229 AB

Hurricane Andrew
Effects on Offshore Platforms

Phase II Joint Industry Project

Final Report

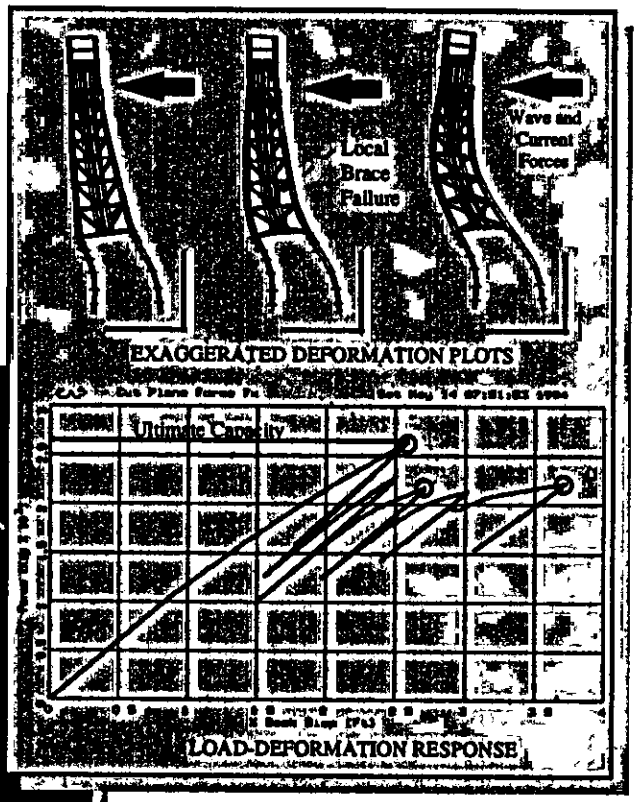

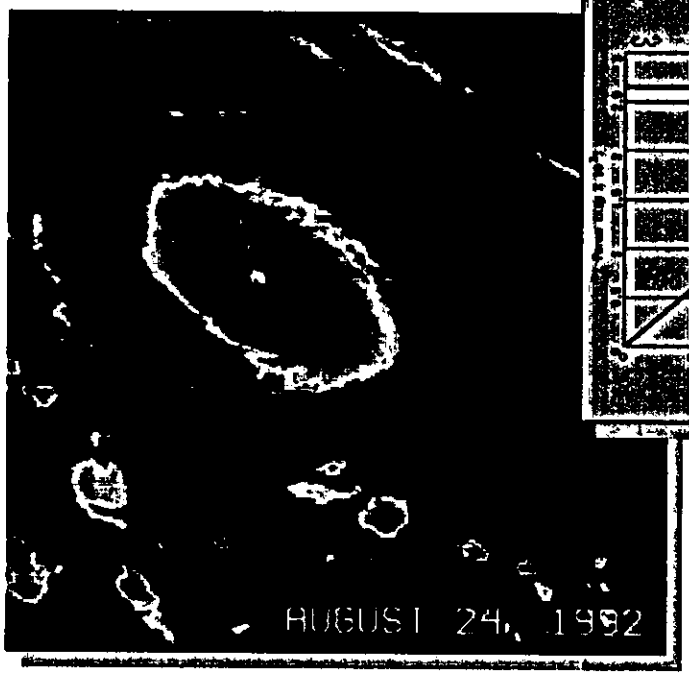

January 1996

PMB Engineering, Inc.

PMB ENGINEERING

NOTE

The use and disclosure of this report are subject to Article 5 of the Participation Agreement between PMB Engineering Inc. and Participating Companies in Hurricane Andrew - Effects on Offshore Platforms Project - Phase II. Distribution and disclosure other than those stipulated in the said article are prohibited.

Contents

Section Page

LIST OF ILLUSTRATIONS

Figure

Table

Section 1
Introduction

1.1 BACKGROUND

Hurricane Andrew

Hurricane Andrew was a very intense storm that passed through the Gulf of Mexico on August 24, 25 and 26, 1992. The hurricane passed through a region of Gulf that is very densely populated with offshore platforms. As shown in Figure 1-1, the center of the hurricane traversed the Mississippi Canyon, South Timbalier, Ship Shoal, and Eugene Island areas. Along its path through the platform areas, Andrew's waves typically exceeded the 100 year return period criteria used for the design of new structures. The region of platforms most significantly loaded by Andrew, as defined by the MMS, included approximately 700 platforms located in the Eugene Island, Grand Isle, Mississippi Canyon, Ship Shoal, South Marsh, South Pelto, South Timbalier, and West Delta areas. Many of these platforms were older structures that were not designed to withstand the forces created by a hurricane of Andrew's magnitude.

Most of the platforms affected by Andrew were not significantly damaged. Many structures suffered minor damage such as bent handrails, although a number of structures experienced significant local structural damage such as a buckled underwater braces and/or joint fracture. There were 28 jacket type platforms that collapsed or were rendered completely unserviceable as a result of the hurricane. In addition, 47 caissons were also significantly damaged or collapsed [1].

Andrew caused significant financial losses offshore and devastating financial losses, injuries and deaths onshore. Although destructive to the oil industry, the Andrew experience provided very valuable data that can be used to further understand the performance of offshore structures subjected to large hurricanes. It provided an opportunity to learn from the experience by reviewing the platforms that survived, were damaged, or failed during the hurricane. Andrew thus provided a unique opportunity to study offshore structures tested under "real-life" full scale conditions.

The objective of this study has been to use the data that were gathered as a result of Andrew to better understand the nature of platform response during extreme hurricanes. It is intended that the results of this study will be used by the industry to improve methods for the ultimate capacity assessment of existing structures, which is a key element in assuring the safety of all offshore facilities.

Phase I Study

In October, 1993, PMB completed a joint industry project, "Hurricane Andrew-Effects on Offshore Platforms," (hereafter called Andrew Phase I or Phase I) [1, 4]. The objective of this study was to review the accuracy of existing assessment procedures based on comparison of predictions of platform response against observations collected for 13 specific platforms This study determined that, for the population investigated, the wave loading and ultimate capacity evaluation procedures contained in API RP2A, 20th Edition and its Section 17 supplement [3] were conservative. Specifically, the study concluded that the capacity to demand (peak lateral load during the

hurricane) ratio is conservatively biased by 19 percent. This result was determined with the use of capacity analyses completed by PMB and some of the participants. The results of these analyses formed the input to a structural reliability analysis and Bayesian updating to calculate the bias factor. This bias factor reflected correction to the analytical predictions required to achieve better agreement with the observed results

The Andrew Phase I study resulted in the following observations and recommendations:

- The capacity analysis predicted failure of joints in many of the jackets analyzed. The inspection of these platforms indicated that, in most cases, joints that were predicted to have failed did not. The joint strengths considered in the analysis were based on API RP2A, 20th Edition, which are lower bound estimates, and the joint stiffness effect was not included in the Phase I modeling Therefore, for Phase II use of mean estimates of the joint strength and explicit modeling of joint stiffness were recommended.

- The capacity analysis predicted failures in pile/soil foundation elements for a significant number of platforms. The inspection of these platforms indicated that, in all cases, piles that were predicted to have failed did not. The foundation failure modes that were predicted were: first yield of pile sections, full plasticity of pile sections, inadequate axial soil capacity leading to pile pullout or plunging. In many cases, the predicted failure mechanisms were due to multiple events in the pile/soil foundation system and controlled the ultimate capacity estimates. Therefore, further investigation of pile/soil capacity formulations were recommended to determine bias specific to the foundation capacity.

- Deck inundation from high waves occurred for a number of platforms and was a primary cause of platform collapse The load profile changes significantly when the wave reaches the deck level. The Phase I analysis utilized a pushover load profile based on maximum wave height during Andrew at a platform location. The capacity analysis results may be improved if the variation in pushover load profile with wave height is included, essentially to determine the effect of significant change in load profile due to wave-in-deck on the occurrence of inelastic events.

- The bias factor (B) was determined to be 1.19. It was an overall (system) correction factor and was not specific to the biases associated with the individual failure modes of the jacket and its foundation. Therefore, multiple bias factors related to the failure modes shall be more appropriate.

- The bias factor was based on a total sample of 13 platforms which represented a relatively small percentage of the total population of platforms significantly loaded during the hurricane. Including additional platforms would improve the definition of the bias factor; however, detailed analysis of a significant number of platforms is prohibited both by the cost of such analyses and the lack of necessary data. It was suggested that a simplified "weighting" procedure could be used to enlarge the sample size without detailed analysis.

Andrew Foundation Study

To further investigate the perceived biases in the foundation capacity estimates for the steel jacket platforms, the API and MMS awarded a study to PMB to specifically evaluate the effects of Hurricane Andrew on platform foundations. This study was completed in May 1995 [5]. The various factors that would influence pile axial and lateral capacity estimates were discussed. Several jacket platforms and caissons were analyzed to establish ultimate capacity estimates as input to the structural reliability calculations. Bias factors of 1.3 and 1.7 were established for the foundation lateral and axial ultimate capacity to load ratios (R_u/S). These estimates confirmed the need to determine ultimate capacity and bias factor estimates specific to failure modes.

Updated Hindcast

The MMS commissioned Oceanweather Inc., to generate new hindcast data for Hurricane Andrew using an improved hindcast model. Oceanweather developed a surface wind model using an improved version of a numerical model of the vortex planetary boundary layer model and surface waves were modeled using a third-generation model which included shallow water physics [see Appendix D]. The new hindcast [13] was developed at a finer grid compared to the 1992 hindcast [12] and in general the new hindcast provided lower significant wave heights than previous. This lead to a need to investigate effects of new hindcast on platform behavior predictions and bias factor.

Phase II Study

PMB was awarded this study by the MMS and 7 operating companies, all of which participated in the Andrew Phase I study. The primary focus of Phase II has been to develop multiple bias factors for different failure modes (failure in jacket structure and failure of pile foundation system) using the new hindcast, updated capacity analysis procedure (with improved joint strength and stiffness modeling), and with improved procedures for calibration

1.2 OBJECTIVES

There were two primary objectives for the Andrew JIP - Phase II study:

1. **Capacity Analysis** — Perform capacity analysis for several platforms which were affected by Hurricane Andrew using the updated analysis procedures. The Andrew Phase I project identified several areas in capacity analysis procedures that required further investigation and development. The objective of this portion of the project was to develop a refined "procedure" for platform capacity analysis to provide a better comparison of analytical results with observed behavior during Andrew.
2. **Calibration** — Perform a calibration of procedures for capacity analysis of the jacket and its foundation (lateral and axial), for assessing existing platforms The process includes reconciling analytically predicted platform damage and failure with observed field performance during Andrew. Multiple bias factors applicable to the ratios of

computed ultimate capacities to load, for the jacket and its foundation were to be developed using an updated procedure for calibration

The API TG 92-5 has recently issued a draft supplement to RP 2A, "Assessment of Existing Platforms to Demonstrate Fitness For Purpose." These guidlines recommend the use of ultimate capacity analysis as the most rigorous procedure for the assessment of existing platforms.

A major goal of this project was the calibration of some of the platforms that survived, were damaged or collapsed during Andrew with the intent to primarily determine the bias in the ratio of predicted ultimate capacity to load estimates.

1.3 PLATFORM SELECTION

The platforms considered in Andrew Phase I and other platforms from the MMS database were considered in the selection process. The participating companies were contacted for providing information for additional identified platforms and any other platforms, which might have been of interest for calibration

The platforms were selected from a detailed evaluation using the following available information:

- Structural characteristics and details of platforms
- Damage to platforms during Andrew
- Geotechnical information in the vicinity of platforms
- Hindcast information (using the 1992 hindcast)
- Ultimate capacity and calibration results from the Phase I

Table 1-1 presents a list of platforms that were selected for investigation in this project. Several other structures were reviewed to assess their value to the calibration (e.g , SS114H and ST86); however, many of these were determined to be unsatisfactory due to either their performance during the hurricane (expected survival) or due to the lack of good data.

There were no jacket type platforms available that were believed to have experienced a foundation failure; however, there were several caissons that experienced full or partial foundation failure. Three caisson platforms which were damaged during Andrew were included in the API/MMS Foundation study to investigate their effect on the foundation lateral capacity bias factor. The expectation was that the caissons would provide a limit to the bias factor established based on jacket platforms However, the caissons' effect on the bias factor was presented separately, to distinguish between individual contributions of jackets and caissons. These caissons are also included in the calibration work in this study, to evaluate their influence on the foundation lateral bias factor.

The following structures were finally selected for calibration in this project:

Steel Jacket Platforms

Observed survival category	ST151K, ST130Q, WD103A
Observed damage category	ST177B, ST151J, SS139 (T25)
Observed failure category	ST151H, ST130A, ST72 (T21)

Caissons

Observed damage category	SPelto 10, SS135, SS136

Figure 1-1 provides locations of these platforms. Note that platform ST177B was considered under observed failure category in Phase I due to lack of specific damage information available at that time. Significant damage information obtained during its salvage lead to its classification under observed damage category.

The physical characteristics and other information for the jacket platforms are summarized in Tables 1-2 and 1-3 The caissons information is summarized in Table 1-4. Platform orientations, structural framings, soil shear strength profiles, and hindcast data are provided in Appendix A.

1.4 ACKNOWLEDGMENTS

The efforts of the technical representatives of the participating companies are greatly appreciated. The input received during the three project meetings included very valuable direction to the project. The participating companies and their technical representatives are as follows:

AMOCO	— Jim Light
CHEVRON	— Dirceu Botelho
EXXON	— Ward Turner
MINERALS MANAGEMENT SERVICE	— Charles Smith
MOBIL	— Damo Nair
MSL	— Minaz Lalani
PHILLIPS	— Roger Thomas
SHELL	— Kris Digre
UNOCAL	— Jared Black

In particular, the following should be commended for their input:

- **Dr. Allin Cornell,** Stanford University - As a consultant to PMB, Allin provided input to the calibration and structural analysis.
- **Dr. Fred Moses,** University of Pittsburgh - As a consultant to PMB, Fred provided input to weighting approach development.

- **MSL Engineering, U.K.** - As a consultant to PMB, MSL provided joint strength and stiffness information.
- **Risk Engineering, Inc.** Provided clarifications on the use of RELACS and provided revisions that were necessary to complete the project.
- **Chevron.** Provided several geotechnical reports, information for a number of platforms and assistance with the interpolation of hindcast data.
- **Oceanweather, Inc.** Through a project funded separately by the MMS, Oceanweather provided the meteorological and oceanographic site specific hindcast information for Hurricane Andrew.
- **Minerals Management Service.** Provided new hindcast data for use in this project.
- **Shell.** Provided details for an 8-leg steel jacket platform for use in this project.
- **Trunkline.** Provided geotechnical reports and other data for two platforms during this study.
- **Mobil** Provided structural information and drivability records for two caissons damaged during Andrew.
- **Murphy.** Provided information including original design summary reports for five caissons damaged during Andrew.

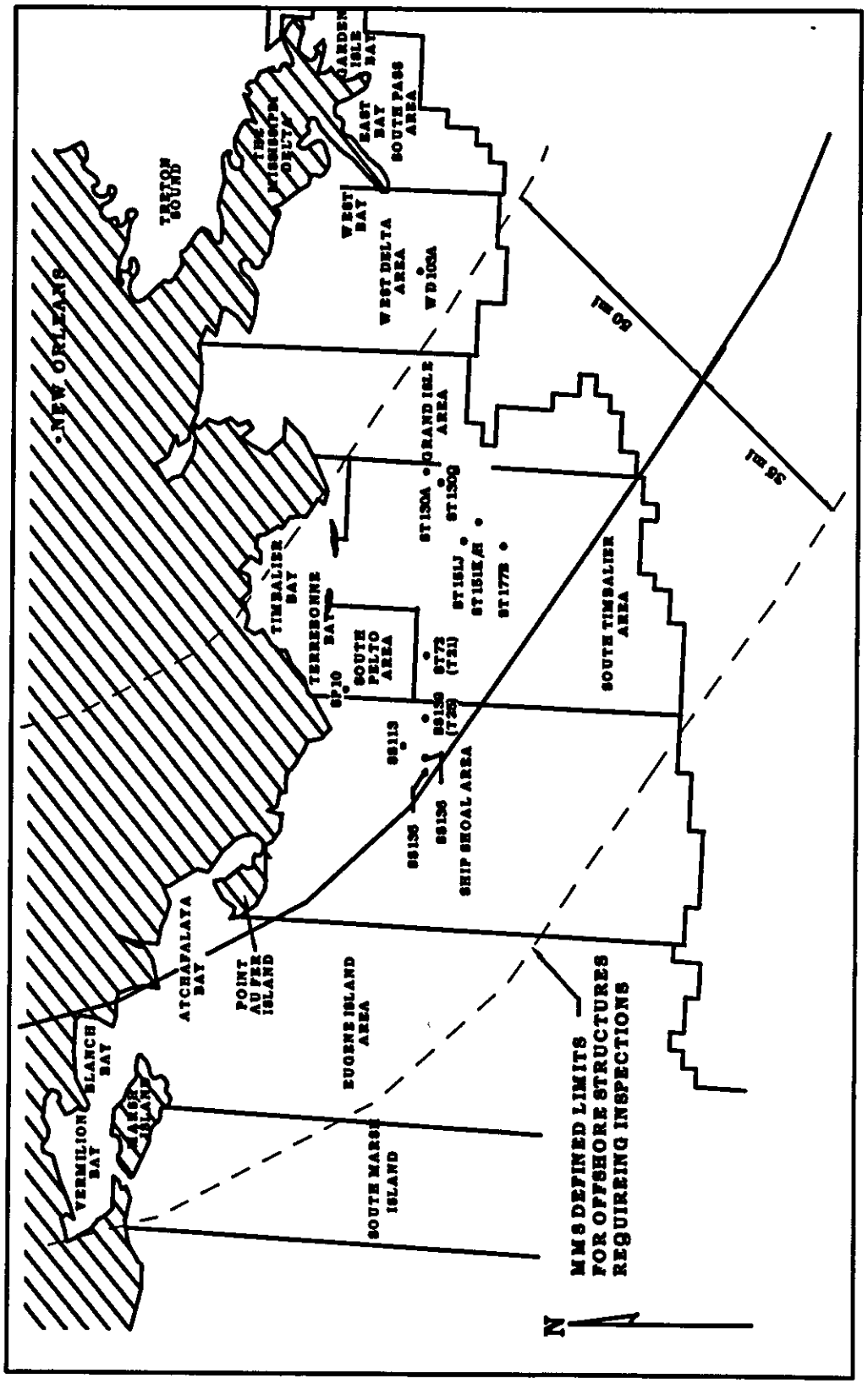

Figure 1-1: Path of Hurricane Andrew with Platforms Used in Phase II

Note: SP10, SS135, and SS136 are caissons

Table 1-1: Platforms Selected for Andrew JIP - Phase II

Platform Name	Water Depth ft.	Year of Installation	Number of legs	Availability of Inspection Information	Availability of Soil Report (#1)	Platform Classification Based on Phase I Calibration
Survival Platform Cases:						
ST151K	137	1963	8	Yes	ST151 block	Unexpected Survival
ST130Q	170	1964	4	Yes	GI 86 block	Unexpected Survival
WD103A	223	1965	8	Yes	WD103 block	(#3)
Damage Platform Cases:						
SS139 (T25)	62	1969	4	Yes	SS139 block	Unexpected Survival/Likely to Damage
ST177B	142	1965	8	Yes	ST189 block	Expected to Damage
ST151J	137	1962	8+2 tripods	Yes	ST151 block	(#3)
Failure Platform Cases:						
ST151H	137	1964	8	Collapsed (#2)	ST151 block	Expected Failure
ST130A	140	1958	8	Yes	GI 86 block	Likely Failure
ST72 (T21)	61	1969	4	Collapsed (#2)	ST72 block	Likely Failure

Notes:
(#1) - Soil information recommended by operators for the platform
(#2) - Detailed information not available
(#3) - Platform was not evaluated in Phase I

Table 1-2: Steel Jacket Platforms - Characteristics and Available Data

Platform Identification	Block Number	Year Installed	Water Depth (ft.)	Number of Legs/Piles	Foundation Features		Damage Location (Elements) (#1)	Availability of Soil Report	Case for Calibration
					Pile Diameter (inch)	Penetration Below Seabed (ft.)			
ST 151K	South Timbalier 151	1963	137	8	30	175	No damage to primary elements	Yes (same block)	Survival
ST130Q	South Timbalier 130	1964	170	4	30	210	No damage	No (used GI 86 Well Site 3) (#2)	Survival
WD103A	West Delta 103	1965	223	8	42	270	No damage	Yes (same block)	Survival
ST151J	South Timbalier 151	1962	137	8 + 2 tripods	30	180	Diagonal braces	Yes (same block)	Damage
ST 177B	South Timbalier 177	1965	142	8	30	187	K-joints, X-joints (Jacket salvaged)	No (used ST189 borelog @ 1 mile) (#2)	Damage
SS139 (T25)	Ship Shoal 139	1969	62	4	36	165	Tearing of K-joints (Jacket salvaged)	Yes (same block)	Damage
ST 151H	South Timbalier 151	1964	137	8	30	180	Rubbled Details not available	Yes (same block)	Collapse
ST 130A	South Timbalier 130	1958	140	8	30	175	Leg failure occurred before pile yield	No (used GI 86 Well Site 3) (#2)	Collapse
ST72 (T21)	South Timbalier 72	1969	61	4	36	170	Collapsed	Yes (same block)	Collapse

Notes:
#1 Damage observed post Hurricane Andrew Refer to Table 1-3 and Appendix A
#2. Soil information provided by operator

Table 1-3: Damage Description - Platform ST177B

Damaged Elements	Damage Description
X- Joints	Crushing (ovalization) of brace in tension Crack (> 2 ft long) at the centerline (narrow apex of the oval) of the tension (through) member.
K- Joints	All K-joints completely severed at gap (zone within braces) in chord. Failure plane located along a line parallel to the compression K-brace.
KT -Joints	Interior frame KT joints located near the conductors showed bulging and cracks, but were generally still intact.
Platform Legs	Slight curvature of legs along the wave direction at lower bays where K joints were completely severed

Table 1-4: Free Standing Caisson Platforms - Characteristics and Available Data

Block Number	Year Installed	Water Depth (#1) (ft.)	Structural Features		Damage Description (#2)	Availability of Soil Report	Case Type for Calibration
			Caisson Diameter (inch)	Penetration Below Seabed (ft.)			
South Pelto 10	1984	35	30	195	Leaning 12 degree	Yes (borelog within 0 2 miles)	Failure case (Foundation failure)
Ship Shoal 135	1983	53 (48' original)	48	100	Leaning 15 degree	Yes (borelog within 0 8 miles)	Failure case (Foundation failure)
Ship Shoal 136	1983	50	48	100	Leaning 30 degree	Yes (Same well location)	Failure case (Foundation failure)

Notes:
#1: As-is water depth is mentioned, where information was available
#2: Damage observed post hurricane Andrew

Section 2
Capacity Analysis Procedures

The procedures used for the nonlinear ultimate capacity analysis of the platforms were based upon the API RP 2A, 20th Edition and its Section 17 supplement [3], with several modifications as required for this project. Several case studies were performed to resolve issues related to the recipe. The following two issues were investigated in detail to establish the updated recipe:

- Pushover Wave Load Pattern
- Conductor modeling

2.1 LOAD AND RESISTANCE RECIPE

There are several modeling issues which would not receive a consensus opinion within the industry. These issues, such as choice of F_y (steel yield strength), were based upon a vote by participants during Phase I meetings. Additional recipe issues were proposed by PMB and were accepted or modified by the participants, during Phase II meetings.

A summary of the key items of the recipe that are applicable to this project are given below. Additional details of the recipe are given in Appendix B.

- **Wave Load on the Deck.** In cases where waves impact the deck, the simplified procedure developed by API Task Group 92-5, given in the Draft Section 17 (April 20, 1994 version) was used.
- **Pushover Wave Load Pattern.** Variable pushover load patterns were used for cases where deck inundation occurred. (See Section 2.3.1 for detail of the case study)
- **Factors of Safety.** No factors of safety were included in defining the capacities of structural elements.
- **Material Strength.** Most of the platforms were fabricated using steel with a 36 ksi nominal yield strength. Participants voted on using a yield strength of 42 ksi for these cases to account for the difference between nominal and mean yield strength and to account for the increase in strength due to strain rate effects (rapid loading in storms) [14].
- **Brace Modeling.** The braces were modeled using Struts, Beam Columns or with a new "Fiber Element." The diagonal braces (leg-to-leg) were modeled as Marshall Struts. The K-braces (or K-joints braces) were modeled using a Fiber Element (a modified beam column element to include the joint capacity/stiffness information) in all instances where the joint capacity governed joint/brace strength. The horizontal braces near the mudline and waterline were checked for the axial vs. flexural behavior dominance and, in general, were modeled with beam columns.
- **Brace Capacity (Buckling).** The brace capacity is defined by Equation D.2.2-2 of API RP 2A LRFD [15]
- **Effective Length (k) Factors.** Section 17 does not recommend values of k (the effective length factor) for use in ultimate capacity analysis Recent tests and analytical studies [16,17,18] have

indicated the appropriate values of "k", without factors of safety, are 0.5 for X- braces, 0.55 to 0.65 for diagonal braces (depending upon end fixity) and 0.65 for K- braces

An effective length factor of 0.65 was used for "k" and "diagonal" braces. The length was taken as node-to-node distance (not face-to-face of the leg). An effective length factor of 0.55 was used for "X" braces with the member length taken as one-half the longest segment length(i.e. out-of-plane buckling is not considered due to the compensating effect of the tension brace).

- **Joint Capacity.** The capacity of braces and their connections were evaluated based on conservative joint capacity formula (i.e., API RP 2A) and prior experience. An explicit joint model was developed in all instances where the joint strength was determined to control. Joint strength and load-deformation formulations, (P-δ) and (M-θ), were developed for these joints by MSL Engineering. Section 2.2 includes further details on joint modeling. These formulas were used to define the properties of the corresponding beam-column and fiber element models.

- **Grouted Joints.** The API RP 2A equations for joint capacity were used, without safety factors, and with an equivalent thickness for the leg representing strength of the composite section (leg/pile) [19].

- **Conductor Modeling.** Conductors were always modeled to capture their wave load contribution The structural resistance of the conductors, which increase the lateral load carrying capacity of the foundation, were modeled only in instances where the conductors were guided at the mudline and initial analysis predicted a pile yield/hinge failure mode. The conductors were guided at the mudlevel horizontal framing for only two platforms (WD103A, ST130A) and were modeled for structural resistance in only ST130A

- **Soil Shear Strength.** Shear strength profiles were developed based on comparison of the following profiles:

  * Based on Strength Ratio (S_u/σ_v') of 0.23 and assuming an over consolidation ratio (OCR) of 1.0
  * Miniature Vane (MV) tests on undisturbed samples
  * Interpreted or Design shear strength profile from soil reports

  In case of driven samples a modification factor of 1.2 was used to account for the effect of sample disturbance if it was not already included in the soil report. In case of pushed samples no modification factor was used.

  The soil shear strength data were based on available geotechnical reports in the same or nearby blocks of platform locations

- **Lateral Soil Capacity.** The AIM projects [20] and other assessment-type studies have typically used degraded soil-pile capacity to develop p-y nonlinear soil springs for pushover analysis. This is based upon the assumption that the soil strength is degraded at the time of the peak wave due to cyclic action of other large waves during storm build-up. However, recent laboratory tests by Exxon [21] indicated that, for pushover type analysis, the static lateral soil

strength is a better measure. Therefore, static p-y soil strength was used and was defined by the API RP 2A formula.

- **Axial "t-z" Springs:** Static soil strength (no degradation) per API RP2A were used

Pile axial capacity estimates per API RP 2A are affected by loading (or strain) rate, cyclic loading, reconsolidation (time effect), compressibility (pile length effect) and pile aging effects. The influence of these factors reported in the literature was summarized in the API/MMS foundation study [5] The contribution of these factors to the pile axial capacity is uncertain and thus, in Phase II, a correction factor was not applied to the pile axial capacities The cumulative effect of all of these factors will be reflected in the resulting foundation axial bias factor.

2.2 JOINT MODELING

2.2.1 Information from MSL

The load-displacement and moment-rotation formulations for 25 joints were developed by MSL Engineering for use in the capacity analysis. MSL did not provide the general formula for axial and bending capacities of joints (these formula are proprietary to an MSL JIP and will be under confidentiality agreement for a period of two years [22]). The following MSL document includes details of joint strength and stiffness formulations.

MSL Engineering Ltd. "JIP on Assessment Criteria, Reliability and Reserve Strength of Tubular Joints. Technical Report No 10: Load/Displacement Characteristics of Simple Joints". Doc Ref. C14200R010 Rev 0, February 1995.

A majority of the participating companies in this project are also participants of the MSL JIP.

MSL provided data in the form of continuous load-deformation plots for the P-δ and M-θ relationships for all joints. Data was provided based on 100% K and 100% Y joint classifications for the P-δ relationship. MSL noted that there is a distinct lack of data for K-joints under moment loading They advised to use T-joint data to estimate the K-joint moment response. The same M-θ curve applies for both K and Y joints of corresponding geometry so one curve was provided to define M-θ for each joint.

The plots relate to mean curves (i.e., not lower bound) and are presented in the non-dimensional form of P/P_u vs. δ/D (or M/M_u vs.θ) where:

P	=	axial load	D	=	chord diameter
Pu	=	basic ultimate axial capacity	M	=	moment load
δ	=	axial deformation in direction of brace			
M_u	=	basic ultimate moment capacity			
θ	=	brace rotation measured at chord surface			

The basic values for P_u and M_u were adjusted for:

- Brace load interaction effect
- Chord load effect
- Joint classification

Brace Load Interaction Effect

MSL recommended consideration of the following interaction equation, which is reflected in all codes except API and DnV, and is believed to more accurately reflect the generally accepted view

$$\left|\frac{P}{P_u}\right| + \left(\frac{M_{ipb}}{M_{u,ipb}}\right)^2 + \left|\frac{M_{opb}}{M_{u,opb}}\right| \leq 1.0 \qquad [2\text{-}1]$$

that OPB (Out-of-Plane Bending) is more important than IPB (In-Plane Bending):

The basic P_u values were scaled down using the following relationship:

$$P_{u,combination} = P_{u,tabulated}\left[1 - \left(\frac{M_{ipb}}{M_{u,ipb}}\right)^2 - \left|\frac{M_{opb}}{M_{u,opb}}\right|\right] \qquad [2\text{-}2]$$

The basic M_u values were scaled down in a similar way.

Chord Load Effect

The basic strength (P_u) was also reduced to account for the presence of chord loads. Present code guidance is somewhat conservative in estimating the degree of reduction in axial strength due to chord load effects. The following bi-linear approximation was recommended by MSL and was suggested to provide a more realistic definition for Q_f (the factor to account for the presence of nominal longitudinal stress in the chord) in the case of brace axial loading The MSL bi-linear approximation is applicable to K and Y joints but not to X joints.

$$\begin{aligned} Q_f &= 1.0 && \text{when } A < 0 \\ &= 1.0 - 0.21\,A && \text{when } 0 < A < 0.5 \\ &= 1.21 - 0.63\,A && \text{when } A > 0.5 \end{aligned} \qquad [2\text{-}3]$$

where A is given by the following expression:

$$A = \left[f_{ax} + 0.5\left(f_{ipb}^2 + f_{opb}^2\right)^{\frac{1}{2}}\right] \Big/ F_{yc} \qquad [2\text{-}4]$$

where f_{ax}, f_{ipb}, and f_{opb} are the nominal axial, in-plane and out-of-plane bending stresses in the chord ('f_{ax}' is negative if axial load in chord is tensile). F_{YC} is the yield strength of the chord material.

The value of Q_f changes as the pushover load level increases. The estimates of Q_f were developed based on the load distribution corresponding to the estimated ultimate strength of each platform.

Joint Classification

The classification of a joint is a primary factor in determining capacity. Some of the "K" joints were found to have well balanced load distributions and can be properly classified as K joints. However, unbalanced joints have to be classified as part K and part Y. In these cases the load-deformation response for mixed behavior (part K and part Y) was obtained by summing the appropriate contribution of K joint load and Y joint load for various values of deformation (δ). In cases where the ratio of axial components in the braces change significantly during the non-linear analysis the classification (e.g., 80% K : 20% Y) was also changed.

COV's of the test data on which the MSL information is based

The COV's of the mean joint strengths are as follows:

Joint Type	COV
Gapped K joints under balanced axial loading	0.13
T joints under IPB	0.11
T joints under OPB	0.14
DT/X joints under compression	0.09

The above COV's are based on available test data and would change if more test data were available. The COV's relate to specific definitions of failure (e.g., the first peak in the load-deflection behavior or, especially in the case of moment loaded joints, to some deformation limit). MSL noted that some investigations have continued their joint tests well beyond those particular failure criterion and, in these few tests, the stiffness is regained and the capacity of the joint may well exceed the initial peak for a K joint, as shown in Figure 2-1. They noted that such stiffening behavior does not always appear.

2.2.2 Modeling by Fiber Element

Selected K, KT, and X joints were modeled using a new fiber element incorporated in the CAP/SEASTAR software [23] The element provides a concentrated joint sub element at each end of the beam as shown in Figure 2-2. The multi-linear axial and bending behavior defined above was modeled using this element. The first yield, full yield, and post-yield behavior of joints and their associated flexibilities were modeled.

The basic capacities provided by MSL were adjusted to include effects of brace load interaction, chord load and joint classifications. Several iterations were made to determine the joint capacity estimates applicable at inelastic events.

2.3 CASE STUDIES

Two case studies were performed to finalize the analysis procedures used in this project

- Pushover Wave Load Pattern
- Conductor Modeling

2.3.1 Pushover Wave Load Pattern

The objective of this case study was to quantify the error in using a constant wave load profile in pushover analysis Pushover analysis is typically performed using a wave load pattern that is established based on a specific wave height. This pattern is applied to a model with increasing scale factors (e.g., 0 to 1.3) until ultimate strength is reached. In this analysis the scale factors are intended to represent the effect of increasing wave height and its associated increase in load However, in using a single wave load pattern, the change in load profile corresponding to different wave heights is not considered. The change in pattern is significant in instances where deck wave inundation occurs.

A more rigorous method of applying the static pushover load pattern to more closely mimic its variation with increasing wave height was tested. An example was developed to demonstrate the impact of two different approaches for pushover load patterns on ultimate capacity estimates. The following two analyses were done:

- Monotonic pushover load pattern based on maximum wave height during Andrew
- Variable pushover load patterns developed for increasing wave heights

The capacity analysis results for the Andrew Phase I [1] and MMS Inspection projects [6,7] were reviewed and platform ST151K was selected for this case study due to high wave-in-deck loads. The soil shear strength was artificially increased for these analyses to force failures in the jacket portion of the structure.

The change in load pattern with wave height was handled automatically within the CAP/SEASTAR program. A procedure for a 2-step wave height incremental pushover is illustrated in Figure 2-3. A load pattern is developed for an initial wave that is well below the height of the wave expected to define the ultimate strength of the platform. This pattern is applied to the model The load pattern for a somewhat larger wave is calculated and the nodal load differences between this second load pattern and the first load pattern are determined. This establishes an incremental pattern that is applied in the second step of the analysis. The total load applied to the model after the second step is thus equal to that of the second wave height both in term of

magnitude and distribution. This process of applying incremental loads is continued until the ultimate capacity of the platform is reached

The Andrew wave height of 60.86 ft was used to generate the pushover load pattern and wave-in-deck forces. The incremental load patterns were determined for wave heights from 51 ft to 63 ft at increments of 2 ft. Loads were also determined for three additional wave heights (30 ft, 40 ft, and 49.5 ft) which were chosen to complete the wave height vs. load curves. A comparison of the pushover load profiles for different wave heights from 30 ft. to 63 ft. is shown in Figure 2-4.

The comparison of pushover results for the case with a single pushover load profile and the case with incremental load profiles is shown in Figure 2-5. In general the results are very similar and the ultimate strength defined with the more accurate method is approximately 1% lower than that that associated with the constant load pattern. The incremental load analysis case shows higher stiffness and thus lower deck displacements for pushover load of less than 4,500 kips (corresponding to a wave height of 60 ft). This is due to the fact that, for wave heights less that 60.86 ft, the centroid of applied load for the incremental load case is lower than that associated with the constant load pattern, therefore resulting in lower overturning moment The incremental load case produces larger displacements, and less ultimate strength, for wave heights greater that 60.86 ft as the centroid of applied load is then higher than that associated with the constant load pattern.

A comparison of the load levels corresponding to failure of different elements in the platform for the two analysis cases indicated that a majority of element failures occur at approximately the same load levels, but differ by 5 percent for the first element (K-joint) failure [Table 2-1].

The following conclusions can be drawn from this analysis:

- The incremental load pattern gives a more realistic interpretation of loads applied to the structure particularly when wave deck inundation occurs.
- The vertical centroid of the load patterns changed significantly for the variable load pattern case as the analysis progressed, suggesting that a different failure path could be triggered using these load patterns verses using a single fixed load pattern However, for the example structure, the resulting pushover capacity was essentially the same for both constant and variable load pattern approaches, but the load levels at element events did vary for two cases.
- The influence of incremental load pattern on ultimate capacity of platform depends upon the characteristics of platform (e.g., deck elevations, location of failure modes). The method would be particularly useful for platforms with non-redundant framing (first element failure controlling ultimate capacity) and also for platforms in deeper water depths.

In Phase II analysis, variable pushover load patterns were used for cases where the hindcast waves inundated the deck. This was the case for all but three platforms (ST130A, SS139, ST72) which had deck elevations well above the Andrew wave heights for their locations.

2.3.2 Conductor Modeling

The objective of this case study was to estimate the contribution of conductors to platform ultimate capacity. This study was performed on a single 30" diameter conductor having a wall thickness of 5/8" (taken from platform ST151K).

The entire conductor was explicitly modeled above and below the mudline Nodes for the conductor were placed at the major jacket elevations. The gap between the conductor guide and conductor wall was modeled explicitly. The effects of geometric stiffness, P-delta were not included in the study. The loads induced within the supporting conductor framing was not checked for any of these analyses.

The pushover of a single conductor was performed for the following models:

- Conductor with no guide at mudlevel (see Figure 2-6)
- Conductor with guide at mudlevel (see Figure 2-7)
- Conductor/guide gap model (see Figure 2-6 and Figure 2-7)

Conductor Model with No Guide at Mudlevel

Two analyses were performed, the first using equal lateral displacements along the full height of the conductor, the second using a displacement pattern taken from the ST151K pushover analysis Displacements were applied to the conductor at the guide elevations as imposed deformations.

The results of these analysis show that the lateral ultimate capacity of the single conductor was approximately 80 kips. Both analyses showed that maximum bending occurs in the element below the last imposed displacement (at 37 ft above mudlevel). Yielding occurs in the elements close to the mudlevel.

The effectiveness of the conductors to provide additional capacity to the platform is also dependent upon their lateral stiffness, so load-displacement behavior was also examined. The variable displacement case shows a much greater deflection at the top node than the uniform displacement case before failure occurs. A comparison of the deflections of top nodes for the uniform and variable imposed displacement cases is shown in Figure 2-8 (a).

Conductor Model with Guide at Mudlevel

In this case the imposed displacements (uniform and variable) were also applied to the mudlevel node of the conductor. The ultimate capacity of the conductor increases to approximately 270 kips. Figure 2-8 (b) presents a comparison of load-deformation results for three analysis:

- Uniform displacements at guides
- Variable displacements at guides with top node displacements noted

- Variable displacements at guides with the mudlevel node displacement noted

The comparison of the mudline and top node load-deformation curves is presented to assess the effects of platform overturning on conductor resistance. The results show that the mudline node load-deformation plot is very similar to the uniform displacement result. This indicates that mudline lateral displacement dictates the resistance of the conductors and that the rotation of the platform due to overturning has a secondary effect.

Conductor/Guide Gap Model

In this case the gap between the conductor and its guides were modeled using a spring element with negligible resistance for the first inch of lateral deflection (either positive or negative) and resistance comparable to that of the conductor guide framing for deflections larger than one inch. The conductor was assumed to be initially located in the center of the guides over its entire length. This model was used with variable imposed displacements with and without mudline guides.

The load-deformation results of these analyses are provided in Figure 2-9. The ultimate strengths defined with this model were very similar to those with the prior models. The presence of the gap does cause a delay in the mobilization of the conductor resistance. The top of the conductor displaces approximately 0 4 ft before base shear begins to increase.

A comparison of conductor and platform load-displacement behavior is presented in Figure 2-10. This analysis assumes 12 conductors Results are provided for both guided and unguided cases. The following observations are made based on these analysis:

- Conductors may contribute up to 20 percent additional capacity (for the case analyzed) in the unguided condition.
- Conductors may contribute significant additional resistance when mudline guides are present and could significantly increase ultimate strength when foundation failure modes are indicated.
- The comparison of the load displacement results indicates that, if the contribution of the conductors is to be included, it is important that the resistance of the conductors be added at the lateral displacement corresponding to the ultimate strength of the platform. This is due to the fact that a failure mechanism may be reached within the platform prior to the mobilization of the full resistance of the conductors.
- If the conductors are included in the ultimate strength of the platform it is important to check the load levels in the conductor framing to assure that local failures do not occur.

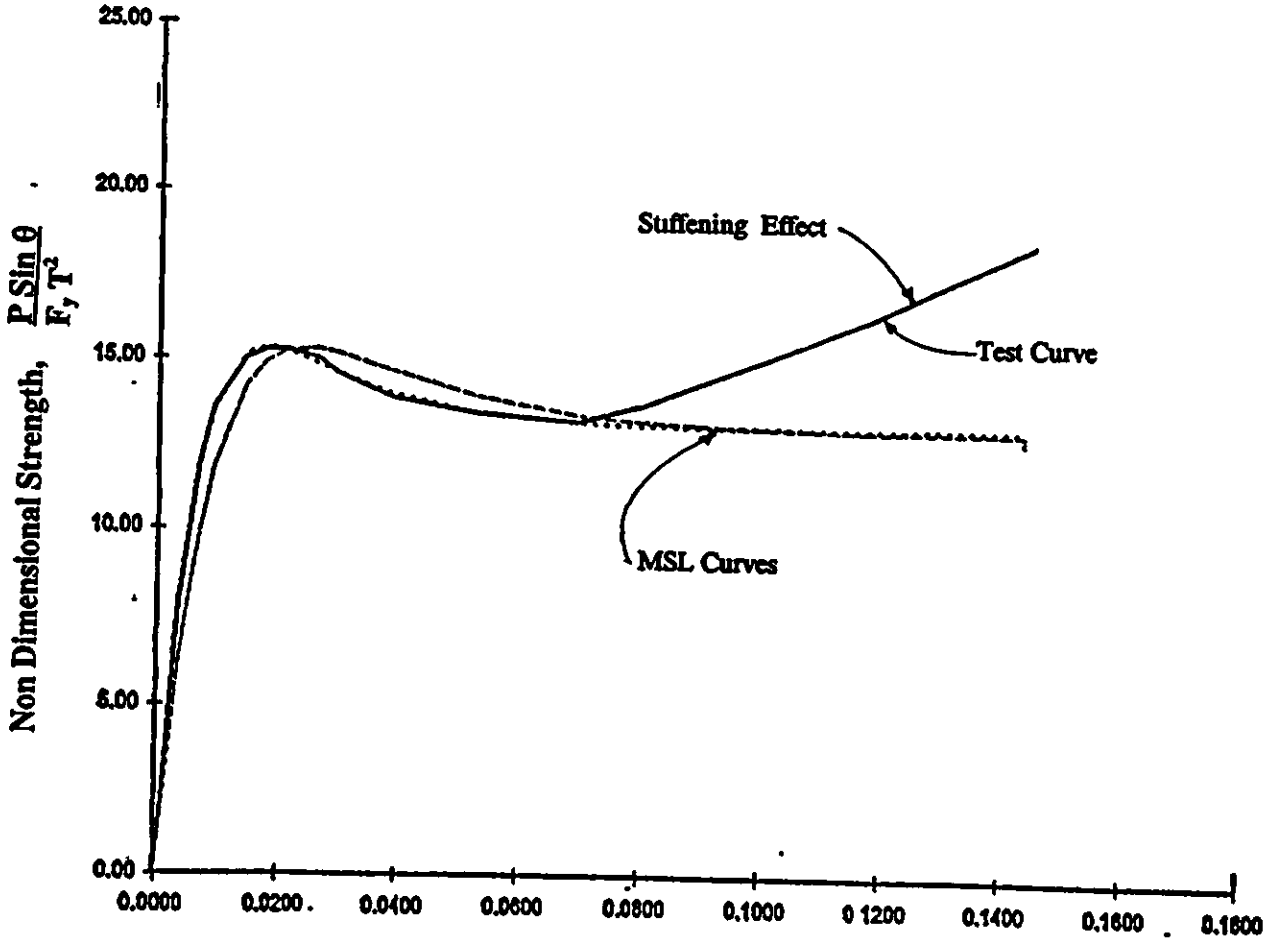

Figure 2-1: Load - Deformation Behavior of K-Joints

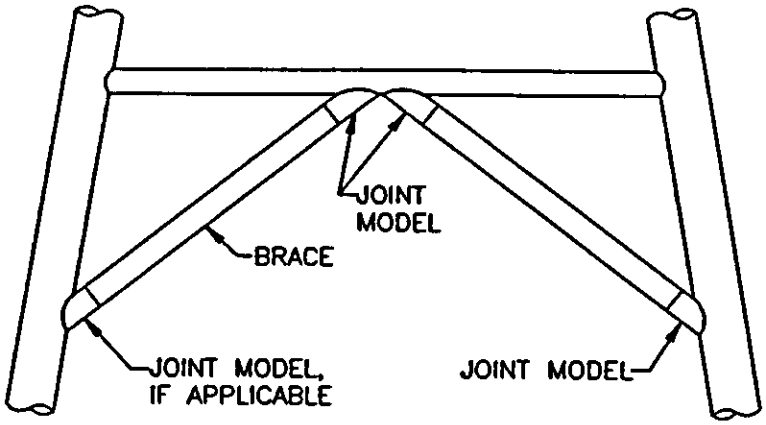

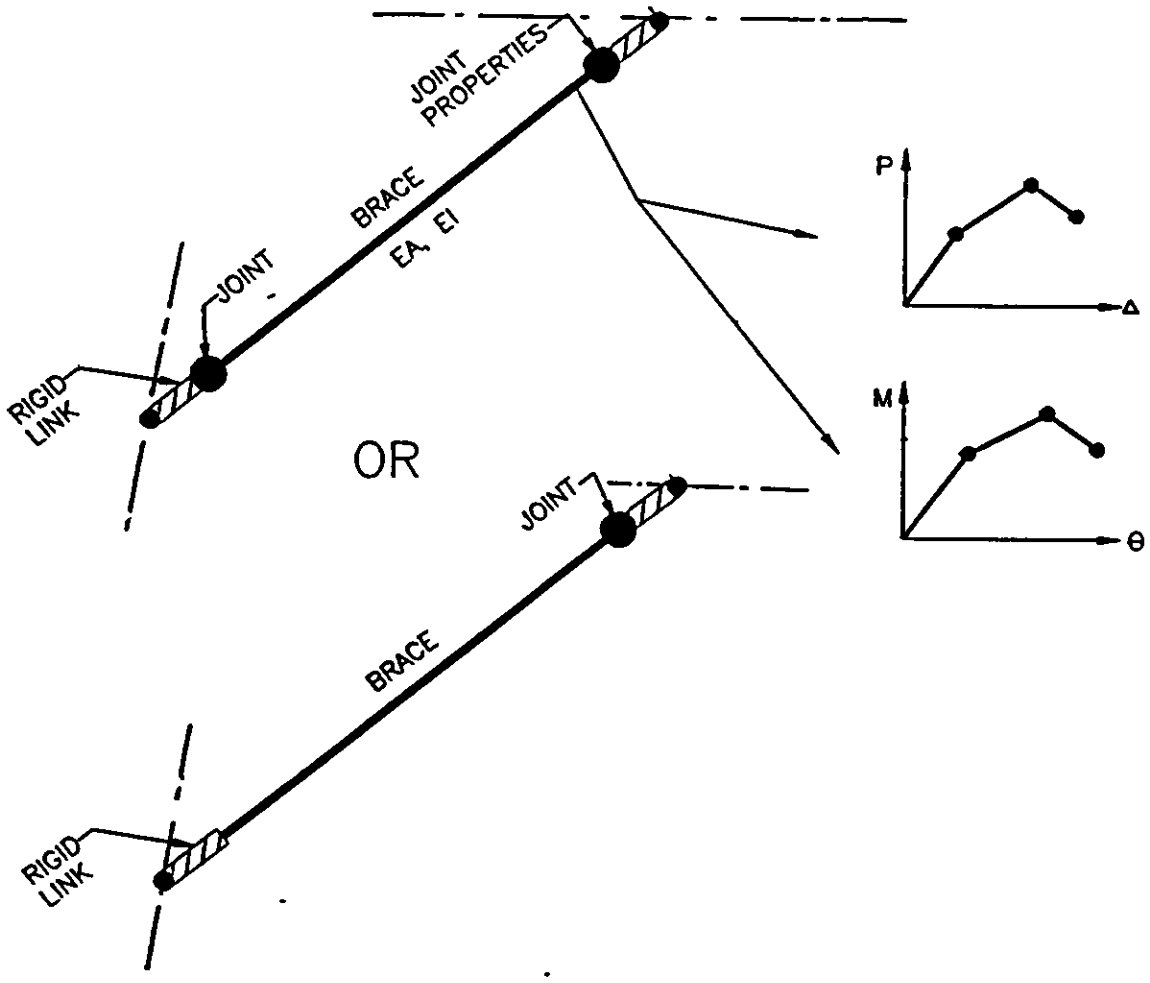

Figure 2-2: Joint Modeling - Phase II

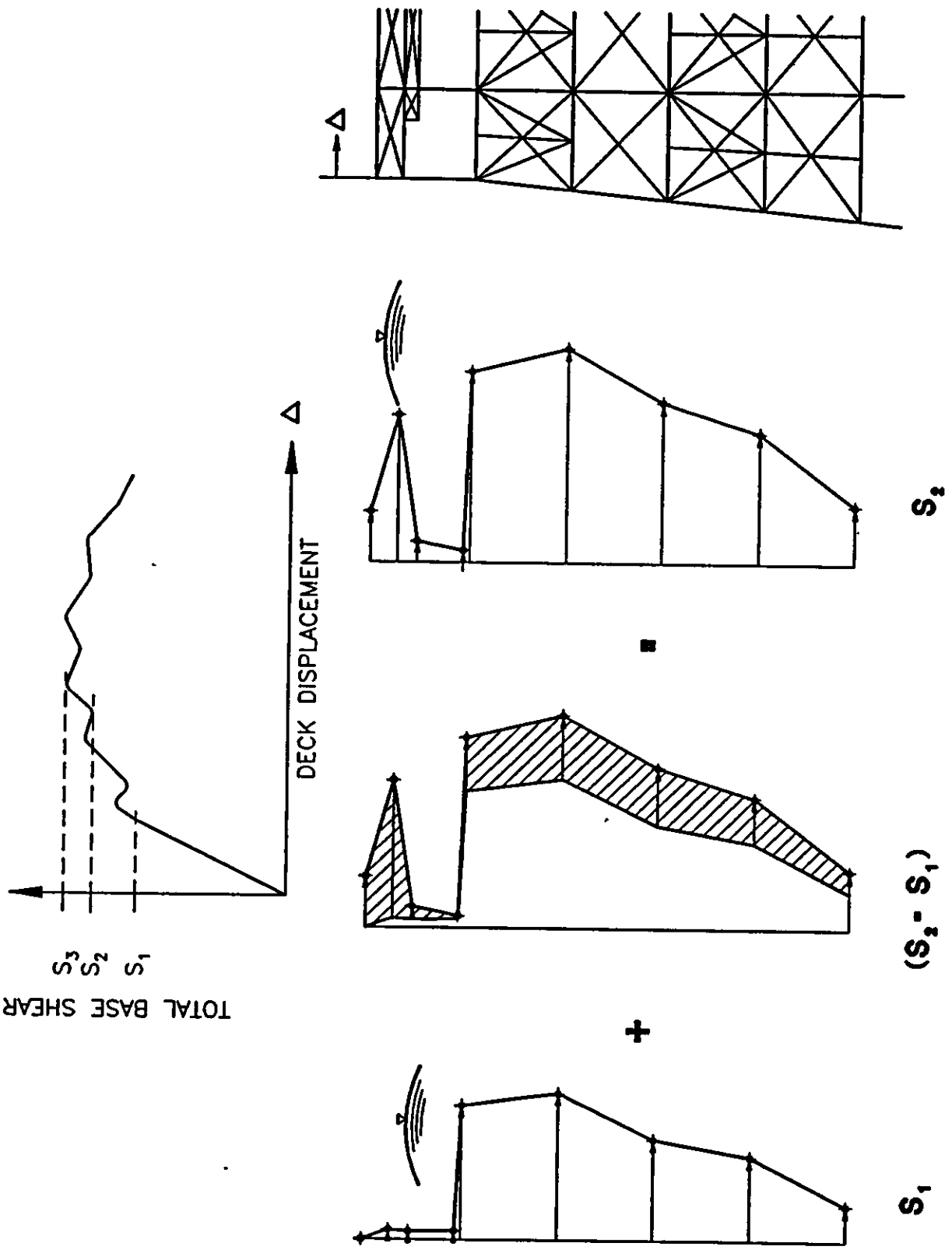

Figure 2-3: Incremental Wave Height Pushover Analysis

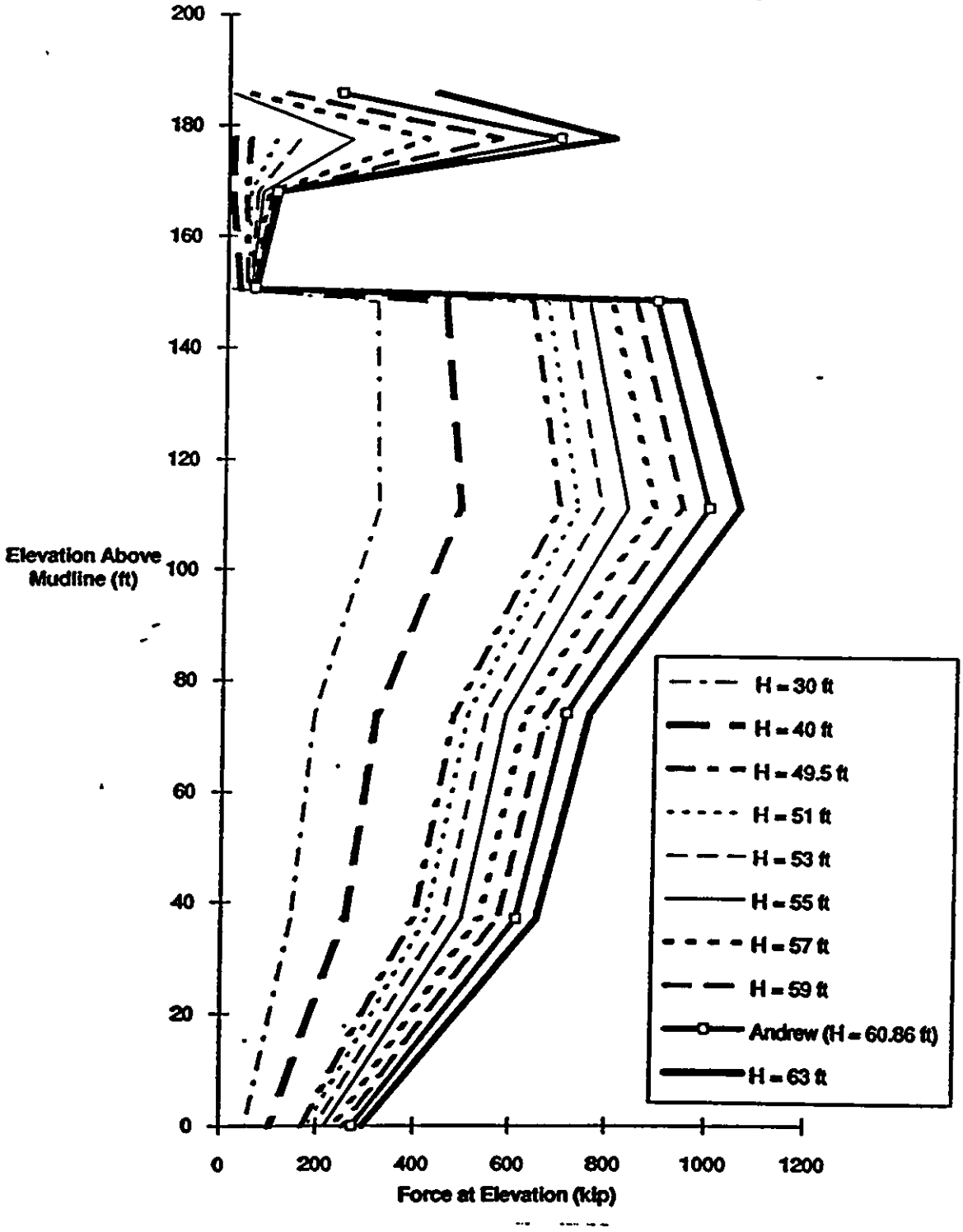

Figure 2-4: Wave Force at Major Elevations for Incremental Wave Heights

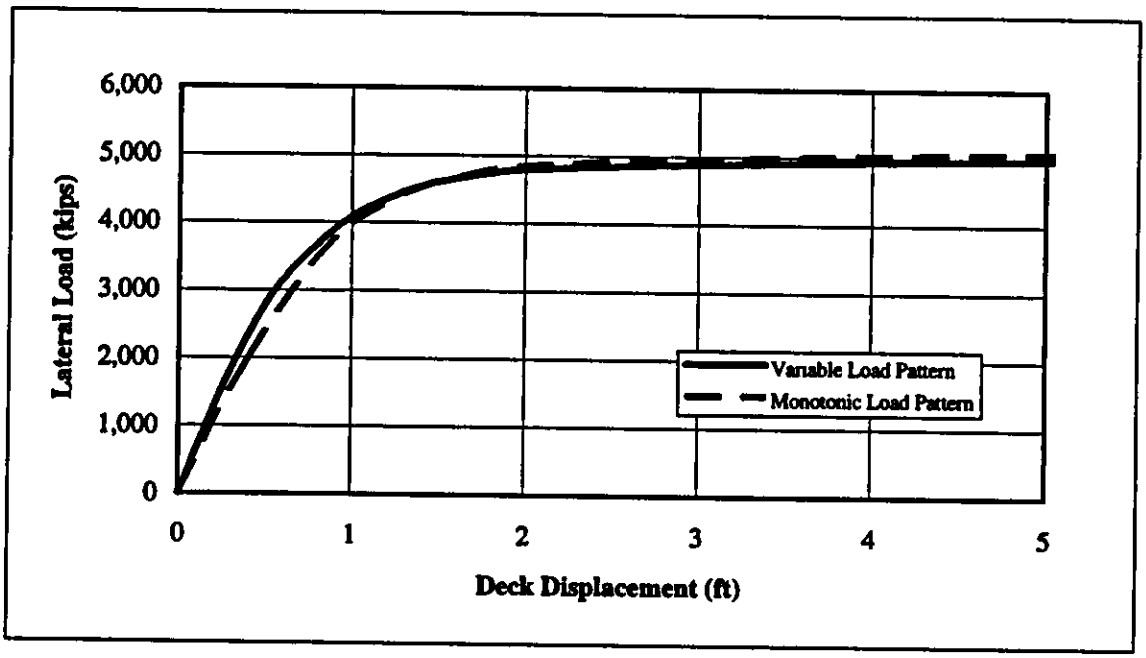

Figure 2-5: Load-Displacement Behavior- Variable vs. Monotonic Load Pattern

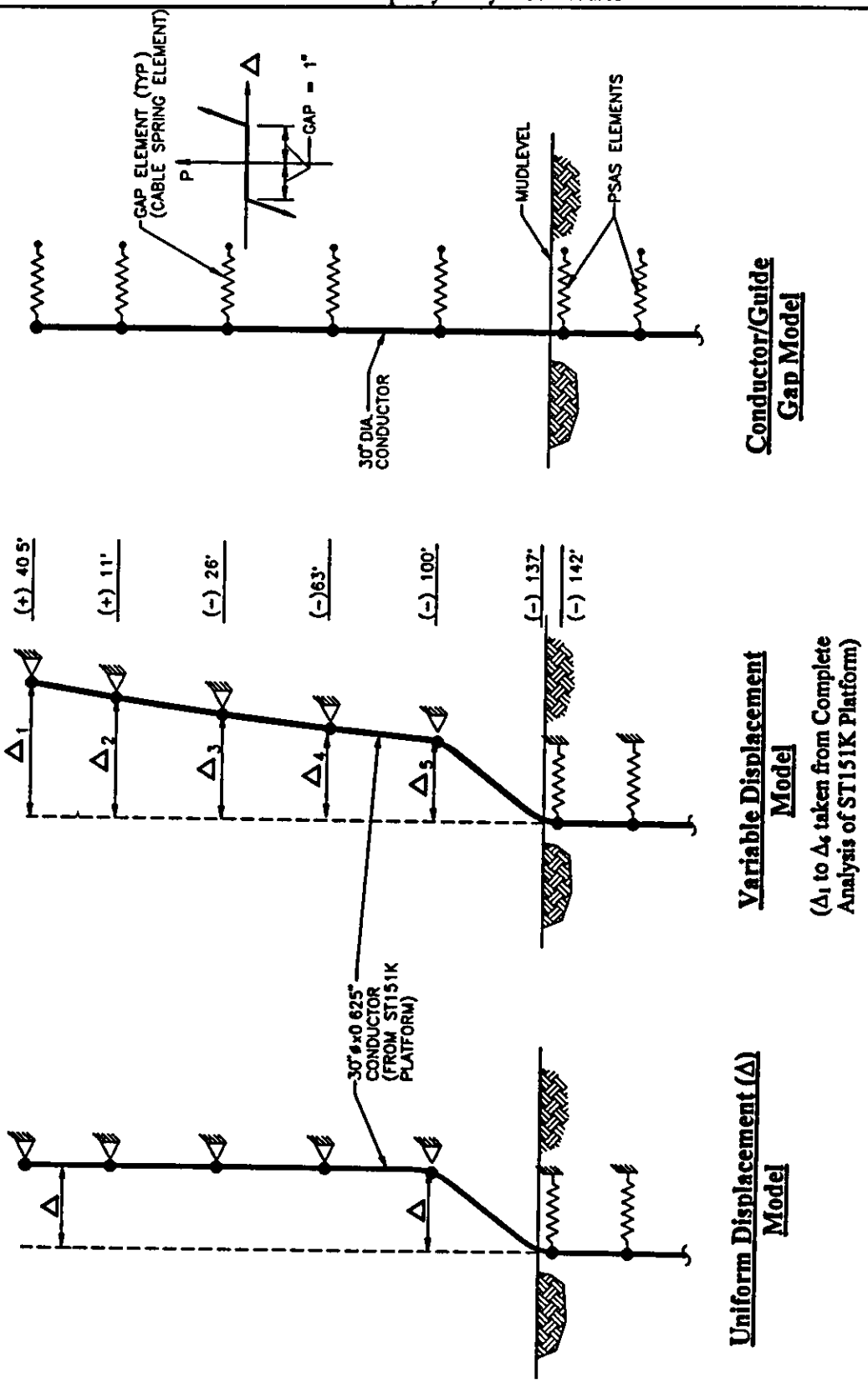

Figure 2-6: Conductor Model with No Guide at Mudlevel Framing

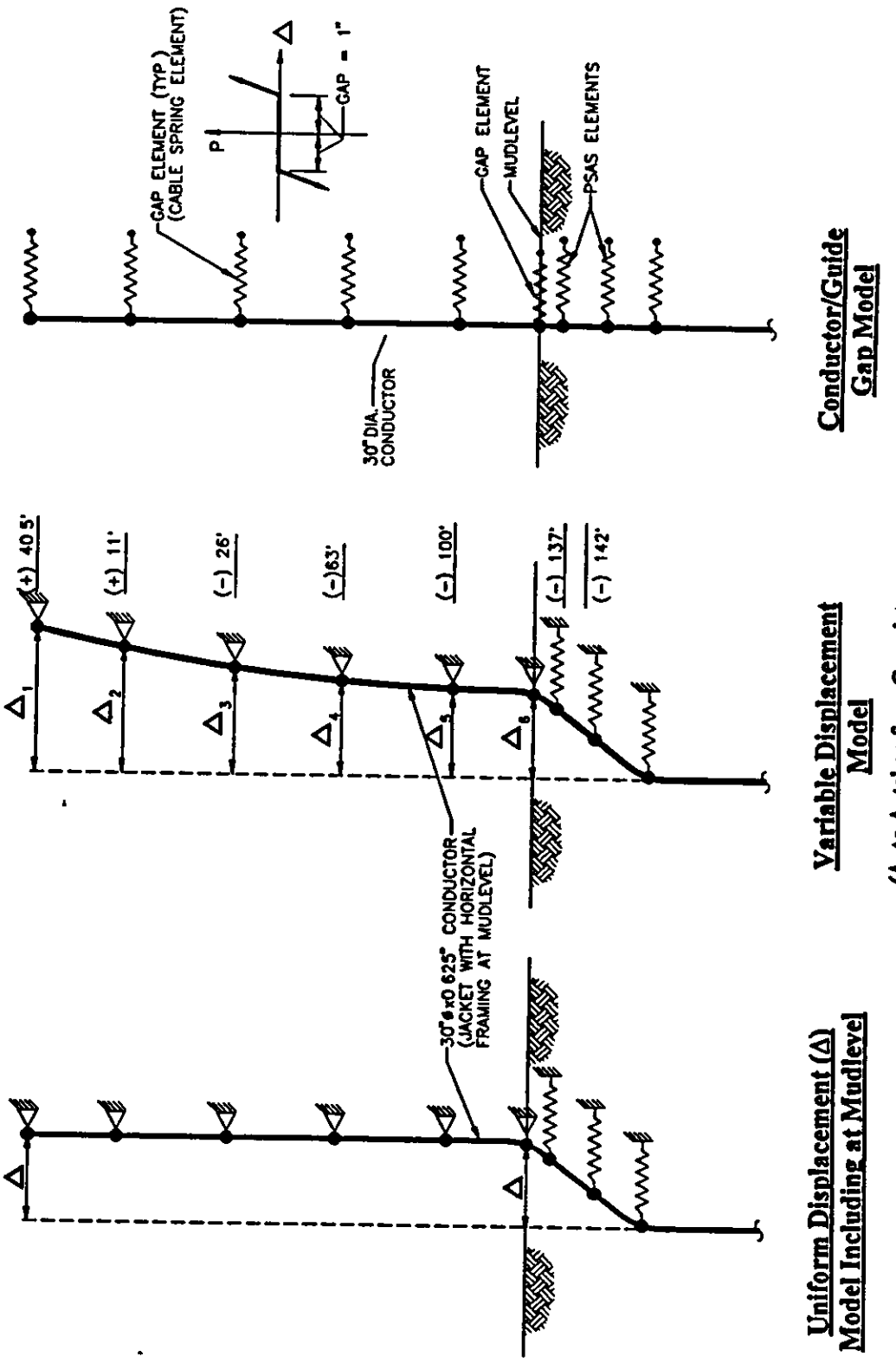

Figure 2-7: Conductor Model with Guide at Mudlevel Framing

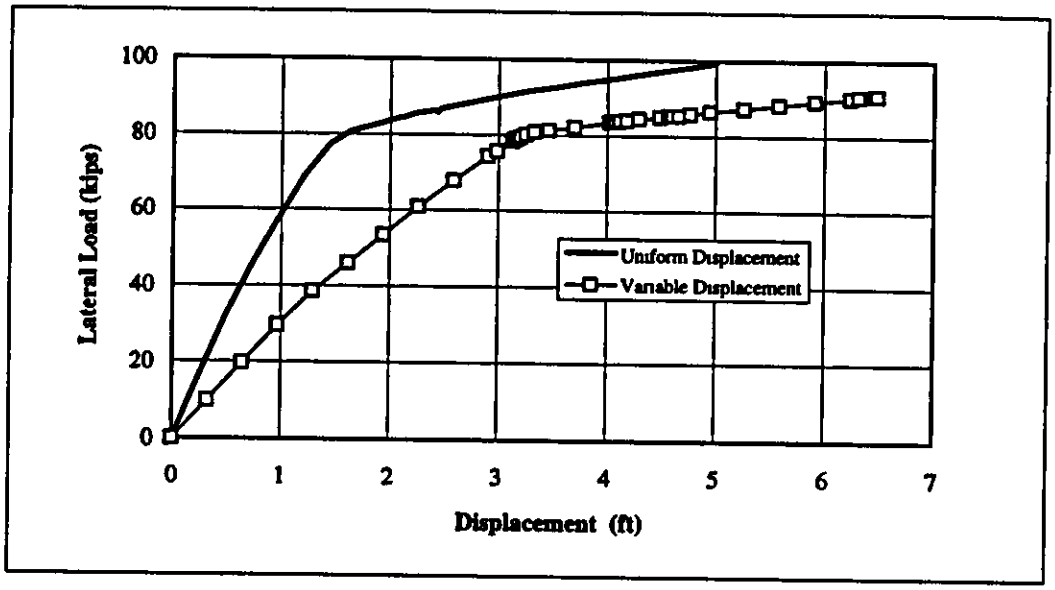

a): Conductor Model with No Guide at Mudlevel Framing

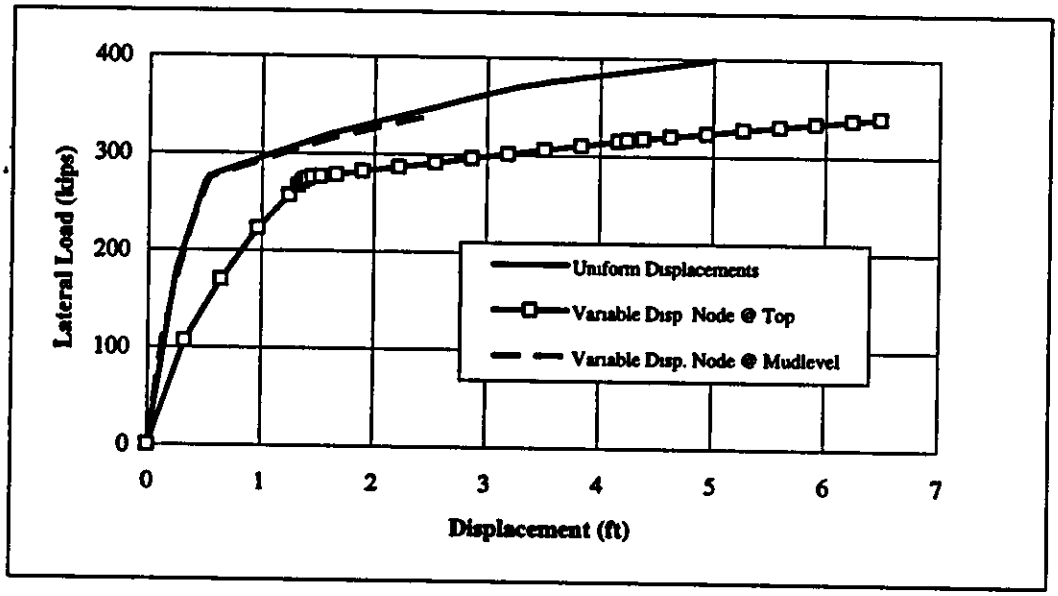

b): Conductor Model with Guide at Mudlevel Framing

Figure 2-8: Load - Displacement Behavior Comparison - Uniform vs. Variable Imposed Displacements (Conductor/Guide Gap Not Modeled)

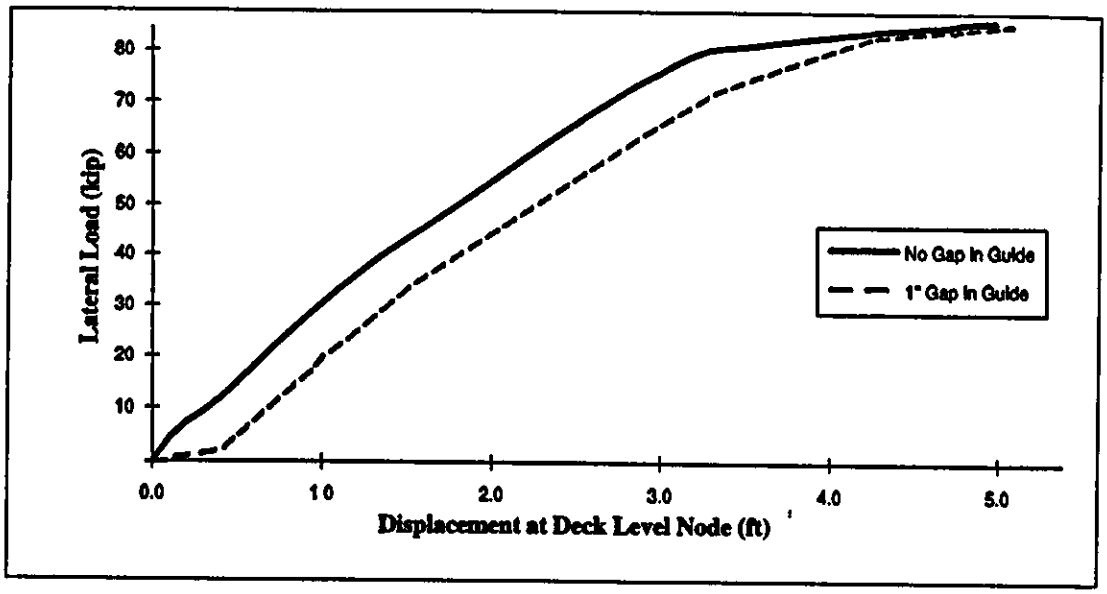

a): Conductor Model with No Guide at Mudlevel Framing

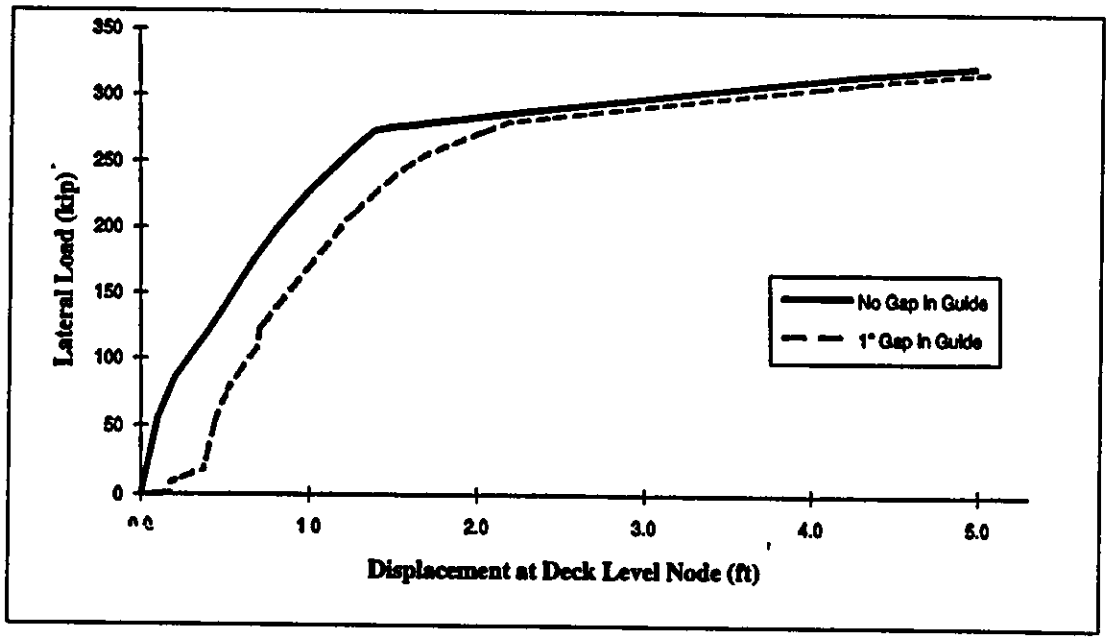

b): Conductor Model with Guide at Mudlevel Framing

Figure 2-9: Load - Displacement Behavior Comparison - Conductor/Guide Gap Model vs. No Gap Model

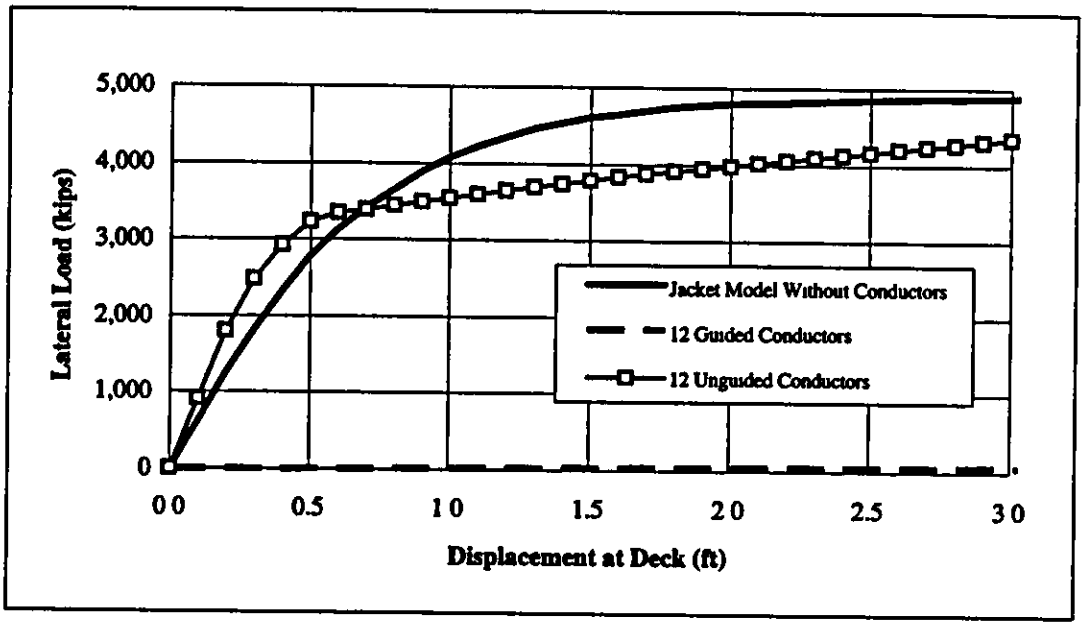

a): Uniform Imposed Displacements Case

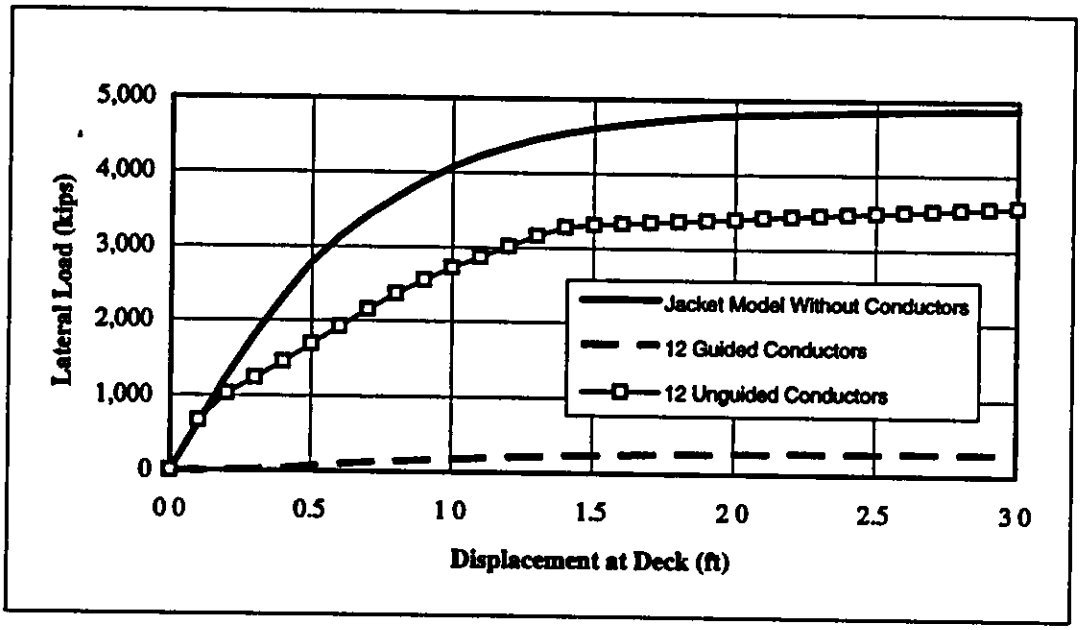

b): Variable Imposed Displacements Case

Figure 2-10: Load - Displacement Behavior for Conductor Strength (12 Number) vs. Jacket Strength

Table 2-1: Pushover Wave Load Pattern - Comparison of Results

Event Number	Event Description	Lateral Load from Pushover Analysis Using Variable Load Pattern (#1) (kips)	Lateral Load from Pushover Analysis Using Monotonic Load Pattern (#2) (kips)	%ge Difference (#2 compared to #1)
1	Failure of Bottom Bay K-Brace	3,235	3,380	4 48
2	First Yield of a Pile Section	3,700	3,700	0 00
3	Failure of Top Bay K-Brace	4,410	4,375	-0 79
4	Pile/Soil Axial Failure	4,765	4,815	1.05
5	Failure of Middle Bay K-Brace	4,905	4,940	0 71
6	Fully Plastic Section in a Pile	4,885	4,950	1.33

Section 3
Weighting Evaluation

3.1 OVERVIEW

One of the constraints of the Phase I and Phase II studies was that only a limited number of platforms were included in the calibration analyses. This sample size was restricted in both studies due to the limited resources (i.e., funding) available for the data collection and analysis, which represented the majority of the work performed. Another factor that affected the selection of platforms was that of the availability of information required for the analysis. Information was typically available for platforms that were owned by one of the sponsoring organizations, however, there were many platforms that would have been useful to the calibration but did not have information that could be accessed.

It was recognized at the conclusion of the Phase I study that the limited sample size affected the calibration in two ways. Firstly, the small sample size impacted the reliability analysis directly due to the statistical formulations involved (i.e., a greater sample size would reduce the COV of the resulting bias factors). A second effect that was generally considered to be more significant was that, with the limited number of platforms that could be selected, those that were used in the calibration were chosen based on their expected degree of impact on the bias factor. This selection criterion resulted in a sample that included a disproportionate number of platforms where damage or failure was observed. As summarized in Table 3-1, the 13 platforms that were included in the Phase I sample represented 25% of the observed damage and failure cases (combined) but just 1% of the survival cases. It was established during the Phase I study that this distribution resulted in conservative bias factor, however, the extent of this conservatism was unknown. A sensitivity study was therefore proposed for Phase II to address the effect of including a larger, more representative, population of platforms in the calibration sample.

3.2 PROCEDURE FOLLOWED

The method that was developed to assess the impact of a larger population of platforms involved making comparisons of platforms outside of the explicit sample set to those for which detailed analyses were performed The observations of this larger population of structures could then be used to scale the impact of, or "weight", the calibration results for individual platforms. This process was executed to extend the explicit sample set of 13 to include an additional 156 survivals so that the representation of survivals roughly equaled that of the damage and failure cases This extended sample set is summarized in Table 3-1.

The Phase I analysis indicated that platforms that were found to have surprising observations (e g , the analysis indicated that a failure was very likely but the platform was observed to survive without damage) had the greatest impact on the bias factors. It was therefore important to identify the "degree of expectedness" of all of the platforms within the survival classification (648) into the more specific categories (unexpected survival, expected survival and sure survival) This distribution was made based on an assessment of platform age and hindcast wave height. A more rigorous application of this process would include a distribution based on more specific physical data (e.g., number and size of legs and piles, bracing pattern, deck elevation, extent of damage and corrosion), however, such an effort was considered beyond the scope of the sensitivity study.

The platform survival database given in Appendix A of the Phase I report [1], which included significant wave heights to which platforms were subjected, was used to perform the classifcation. The Phase I database was based upon the MMS database and updated based on feedback from several participants. The results of this classification are provided in Table 3-2. The total population of 648 survivals were allocated into groups of 34 unexpected survivals, 147 expected survivals and 467 sure survivals.

Following the allocation of the extended population, each group of platforms in the survival category was matched to a single platform from the explicit sample set (13). Platforms ST130Q, WD90A and MC397 were selected as being most representative of the unexpected survival, expected survival and sure survival classifications. respectively. This selection is presented in Figure 3-1 which provides a comparison of the likelihood functions for survival platforms obtained from Phase I work [1] Three zones are identified in this figure based on the degree of expectedness of survival of the platforms. The allocation of the full population (648) was then factored by 25% to obtain the necessary number of platform for each category that would be consistent with the percentage of damaged and failure platforms in the sample. This distribution is summarized in Table 3-3.

3.3 RESULTS OF SENSITIVITY ANALYSIS

The effect of the extended sample set on the survival likelihood function is provided in Figure 3-2. These curves show the extent of change resulting from the addition of each of the categories of survivals separately as well as their total combined effect. These results show that the 6 additional unexpected survivals have the greatest impact on the likelihood function. The 35 expected survivals are shown to have an impact similar to that of the unexpected survivals while the 115 sure survivals are shown to have very little impact.

The effect of the extended sample set on the bias factor is summarized in Table 3-4. The results indicate that the global bias factor established during Phase I would increase from 1.19 to 1.40 (an increase of 18%) as a result of the full extended sample (i e , 156 additional survivals). The increase in bias factor resulting from the addition of each of the separate categories is also provided (Cases II, III and IV) to identify the relative contributions. The 35 additional platforms in the expected survival category produced the largest individual change to the bias factor which increased to 1.35 (an increase of 13%). The 6 platforms in the unexpected survival category increased the bias factor to 1.29 (an increase of 8%) and the 115 platforms in the sure survival category produced only a slight increase to 1.20 (an increase of (an increase of 1%).

An additional calculation was performed to assess the increase in the mean of the bias factor resulting from the addition of any number of unexpected, expected and sure survivals. The results of this analysis are provided in Figure 3-3. Each of these curves includes the effect of the original number (i.e., 7) damage/failure cases considered in the Phase I. These results show that the change in the bias factor is very much dependent upon the degree of "unexpectedness" of the survivals included in the sample.

The results of this sensitivity analysis indicate the bias factors determined using the explicit sample (13) from Phase I are likely to be somewhat conservative but not excessively so The results indicate that the addition of a number of expected and/or unexpected survivals in the sample would provide the greatest increase while a large number of sure survivals would produce a slight increase. This comparison is significant in that the process of a rigorous identification and classification of the sure survivals would require substantially less effort than that required for the expected and unexpected survivals. A complete and rigorous application of the weighting process on the Andrew survival population is therefore not considered practical due to the effort and physical data required to identify and classify the expected and unexpected survival platforms.

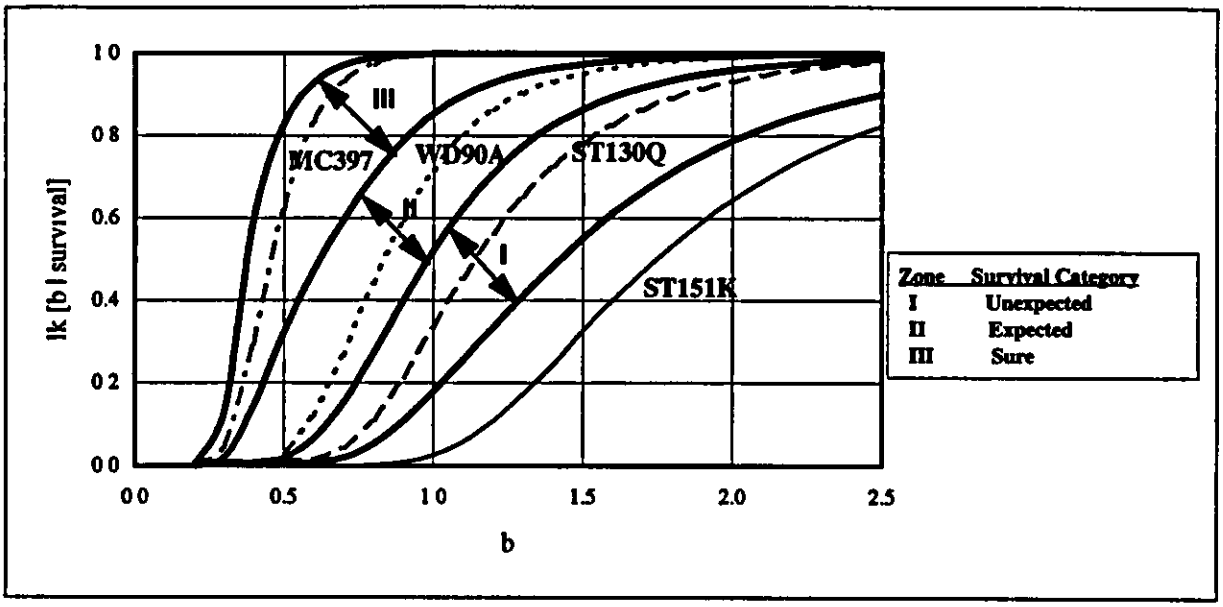

Figure 3-1: Likelihood Functions - Success Cases (from Andrew JIP - Phase I)

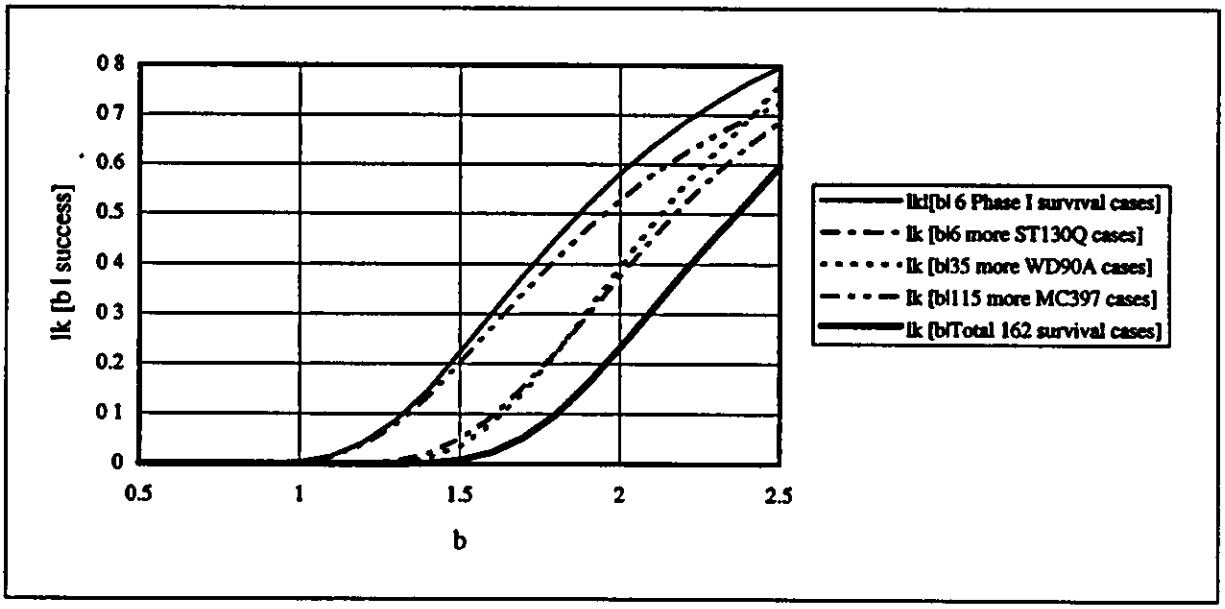

Figure 3-2: Likelihood Function Variation Due to Additional Survival Case

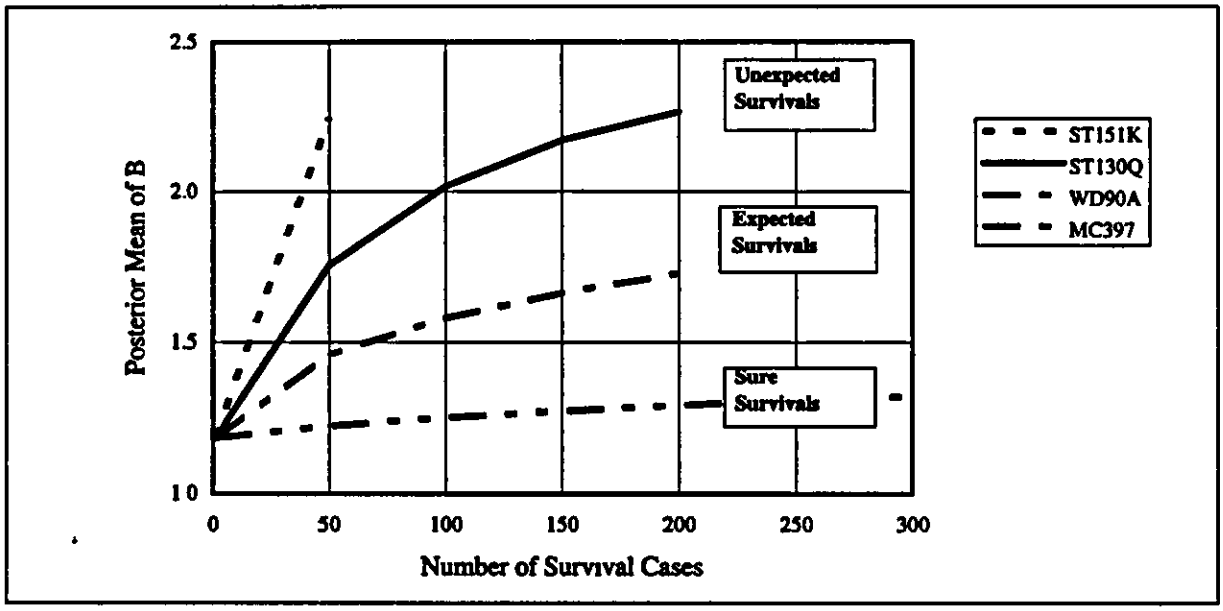

Figure 3-3: Variation in Mean of Posterior of B with Number of Survival Platforms Under Different Categories

	Classification			Total
	Survivals	Damaged	Failures	
Observations	648	14	14	676
Phase I Sample	6	3	4	13
Percentage	*1%*	*21%*	*29%*	*1.9%*
Extended Sample	162	3	4	169
Percentage	*25%*	*21%*	*29%*	*25%*

Table 3-1 Distribution of Platforms by Classification

		Unexpected Survivals			Expected Survivals			Sure Survivals	
	12							2	3
	11		10	16			2	5	5
H_s	10			8			7	4	6
(m)	9						9	6	4
	8						25	10	4
	7	16	20	29	25	42	37	23	13
	6	35	20	17	32	12	28	15	8
		upto 1959	1960-64	1965-69	1970-74	1975-79	1980-84	1985-89	after 1989

Year Installed

Table 3-2 Detailed Classification of Survival Platforms

Survival Category	Total Population	Extended Sample	Total Sample (explicit plus extended)	Representative Platform Type
Unexpected	34	6	8	ST130Q
Expected	147	35	37	WD90A
Sure	467	115	117	MC397
Total	**648**	**156**	**162**	

Table 3-3 Allocation of Extended Sample

Calibration Case	Description	Mean Value of Bias Factor	COV of Bias Factor
I	13 Phase I Platforms (includes 6 survivals)	1.19	0 10
II	Case I + 6 more unexpected survivals	1.29	0.09
III	Case I +35 more expected survivals	1.35	0.08
IV	Case I + 115 more sure survivals	1.20	0.09
V	Case I + 156 more survival cases	1 40	0.08

Table 3-4 Effect of Extended Sample on Bias Factors

Section 4
Capacity Analysis

4.1 APPROACH

Structural analyses were performed to establish the response characteristics of each of the 9 platforms selected for the calibration. These analysis defined response up to, and in some cases beyond, the point at which the ultimate lateral resistance (ultimate capacity) of the structure was obtained. All of the analyses utilized explicit nonlinear representations of the platform structure, piles and foundations based on the analysis recipe that was developed during the study (Reference Section 2) All analyses were performed using the CAP (Capacity Analysis Program) which has been developed and is licensed by PMB Engineering [23]

The type of analysis performed is typically referred to as "static pushover" and involves defining a representative profile of lateral forces (wind, wave, and current) acting on the platform (including any wave forces acting on the deck) and then applying this profile with incrementally increasing amplification factors until the platform's ultimate capacity is defined. The ultimate capacity of the platform can then be used to estimate the wave height that would induce platform collapse or it can be compared with the loads due to any reference level loading (e g , the 100-year return period wave) to determine the platform's reserve strength ratio (RSR).

The lateral load applied to the platform was monitored during the pushover to establish the load at which key response states occur. The results of these analyses were used to determine the predictions of lateral loads associated with successive inelastic events (failures) in elements, and to determine the ultimate capacity of jacket and its foundation.

4.1.1 Specific Failure Modes

The results of these analyses were used in the calibration study to determine bias factors specifically for the jacket, lateral foundation and axial foundation components. The definition of component specific bias factors made it necessary to establish the platform capacities associated with failure mechanisms developed in each of the three areas. The failure modes and mechanisms in the jacket frame and the foundation system were therefore isolated to establish component specific ultimate capacity and to eliminate the effects of uncertainties in the modeling of one component on the definition of the capacity associated with another. A total of four analyses were therefore performed for each steel jacket platform to obtain uncoupled estimates of platform capacity for specific failure modes, using the following models:

- Base Case analysis

  This analysis was performed to establish the expected mode of failure based on the best estimate of the physical properties and local response characteristics of all of the components of the structure. All components (jacket elements, piles and supporting soils) that could potentially contribute to a failure mechanism of the platform were represented to capture their elastic and inelastic response.

- Case 1 analysis (foundation failures suppressed)

  This analysis was performed to estimate the ultimate capacity of the platform associated with jacket structure failure modes (local failure and inelasticity in the braces, joints, horizontals and legs). This analysis was completed by suppressing any inelastic behavior in the pile and soil elements The model included a nonlinear of the jacket and a linear model of the foundation. The effects of uncertainties associated with the modeling of the strengths and stiffnesses of pile and soil-pile interaction (p-y, t-z and q-z) elements were eliminated. The analysis therefore defined an uncoupled estimate of the ultimate capacity of the platform as controlled by jacket frame failure modes.

- Case 2 analysis (jacket and axial foundation failures suppressed)

  This analysis was performed to estimate the ultimate capacity of the platform associated with the pile yielding/hinging mechanism. This analysis was completed by suppressing any inelastic behavior in the jacket and by limiting inelastic behavior in the axial soil-pile interaction elements to the extent that pile axial failure could not occur. The effects of uncertainties associated with the modeling of strengths and stiffnesses of jacket and axial soil-pile interaction elements were eliminated. This analysis therefore defined an uncoupled estimate of the ultimate capacity of the platform as controlled by lateral foundation failure modes

- Case 3 analysis (jacket and lateral foundation failures suppressed)

  This analysis was performed to estimate the ultimate capacity of the platform associated with a pile plunging/pullout failure mechanism. This analysis was completed by suppressing any inelastic behavior in the jacket and pile elements and by limiting inelastic behavior in the lateral soil-pile interaction elements to the extent that pile lateral failure could not occur. The effects of uncertainties associated with the modeling of strengths and stiffnesses of jacket, piles and lateral soil-pile interaction elements were eliminated. This analysis therefore defined an uncoupled estimate of the ultimate capacity of the platform as controlled by axial foundation failure modes.

4.2 HINDCAST DATA

The updated hindcast developed by Oceanweather [13] was used to define the loading conditions for the capacity analysis The hindcast provided wave heights, currents, wind velocities and directions at specific grid points for the significant period of the storm. This data was analyzed to generate metocean data for each of the platform locations. A summary of the resulting information is provided in Appendix A. A summary of the procedure used to generate the metocean data for the specific platform locations is provided in Appendix D along with excerpts of the Oceanweather report. The wave heights that were generated from the updated hindcast were found to differ from those generated from the previous hindcast [12] that was used in the Phase I work [1]. The new hindcast was developed using a finer grid and utilized improved surface wind and wave models.

The change in the hindcast data was found to be a very important contributor to the accuracy of the calibration.

A review of the wave height and current information indicated that the most intense portion of the storm occurred within a 3 to 5 hour segment. The wave heights and currents for time segments outside of this range were of substantially reduced intensity and were therefore not expected to effect the calibration. The variation in storm direction during these 3 to 5 hour segments was found to be less than 20 degrees, which indicated that it would be adequate to perform capacity analysis for only one direction This was supported by the findings of the Phase I study which showed that the dominant contribution to the probability of failure typically came from the maximum wave within the storm and that lesser waves in other directions (±22.5 degrees) had little or no effect on failure probability. Capacity analysis were therefore performed for only one storm approach direction for each platform. The wave direction for the storm hour with the maximum wave height was selected. The orientations of the platforms (from True North) and the storm directions analyzed for each platform are given in Appendix A.

4.3 ANALYSIS MODELS

A schematic representation of the element types used for the capacity analysis is shown in Figure 4-1. A fully coupled nonlinear jacket-pile-soil model was developed for each platform using the distribution of element types·

- **Deck** - The deck structures were modeled with the objective of providing an accurate distribution of gravity, wind and deck wave inundation forces amongst the supporting jacket legs. The deck structures were not expected to experience inelastic behavior or participate in the development of failure mechanisms and, therefore, most of the deck structural members were modeled with linear elements Secondary deck structural elements were not modeled explicitly but were included in terms of their contribution to gravity, wind and wave load. The deck legs were modeled as nonlinear beam-column elements.

- **Jacket Legs and Piles** - The jacket legs and piles were modeled with explicit nonlinear beam-column elements. These elements are defined with a three dimensional failure surface (i e., axial, in-plane and out-of-plane bending). The load deformation behavior of the elements (P-δ and M-θ) utilize a tri-linear formulation that is set based on initial outer fiber yield and full plasticity.

- **Braces** - The selection of the element type used to model the braces was based on the calculated mode of failure of the brace and its connections The joint capacities were checked using a conservative formulation and compared to capacities of the corresponding braces. The axial capacity of the diagonal braces (leg-to-leg) was never limited by joint strength and these members were therefore modeled with axial struts to capture the buckling and post-buckling behavior of the brace. The joint capacity limited brace strength for some of the K-braces and, in these instances, the brace-joint system was modeled using a modified beam

column element (Fiber Element) which represented the strength and stiffness of both the joint and the brace. The horizontal braces near the mudline and waterline were checked to assess their likely mode of failure (i.e., axial buckling or plastic hinge development) and were modeled with struts or nonlinear beam-columns. In most instances the mudline horizontals were modeled with beam columns (see Section 2 for additional details).

- **Joints** - The joints were modeled where the joint capacities were lower than the brace capacity estimates. In general, the capacities of K and KT joints without can sections were lower than the brace capacity (buckling) for the platforms investigated in the study. The K, KT, and X joints strengths and stiffnesses were modeled with a Fiber element which represented the brace and joint response characteristics The joints which were modeled this way are identified in Appendix C.

- **Conductors** - The conductors were always modeled to capture their contribution to wave load and p-delta. The conductors were also modeled to include their contribution to foundation lateral capacity (i.e., modeled as piles) in situations where:

    1) The conductors were guided at the mudline
    2) Initial analysis predicted pile yield/hinge failure modes

  This situation only occurred for the ST130A platform in which the conductors were modeled with nonlinear beam column elements. The conductors were modeled using wave load elements (i.e., non-structural beams with wave load properties) for all other platforms.

- **Soils** - The soil-pile interaction (i.e., p-y, t-z, and q-z) was modeled using the PSAS (pile-soil analysis system) suite of elements included in the CAP program. These elements include a nonlinear representation of each mode of response which, in this study, was based on API RP 2A recommend formulations. The static API RP 2A capacities were modeled for both p-y and t-z springs (see Section 2.1 for discussion).

4.4 ANALYSIS RESULTS

The pushover analysis results for the nine steel jacket platforms are summarized in Tables 4-1 to 4-3. The capacity analysis results for three caissons are provided in Table 4-4 (results taken from the API/MMS Foundation Study [5]). The wave approach direction, and associated wave height and current for the storm hour with maximum wave height are provided in Table 4-5. The analysis was performed for this approach direction [see Appendix A for details].The information found in columns of Tables 4-1 to 4-4 is organized as follows:

- **Background Information** - The first three columns describe the general information and physical characteristics of platforms. The jacket and pile configurations, and soil shear strength profiles are provided in Appendix A.

- **Analysis Cases** - Each jacket platform was analyzed for several cases to determine the capacity of the platform as controlled by failure mechanisms within the jacket and foundation. The caissons were analyzed using the basic shear strength profile, increased soil shear strength, or with the intermittent thin sand layer ignored.

- **Expected Maximum Hindcast Base Shear** - An estimate of the expected maximum lateral loads during Andrew based on the maximum hindcast wave height (H_{max}) and associated seastate parameters

- **Base Shear at Failure of First Component** - The lateral load levels at which the initial inelastic events (brace buckling, joint failures, yielding/hinging or plastification of pile sections, axial pile/soil failures) were predicted.

- **Base Shear at Failure of Multiple Components** - The lateral load level at which multiple inelastic/failure events occurred in each component type (brace/joint, pile, or soils).

- **Ultimate Capacity of Platform** - The load level at which the platform is considered to have no additional lateral load carrying capacity. The ultimate capacity was considered to have been achieved either when a definitive peak in the resistance-deformation curve was obtained or when the global stiffness of the platform was reduced to a very low value and the displacements at the deck level were in excess of 5 ft.

- **Collapse Modes** - The primary events and failure modes predicted from static pushover analysis.

  Jacket Platforms - Jacket frame failure was typically initiated by the failure of K-joints and braces followed by yield/hinge formation in the legs. Pile foundation failure was indicated by fully plastic hinge formation in multiple piles at one or two depths below mudline. Pile pullout/plunging failures was indicated by the mobilization of full resistance of the q-z spring and all t-z springs for a pile. The detailed load-displacement results and the specific location of inelastic events is presented in Section 4.4.1.

  Caisson Platforms - Failure is indicated by the development of full plasticity at some depth below the mudline. The collapse state is reached when local buckling is initiated in the plastic section.

- **Ratio of Ultimate Capacity (R_u) to Expected Maximum Lateral Loads During Andrew (S)** - Provides a deterministic comparison of the platform capacity with the lateral load estimate.

- **System Factor** - Provides an estimate of the platform capacity beyond the load level associated with the first event. This is computed as the ratio of the ultimate capacity to the load level at the inelastic event in the first element (including first yield of a pile section).

- **System Factor (Pile Lateral Capacity)** - Provides an estimate of the platform capacity beyond the load level associated with the development of full plasticity in the first pile. This is computed as the ratio of the load level at which full plasticity (hinge formation) occurs in multiple piles to the load level at which full plasticity occurs in one pile.

- **System Factor (Pile Axial Capacity, Jacket Platforms only)** - Provides an estimate of the platform capacity beyond pullout or plunging of the first pile. This is computed as the ratio of the load level at which pullout or plunging occurs for multiple piles to the load level corresponding to pullout or plunging of the first pile.

4.4.1 Steel Jacket Platforms

In general, the predicted failure modes varied from failure of K and KT joints, buckling of diagonal braces, full plasticity of horizontal brace sections, yielding/hinging of leg sections for the jacket, yielding/hinging of pile sections at one or two levels (at mudline and some depth below), and pullout/plunging of piles.

Significant differences in the ultimate capacity estimates were noted for some platforms by suppression of some failure modes. Therefore, it is beneficial to perform several analysis (Base Case to Case 3 analysis) to estimate the range of ultimate capacities based on deterministic characterization (mean estimates) of individual element capacities

The analysis did not include some secondary effects such as local buckling of the beam column elements at large deformations. The results of these analyses were examined to determine if these effects would limit the ultimate capacity. Therefore, in some cases the load-displacement curves indicate greater capacities than those have been summarized in the tables.

Survival Platforms (Table 4-1).

ST151K

This platform experienced minor damage as a result of Andrew. The most extensive damage that was recorded during post-hurricane field inspections was that of flooding of some horizontal braces near mudlevel. The hindcast estimated a maximum wave height of 59.05 feet for this location which resulted in a total peak metocean loading of 3,700 kips.

The analysis determined a Base Case ultimate capacity of 3,800 kips which was limited by the development of a mechanism in the base of the jacket. The load-displacement results for the Base Case analysis are provided in Figure 4-2-a and the inelastic events occurring up to the ultimate capacity are shown in Figure 4-2-b. The analysis predicted that the K and KT joints in the lower two bays of the structure would fail at approximately 3,000 kips of lateral load followed immediately by yielding of horizontals. Pile pullout was predicted at 3,450 kips and fully plastic

pile sections between 3,570 and 3,700 kips. The Base Case analysis predicted that significant damage should have occurred for load levels below that corresponding to the maximum wave height. Initial joint failure was predicted to occur at 2,900 kips which is 22% less than the maximum load. The inspections of this platform revealed no damage of the elements that were predicted to fail. The analysis is therefore conservatively biased.

The load-displacement results of the Phase I analysis are also presented in Figure 4-2-a as a means of comparison of the Phase I and II analysis recipes.

ST130Q

The inspections revealed that this platform experienced no damage during Andrew. The hindcast estimated a maximum wave height of 58.29 feet for this location which resulted in a peak metocean loading of 990 kips. The analysis determined a Base Case ultimate capacity of 1,430 kips, which was limited by development of a mechanism in the pile foundation by formation of fully plastic sections. The load-displacement results for the Base Case analysis are provided in Figure 4-3-a and the inelastic events occurring up to the ultimate capacity are shown in Figure 4-3-b. The analysis predicted that first yield in pile sections would occur at 800 kips and fully plastic pile sections would develop between 1,010 kips to 1,380 kips. The analysis predicted some damage to the foundation.

The Case-1 analysis predicted yielding of leg sections at 955 kips and that the KT joints in the bottom bay would fail at approximately 1,380 kips, which is 39 % higher than the maximum load. The analysis predicted no damage to the jacket

WD103A

This platform experienced no damage during Andrew. The hindcast estimated a maximum wave height of 50.21 feet for this location which resulted in a peak metocean loading of 2,140 kips. The analysis determined a Base Case ultimate capacity of 4,660 kips, which was limited by development of a mechanism below the mudline by formation of fully plastic sections in legs and piles. The load-displacement results for the Base Case analysis are provided in Figure 4-4-a and the inelastic events occurring up to the ultimate capacity are shown in Figure 4-4-b. The analysis predicted that first yield in pile sections would occur at 3,880 kips and fully plastic pile sections would occur at 4,660 kips, which is more than twice of the maximum load. The analysis predicted no damage to the platform and a sure survival.

<u>Damaged Platforms (Table 4-2):</u>

ST151J

The platform ST151J strengthened with two tripods is shown in Figure 4-5-a. The jacket configuration for this platform is similar to ST151H and ST130A (see Appendix A), provided with single batter legs, which both failed during Andrew. ST151J was damaged during Andrew,

with the damage limited to buckling and yielding of diagonal braces in the lower two bays (see figure in Appendix A). The hindcast estimated a maximum wave height of 58.77 feet for this location which resulted in a total peak motocean loading of 4,450 kips.

The analysis determined a Base Case ultimate capacity of 5,000 kips which was limited by pullout and plunging of several piles in the jacket and tripod, and development of fully plastic sections in the piles and at jacket-tripod connections The load-displacement results for the Base Case analysis are provided in Figure 4-5-b and the inelastic events occurring up to the ultimate capacity are shown in Figure 4-5-c. The analysis predicted initial pullout of piles at 3,460 kips, which is 22 % lower than Andrew loads, followed by failure of several diagonal braces, and KT joints between 3,750 kips to 4,520 kips. The Base Case analysis predicted more damage than were observed in the post-Andrew inspections, thus it was conservatively biased.

Case 1 analysis predicted buckling of 3 braces and yielding of 1 brace starting at 4,640 kips, which is 4 % higher than the maximum loading. These failures were observed in the inspections. Thus, the analysis in Case 1 is marginally unconservative and the predictions of brace buckling and yielding behavior are closer than the Base Case analysis. Up to 5,100 kips, the analysis also predicted failure of one KT joint in the bottom bay, which was not observed.

A comparison of Case 1 ultimate capacity of 5,800 kips with the Base Case ultimate capacity of 5,000 kips indicate that the lower load at failure of braces in the Base Case is influenced by initial pullout and plunging of piles at 3,460 kips Therefore a conservative bias in estimates of pullout and plunging of piles would influence the predictions of damage and platform capacity.

ST177B

This platform experienced significant damage as a result of Andrew. The damage that was recorded during post-hurricane field inspections consisted of failure of K, KT, and X joints, and yielding of legs at lower bays where K joints were completely severed (see Table 1-3 for details). This platform was later salvaged. The hindcast estimated a maximum wave height of 59.60 feet for this location which resulted in a total peak metocean loading of 4,390 kips.

The analysis determined a Base Case ultimate capacity of 3,800 kips which was limited by pullout and plunging of several piles, and development of fully plastic sections and local buckling in a pile. The load-displacement results for the Base Case analysis are provided in Figure 4-6-a and the inelastic events are shown in Figure 4-6-b. The analysis predicted pullout and plunging of six piles in the 3,200 kips to 3,700 kips load range, which is followed by inelastic events in several K, KT and X joints starting at loading of 3,850 kips, which is 12% lower than the maximum load. The Base Case analysis predicted more damage than were observed in the post-Andrew inspections, thus it was conservatively biased.

Case 1 analysis predicted initiation of failure of KT joints in the bottom bay at same loading as for the Base Case, but due to elimination of pile failure events the ultimate capacity of the platform is 6,000 kips, which is 58 % higher than the Base Case estimate. All of the observed

damage was predicted at 4,000 kips load, which is 9 % lower than the maximum estimated Andrew load. The analysis is therefore marginally conservative.

The Case 1 to Case 3 analysis predicted initial failures (joint or pile yield or pile pullout) at same loads as in the Base Case for respective elements The ultimate capacity estimate of 3,800 kips was the same for both Base Case and Case 3. The Case 1 ultimate capacity was predicted as 6,000 kips, which is 37% higher than the maximum load. The ultimate capacity for Case 2 is 4,700 kips, which is marginally higher than maximum load. The analysis indicated conservative bias in foundation capacity estimates.

The platforms ST151K and ST177B have identical jacket configuration, but their Case 1 ultimate capacity estimates are 3,880 kips and 6,000 kips respectively. The significant difference in jacket frame capacities for these two identical platforms is largely due to the differences in their orientations and wave approach directions, which lead to differences in loading on the tendon frames with weaker K, KT, and X joints. Platform ST177B is oriented 20 degree more westward compared to ST151K and the approach directions of the maximum waves for the two platforms differ by 5 degree. Due to these reasons, the first KT joint fails at 2,900 kips for ST151K platform and at 3,900 kips for ST177B platform.

SS139 (T25)

This platform experienced significant damage as a result of Andrew. The damage that was recorded during post-hurricane field inspections consisted of failure of K and KT joints (see Appendix A for details). This platform was later salvaged. The hindcast estimated a maximum wave height of 43.50 feet for this location which resulted in a total peak metocean loading of 1,060 kips.

The analysis determined a Base Case ultimate capacity of 1,640 kips which was limited by development of fully plastic sections in piles and failure of a K-joint in the middle bay. The load-displacement results for the Base Case analysis are provided in Figure 4-7-a and the inelastic events occurring up to the ultimate capacity are shown in Figure 4-7-b. The analysis predicted all observed damage to occur up to 1,640 kips, the load level at the ultimate capacity. The failure of first K-joint occurred at 1,230 kips, which is 16 % higher than the expected maximum load. The analysis is therefore unconservative.

Failure Platforms (Table 4-3):

ST151H

This platform collapsed as a result of Andrew. The platform was know to have rubbled and explicit damage details were not known. The hindcast estimated a maximum wave height of 59 05 feet for this location which resulted in a total peak metocean loading of 3,560 kips.

The analysis determined a Base Case ultimate capacity of 3,250 kips which was limited by the development of a mechanism in the base of the jackets. The load-displacement results for the Base Case analysis are provided in Figure 4-8-a and the inelastic events occurring up to the ultimate capacity are shown in Figure 4-8-b. The analysis predicted that the K and KT joints in the lower bays of the structure would fail at approximately 3,240 kips of lateral load, which is preceded by pullout of one pile at 3,140 kips. The Base Case analysis predicted that significant damage should have occurred for load levels below that corresponding to the maximum wave height. Initial joint failure was predicted to occur at 2,680 kips which is 25% less than the maximum load. The analysis predicted collapse of the platform due to jacket failure.

ST130A

This platform collapsed as a result of Andrew. The platform is know to have collapsed due to yielding of legs and the inspections indicated that the leg failure may have occurred before pile. Complete details of damage to this platform were not known. The hindcast estimated a maximum wave height of 55.43 feet for this location which resulted in a total peak metocean loading of 1,990 kips.

The analysis determined a Base Case ultimate capacity of 1,830 kips which was limited by the development of a mechanism in the pile and leg sections due to development of fully plastic sections. The load-displacement results for the Base Case analysis are provided in Figure 4-9-a and the inelastic events occurring up to the ultimate capacity are shown in Figure 4-9-b. The analysis predicted that development of fully plastic section in the first pile would occur at 1,720 kips, which is 14 % lower than the maximum load.

The Case 1 analyses indicated that initially a brace would buckle at 2,000 kips but thereafter all 8 legs would develop fully plastic sections up to 2,200 kips, which is 10 % higher than the expected maximum load.

A comparison of the Base Case and Case 1 analysis indicate that the analysis predictions are very close to observations.

ST72 (T21)

This platform collapsed as a result of Andrew. No information was available where the damage occurred. The hindcast estimated a maximum wave height of 46.90 feet for this location which resulted in a total peak metocean loading of 1,380 kips

The analysis determined a Base Case ultimate capacity of 1,610 kips (17% higher than the maximum load) which was limited by the development of a mechanism in the bottom two bays. The load-displacement results for the Base Case analysis are provided in Figure 4-10-a and the inelastic events occurring up to the ultimate capacity are shown in Figure 4-10-b. The analysis predicted that first KT joint would fail at 1,250 kips, which is 10% lower than the maximum load. The Case 2 analysis predicted first yield in a pile section at 2,110 kips, which is 53% higher

than the maximum load. The analysis predicted that the jacket structure was weaker than its foundation.

4.4.2 Caisson Platforms

The capacity analysis results for three caisson platforms are given in Table 4-4, which were taken from the API/MMS Foundation Study [5] The 3-D non-linear analysis model used for the analysis of caissons is shown in Figure 4-11. The caisson information was used in the calibration work to determine the sensitivity of the foundation lateral bias factors resulting from the addition of structures that experienced foundation failures.

The capacity analysis results indicate that the Andrew load level was higher than the ultimate capacity for caissons SPelto 10 and SS135. The capacity estimate of SS136 was 60 percent higher for the basic shear strength case, and was 30 percent higher for the case with intermittent sand layer ignored. The results for the case which ignored the sand layer were used in calibration.

4.5 COMPARISON OF PHASE II AND PHASE I RESULTS

There were seven platforms that were included in both the Phase I and Phase II studies. The results of the analyses of these platforms are compared below. An overview of the differences between the Phase I and Phase II studies is provided as follows:

- Information from detailed inspections (including MPI) performed for several of platforms became available after the Phase I work. This information provided the basis for the selection of more precise calibration conditions.
- Improved information on the number of conductors, boat landings, etc. on the platforms was obtained for the Phase II study.
- Site-specific geotechnical information for most platforms was obtained for the Phase II study.
- A new hindcast (1994) with improved physics and numerical models was performed following the Phase I study.
- Improved procedure for joint modeling, including effect of joint stiffness, was incorporated into the Phase II analysis recipe.
- A variable pushover load profile was used for the Phase II analysis.

Platform Data:

Site specific soil reports were obtained for six platforms. Soil data from adjacent blocks were used for ST177B, ST130A and ST130Q.

The 1993 field inspections of ST151K indicated that there was only one boat landing and that only 12 of the planned 16 conductors were in-place. The Phase I analysis included 2 boat landings and 16 conductors.

The 1993 salvage of platform ST177B provided detailed damage information that lead to its re-classification as a damaged platform. The Phase I calibration was based on a failure classification of this platform.

Hindcast Data

Comparisons of the maximum wave heights, associated wave approach directions and current speeds from two Andrew hindcasts [12, 13] are provided in Table 4-5 and Figure 4-12 for the common platforms. The 1994 hindcast wave heights were 1% (ST177B) to 14% (SS139) lower than those of the 1992 hindcast. The wave approach angles changed by 2.5 (ST130Q) to 30.7 degrees (ST72). The largest changes in wave height and direction occurred for the platforms located in shallow water. The current speeds were reduced from 3% (ST130Q) to 16% (ST130A). Current speeds were reduced for all but two platforms. In these other two cases the current speed increased from 5% (SS139) to 20% (ST177B).

Expected Maximum Lateral Loads:

A comparison of the expected maximum base shear for seven platforms investigated in both Phase I and Phase II is given in Table 4-6 and Figure 4-13. The total effect of 1994 hindcast was a reduction in expected maximum lateral loads (base shear) of 15% (ST177B, ST151H, ST72) to 37% (SS139) from those that were based on 1992 hindcast. The large reduction in the expected maximum base shear for platform ST151K was due to the combined effect of the following factors:

- 3% reduction in the maximum wave height
- Reduction in the wave-in-deck load estimate from 930 kips to 340 kips
- Number of conductors reduced from 16 to 12
- Reduction in the conductor shielding factors

Ultimate Capacity Estimates:

The Phase II ultimate capacities for the seven common platforms are provided in Table 4-6 and Figure 4-13. On average, the ultimate strengths calculated were 6% than those determined during the Phase I study. The Phase I to Phase II capacity ratios were in the range of 0 81 to 1.22.

The ultimate capacity results for the Base Case analysis (all failure modes included) indicate higher capacity predictions for platforms ST151K, ST130Q, and SS139 by 10% to 20% of the Phase I estimates. Whereas, for platforms ST177B, ST151H, and ST130A, the Phase II capacity estimates are lower by 10% to 20% of the Phase I estimates.

Ratios of Ultimate Capacity to Expected Maximum Base Shear:

A comparison of the Phase II - Base Case ratios with the Phase I indicated higher ratios for all survival and damaged platforms in the Phase II analysis. The ratios were higher by 40% for survival cases and by 7% to 95% for damage cases, and were lower by 16% for failure cases. On average, the ultimate capacity to the base shear ratios were 22% higher than the Phase I results with a range of ratios between 0.85 to 1.95. Note that some differences in the ultimate capacity estimates were due to differences in the wave approach directions in the two hindcasts.

These results indicate that the capacity analysis using the updated recipe and procedures (Section 2.2) provided better predictions of the platform behaviors during Andrew primarily due to explicit joint strength and stiffness modeling and a general reduction in the Andrew load levels estimated using new hindcast. A comparison of the Base Case and "failure mode specific" analyses provided very useful insight regarding the expected modes of failure.

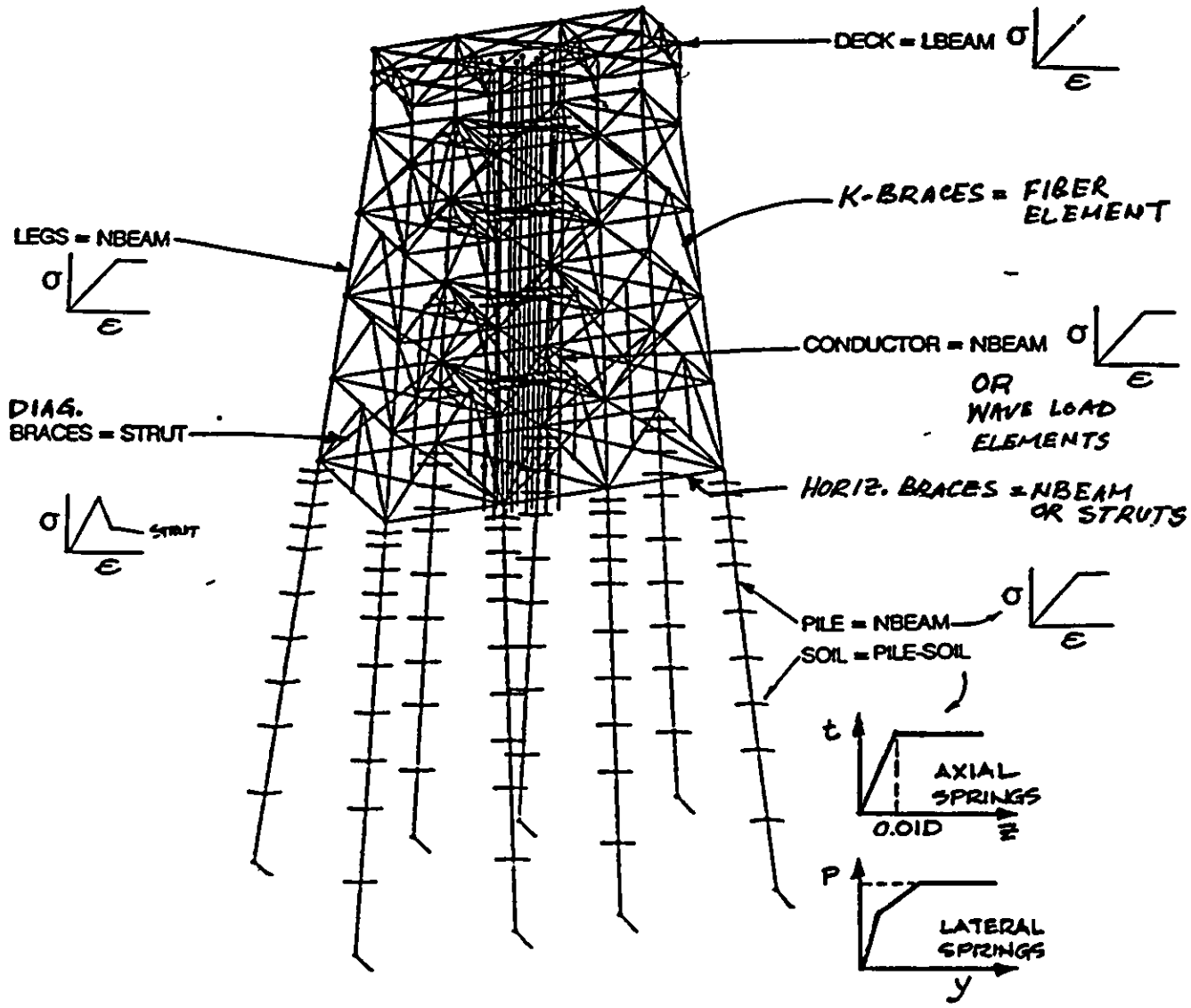

Figure 4-1: Nonlinear Analysis Computer Model - 8 Leg Steel Jacket Platform

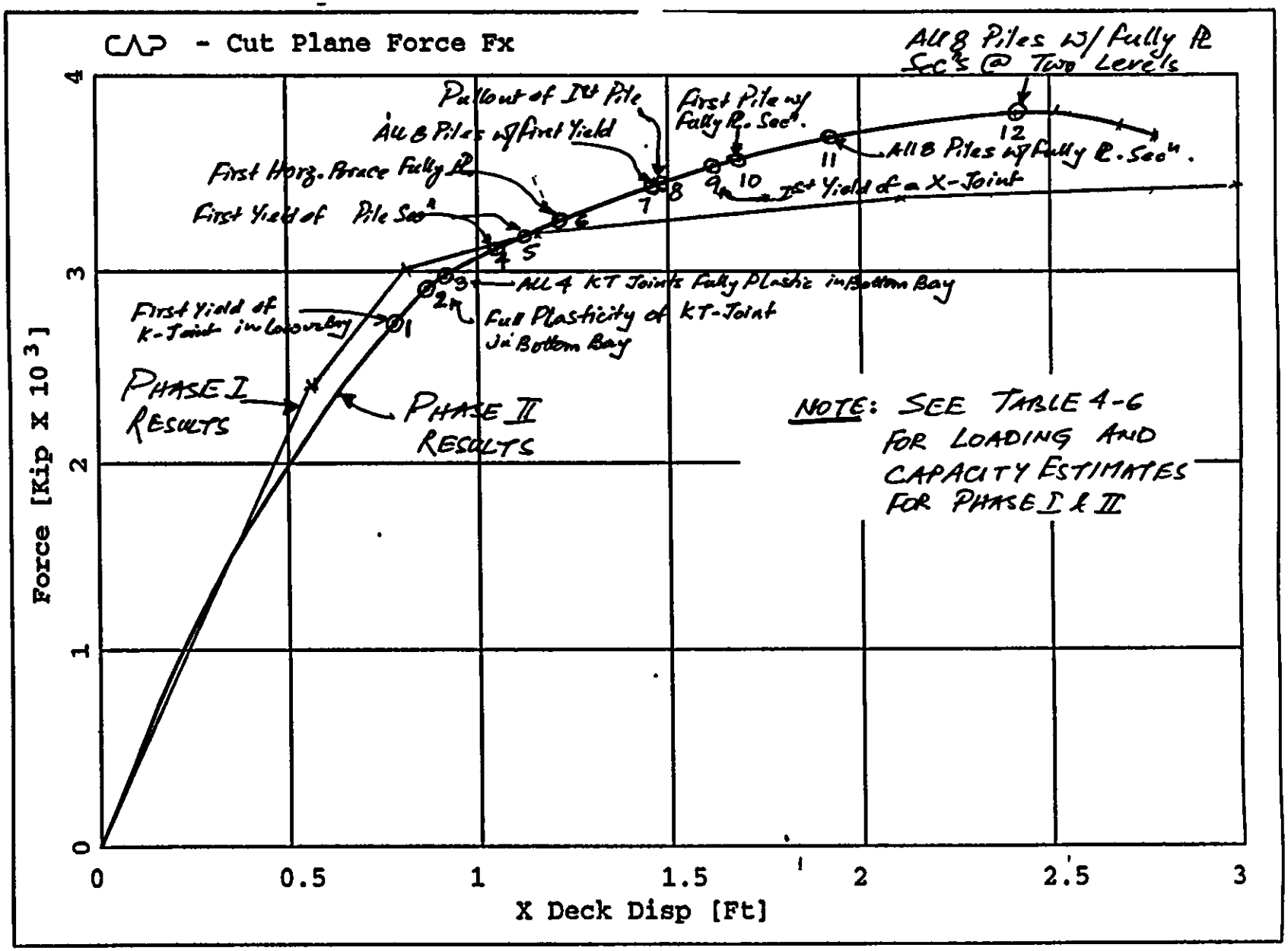

Figure 4-2(a): Load - Displacement Behavior — Platform ST151K - Base Case Analysis

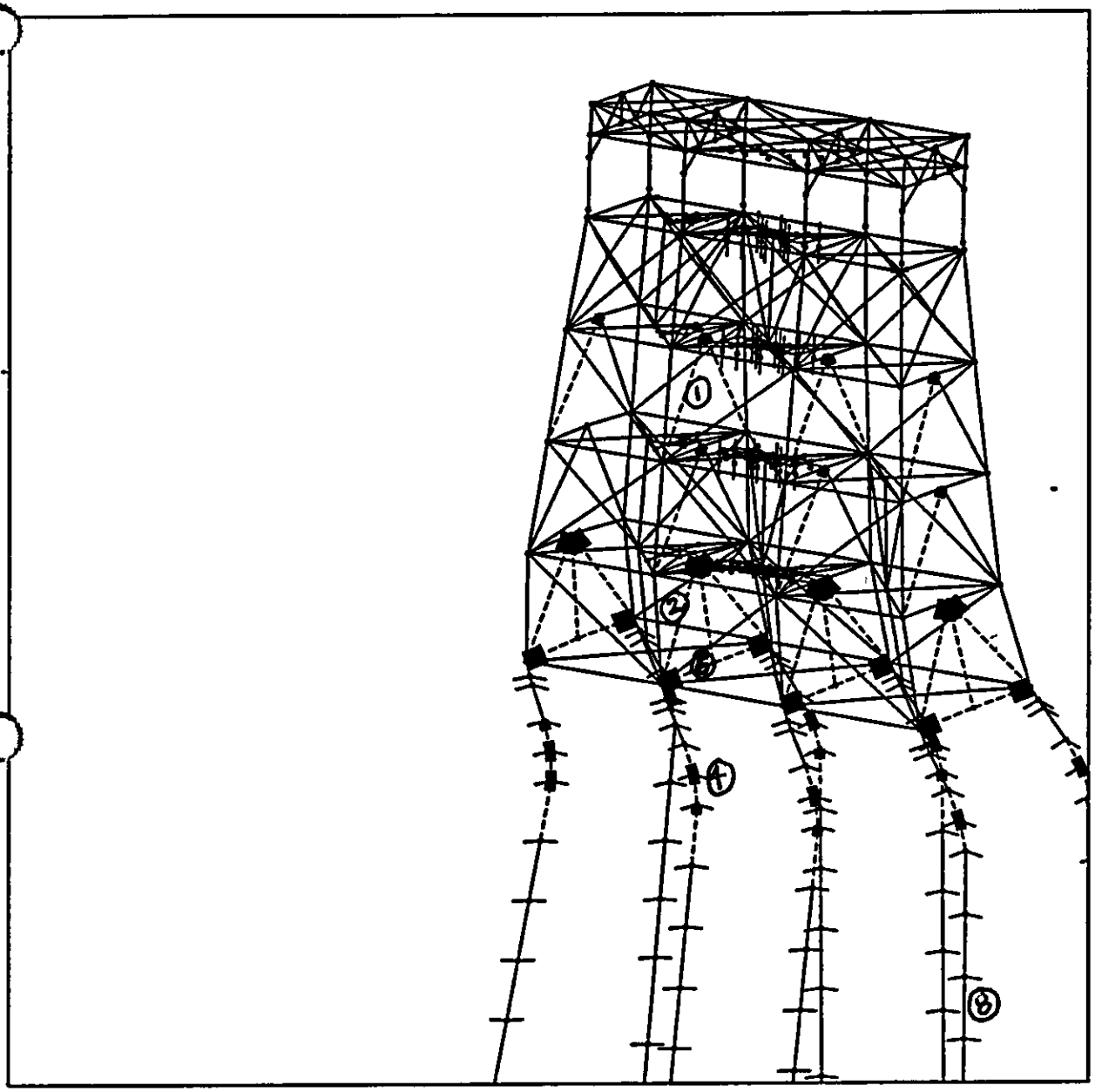

Figure 4-2(b): Inelastic/ Failure Events — Platform ST151K

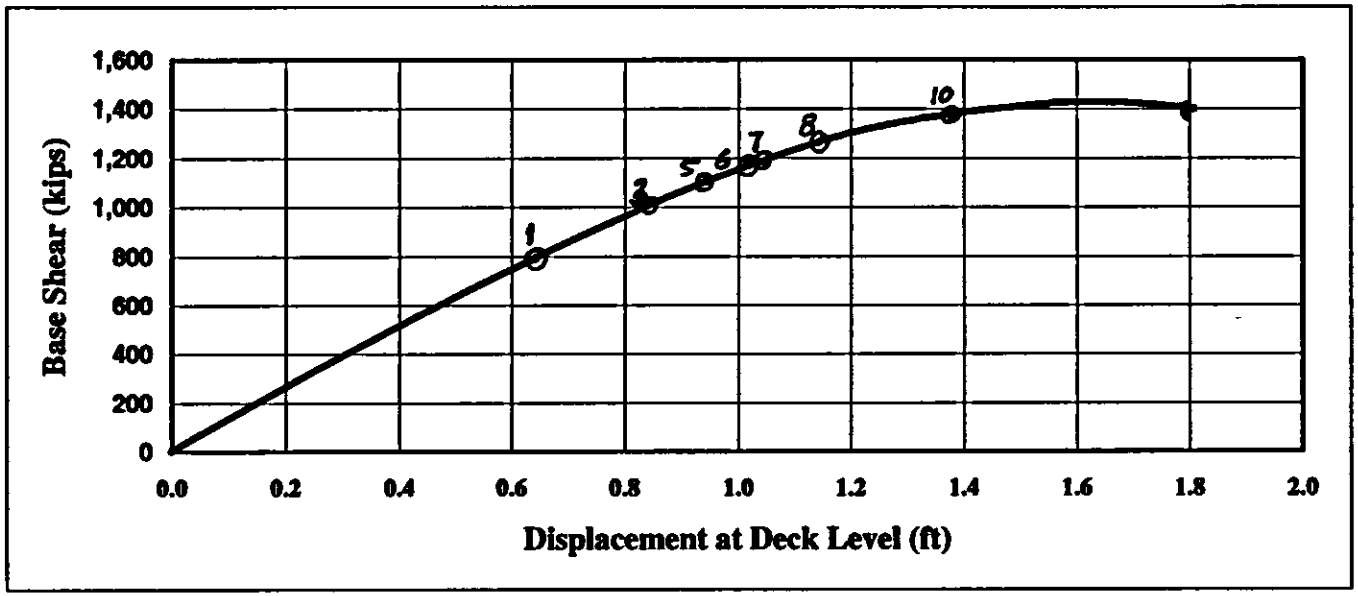

Point	Inelastic Events	Point	Inelastic Events
1	First yield in a pile section	6	First yield in a K-joint
2	First yield in all 4 piles	7	First yield in a leg section
3	Fully plastic section in a pile	8	First fully plastic section in a pile at second level
4	Fully plastic section in second pile	9	Second fully plastic section in a pile at second level
5	Full plasticity section in third pile	10	Third fully plastic section in a pile at second level

Figure 4-3(a): Load - Displacement Behavior — Platform ST130Q - Base Case Analysis

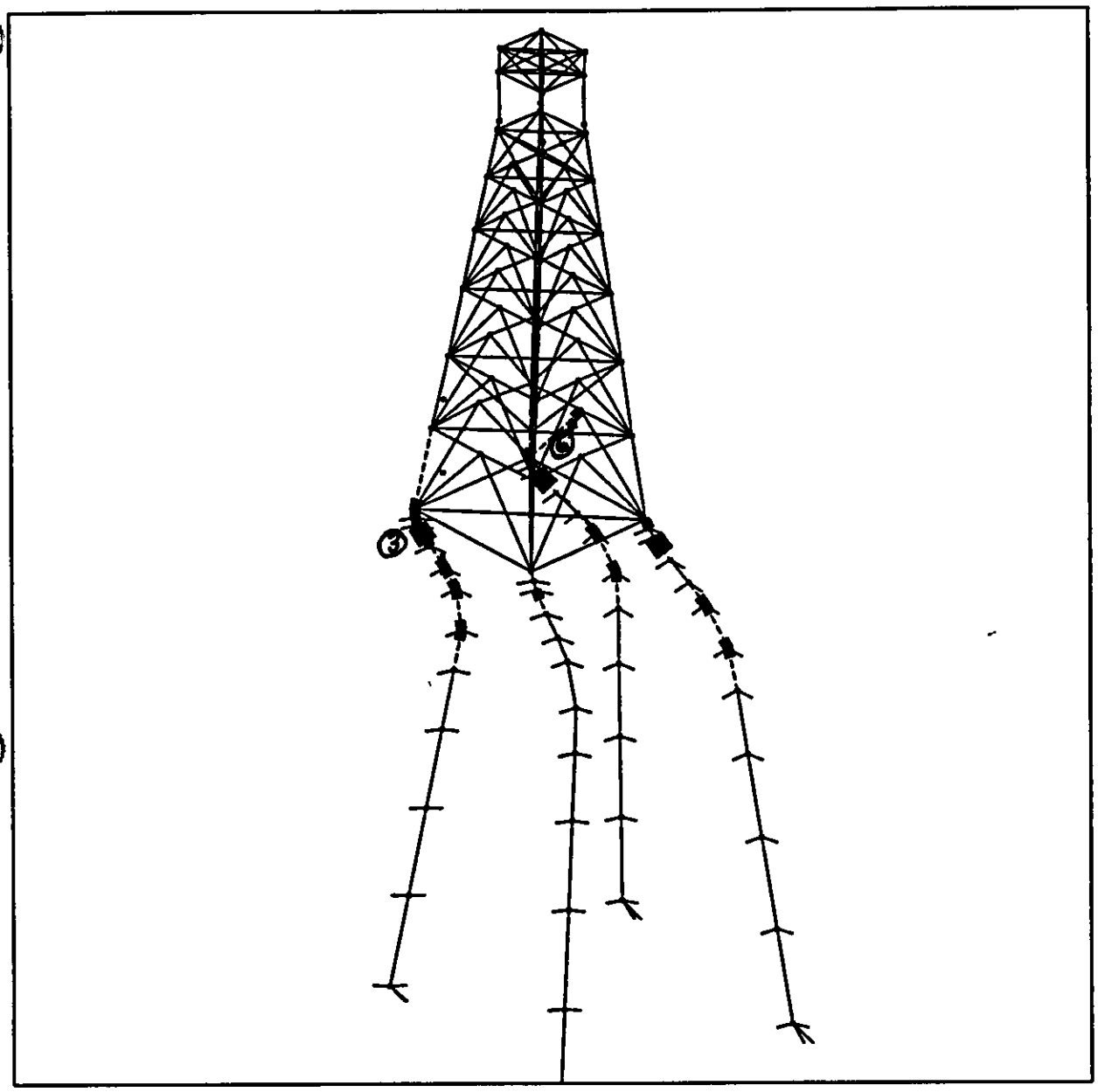

ST130Q NL jacket model

Inelastic Events Legend

_____	Elastic	.....	Strut Buckling
_ _ _ _ _	Strut Residual	_ . _ . _	Strut Reloading
.....	Plastic Strut/NLTruss	_ _ _ _	Beam Clmn Initial Yield
_____	Beam Clmn Fully Plastic	.....	Fracture

Figure 4-3(b): Inelastic/ Failure Events — Platform ST130Q

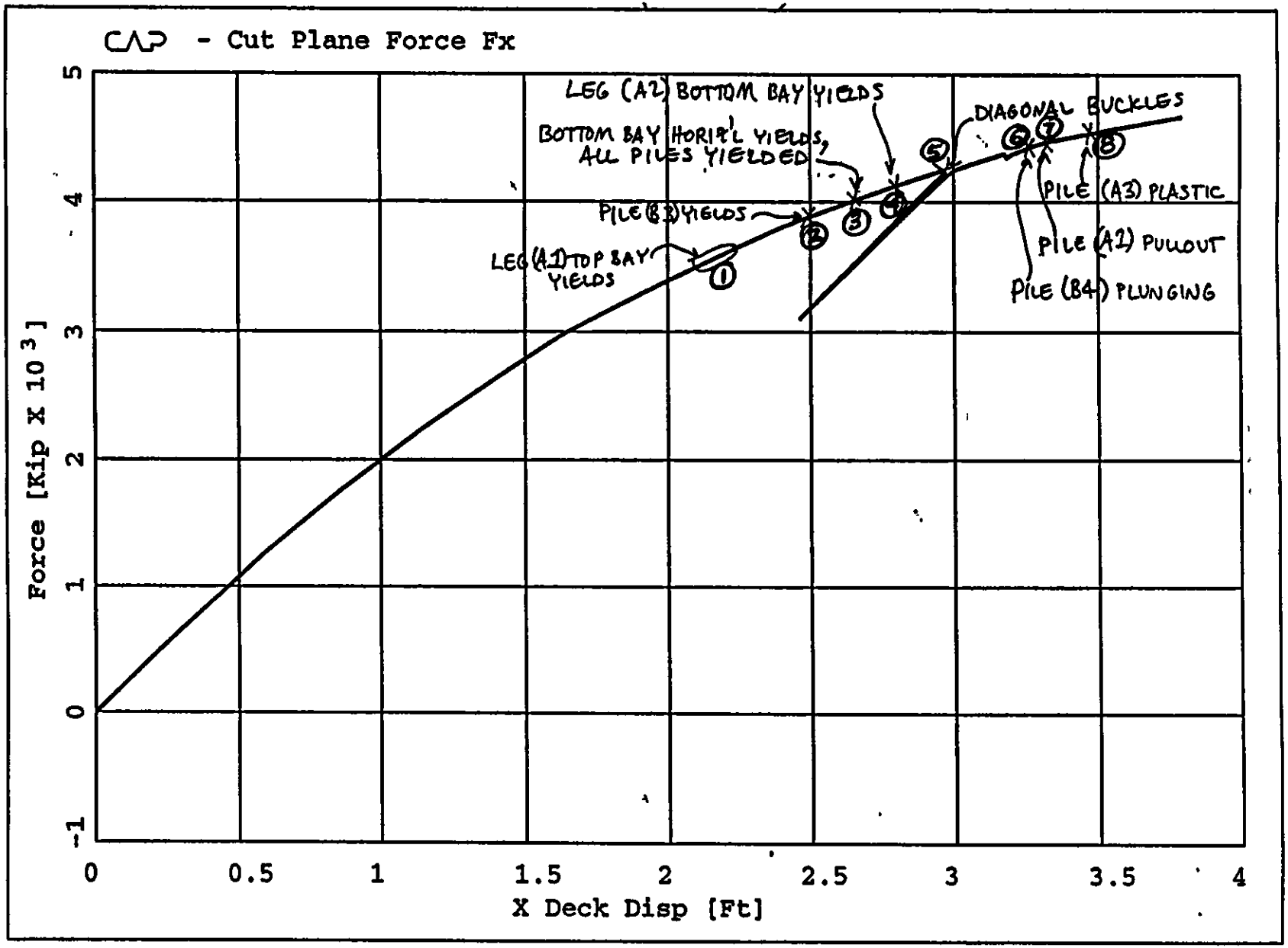

Figure 4-4(a): Load - Displacement Behavior — Platform WD103A - Base Case Analysis

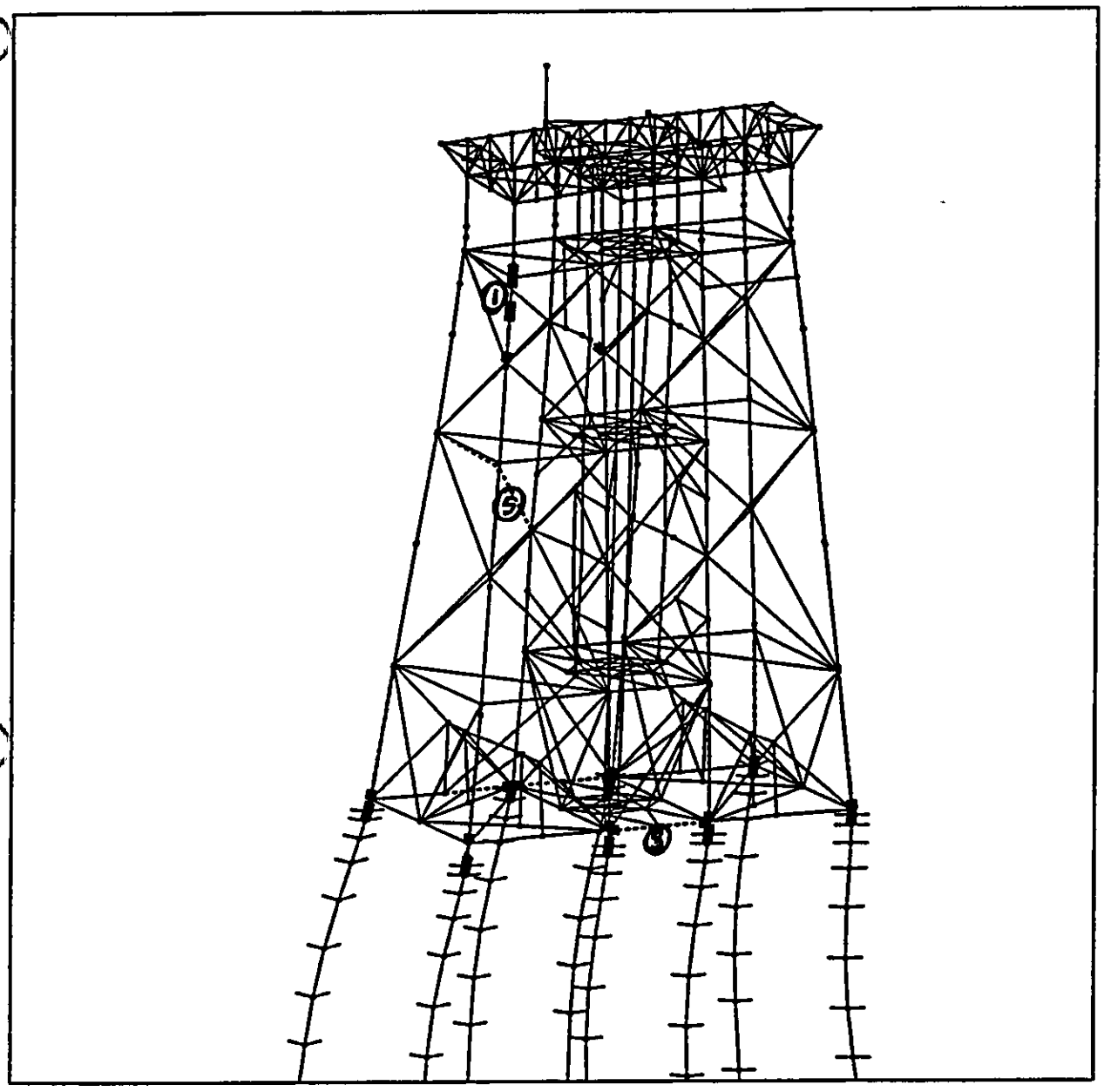

WD103A: Step 248, 4530 k

Inelastic Events Legend

Elastic	Strut Buckling
Strut Residual	Strut Reloading
Plastic Strut/NLTruss	Beam Clmn Initial Yield
Beam Clmn Fully Plastic	Fracture

Figure 4-4(b): Inelastic/ Failure Events — Platform WD103A

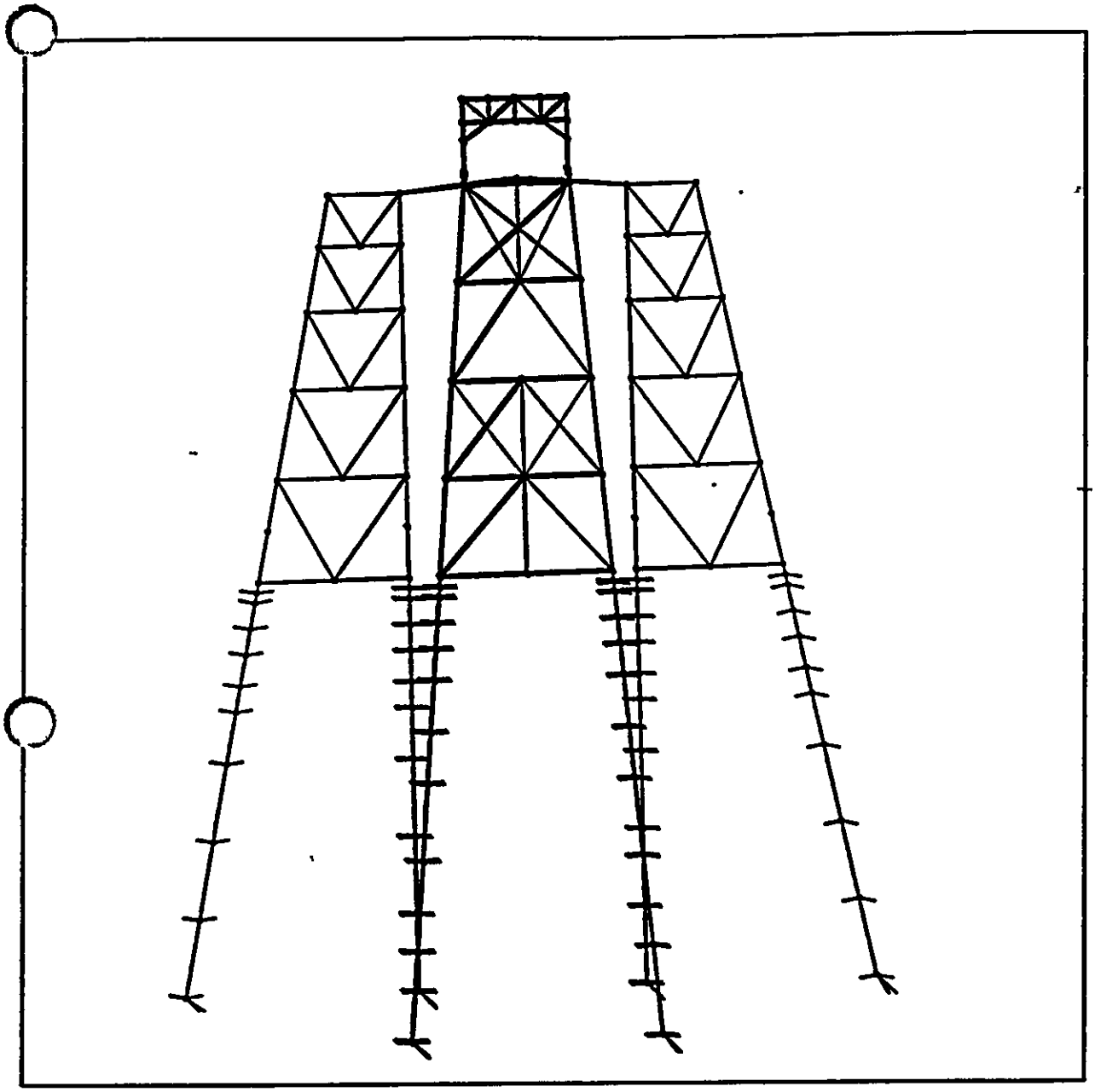

Figure 4-5(a): Structural Configuration — Platform ST151J with Tripod

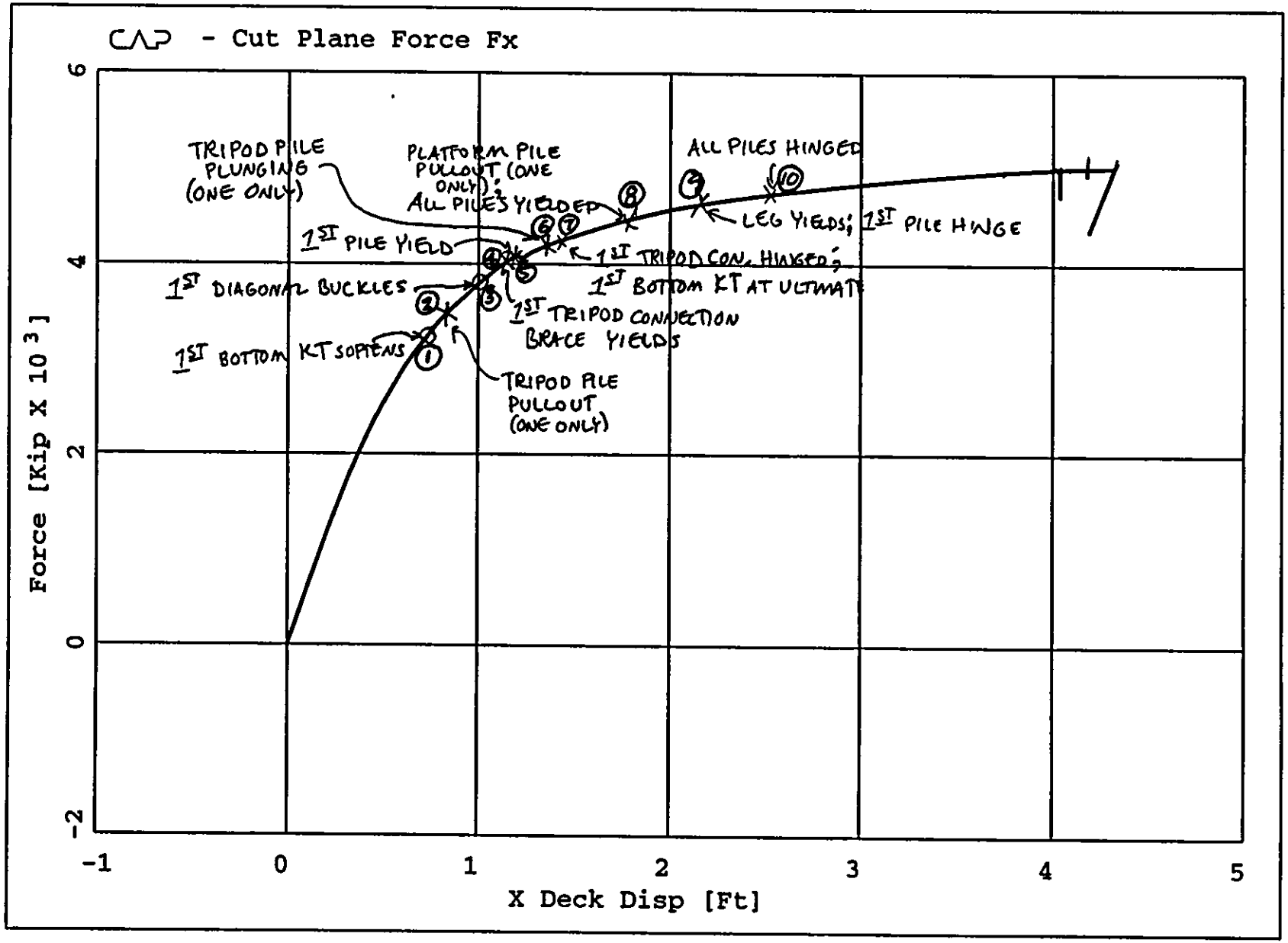

Figure 4-5(b): Load - Displacement Behavior — Platform ST151J - Base Case Analysis

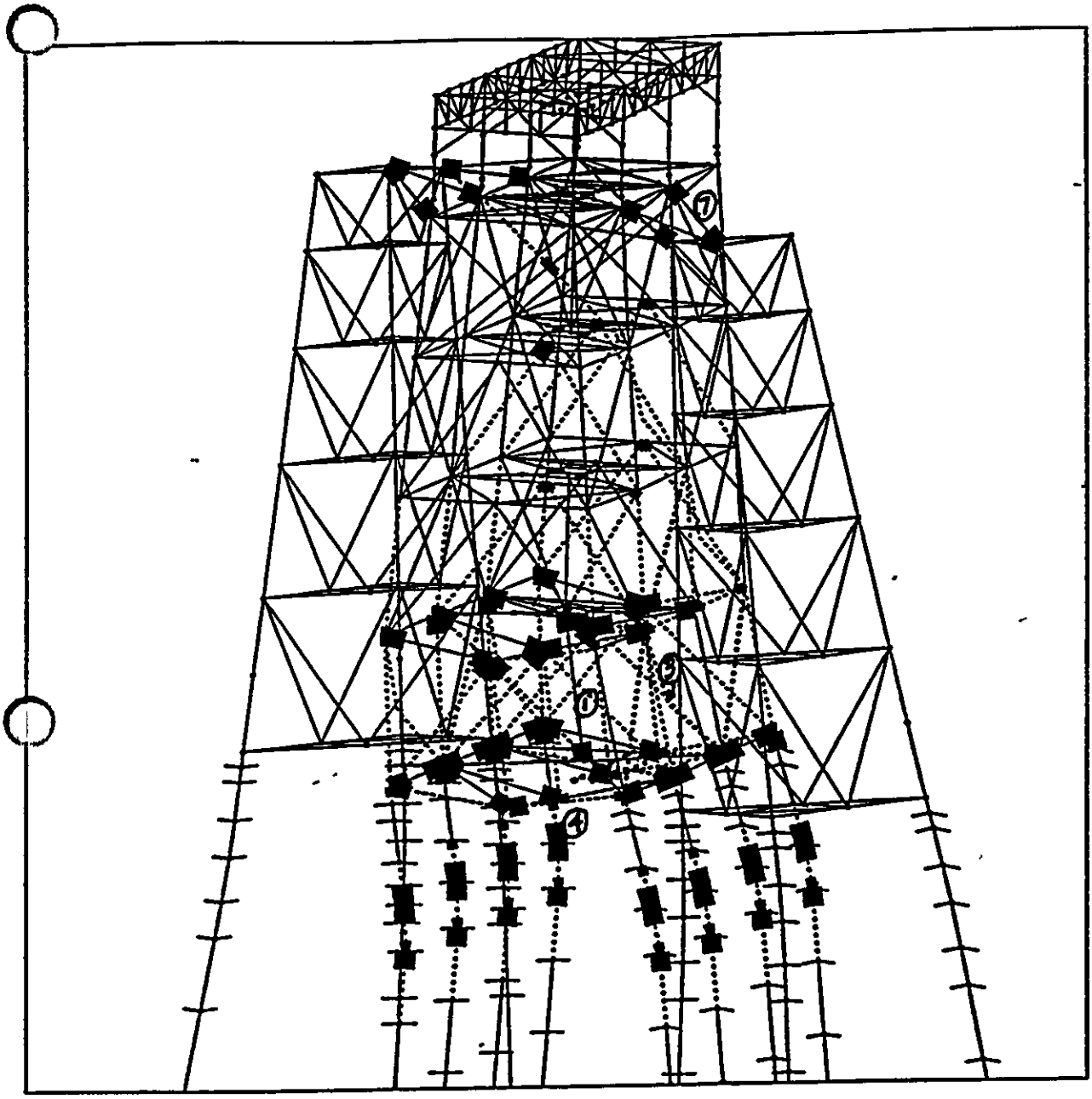

CAP ST151J run 1: Step 267, 5020 kips

Inelastic Events Legend

- Elastic
- Strut Residual
- Plastic Strut/NLTruss
- Beam Clmn Fully Plastic
- Strut Buckling
- Strut Reloading
- Beam Clmn Initial Yield
- Fracture

Figure 4-5(c): Inelastic/ Failure Events — Platform ST151J

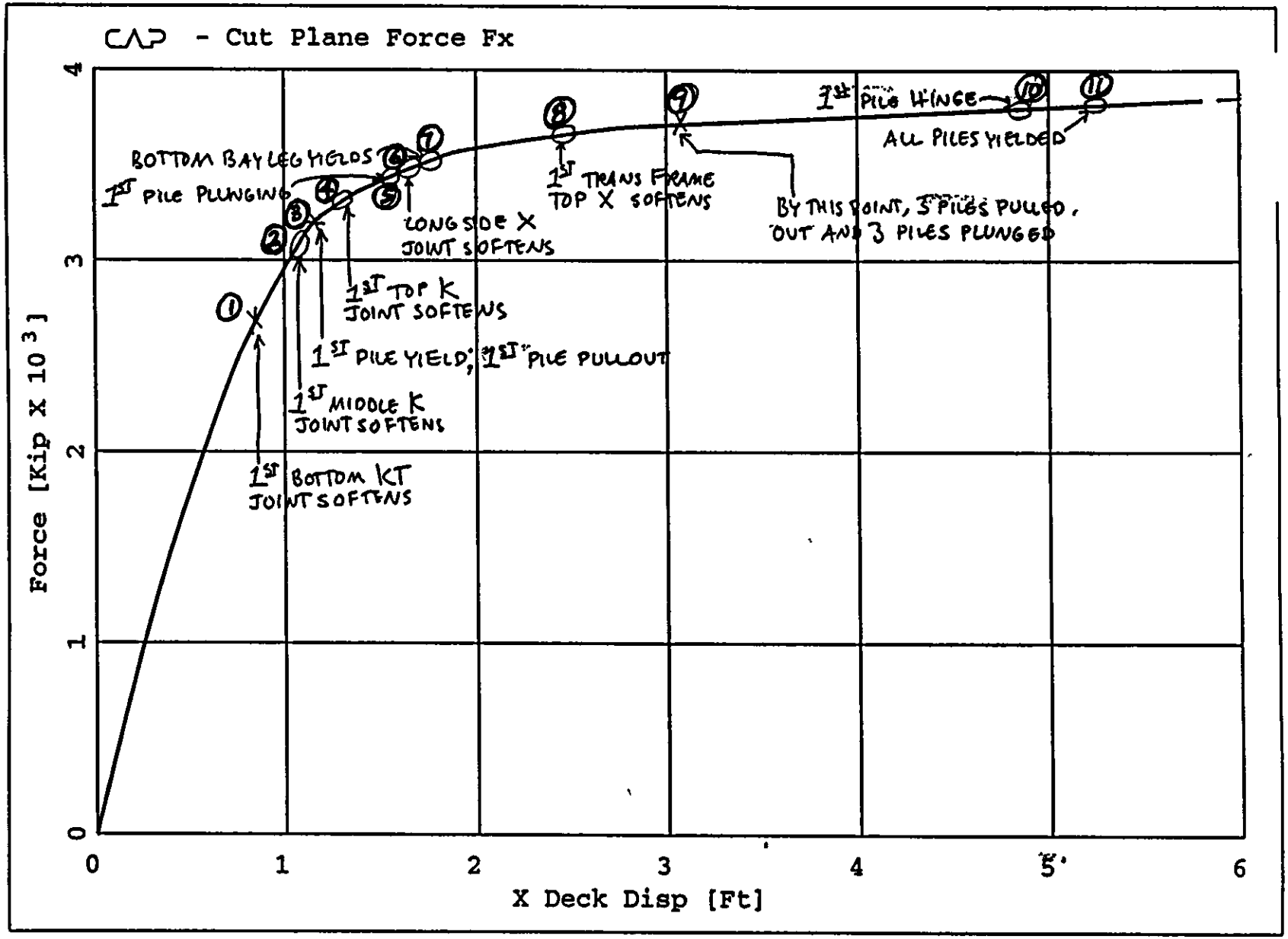

Figure 4-6(a): Load - Displacement Behavior — Platform ST177B - Base Case Analysis

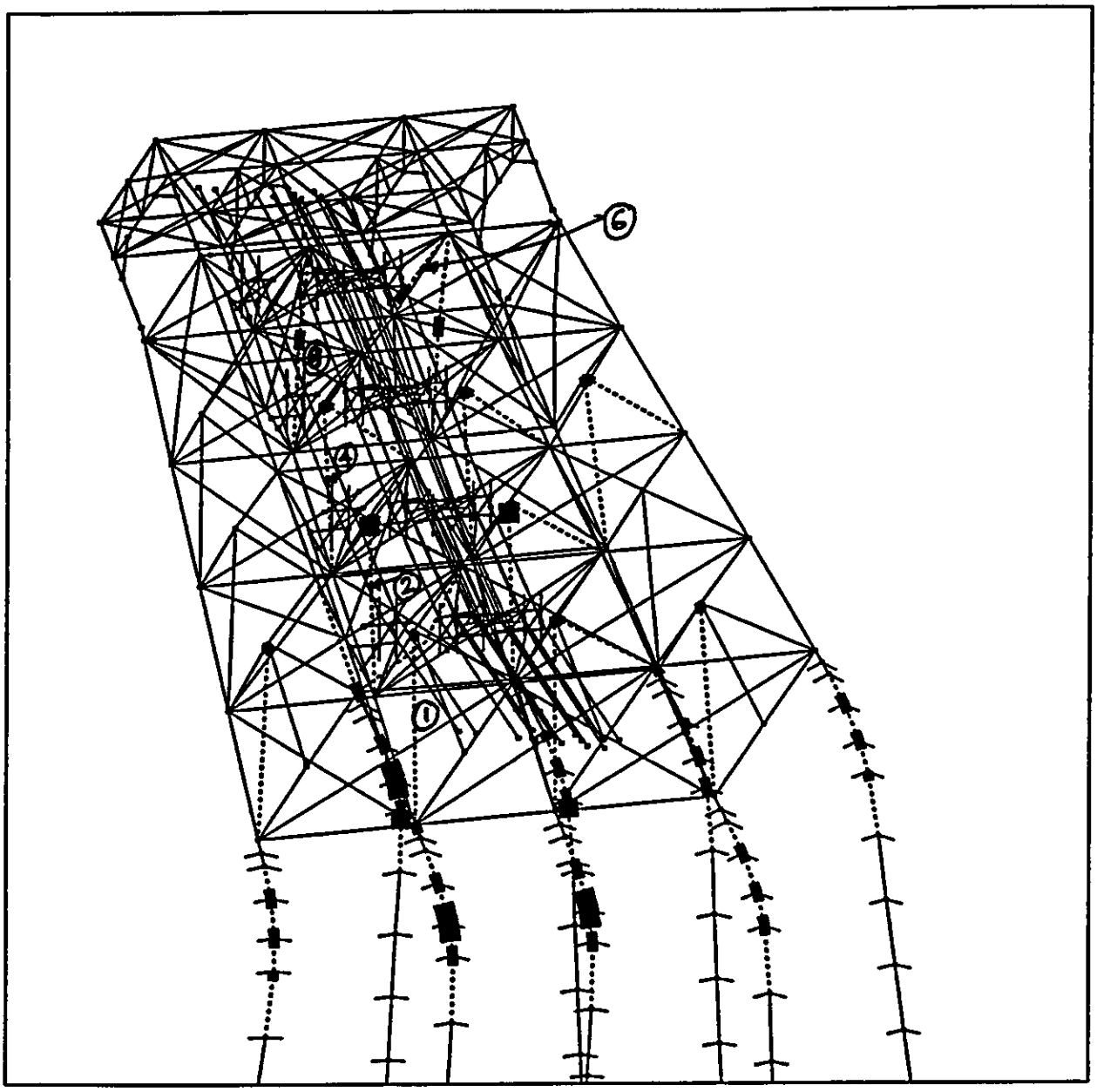

CAP z x ST177B (v4): Step 138, 3970 kips (disp x10)

Inelastic Events Legend

Elastic	Strut Buckling
Strut Residual	Strut Reloading
Plastic Strut/NLTruss	Beam Clmn Initial Yield
Beam Clmn Fully Plastic	Fracture

Figure 4-6(b): Inelastic/ Failure Events — Platform ST177B

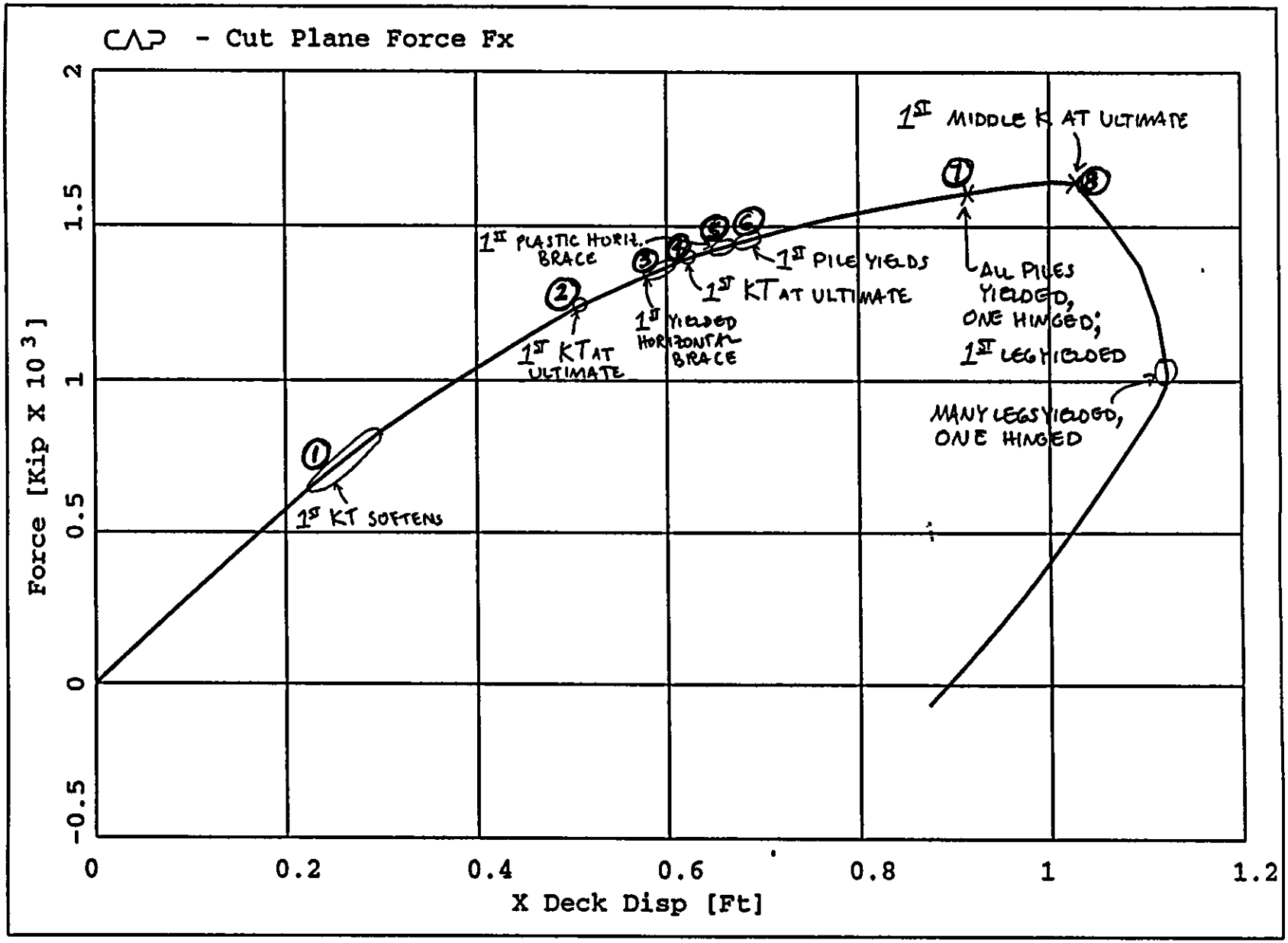

Figure 4-7(a): Load - Displacement Behavior — Platform SS139(T25) - Base Case Analysis

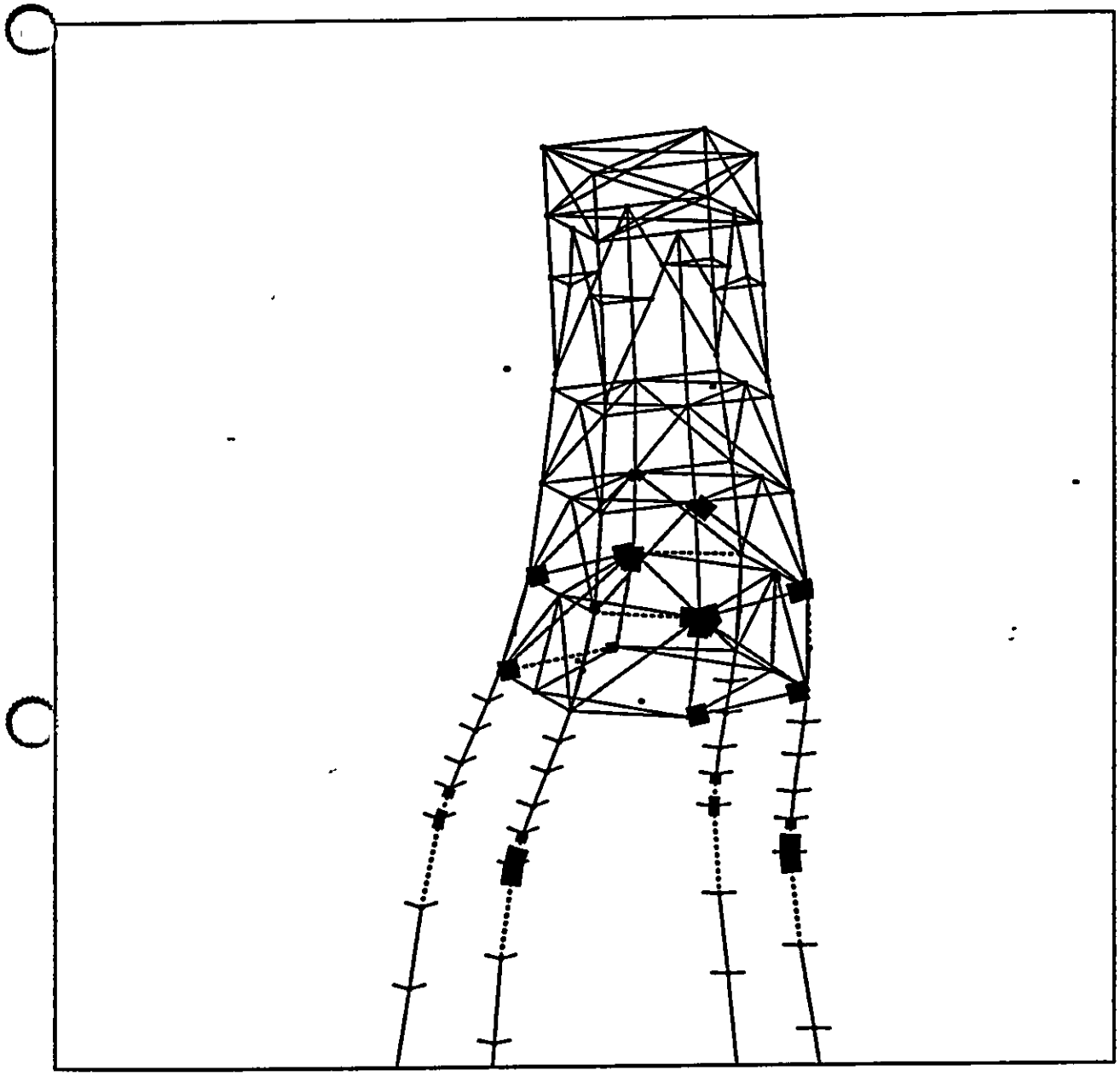

CAP T25: Step 57, 1640 kips; max load (x10)

Inelastic Events Legend

_____	Elastic	.....	Strut Buckling
_ _ _ _ _	Strut Residual	.....	Strut Reloading
.....	Plastic Strut/NLTruss	.....	Beam Clmn Initial Yield
_____	Beam Clmn Fully Plastic	.....	Fracture

Figure 4-7(b): Inelastic/ Failure Events — Platform SS139(T25)

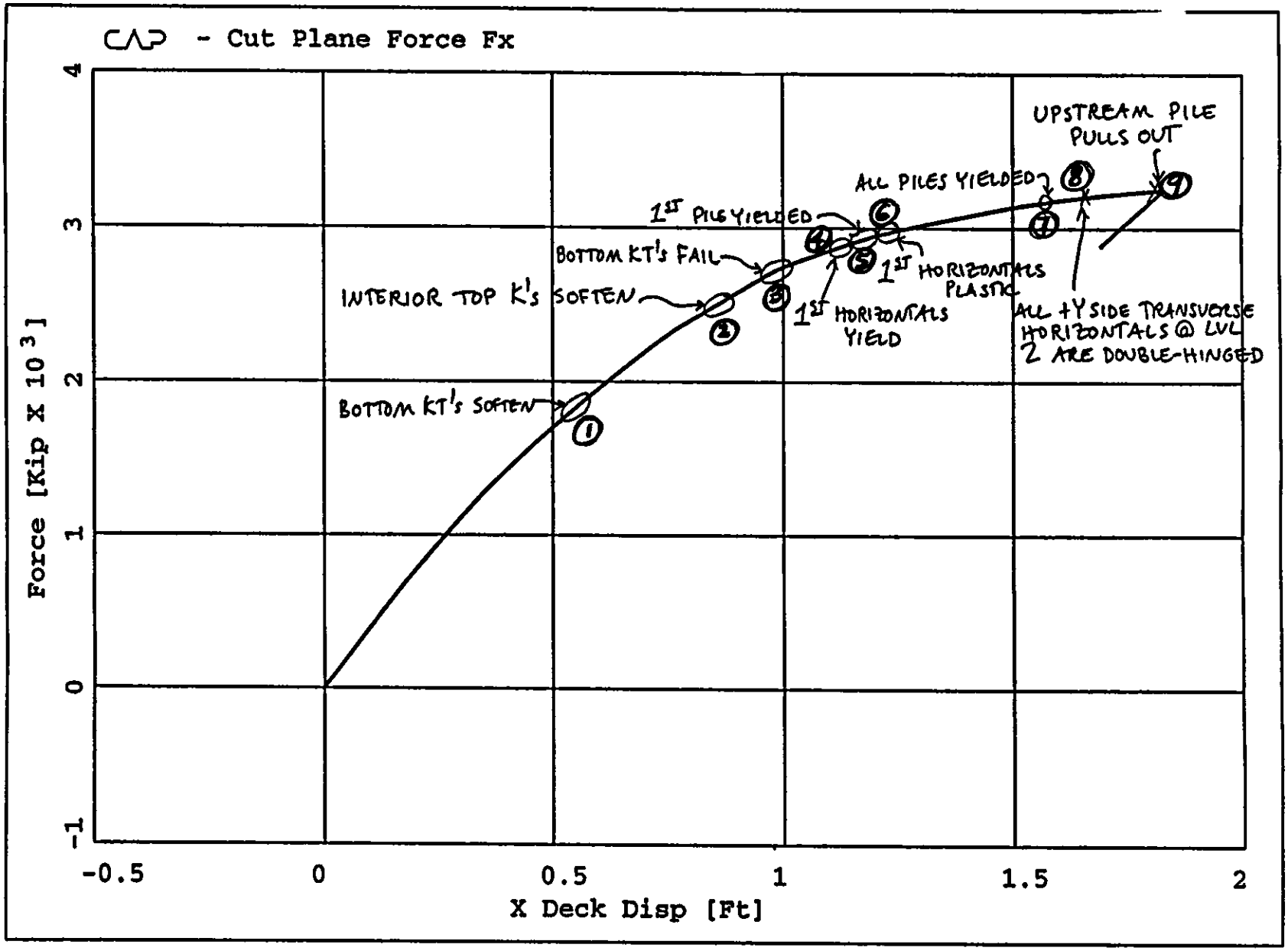

Figure 4-8(a): Load - Displacement Behavior — Platform ST151H - Base Case Analysis

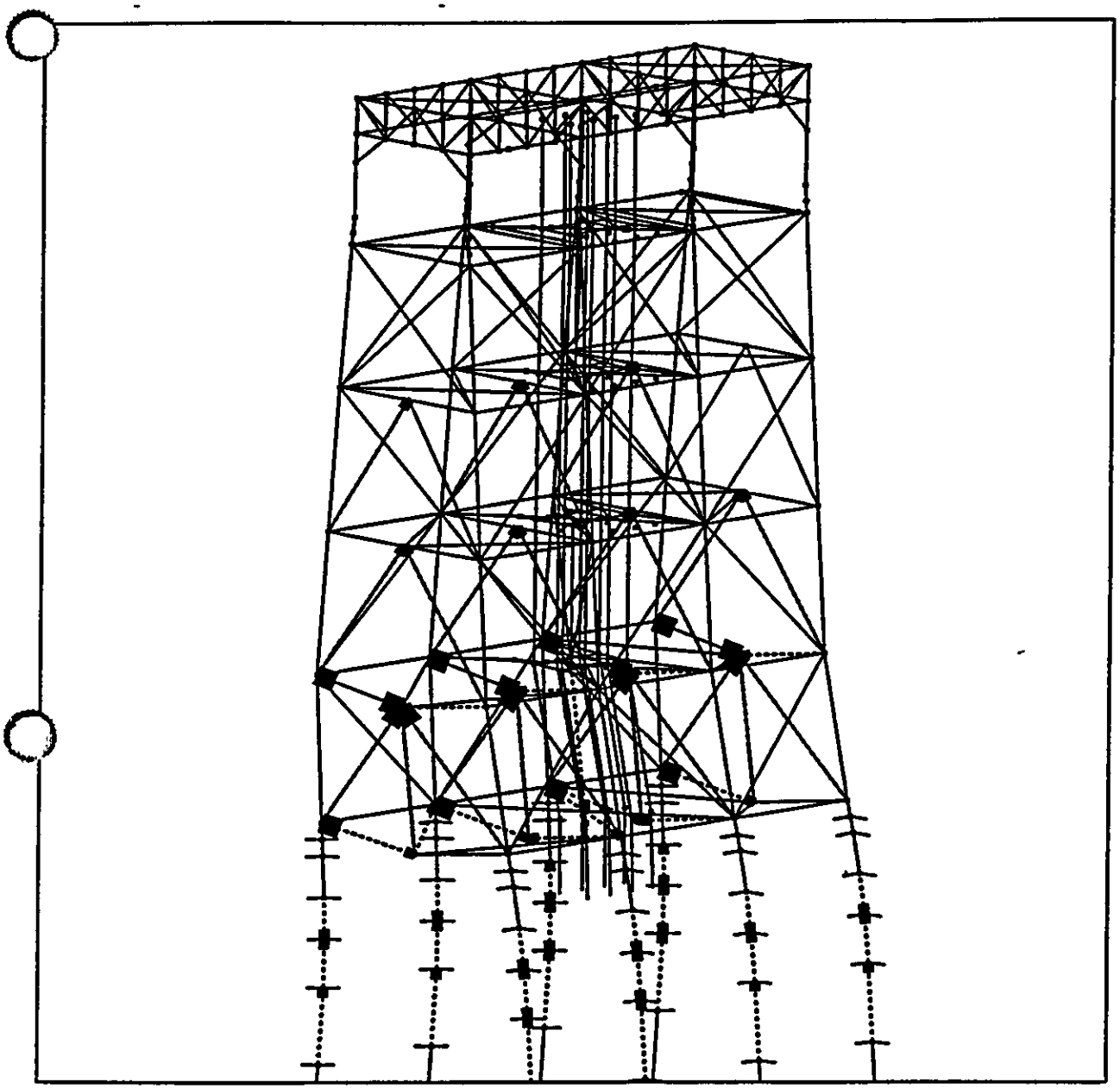

ST151H(run2): Step 60, 3240 k (displ x10)

Inelastic Events Legend

———	Elastic	.....	Strut Buckling
- - - - -	Strut Residual	- - - - -	Strut Reloading
.....	Plastic Strut/NLTruss	.....	Beam Clmn Initial Yield
———	Beam Clmn Fully Plastic	.....	Fracture

Figure 4-8(b): Inelastic/ Failure Events — Platform ST151H

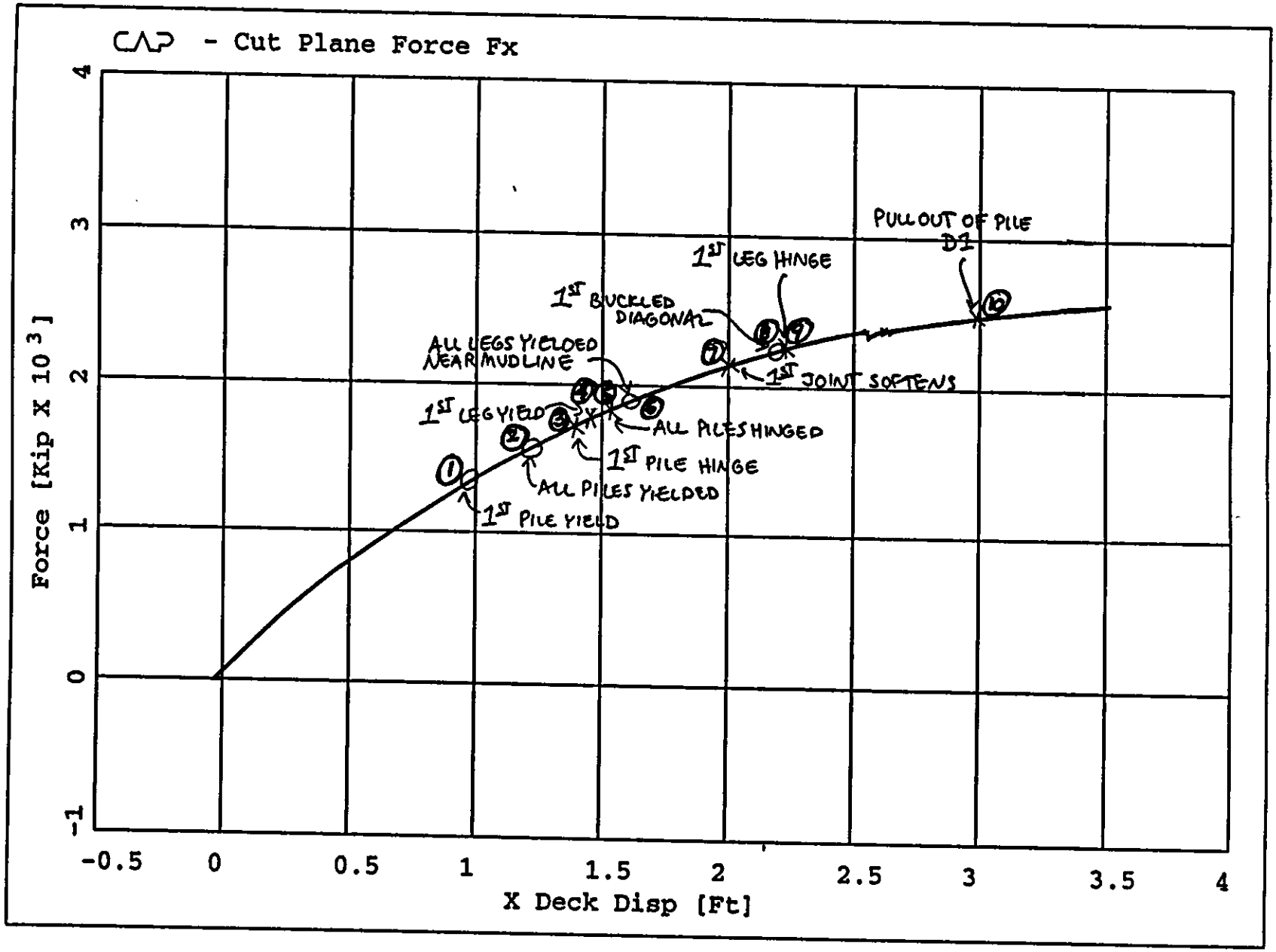

Figure 4-9(a): Load - Displacement Behavior — Platform ST130A - Base Case Analysis

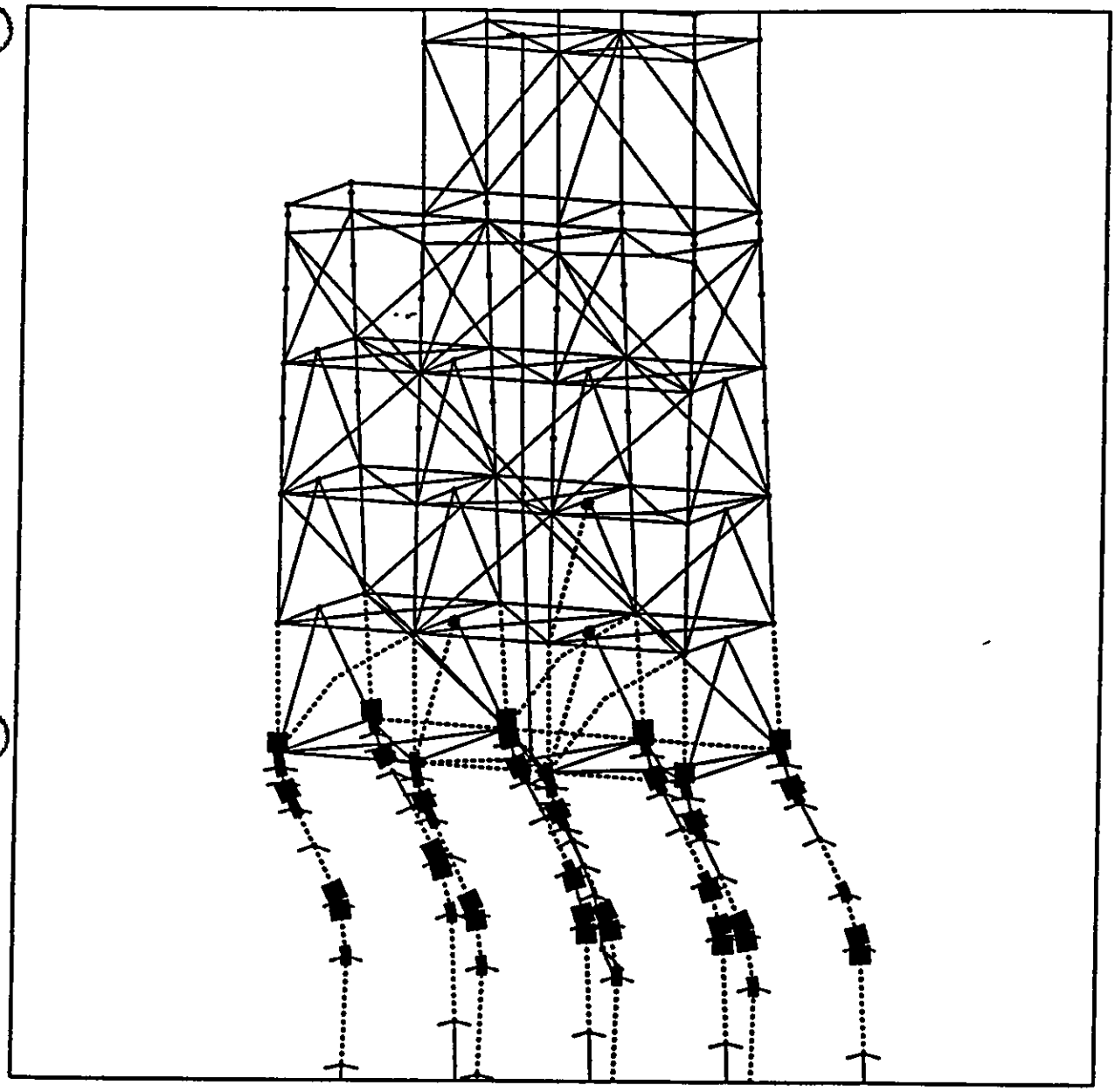

Figure 4-9(b): Inelastic/ Failure Events — Platform ST130A

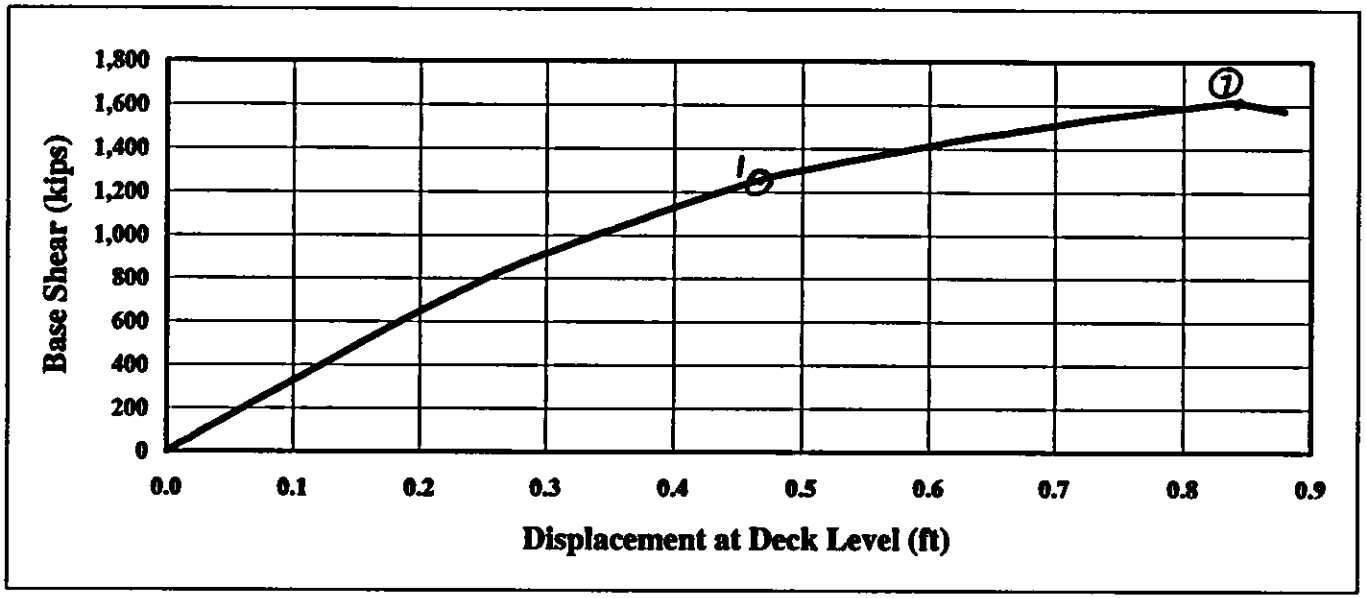

Point	Inelastic Events	Point	Inelastic Events
1	First yield of KT joint in bottom bay	5	First yield of horizontal brace at 2nd level
2	Full plasticity of KT joint in bottom bay	6	Full plasticity of horizontal brace at 2nd level
3	First yield of K joint in middle bay	7	Full plasticity of K joint in middle bay
4	Full plasticity of horizontal brace at bottom level		

Figure 4-10(a): Load - Displacement Behavior — Platform ST72(T21) - Base Case Analysis

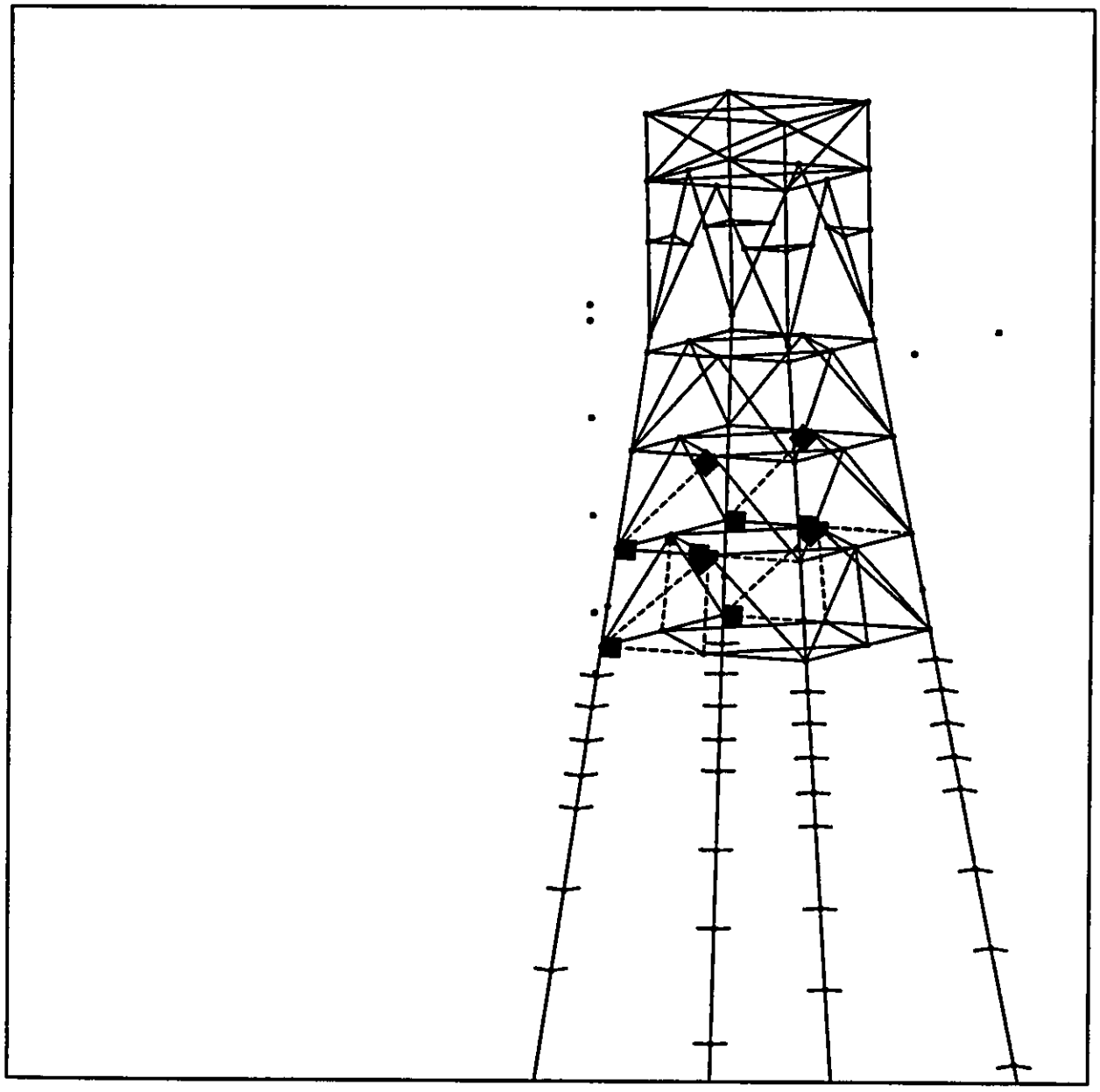

CAP z x T21 Base Case LS 36

Inelastic Events Legend

Elastic	Strut Buckling
Strut Residual	Strut Reloading
Plastic Strut/NLTruss	Beam Clmn Initial Yield
Beam Clmn Fully Plastic	Fracture

Figure 4-10(b): Inelastic/ Failure Events — Platform ST72(T21)

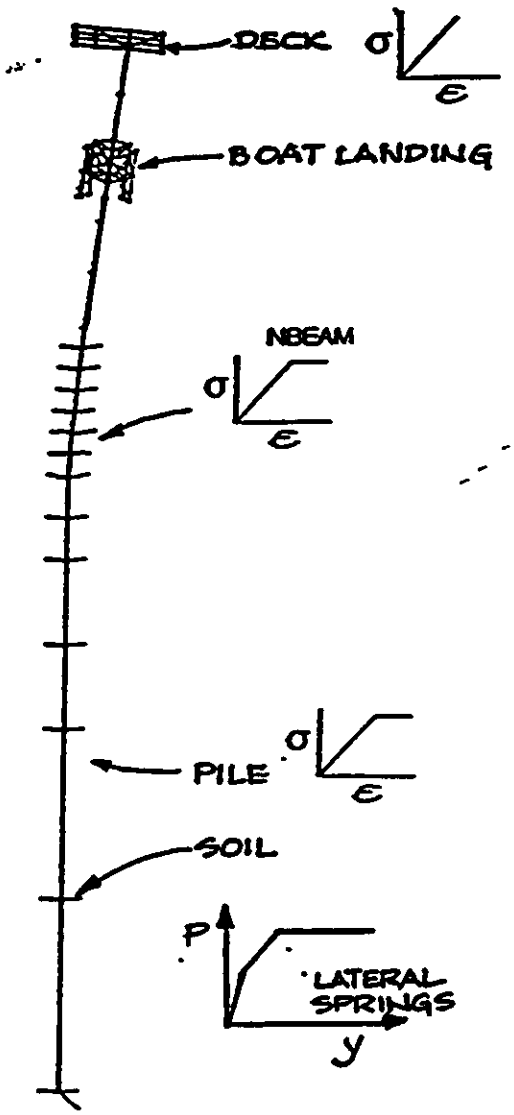

Figure 4-11: Nonlinear Analysis Computer Model - Caisson Platform

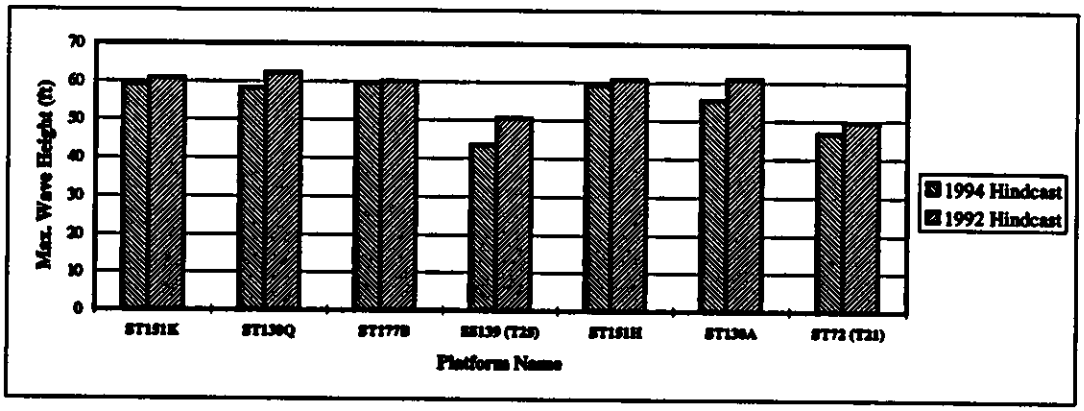

(a): Hindcast Maximum Wave Heights

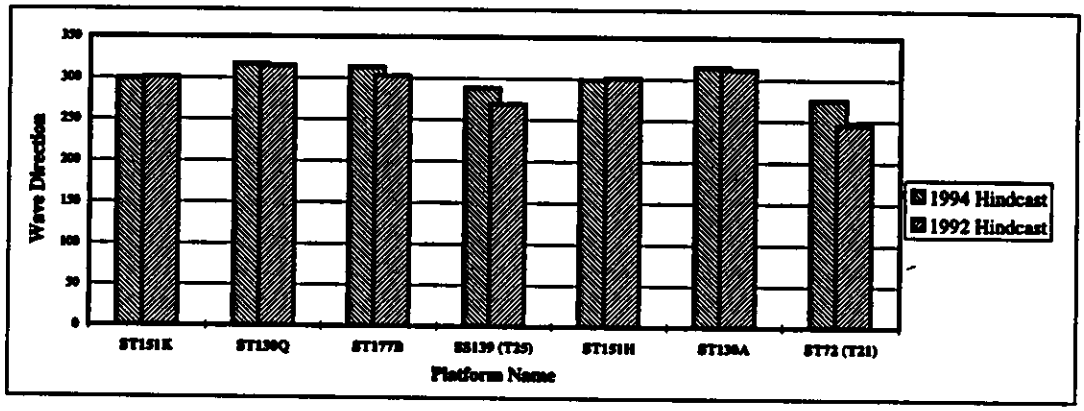

(b): Hindcast Wave Directions from True North

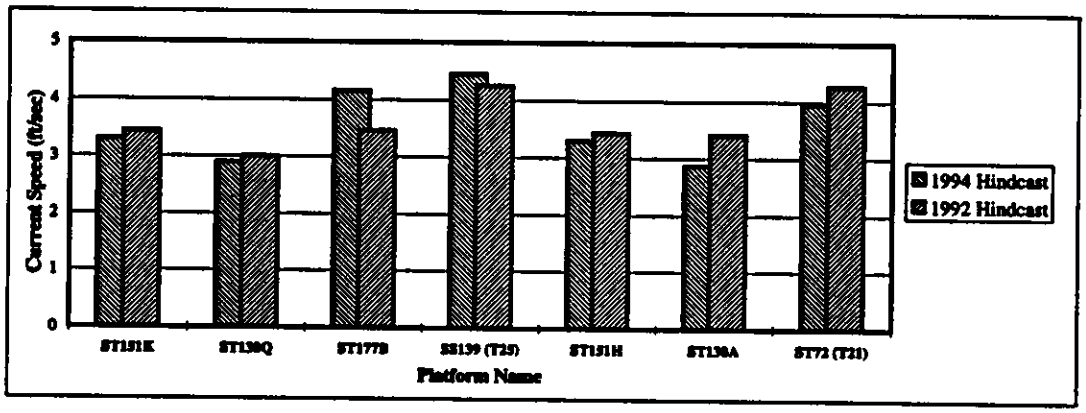

(c): Hindcast Currents

Figure 4-12: Comparison of Hindcast Data - Phase II (1994 Hindcast) vs. Phase I (1992 Hindcast)

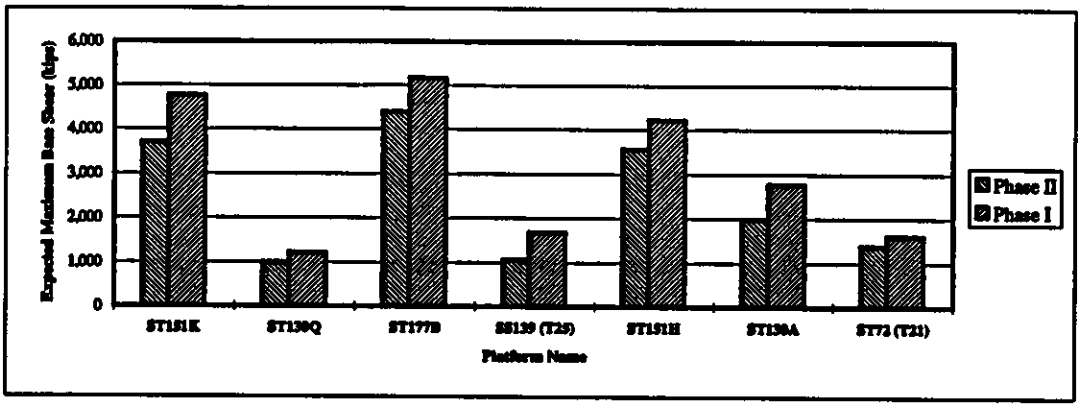

(a)· Expected Maximum Base Shear (S), kips

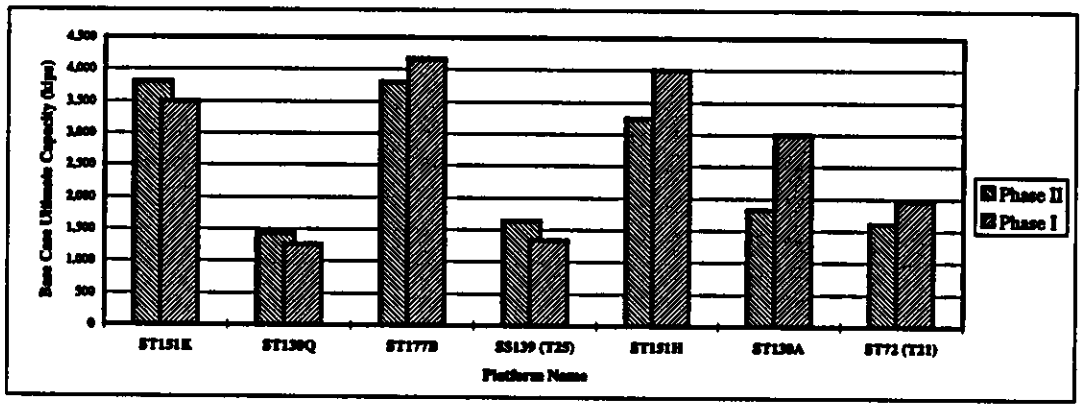

(b): Base Case Ultimate Capacity (Ru), kips

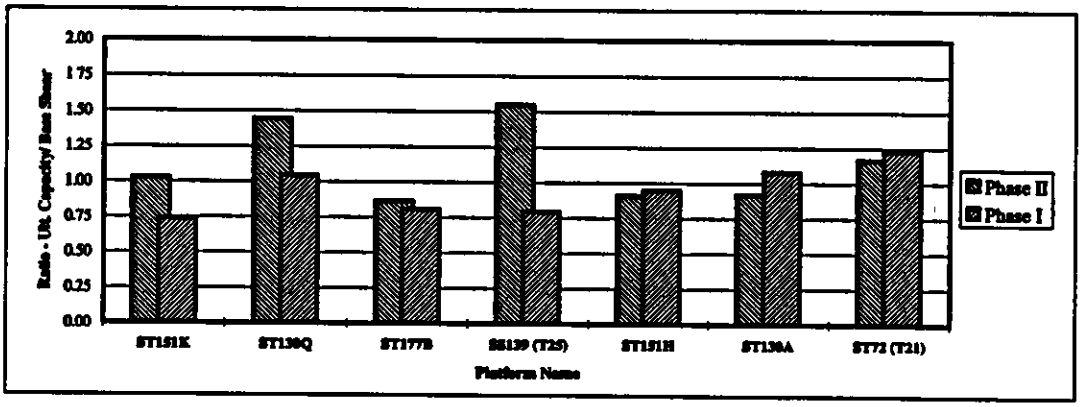

(c): Ratio of Ultimate Capacity (Ru) to Base Shear (S)

Figure 4-13: Comparison of Base Case Capacity Analysis Results - Phase II vs. Phase I

Table 4-1: Capacity Analysis Results - Steel Jacket Platforms - Survival (No Damage) Cases

Platform	Platform Characteristics		Analysis Case	Expected Maximum Hindcast Base Shear	Base Shear at Failures of First R1 (#2)				Base Shear at Failure of Multiple (#2)			Ultimate Capacity	Element Failures at Platform Collapse State	Ratio of Ult. Cap./ Andrew Base Shear	System Factor	System Factor (Pile-Lateral Capacity)	System Factor (Pile-Axial Capacity)
	Configuration (see Appendix-A for platform configuration)	Water Depth/ Year Installed (ft.)	(see Section 4.1.1 for Description) (see Appendix A for analysis direction and hindcast data)	(S) (#1) (kips)	Brace/ Joint (RJ1,1) (kips)	Pile or Leg First Yield (RJ1,2) (kips)	Pile or Leg Plasticity (Rf1) (kips)	Pile Pullout/ Plunging (Rfa1) (kips)	Brace/ Joint (RJ) (kips)	Pile or Leg Plasticity (Rf) (kips)	Pile pullout/ Plunging (Rfa) (kips)	Rs (Raj or Rsfl or Rsfa) (kips)	(See Figures 4-2 to 4-4 for locations of failure events)	= (Rs/S)	= (Rs/R1) (#3)	= (Rf/Rf1)	= (Rfa/Rfa1)
ST 151 K	8 Leg - Grouted Double Battered K Brand 30" dia. piles 175' penetration	177 ft. 1963	Base Case	3,700	2,900	3,100	3,570	3,450	3,000	3 700	-	3,000	Bottom bay KT-joints, horiz. fully plastic; all piles fully plastic at depth below mudline; 1 pile pullout	1.03	1.10	-	-
			Case-1	3,700	2,900	-	-	-	3,000	-	-	3,000	Bottom bay KT joints and inner verticals, and bottom horizontals fully plastic	1.05	1.03	-	-
			Case-2	3,700	-	3,200	3,850	-	-	4,230	-	4,400	All 8-piles with fully plastic sections at two levels (just below and at depth below mudline)	1.19	-	1.10	-
			Case-3	3,700	-	-	-	3,430	-	-	4,000	4,000	3 piles pullout and 3 plunge	1.08	-	-	1.17
ST130Q	4 Leg - Grouted Double Battered K Brand 30" dia. piles 210' penetration	170 ft. 1964	Base Case	990	-	800	1,010	-	-	1,300	-	1,430	Fully plastic pile sections	1.44	1.79	-	-
			Case-1	990	1,300	955 (leg event)	1 100 (leg event)	-	1,410	-	-	1,410	Bottom bay leg sections and bottom horiz. braces with fully plastic sections; 2-KT joints fail	1.42	1.48	-	-
			Case-2	990	-	800	1,000	-	-	1,470	-	1,500	All four piles with fully plastic sections at two levels (just below and at depth below mudline)	1.52	-	1.36	-
			Case-3	990	-	-	-	1,820	-	-	1,860	1,860	1 pile pullout and 1 pile plunge	1.88	-	-	1.82
WD103	8 Leg Ungrouted Double Battered K Braced/Diagonals 42" dia. piles 270' penetration	223 ft. 1965	Base Case	2,140	4,250	3,800	4,570	4,150	4,520	4,660	4,460	4,460	All legs and piles yield near the mudline	2.18	1.28	-	-
			Case-1	2,140	4,300	-	-	-	4,425	-	-	4,700	Three diagonals buckled and leg sections with first yield	2.20	1.07	-	-
			Case-2	2,140	-	4,120	4,480	-	-	4,880	-	4,880	All 8 piles with fully plastic sections below mudline	2.28	-	1.09	-
			Case-3	2,140	-	-	-	4,100	-	-	5,040	5,060	3 piles pullout and 3 piles plunge	2.36	-	-	1.23

Notes: (#1)- Includes wave in deck load of 340 kips for ST151K.
(#2)- Values in bold indicates those picked for calibration.
(#3)- Rl the lesser of RJ1,1; RJ1,2; Rfl1; and Rfa1.

Table 4-2: Capacity Analysis Results - Steel Jacket Platforms - Damage Cases

Platform	Platform Characteristics		Analysis Case	Expected Maximum Hindcast Base Shear	Base Shear at Failures of First RI (#2)				Base Shear at Failure of Multiple (#2)			Ultimate Capacity	Element Failures at Platform Collapse State	Ratio of Ult. Cap./ Ambrose Base Shear =	System Factor =	System Factor (Pile-Lateral Capacity) =	System Factor (Pile-Axial Capacity) =
	Configuration (see Appendix-A for platform configuration)	Water Depth/ Year Installed (ft.)	(see Section 4.1.1 for Description) (see Appendix A for analysis direction and hindcast data)	(S) (#1) (kips)	Brace/ Joint (RJ1,1) (kips)	Pile or Leg First Yield (RJ1,2) (kips)	Pile or Leg Plasticity (Rf1) (kips)	Pile Pullout/ Plunging (Rfa1) (kips)	Brace/ Joint (RJ) (kips)	Pile or Leg Plasticity (Rf) (kips)	Pile pullout/ Plunging (Rfa) (kips)	Ru (Ruj or Ruf or Rufa) (kips)	(See Figures 4-5 to 4-7 for locations of failure events)	(Ru/S)	(Ru/R1) (#3)	(Rf/Rf1)	(Rfa/Rfa1)
ST 151 J	8 Leg - Grouted Single Battered K Braced 30" dia. piles 180' penetration Strengthened by 2 Tripods	177 ft. 1982	Base Case	4,450	3,750	4,040	4,630	3,460	4,520	4,730	4,935	5,000	Pullout and plunging of piles; failure of braces & KT joints; fully plastic section in jacket piles & at jacket-tripod connections	1.12	1.45	-	-
			Case-1	4,450	4,640	-	-	-	5,100	-	-	5,000	3-braces buckle and 1 yields and 1 KT joint fails in the bottom bay	1.30	1.25	-	-
			Case-2	4,450	-	4,870	5,710	-	-	6,000	-	6,020	Fully plastic section at two levels in all 8 piles of jacket; no event predicted in tripod piles	1.35	-	1.05	-
			Case-3	4,450	-	-	-	3,550	-	-	5,785	6,010	3 piles pullout and 3 piles plunge in jacket & 2 piles pullout and 2 plunge in the tripods	1.35	-	-	1.63
ST 177B	8 Leg - Grouted Double Battered K Braced 30" dia. piles 187' penetration	142 ft. 1965	Base Case	4,390	3,850	3,200	3,800	3,200	-	3,900	3,720	3,800 (#4)	Three piles pullout and 3 piles plunge; first yield in K and X joints; fully plastic section and local buckling in a pile	0.87	1 19	-	-
			Case-1	4,390	3,900	-	-	-	5,210	-	-	6,000	All bottom bay KT-joints fail and horiz. braces with plastic sections and 3 diag. buckle; 3 K-joints in 2 bays above fail	1.37	1.54	-	-
			Case-2	4,390	-	3,180	4,200	-	-	4,700	-	4,700	Fully plastic section at two levels in all 8 piles	1.07	-	1.12	-
			Case-3	4,390	-	-	-	3,200	-	-	3,700	3,800	Three piles pullout and three piles plunge	0.87	-	-	1.16
SS139 (T25)	4 Leg - Grouted Double Battered K Braced 36" dia. piles 165' penetration 15' leg extension	62 ft. 1969	Base Case	1,060	1,230	1,440	1,625	-	1,640		-	1,640	First yield in all 4 piles, joint failures, yielding of jacket legs, and hinge in a pile	1.55	1.33	-	-
			Case-1	1,060	1,230	-	-	-	1,640	-	-	1,640	KT joints in bottom bay and K joints in 2nd bay fail; horiz. at bottom 2 levels fully plastic	1.55	1.31	-	-
			Case-2	1,060	-	1,860	2,070	-	-	2,240	-	2,300	Fully plastic section at two levels in all 4 piles	2.17	-	1.86	-
			Case-3	1,060	-	-	-	2,190	-	-	2,665	2,740	One pile pullout and one pile plunge	2.58	-	-	1.22

Notes. (#1): Includes wave in deck load of 330 kips for ST151J and 265 kips for ST177B.
(#2): Values in bold indicates those picked for calibration.
(#3): RI the lesser of RJ1,1; RJ1,2; Rf1; and Rfa1.
(#4): Ultimate capacity at local buckling of non compact pile sections

Table 4-3: Capacity Analysis Results - Steel Jacket Platforms - Failure Cases

Platform	Platform Characteristics		Analysis Case	Expected Maximum Hindcast Base Shear	Base Shear at Failures of First R1 (#2)				Base Shear at Failure of Multiple (#2)			Ultimate Capacity	Element Failures at Platform Collapse State	Ratio of Ult. Cap./ Andrew Base Shear	System Factor	System Factor (Pile-Lateral Capacity)	System Factor (Pile-Axial Capacity)
	Configuration (see Appendix-A for platform configuration)	Water Depth/ Year Installed (ft.)	(see Section 4.1.1 for Description) (see Appendix A for analysis direction and hindcast data)	(S) (#1) (kips)	Brace/ Joint (Rj1,1) (kips)	Pile or Leg First Yield (Rj1,2) (kips)	Pile or Leg Plasticity (Rf1) (kips)	Pile Pullout/ Plunging (Rfa1) (kips)	Brace/ Joint (Rj) (kips)	Pile or Leg Plasticity (Rf) (kips)	Pile pullout/ Plunging (Rfa) (kips)	Ru (Rufj or Rufl or Rufa) (kips)	(See Figures 4-8 to 4-10 for locations of failure events)	= (Ru/S)	= (Ru/R1) (#3)	= (Rf/Rf1)	= (Rfa/Rfa1)
ST 151 H	8 Leg - Grouted Single Battered K Braced 30" dia. piles 180' penetration	137 ft. 1964	Base Case	3,560	2,680	2,900	-	3,140	3,240	-	-	3,250	Failure of KT joints; first yielding of all piles; fully plastic section in the bottom horizontals	0.91	1.21	-	-
			Case-1	3,560	2,680	-	-	-	3,140	-	-	3,250	Failure of KT joints and fully plastic sections in the bottom horizontals	0.91	1.21	-	-
			Case-2	3,560	-	3,120	3,830	-	-	3,970	-	4,070	Fully plastic sections in all 8 piles at two levels	1.14	-	1.04	-
			Case-3	3,560	-	-	-	3,240	-	-	3,580	3,600	Three piles pullout and two piles plunge	1.01	-	-	1.10
ST 130A	8 Leg - Grouted Single Battered K Braced 30" dia. piles 175' penetration	140 ft. 1958	Base Case	1,990	-	1,300	1 720	-	-	1,830	-	1,830	First yielding in all piles; fully plastic section in piles	0.92	1.41	-	-
			Case-1	1,990	2,000 2,790	(strut) (joint)	1720 (leg 1st yield) 2100 (leg fully plastic)		2,400 2,930 2,200 (8 legs fully plastic)	(struts) (joints)	-	2,930	3-K joints fail, 6 struts buckle/ yield; fully plastic leg sections (all 8 legs in bottom bay)	1.47	1.20 1.05	(struts) (joints)	-
			Case-2	1,990	-	1,360	1,820	-	-	1,800	-	1,800	Fully plastic sections in all 8 piles below jacket leg extensions	0.90	-	1.11	-
			Case-3	1,990	-	-	-	2,500	-	-	2,860	2,880	Three piles pullout and four piles plunge	1.45	-	-	1.14
ST72 (T21)	4 Leg - Grouted Double Battered K Braced 36" dia. piles 170' penetration 15' leg extension	61 ft. 1969	Base Case	1,300	1,250	-	-	-	1,610	-	-	1,610	K and KT joints in two frames fail with fully plastic sections in bottom two jacket bays.	1.17	1.29	-	-
			Case-1	1,300	1,260	-	-	-	1,610	-	-	1,610	K and KT joints in two frames fail with fully plastic sections in bottom two jacket bays.	1.17	1.28	-	-
			Case-2	1,300	-	2,114	2,800	-	-	3,250	-	3,250	All four piles with fully plastic sections at two levels	2.36	-	1.25	-
			Case-3	1,300	-	-	-	2,700	-	-	2,700	2,770	Two piles pullout	2.01	-	-	1.00

Notes: (#1): Includes wave in deck load of 330 kips for ST151H
(#2): Values in bold indicates those picked for calibration.
(#3): Rl the lesser of Rj1,1; Rj1,2, Rfl1; and Rfa1.

Table 4-4: Capacity Analysis Results for Caisson Cases (Source - API/MMS Foundation Study [5]

Platform	Platform Characteristics		Analysis Case (#1)	Expected Maximum Hindcast Base Shear (kips)	Base Shear from Static Pushover Analysis (#2)			Displacement		Ratio Ult. Cap./ Andrew BS	System Factor Ult. Cap./ BS at First Member Failure (S2)/(S1)
	Configuration	Water Depth/ Year Installed			at First yield of Ist Section (S1) (kips)	at Fully Plastic Ist Section (kips)	at Ultimate Capacity (S2) (kips)	at Deck Level (ft.)	at Seabed Level (ft.)		
SPelto 10	30" dia. 180' penetration 12 degree lean	35 ft. 1984	Base Case	65	38 at 35' below	44	48	5 63	1 2	0.74	1.26
			Su increased by 100 %	65	54	69	-	-	-	-	-
SS135	48" dia. 95' penetration 15 degree leaning	53 ft. 1983	Base Case	132	119 at 40'-50' below	128 in 1" section	148	7.2	-	1 12	1.24
			Su increased 50 %	132	129	142	165	-	-	1.25	1.28
			Su increased 100%	132	138	154	178	-	-	1.35	1.29
SS136	48" dia. 100' penetration 30 degree leaning	50 ft. 1983	Base Case (upper bound)	139	173	197	224	7 24	1 96	1.61	1.29
			Ignored Sand layer	139	150	153	181	6 78	2.05	1.30	1.21

Notes: #1: Su denotes the undrained shear strength of soil
#2: Values in bold indicates those picked for calibration

Table 4-5: Comparison of Andrew Hindcasts

Platform Name (Orientation)	Water Depth (ft.)	1994 Hindcast (#1)			1992 Hindcast			Difference in Parameters 1994 vs. 1992		
		Maximum Wave Height (H1) (ft.)	Wave Direction from Plat. North (D1) (degree)	Current Speed in Wave Direction (C1) (ft/sec)	Maximum Wave Height (H2) (ft.)	Wave Direction from Plat. North (D2) (degree)	Current Speed in Wave Direction (C2) (ft/sec)	Wave Heights Ratio = (H1)/(H2)	Difference in wave Directions = (D1)/(D2)	Current Speeds Ratio = (C1)/(C2)
ST151K (N15W)	137	59 05	298.6	3 30	60 85	301 40	3 44	0.97	-2.8	0 96
ST130Q (N25W)	170	58.29	316.6	2.90	62.27	314 10	3 00	0 94	2.5	0 97
WD103A (N21W)	223	50.21	329 9	1.51	-	-	-	-	-	-
ST151J (N35W)	137	58 77	318.6	3 31	-	-	-	-	-	-
ST177B (N35W)	142	59.60	313 0	4 15	60.17	302.50	3 46	**0.99**	10.5	**1.20**
SS139 (T25) (N12W)	62	43 50	289 0	4 45	50.63	269 70	4 25	**0.86**	19.3	1 05
ST151H (N15W)	137	59 05	298.6	3 30	60 85	301 40	3 44	0.97	-2.8	0 96
ST130A (N25W)	140	55 43	314.5	2.88	60 95	311 10	3.41	0.91	3 4	**0.84**
ST72 (T21) (N12E)	61	46 90	276 0	3 96	49 74	245 30	4 26	0 94	30 7	0.93

Note : (#1) - See Appendix A for Wave Direction and Hindcast Data

Table 4-6: Comparison of Capacity Analysis Results: Andrew Phase I and II (#1)

Platform Name	Water Depth (ft.)	Andrew Phase II (#2)			Andrew Phase I			Ratios Andrew II/ Andrew I Results		
		Expected Max. Base Shear (kips)	Ultimate Capacity - Base Case (kips)	Ratio of Ult. Cap./ Base Shear (Ru/ S)	Expected Max. Base Shear (kips)	Base Case Ultimate Capacity (kips)	Ratio of Ult. Cap./ Base Shear (Ru/ S)	Expected Max. Base Shear (kips)	Ultimate Capacity (kips)	Ratio of Ult. Cap./ Base Shear (Ru/ S)
Survival Cases:										
ST151K	137	3,700	3,800	1.03	4,765	3,500	0.73	0.78	1.09	1.40
ST130Q	170	990	1,430	1.44	1,210	1,265	1.05	0.82	1.13	1.38
WD103A (#3)	223	2,140	4,660	2.18	-	-	-	-	-	-
Damage Cases:										
ST151J (#3)	137	4,450	5,000	1.12	-	-	-	-	-	-
ST177B	142	4,390	3,800	0.87	5,150	4,170	0.81	0.85	0.91	1.07
SS139 (T25)	62	1,060	1,640	1.55	1,690	1,340	0.79	0.63	1.22	1.95
Failure Cases:										
ST151H	137	3,560	3,250	0.91	4,210	4,000	0.95	0.85	0.81	0.96
ST130A	140	1,990	1,830	0.92	2,780	3,000	1.08	0.72	0.61	0.85
ST72 (T21)	61	1,380	1,610	1.17	1,615	1,980	1.23	0.85	0.81	0.95

Notes: (#1) - The capacity calibrated for both Phase I and Phase II differ from the capacity estimates given in this table.
See tables in Section 5 for the capacity levels calibrated in Phase II.
(#2) - The ultimate capacity estimates for the Base Case are shown.
(#3) - Platforms included in Phase II only.

Section 5
Calibration

5.1 APPROACH

The objective of the calibration is to determine a bias factor that can be used to improve the analytical process to more closely match true platform behavior under extreme storm conditions. The calibration process involves a comparison of platform performance determined analytically to that observed following a severe storm or hurricane. This study utilized 9 platforms that were heavily loaded during hurricane Andrew for calibration.

A number of parameters are required to estimate structural capacity and environmental loads. Parameters that affect the estimate of resistance include, for example, material yield strength, soil strength and density. Parameters that affect the estimate of wave load include, for example, drag and inertia coefficients. In principle, it is possible (with enough data) to "calibrate" the capacity and load models separately and determine bias factors specific to both the load and resistance formulations. It is also theoretically possible to establish bias factors for each of the individual parameters that affect the formulations. Such a calibration would require a significant amount of recorded data regarding both the loading and response of platforms during the hurricane. Unfortunately there were no load measurements available and the only data available regarding response was that of extent of damage. It was therefore not possible to calibrate the load and resistance separately nor was it possible to calibrate many of the specific items of the capacity analysis recipe. The calibration was simplified to determine the bias of a global measure of the platform capacity. Thus, as in Phase I, a bias factor "B" was introduced as a correction to the computed "safety factor" of the platform, defined as the ratio of resistance (R) to load (S):

$$\left[\frac{R}{S}\right]_{true} = B\left[\frac{R}{S}\right]_{computed} \qquad [5\text{-}1]$$

Thus, the "true" safety factor equals the "computed" safety factor (per the assessment process) times a bias (or correction) factor, B. A value of B greater than 1.0 would indicate (on average) that the current ultimate capacity analysis procedures provide conservative results. A value of B less than 1.0 would indicate (on average) unconservative ultimate capacity results. B is a random variable.

The calibration methodology that was used for this study was expanded upon the approach that was developed in the Phase I [1] study. Its main components are as follows (see Figure 5-1):

- Capacity analysis
- Reliability analysis
- Bayesian updating

The procedures and results of the capacity analysis are presented in Section 4. The procedures and results of the reliability analysis and Bayesian updating are presented in this section.

The basic procedure used for calibration has been refined during this study and its direct predecessors: Andrew Phase I and the API/MMS Foundation Study. The results of these earlier studies has affected the Phase II work and an overview of these studies is therefore provided in Section 5.2. The details of the procedure followed in Phase II and the results are provided in Sections 5.3 to 5.5.

5.2 BACKGROUND PROJECTS

The calibration approach and results of the Andrew Phase I and API/MMS Foundation studies are summarized as follows:

Andrew JIP - Phase I [1, 4]:

The capacity analysis results generated during Phase I relate best to the Base Case analysis (nonlinear jacket and foundation) results of Phase II. The probabilities of failure and likelihood functions for 13 platforms were determined using a program developed by PMB (entitled "PF"). The PF program was used to determine the failure probabilities using a 4-level direct integration approach (see Section 5.4 for theoretical details).

The posterior distribution of bias factor (B) was determined to have a mean value and a COV of 1.19 and 0.11. This was a system bias factor applicable to the overall behavior of platform (jacket and foundation combined).

The Andrew Phase I capacity analysis indicated that the ultimate capacity of the foundation is mobilized at very small pilehead displacements. It was determined that these deformations are so small that they may not be observable by a diver during field inspections. Field inspections were performed subsequent to Phase I, specifically addressing foundations failures. No foundation failures were observed [6, 7]. This suggests that:

1. The foundation bias is higher then the global bias or
2. Some damage can occur to a foundation which may not be visible.

The Phase I analysis predicted foundation failures in several platforms, none of which were observed to have failures in the foundation. These results indicated that the biases in foundation capacity predictions could be higher than in the jacket capacity estimates. Thus it would be beneficial to establish bias factors separately for jacket and foundations instead of a single (system) bias factor. This was a key factor in determining the Phase II scope objectives

API/MMS Foundation Study [5]:

This study focused on bias factors specific to the foundation. Therefore, this study included two additional capacity analysis to suppress the jacket failure modes, and thus determine the ultimate capacity associated with foundation failure modes Three steel jacket platforms were analyzed, each

of which had no observed failures of the foundation. Two of these platforms had significant observed damage to the jacket structure, whereas the third had none.

The foundation capacity estimates and earlier API research [27, 28] indicated that the biases associated with the foundation lateral and axial capacities varied significantly and, therefore, the biases in these two modes were separated. The foundation bias factors for the lateral (B_{fl}) and axial (B_{fa}) were determined using the capacity estimates corresponding to analyses performed for those specific failure modes (i.e. similar to that described as Case 2 and Case 3 for the Phase II study).

Due to the inconclusive observations regarding the foundation behavior during Andrew, three alternative structural damage interpretations of field observations were investigated to support the calibration of both bias factors (B_{fl} and B_{fa}) The alternative classifications considered for foundation lateral bias factor (B_{fl}) were:

Case A: Fully plastic section event did not occur in any pile
Case B: Fully plastic section events did not occur in several piles
Case C: Fully plastic section event did occur in one pile and others were undamaged

The classifications considered for foundation axial bias factor (B_{fa}) were:

Case D: Pullout or plunging event did not occur in any pile
Case E: Pullout/plunging events did not occur in several piles
Case F: Pullout/plunging event did occur in one pile and other piles were undamaged

The previous API research completed by Dr. Wilson Tang [27, 28] was used to establish the prior distributions of the foundation bias factors. The prior distributions of the foundation lateral bias factor was assumed to be normally distributed with a mean of 1.0 and COV of 0.3. The prior distribution of the foundation axial bias factor was assumed to have a mean of 1.3 and COV of 0 3.

The reliability analysis and Bayesian updating procedures used in the Foundation Study were the same as those used during the Andrew Phase I study. Two separate analyses were performed to determine uncoupled foundation bias factors. The following results were obtained:

- Assumed prior distributions of bias factors: B_{fl} , N (1.0, 0.3); B_{fa} , N (1.3, 0.3)
- The mean values of the posterior distributions of B_{fl} were similar for Case A and B (Case A B_{fl}= 1.32 and Case B B_{fl}= 1.26).
- The mean value of the posterior distribution of B_{fl} for Case C was the same as that assumed for the prior distribution (i.e. 1.0).
- The mean values of the posterior distributions of B_{fa} were similar for Case D and E (Case D B_{fa} = 1.73 and Case E B_{fa} = 1.66).
- The mean value of the posterior distribution of B_{fa} for Case E was 1.53, which was higher than the value assumed for the prior distribution (i.e. 1.3)

- The foundation lateral bias factor, B_{fl} was reduced by 17 percent (to 1.1 for Case A and to 1.04 for Case B) when the effect of three caissons (with observed foundation damage) was included

A conclusion of this work was that the individual foundation bias factors were estimated to be significantly larger that the global system bias factor determined during Phase I and that the two foundation bias factors were very dissimilar.

Influence of Foundation Study on Phase II Scope:

The original scope proposed for Andrew Phase II was to determine two bias factors, one each for the jacket and foundation. The scope was changed as a result of the API/MMS Foundation project to determine three bias factors (one for the jacket structure and two for the foundation). This change was made due to the significant difference in B_{fl} and B_{fa} seen from the Foundation study. The following three bias factors were therefore identified for Phase II:

- Bias in the jacket structure, B_j
- Bias in foundation lateral capacity, B_{fl}
- Bias in foundation axial capacity, B_{fa}

The bias factors (B_{fl} and B_{fa}) were determined by calibrating the predicted load levels corresponding to fully plastic sections or pullout/plunging of several piles instead of the first pile to assure conservatism. These calibration conditions are the same as the Case B and Case E conditions investigated in the Foundation study. The other four calibration cases investigated during the Foundation study were not repeated in Phase II.

5.3 CALIBRATION PROCEDURE DETAILS

The three stage calibration procedure shown in Figure 5-1 was applied to nine steel jacket platforms selected for this project (see Section 1.3 for platform details) In addition, the three caissons analyzed in the API/MMS Foundation project were considered in this phase to determine the sensitivity of the foundation lateral bias factor.

5.3.1 Capacity Analysis

The capacity analyses described in Section 4 were performed to establish the lateral load levels corresponding to successive inelastic events in the jacket and its foundation and to determine ultimate capacity. Four analyses were completed for each platform for a single storm approach direction (see Sections 4.1 and 4.2 for discussion):

- Base Case - All failure modes modeled
- Case-1 - Only jacket failure modes modeled
- Case-2 - Only lateral pile failure modes modeled
- Case-3 - Only axial pile failure modes modeled

The load levels corresponding to the following failure modes were determined from the capacity analysis (Tables 4-2 to 4-4) to define the calibration load levels and conditions.

- Jacket capacity:
  - Failure of first K-joint or a brace
  - First yield of first leg/pile section
  - Full plasticity of first leg/pile section
  - Failure of observed damage to K-joints or braces
  - Failure of unobserved damage to K-joints or braces (system capacity)
  - Full plasticity of several pile sections (system capacity)
- Foundation lateral capacity:
  - First yield of first pile section
  - Full plasticity of first pile section
  - Full plasticity of several pile sections (system capacity)
- Foundation axial capacity:
  - Pullout/plunging of first pile
  - Pullout/plunging of several piles (system capacity)

In the case of the caisson platforms the load levels at first yield of a section, at fully plastic section, and at ultimate capacity were identified. All three caissons were classified in the damage/failure category.

5.3.2 Calibration Conditions

Load levels defined from the capacity analysis corresponding to the various levels of observed performance (e.g., extent of damage, lack of damage) were selected to define the calibration conditions.

The calibration conditions used in Phase II differed from those in the Phase I study in several ways. A primary difference was that, in Phase II, survival platforms were calibrated at no damage load levels. The net effect of this more accurate assumption is to increase the bias for survival platforms.

The following calibration conditions were used in this phase:

- Survival — No damage or only minor, non-structural, damage identified.
- Type I Damage Case — Known damage to the jacket and foundation assumed to be intact.
- Type II Damage Case — Damage is known but not specifically identified or attributed to the jacket or foundation.
- Type I Failure Case — Known failure of the jacket and foundation assumed to be intact.

- Type II Failure Case — Failure is known but not specifically attributed to the jacket or foundation.

The field observations and interpretations made for calibration are summarized for each of the platforms as follows (In cases where multiple interpretations are identified, all were applied):

Survival cases

Observations: No damage occurred in the jacket or its foundation during Andrew.

Interpretations for calibration: The actual applied Andrew load level was lower than the level of load required to cause first damage to the jacket frame (K-joint or diagonal brace failures).

The actual applied Andrew load level was lower than the level of load required to cause damage to several piles (fully plastic sections formation and/or pullout/plunging).

Platforms in this category: ST151K, ST130Q, WD103

Type I Damage Cases

Observations: Jacket braces and/or joints were damaged during Andrew. No damage occurred to the foundation during Andrew.

Interpretations for calibration: The actual applied Andrew load level was higher than the level of load required to cause the amount of brace or joint damage that was observed.

The actual applied Andrew load level was lower than the level of load required to cause failure of the next primary element in the jacket.

The actual Andrew load level was lower than the level of load required to cause damage to several piles (fully plastic sections formation and pullout/plunging).

The foundation was stronger than the jacket

Platforms in this category. ST151J and ST177B

Type II Damage Cases

Observations:	Platform was damaged during Andrew. Field observations were not conclusive as to where the damage occurred.
Interpretations for calibration:	The actual applied Andrew load level was higher than the level of load required to cause brace or joint damage. The actual Andrew load level was higher than the level of load required to cause damage to several piles (fully plastic sections formation or pullout/plunging)
Platforms in this category:	SS139 (T25)

Type I Failure Cases

Observations:	Platform collapsed or was rendered completely unserviceable and the failure occurred in the jacket part of the platform during Andrew. No damage occurred to the foundation during Andrew.
Interpretations for calibration:	The actual applied Andrew load level was higher than the ultimate capacity of the jacket structure. The actual Andrew load level was lower than the level of load required to cause damage to several piles (fully plastic sections formation or pullout/plunging). The foundation was stronger than the jacket.
Platforms in this category:	ST151H and ST130A

Type II Failure Cases

Observations:	Platform collapsed during Andrew. Field observations did not indicate damage location.
Interpretations for calibration:	The actual applied Andrew load level was higher than the ultimate capacity of jacket structure. The actual Andrew load level was higher than the level of load required to cause damage to several piles (fully plastic sections formation or pullout/plunging)

Platforms in this category: ST72 (T21)

Tables 5-1 to 5-3 present the load levels used in calibration and the calibration conditions for all nine steel jacket platforms. These load levels were used as the best estimate of the capacity (R) in the analysis.

5.3.3 Reliability Analysis

The probabilities of occurrence of failure-survival-or damage was determined by the structural reliability analysis. Some modifications were made to the Phase I probability of failure formulation to suit the FORM/SORM analysis that was used in place of the direct integration approach followed in Phase I.

Base Shear Coefficients:

The load is represented by an empirical formulation in the reliability analysis. This formulation defines the base shear (S) as a function of wave height (h) and current (u). A computer code developed during Phase I study ($C_1C_2C_3$) was updated to include another coefficient, C_4 to provide a better definition of the change in total load as deck wave inundation occurs. The empirical formulation of base shear and the coefficients used are presented in Section 5.4. The program "C1C2C3C4" was used to perform a three-dimensional iteration to determine a single set of the best fit coefficients using base shear values computed for different combinations of wave and current.

This data was developed by performing a large number of wave load analyses. The platform specific base shear coefficients (C_1, C_2, C_3, and C_4), applicable for a range of wave heights and currents, were then determined.

Probabilities of Occurrence:

The joint distributions of three bias factors were determined. The PF program was not adequate to include the multiple interpretations of field observations included in the calibration conditions. The RELACS software [29] was selected for use within the Phase II calibration. This program determines the probabilities of failure by use of advanced reliability analysis methods and also system reliability analysis. The first and second order reliability methods (FORM and SORM) [30, 31, 32] were used in this work. Details of this procedure are given in Section 5 4. Additional features were added to RELACS during the course of this project to obtain the probability of occurrence for specific calibration conditions and for a large number of combinations of the three bias factors The probabilities of occurrence for the different combinations of b_j, b_{fi}, and b_{fa} define the joint likelihood function for each observed behavior.

Likelihood Function for Failure Case:

When a single bias factor is used and a failure is observed the likelihood of the bias factor B being less than a given value ('b') is represented as follows:

$$lk(b \mid failure) = P[failure \mid b] \quad [5\text{-}2]$$
$$= P_f(b)$$

in which $P_f(b)$ is the probability of failure for the platform at B = b. When three bias factors are used the joint likelihood function for a failure case would be represented as follows:

$$lk[b_j, b_{fl}, b_{fa} \mid failure] = P[failure \mid b_j, b_{fl}, b_{fa}]$$
$$= P_f(b_j, b_{fl}, b_{fa}) \quad [5\text{-}3]$$

Likelihood Function for Survival Case:

The likelihood function for survival cases (no observed damage) becomes:

$$lk(b \mid survival) = P[no\ damage \mid b]$$
$$= 1 - P_f(\alpha_1\, b) \quad [5\text{-}4]$$

where α_1 is the ratio of predicted load level at first element failure to the ultimate capacity estimate.

Likelihood Function for Damage Case

The likelihood function for a damaged platform case is defined based on the probability that the observed damage lies in the same fractional interval of the capacity to load ratio as predicted by the pushover analysis. The predicted ratios corresponding to the observed damage and to that of one additional increment of damage (i.e., one more failed component) are denoted by α_1 and α_2 respectively. The resulting likelihood function for a damage platform case would be:

$$lk(b \mid damage) = P_f(\alpha_1\, b) - P_f(\alpha_2\, b) \quad [5\text{-}5]$$

Likelihood Function for Multiple Platforms

The above likelihood functions represent the information about the bias factor resulting from the observed behavior of an individual platform. The combined likelihood function of *B* given the observed behavior of a number of platforms, with a combination of survivals, damages, and failures, is obtained by direct multiplication of the likelihood functions for each of the individual platforms as follows:

$$lk(b|n-observations) = \prod_{platform\ i}^{n} [lk_i(b|observation)] \quad [5\text{-}6]$$

where n is the total number of platforms.

Joint Likelihood Function for Multiple Platforms:

The combined joint likelihood function given the observed behavior of a number of platforms with a combination of survivals, damages, and failures, is obtained by direct multiplication of the individual joint likelihood functions (e.g , Equation 5-3 for a failure case) as follows:

$$lk(b_j, b_{fl}, b_{fa}|n-observations) = \prod_{platform\ i}^{n} \left[lk_i(b_j, b_{fl}, b_{fa}|observation)\right] \quad [5\text{-}7]$$

5.3.4 Bayesian Updating

The objective of the calibration is to establish a distribution on "B" that is consistent with the observed behavior. The updating is based on the Bayes theorem of probability [30] which, for a single bias factor states:

$$f''_B(b) \propto f'_B(b)\ lk(b|\text{new information}) \quad [5\text{-}8]$$

in which f'_B (b) is the "prior" distribution of bias factors, f''_B (b) is its "posterior" distribution, and lk(b|new information) is the "likelihood function" which reflects the information about b obtained through the observations.

In case of multiple bias factors, the joint posterior distribution of the bias factors would become:

$$f''_{B_j,B_{fl},B_{fa}}(b_j, b_{fl}, b_{fa}) \propto f'_{B_j,B_{fl},B_{fa}}(b_j, b_{fl}, b_{fa})\ lk(b_j, b_{fl}, b_{fa}|n-observations) \quad [5\text{-}9]$$

where the joint prior distribution is assumed as the product of independent individual priors:

$$f'_{B_j,B_{fl},B_{fa}} = f'_{B_j}\ f'_{B_{fl}}\ f'_{B_{fa}} \quad [5\text{-}10]$$

The marginal posterior distributions, mean and COV of the three bias factors are determined from this joint distribution. The change in the mean values of the bias factors from the prior to the posterior distribution provides the bias (conservatism or non-conservatism) in the ratios of capacity to load predictions for each failure mode.

In most cases the joint posterior distribution will not simply be the product of marginal posteriors (i.e., the 3 B's are not independent a "posteriori"). The bias factors are interdependent due to the fact that a failure observed in the jacket implies that axial foundation capacity is larger than the jacket capacity.

The Bayesian analysis method was used previously during the cooperative project on offshore platform reliability organized by Amoco [33, 34]. Bayesian applications are also presented in the API PRAC Project 89-22 Report [35], and other literature [36, 37].

5.4 THEORY FOR DEVELOPMENT OF BIAS FACTORS

The conventional formula for computation of the probability of failure of a structure is:

$$P_f = \int_0^{\infty} \{1 - F_s(x)\} f_R(x) dx \qquad [5\text{-}11]$$

where f_R is the probability density function (PDF) of capacity and F_s is the cumulative distribution function (CDF) of load

Normally the random load (S) represents the maximum load in any one-year period. In this hindcast case, the load is the maximum load subjected to the structure during Andrew. The load is represented by the base shear (BS) which, for a single wave, will be represented by

$$BS = [C_1][h + C_2 u]^{C3} \varepsilon_0 \qquad \text{for } h \le h_d \qquad [5\text{-}12\text{-a}]$$

$$BS = [C_1 + C_4(h - h_d)][h + C_2 u]^{C3} \varepsilon_0 \qquad \text{for } h > h_d \qquad [5\text{-}12\text{-b}]$$

in which h is a wave height, h_d is the wave height at which the wave crest hits the deck and u is a current C_1, C_2, C_3 and C_4 are the coefficients that are determined for a range of wave heights and currents in a specific storm direction for a platform. These coefficients are found by fitting this empirical equation to calculated base shears for various pairs of h and u values ε_0 represents a random "correction factor" in base shear estimates, due to wave-to-wave variability, and is assumed to have a log-normal distribution with a mean of 1.0 and COV of 0.20.

The FORM/SORM analysis used in Phase II required a continuous and differentiable function and thus one set of base shear coefficients were determined for the complete range of wave heights. The use of Eq. 5-12-a, over the complete range of wave heights resulted in large differences between the input and computed base shears for cases where the wave inundated the deck. Therefore, an additional coefficient (C_4) was introduced. The differentiability of the function was further improved by introducing a polynomial function for the wave height range (h_d -5) to (h_d +5).

Equations 5-12 a and b represent the (random) base shear associated with a specified wave height h and current velocity u (in a specified direction). In any given 1 hour segment of the storm, with significant wave height h_s and current u, there will be a sequence of N waves with random wave heights, H. We assume N is approximately equal to $3600/T_p$, where T_p is the period associated with the maximum wave of the wave spectrum. It is assumed that the probability distribution of each random wave height (H) follows the empirical Forristall distribution [38]:

$$f_{H|H_s}\left(h\middle|H_{sj}=h_s\right)=\frac{\alpha 4^{\alpha}}{\beta H_s}\left(\frac{x}{H_s}\right)^{\alpha-1}\exp\left[-\frac{4^{\alpha}}{\beta}\left(\frac{x}{H_s}\right)^{\alpha}\right] \qquad [5\text{-}13]$$

in which $\alpha = 2.126$, $\beta = 8.42$, and H_s is the significant wave height.

Using the probability distribution of H and the formulation of base shear, the final (marginal) CDF for the maximum base shear, F_{MBS}, during the multi-hour (unidirectional) "storm" is obtained as follows:

$$F_{MBS}(x)=\int_{-\infty}^{\infty}\int_{-\infty}^{\infty}\prod_{\substack{hour\\ j}}^{No.ofSig\ Hours}\left\{\int F_{BS}\left(x\middle|H=h,U=u_j\right)\quad f_{h|H_s}\left(h\middle|H_{Sj}=h_{sj}\right)dh\right\}^{Nj} f_{\varepsilon_1}(\varepsilon_1)f_{\varepsilon_2}(\varepsilon_2)d\varepsilon_1 d\varepsilon_2 \qquad [5\text{-}14]$$

in which F_{BS} is the lognormal cumulative distribution implied by Equations 5-12 a and b, N_j denotes the number of random waves in an hour with significant wave height h_{sj} and current u_j. ε_1 and ε_2 represent the significant wave height and current errors in the hindcast. In this equation h_{sj} is equal to (H_{sj} ε_1) and u_j is equal to (U_j ε_2), where H_{sj} and U_j are the hindcast estimates.

The probability of failure is then calculated by numerical integration of Eq. 5-11, assuming a lognormal distribution on R, with a specified mean and COV. Failure is presumed to be associated with $BR/S < 1$ rather than $R/S < 1$, where B is the bias factor. The probability of failure for a given bias factor (B) is obtained as follows:

$$P_f(b)=\int_0^{\infty}\left\{1-F_s(bx)\right\}f_R(x)dx \qquad [5\text{-}15]$$

The "nested FORM/SORM" reliability analysis methods [39] were used to determine the probability of failure. The ISSORM (second order reliability method with a correction based on importance sampling) method [31, 32] was also used to provide a check on the FORM/SORM results. A test performed by Risk Engineering, Inc. during Phase I indicated that the RELACS results were comparable to those obtained using PF program.

The "nested FORM/SORM" analysis utilized different random variables that are integrated in inner and outer loops of the algorithm. The model was formulated as follows:

Inner loop random variables, Y

- individual wave height, $H \mid H_s$
- error in base shear, ε_o

Outer loop random variables, X

- capacity, R
- significant wave height, H_s
- current, V_c (note that in equations 5-12 to 5-14, current is denoted by U)

The distributions and uncertainties of various quantities used in the analysis were as follows:

Item	Distribution	Expected Value	COV
Capacity, R	Log-Normal	per analysis	0 15 for jacket capacity 0 20 for lateral pile capacity 0 30 for axial pile capacity
Individual wave height, (H/H_s)	Fornstall	per hindcast	per formula
Hindcast error in H_s, ε_1	Log-Normal	1 0	0 10
Hindcast error in current U (or V_c), ε_2	Log-Normal	1.0	0 15
Wave-to-wave error in base shear S, ε_o	Log-Normal	1 0	0 20 for wave-below-deck case 0.25 for wave-in-deck case

The reliability analysis model was based on the following correlation of random variables:

- Wave-to-wave variabilities in H and ε_o were assumed to be independent.
- Hour-to-hour uncertainties in H_s and U were considered to be independent.
- Uncertainties in H_s and U were considered to be independent from site-to-site during Andrew (i.e., it was assumed that no overall overprediction or underprediction of the wind field or errors in track location, which would affect all H_s values, exists in the hindcast).
- Platform-to-platform uncertainties in capacities (R) were considered independent. Some dependence in capacity could come from common material properties of steel, soil, general scour effect, bias in platform designs, etc. Variation in the uncertainties in capacity were found to have a minor impact on the likelihood functions. Defining a correlation in capacity

would be very difficult. It was therefore not considered practical to include such correlations in the analysis

Some of these assumptions were made based on the results of sensitivity analysis completed in Phase I that determined the effect of variations in the magnitudes of mean and COV's of various random variables on the likelihood functions. The Phase I sensitivity analysis also indicated that the uncertainties in H_s and in the error in base shear (ε_o) have a dominant effect on the analysis as compared to all the other variables.

In order to solve this problem using the FORM/SORM algorithms, Eq 5-15 had to be modified to the conditional form as follows:

$$P_f(b) = \int P_f(x;b) f_X(x) dx \qquad [5\text{-}16]$$

where,

$$P_f(x;b) = P\left[g(Y,X;b) < 0 | X = x\right] \qquad [5\text{-}17]$$

where $P_f(x; b)$ represents the conditional failure probability of a component or a system for a given set of random variable values denoted by vector X (H_s, V_c, R) and a given value of b. The random variables for each wave height (H) and error in base shear (ε_0) are denoted by vector "Y." $f_X(x)$ represents the joint distribution of H_s, V_c (current), and R. The form of the limit state function (or g-functions) in the FORM/SORM analysis for the conditional inner loop is as follows:

$$g(Y, x; b) = bR - S \qquad [5\text{-}18\text{-}a]$$

or

$$g(Y, x; b) = bR - \left[C_1 + C_4(h - h_d)\right]\left[h + C_2 u\right]^{C3} \varepsilon_0 \qquad [5\text{-}18\text{-}b]$$

The inner loop determines the probabilities of failure for a single wave and set of outer loop variable values (denoted by X).

The outer loop (external) limit state function for a single event (probability of failure during a seastate) is as follows:

$$g(U, X; b) = U - \Phi^{-1}\left[P_f(X; b)\right] \qquad [5\text{-}19]$$

The outer loop limit state function includes an auxiliary variable (U) which was originally proposed by Wen and Chen [39]. The auxiliary random variable U has a standard normal distribution with a mean of 0 and a standard deviation of 1.

The integration over all possible outcomes of combinations of random variables in vector "X" is obtained by use of the law of total probability as follows:

$$P_f\ (b) = \int P\left[\left\{U - \Phi^{-1}\left(P_f(X;b)\right)\right\}<0\right] f_X(x)dx \qquad [5\text{-}20]$$

In case of multiple waves within a seastate and considering that events within each seastate are independent of each other, the outer loop g - function is generalized as:

$$g(U,X;b) = U - \Phi^{-1}\left[P\left\{g(Y,X;b)<0 \middle| X=x\right\}^n\right] \qquad [5\text{-}21\text{-a}]$$

or

$$g(U,X;b) = U - \Phi^{-1}\left[\nu\left\{1-\left(1-P_f(x;b)\right)^n\right\}\right] \qquad [5\text{-}21\text{-b}]$$

Where "n" is the number of waves in a storm hour ($n=3600/T_p$) and "ν" represents the storm rate of occurrence (which is 1.0 in this case). Variability in T_p was not considered in this analysis. The Phase I sensitivity analysis indicated that variation in the COV of T_p, had no effect on the likelihood function. It was therefore considered adequate to ignore variability in T_P and therefore, the number of waves for each storm hour were equal. $P_f(x; b)$ represents the failure probability for one wave and is determined by the condition in Eq. 5-17.

The likelihood function is obtained by processing Eq 5-20 for a number of different "b" values.

$$lk\ [b \mid failure\ ] = P[failure \mid b] = P_f(b) \qquad [5\text{-}22]$$

The above formulation is given for a single component. This formulation is extended to multiple "components," (i e., multiple modes of failure and multiple hours during which the event might occur). The multiple component calibration conditions are discussed in the next section.

5.5 CALIBRATION TASKS AND RESULTS

The following five calibration tasks were performed:

Task #1: Develop the joint and marginal distributions of the three bias factors. Evaluate the effect of the three selected caissons on the marginal distribution of the foundation lateral bias factor.

Task #2: Develop a single (system) bias factor using the new hindcast, base case capacity analysis results and calibration conditions.

Task # 3: Determine the sensitivity of the bias factors to alternative interpretations of field observations for the two platforms in the failure category.

Task #4: Determine the sensitivity of posterior distributions to variations in the prior distributions of the bias factors.

Task #5: Develop an example application of the bias factors to determine the annual failure probability of a platform

5.5.1 Joint and Marginal Distributions of Bias Factors

The calibration conditions for each platform are summarized in Tables 5-1 to 5-3. These conditions were based on a comparison of capacity analysis predictions with the post Andrew field observations, as discussed in Section 5.3. The expected maximum base shear and the load levels corresponding to specific levels of response shown in these tables were based on the capacity analysis results which were presented in Tables 4-1 to 4-3.

The five calibration conditions identified in Section 5.3.2 were formulated to perform multiple component system reliability. The reliability analysis was performed for 3 to 5 hour segments of the hindcast data and included all hours which were likely to contribute to the probability calculations.

The system reliability analysis with 3 to 5 storm hours of data would require 9 to 15 components (a product of the number of storm hours and the number of bias factors) respectively. This produced a prohibitive level of complexity and an approach was therefore developed to reduce the number of components to the number of storm hours considered for a platform. This was done by introducing a new distribution to represent the minimum of two or three log-normal distributions of capacity.

The analysis was performed using both FORM and SORM and the results were found to be similar. The inner loop system reliablility analysis was done using first order reliability method. Second order reliability method results were determined in the outer loop analysis for each combination of three bias factors.

5.5.1.1 Formulation of Calibration Conditions

The formulations for each of the calibration conditions are presented for two models as follows:

- A complete system reliability analysis including two storm hours and all three capacities (i e. 6 components)
- A reduced system with only two components

Survival Cases:

The probability of survival (P_s) with no damage was computed based on the following calibration condition:

P_s = P [Andrew load level during hour-1 and hour-2 < Capacity level associated with the first predicted event in the jacket and its foundation system]

$$= P[\{(S < b_j R_{j1}) \cap (S < b_{fl} R_{fl1}) \cap (S < b_{fa} R_{fa1})\}_{hour\text{-}1} \cap \{(S < b_j R_{j1}) \cap (S < b_{fl} R_{fl1}) \cap (S < b_{fa} R_{fa1})\}_{hour\text{-}2}]$$

$$= P[\{S < \min.(b_j R_{j1}, b_{fl} R_{fl1}, b_{fa} R_{fa1})\}_{hour\text{-}1} \cap \{S < \min.(b_j R_{j1}, b_{fl} R_{fl1}, b_{fa} R_{fa1})\}_{hour\text{-}2}] \quad [5\text{-}23]$$

The system reliability analysis was reduced from 6 parallel components (3 failure modes, 2 storm hours) to 2 components (2 storm hours) in this case by introducing a distribution which represents the minimum of the three log-normal distributions (jacket, foundation lateral and axial capacities). These components represent the probability of survival of a platform against all failure modes during each storm hour.

The platforms analyzed in this category included ST151K, ST130Q, WD103A.

Type I Failure Case:

The platforms analyzed in this category included ST151H and ST130A. The structural damage to the jackets (K-joints and braces) was known. No foundation damage was observed in the field inspections. This case was formulated as a conditional failure probability problem; the jacket collapsed and the foundation was not damaged, implying that the foundation was stronger than the jacket.

$$P_f = P[\text{jacket collapsed} \mid \text{foundation survived}] \times P[\text{foundation survived}]$$

$$= P[E_1 \mid E_2] \times P[E_2]$$

$$= P[\{S > b_j R_j \mid (b_j R_j < b_{fl} R_{fl} \cap b_j R_j < b_{fa} R_{fa})\}_{hour\text{-}1} \cup \{S > b_j R_j \mid (b_j R_j < b_{fl} R_{fl} \cap b_j R_j < b_{fa} R_{fa})\}_{hour\text{-}2}] \times P[(b_j R_j < b_{fl} R_{fl} \cap b_j R_j < b_{fa} R_{fa})]$$

$$= P[\{S > b_j R_j \mid \min.(b_{fl} R_{fl}, b_{fa} R_{fa}) > b_j R_j\}_{hour\text{-}1} \cup \{S > b_j R_j \mid \min.(b_{fl} R_{fl}, b_{fa} R_{fa}) > b_j R_j\}_{hour\text{-}2}] \times P[\min.(b_{fl} R_{fl}, b_{fa} R_{fa}) > b_j R_j] \quad [5\text{-}24]$$

In this expression, each component in the system reliability analysis represents the probability of load exceeding the jacket capacity (event E_1) during each storm hour. This event is conditioned on the second calibration condition; that the foundation survived (i.e., the lateral and axial foundation capacities were more than the jacket capacity (event E_2)).

Type II Failure Case:

Failure was observed for ST72 but was not specifically attributed to either the jacket or foundation. Platform ST72 (T21) was analyzed in this category. The calibration conditions were therefore formulated in the following way:

$$P_f = P[\text{Andrew load level in hour-1 or hour-2} > \text{Ultimate capacity of jacket or its foundation system}]$$

$$= P[\{(S > b_j R_j) \cup (S > b_{fl} R_{fl}) \cup (S > b_{fa} R_{fa})\}_{\text{hour-1}} \cup \{(S > b_j R_j) \cup (S > b_{fl} R_{fl}) \cup (S > b_{fa} R_{fa})\}_{\text{hour-2}}]$$

$$= P[\{S > \min.(b_j R_j, b_{fl} R_{fl}, b_{fa} R_{fa})\}_{\text{hour-1}} \cup \{S > \min.(b_j R_j, b_{fl} R_{fl}, b_{fa} R_{fa})\}_{\text{hour-2}}] \quad [5\text{-}25]$$

This formulation includes 2 components in series, each representing the probability of failure during a storm hour when the loading exceeds any of the capacities.

Type I Damage Case:

Platforms ST151J and ST177B, were analyzed in this category. Both of these platforms experienced damage to the jacket structure. No damage was observed in the foundation in either case. This calibration condition uses the conditional system reliability problem formulated for the "Type I Failure Case." In this case, the probability of occurrence of the Andrew load level being within the calibrated load levels (Table 5-2) was determined by subtraction of the probability computations at the bounds of the load range as follows.

$$P_f = P_{f1} - P_{f2}$$

$$= P[E_1 \mid E_2] \times P[E_2] - P[E_3 \mid E_2] \times P[E_2]$$

$$= P[\{S > b_j R_{j1} \mid \min.(b_{fl} R_{fl}, b_{fa} R_{fa}) > b_j R_{j1}\}_{\text{hour-1}} \cup \{S > b_j R_{j1} \mid \min.(b_{fl} R_{fl}, b_{fa} R_{fa}) > b_j R_{j1}\}_{\text{hour-2}}] \times P[\min.(b_{fl} R_{fl}, b_{fa} R_{fa}) > b_j R_{j1}] -$$

$$P[\{S > b_j R_{j2} \mid \min.(b_{fl} R_{fl}, b_{fa} R_{fa}) > b_j R_{j1}\}_{\text{hour-1}} \cup \{S > b_j R_{j2} \mid \min.(b_{fl} R_{fl}, b_{fa} R_{fa}) > b_j R_{j1}\}_{\text{hour-2}}] \times P[\min.(b_{fl} R_{fl}, b_{fa} R_{fa}) > b_j R_{j1}] \quad [5\text{-}26]$$

where P_{f1} and P_{f2} are formulated in the similar way as the Type I failure case (Eq. 5-24);
R_{j1} represents the capacity level at which observed damage was predicted;
R_{j2} used in P_{f2} represents capacity level at which next damage is predicted;

The conditioning for the foundation capacity for both P_{f1} and P_{f2} were done at the capacity level, R_{j1}.

Type II Damage Case:

Platform SS139 (T25) was analyzed in this category. SS139 experienced some damage to the jacket and the behavior of foundation was not known. The calibration conditions were formulated in the following way:

$$P_f = P\,[\text{ Andrew load level in hour-1 or hour-2} > \text{Capacity level at jacket damage or damage to multiple piles }]$$

$$= P\,[\{(S > b_j R_j) \cup (S > b_{fl} R_{fl}) \cup (S > b_{fa} R_{fa})\}_{\text{hour-1}} \cup \{(S > b_j R_j) \cup (S > b_{fl} R_{fl}) \cup (S < b_{fa} R_{fa})\}_{\text{hour-2}}]$$

$$= P\,[\{S > \min.\,(b_j R_j, b_{fl} R_{fl}, b_{fa} R_{fa})\}_{\text{hour-1}} \cup \{S > \min\,(b_j R_j, b_{fl} R_{fl}, b_{fa} R_{fa})\}_{\text{hour-2}}\,] \qquad [5\text{-}27]$$

This formulation includes 2 components in series, each representing probability of failure during a storm hour.

5.5.1.2 Joint Likelihood Functions and Posterior Distributions

The joint likelihood functions for each of the platforms were determined using the above formulations. The probabilities of occurrence (survival, damage, or failure) were determined for different combinations of values for three bias factors. The values of b_j and b_{fl} were varied from 0.6 to 1.8 and b_{fa} was varied from 1.0 to 2.0. The marginal likelihood functions were generated from the joint likelihood functions for comparison purpose. The joint posterior distributions of the three bias factors were then obtained by product of the joint likelihood functions and the respective prior distributions. The following prior distributions were used,

Jacket structure (B_j)	Mean = 1.0,	COV = 0.3
Foundation lateral (B_{fl})	Mean = 1.0,	COV = 0.3
Foundation axial (B_{fa})	Mean = 1.3,	COV = 0.3

The joint and marginal likelihood functions for each of the platforms are given in Appendix E. The joint and marginal posterior distributions for three selected platforms, ST151K, ST151J, and ST130A (one in each category), are also given in Appendix E. The estimates of the mean and the COV of each of the bias factors are provided in Tables 5-1 and 5-3. The mean and COV for each group are also provided in these tables.

Survival Cases (Table 5-1):

The joint likelihood functions for all three survival platforms are provided in Figure 5-2(a) These three joint distributions (i.e., three different pairs of the three biases) were developed from the joint distributions of all three biases. The marginal likelihood functions for the individual biases are given in Figure 5-2(b). These were developed using the joint distributions of the three pairs of biases. The joint and marginal likelihood functions for the platforms under the survival category are given in Figures E-1, E-3, and E-4 in Appendix E.

The joint and marginal posterior distributions for platform ST151K are given in Figures Figure E-2(a) to E-2(c). The mean values of the bias factors shift to 1.33, 1.15, and 1.40 for B_j, B_{fl}, and B_{fa}, respectively. The COVs reduce from 0.3 to 0.16 to 0.21.

The joint and marginal distributions of each bias factor, including the effect of all three survival platforms, are given in Figures 5-3(a) to 5-3(c). The mean values shift to 1.35, 1.19 and 1.41 for B_j, B_{fl}, and B_{fa}, respectively. The posterior COVs range from 0.16 to 0.20. These results indicate that the contributions of the ST130Q and WD103A platforms are marginal as compared to the contribution of ST151K.

Damage Cases (Table 5-2):

The joint likelihood functions for all three damaged platforms are provided in Figure 5-4(a) The marginal likelihood functions for the individual biases are given in Figure 5-4(b). The joint and marginal likelihood functions for the individual platforms under the damage category are given in Figures E-5, E-7, and E-8 in Appendix E.

The joint and marginal posterior distributions for platform ST51J are given in Figures E-6(a) to E-6(c) The mean values of the factors shift to 1.02, 1.12, and 1.43 for B_j, B_{fl}, and B_{fa}, respectively. The COVs reduce from 0.3 to 0.18 to 0.22.

The joint and marginal distributions of each bias factor, including the effect of all three damaged cases, are given in Figures 5-5(a) to 5-5(c) The mean values shift to 1.00, 1.13 and 1.46 for B_j, B_{fl}, and B_{fa}, respectively. The posterior COVs range from 0.17 to 0.21. These results indicate that, among the damaged cases, no single platform has a dominating effect on the bias factors for the group.

Failure Platforms (Table 5-3):

The joint and marginal likelihood functions for all three failure cases are given in Figures 5-6(a) and 5-6(b). The joint and marginal likelihood functions for individual platforms under the failure category are given in Figures E-9, E-10, and E-12 in Appendix E.

The joint and marginal posterior distributions for platform ST130A are given in Figures E-11(a) to E-11(c). The mean values of the bias factors shift to 0.86, 1.18, and 1.37 for B_j, B_{fl}, and B_{fa}, respectively. The COVs reduce from 0 3 to 0.21 to 0.22.

The joint and marginal distributions of each bias factor, including the effect of all three failure cases, are given in Figures 5-7(a) to 5-7(c). The mean values shift to 0 80, 1.17 and 1.38 for B_j, B_{fl}, and B_{fa}, respectively. The posterior COVs range from 0.19 to 0.21. These results indicate that, among the failure cases, platform ST130A provides more information about B_j and B_{fl}

Effect of All Nine Steel Jacket Platforms (Table 5-4).

The joint likelihood functions resulting from the combination of all nine platforms (survival, damage, and failure cases) are given in Figure 5-8(a). The marginal likelihood functions for the individual biases are given in Figure 5-8(b) The joint and marginal distributions, including the contribution from all platforms, are given in Figures 5-9(a) to 5-9(c). The following posterior distributions of bias factors were obtained using the joint likelihood function for all 9 platforms

Jacket structure (B_j)	Mean = 1.10, COV = 0.13
Foundation lateral (B_{fl})	Mean = 1.32, COV = 0.17
Foundation axial (B_{fa})	Mean = 1.54, COV = 0.15

The posterior estimate for B_j based on the failure cases was 0.8. The posterior estimate for B_j was 1.35 when only survivals were considered. These values are significantly different than the final value of 1.1 which indicates the degree of unexpectedness of observed failure and survival events. The bias factors for three categories do not vary nearly as much for the foundation lateral (1.13 to 1.19) and foundation axial (1.38 to 1.46) cases. The correlation between the jacket structure and foundation bias factors is very low for the survival platforms Higher correlation was found between the jacket and foundation lateral bias factors for the damage and failure cases.

Effect of Caisson Platforms on B_{fl}:

The likelihood functions were also developed for three caisson platforms each of which were damaged during Andrew. The caissons were considered for this sensitivity study due to similarities in their lateral foundation behavior with the jacket platforms and due to the lack of availability of any jacket platform with observable foundation damage.

The calibration conditions given in Table 5-5 were used. The posterior distribution of B_{fl} (mean of 1.32 and COV of 0.17) changed to a distribution with a mean of 1.10 and COV of 0.15 due to the inclusion of the three caissons. The caissons (all under observed failure category) were found to reduce the mean estimate of the posterior of B_{fl} by 17 percent.

The contribution from caissons should be considered with caution due to differences in the characteristics and behavior of jackets and caissons including:

- Differences in pilehead fixity.

- Differences in the failure modes: In case of a jacket platform, the ultimate lateral failure mode would be due to the formation of fully plastic sections (hinges) at two levels in several piles (near the mudline and at some depth below). In case of caissons, the failure mode is due to formation of a single fully plastic section.

- Differences in loads: Jacket wave load is affected by several factors that do not affect caissons, such as conductor shielding factor, and current blockage factor. Therefore, the contributions from loading effects to the bias factor would vary for the two systems.

This bias factor does demonstrate the likely trend for the shift in the jacket foundation (lateral) bias factor, if platforms with observed foundation damage were added to the calibration.

5.5.2 Development of a Single Bias Factor

A single bias factor was determined to assess the effect of various changes from the Phase I study (e.g., hindcast and recipe) Table 5-6 presents a summary of the input data and results of this analysis. It includes the hindcast maximum base shear, base case load levels for selected response conditions, and the calibration conditions for all nine platforms.

The mean values of the bias factors were estimated as 1.37, 1.06 and 0.90 for the survival, damage, and failure categories respectively. An overall bias factor was determined with a mean of 1.15 and COV of 0.13. This compares with a mean of 1.19 and COV of 0.11 from Phase I. The posterior distributions for the three individual categories and for the combined case are given in Figure 5-10.

The single bias factor using the Phase II capacity analysis results and improved calibration conditions is marginally lower than the Phase I value This change is due to the following factors:

- New hindcast (which provided generally lower seastate data) - The new hindcast provided wave heights that were 15 to 37 percent lower than the Phase I estimates. This lowers the mean value of B.
- Updated capacity analysis recipe - The mean capacity of the K-joints have generally increased, based on the new recipe, which has increased the capacity estimates. This lowers the mean value of B.
- Additional soil data - The soil reports obtained for a majority of the platforms established shear strengths lower than those used for Phase I (which were based on ST151 data) This increases the mean value of B. The effect of improved soil information on the bias factor will be significant for platforms that were controlled by foundation failures.
- More precise calibration conditions - The primary change in the new calibration conditions is due to additional inspection information and treatment of the survival cases as having no

damage. This led to calibration at lower capacity levels than used in Phase I. This increases the mean value of B.

The combined effect of all these changes have lead to a marginal reduction in the single (system) bias factor from Phase I.

5.5.3 Sensitivity of Alternative Interpretation of Failure Cases

The sensitivity of the bias factors resulting from alternative interpretations of the field observations for two failed platforms was determined. The alternative interpretation considered was that the observed jacket damage were instigated by initial inelastic events in the foundation (i e., the failure in foundation occurred first)

In this calibration task the initial damage to the foundation was assumed to be hinging or pullout of a pile. The following calibration conditions describe this interpretation:

- Initial damage occurred in the foundation. The actual applied Andrew level of load was higher than the load level required to cause initial damage to the foundation.

- Jacket capacity was higher than the capacity (load) level at initial foundation failure.

The following conditions are identified for platforms ST151H and ST130A:

Platform ST151H : $S > 3{,}240\ b_{fa}$ and $2{,}680\ b_j > 3{,}240\ b_{fa}$.

Platform ST130A : $S > 1{,}620\ b_{fl}$ and $2{,}000\ b_j > 1{,}620\ b_{fl}$

P_f = P [foundation damaged | (load at first event in the jacket > load at first event in the foundation)] x P [(load at first event in the jacket > load at first event in the foundation)]

$$= [\, P\, \{S > (b_{fl} R_{fl1} \text{ or } b_{fa} R_{fa1}) \mid (b_{fl} R_{fl1} \text{ or } b_{fa} R_{fa1}) < b_j R_{j1})\}_{\text{hour-1}} \cup \{S > (b_{fl} R_{fl1} \text{ or } b_{fa} R_{fa1}) \mid (b_{fl} R_{fl1} \text{ or } b_{fa} R_{fa1}) < b_j R_{j1})\}_{\text{hour-2}}] \times P\,[(b_{fl} R_{fl1} \text{ or } b_{fa} R_{fa1}) < b_j R_{j1})] \qquad [5\text{-}28]$$

The conditioning event is similar to the known failure cases in Eq. 5-24 (Section 5.5.1).

The following procedure was used to determine the variation in the posterior bias factors·

- Reliability analysis was performed for the two platforms for both the stronger foundation (Section 5.5.1 approach) and weaker foundation (Section 5.5.3 approach) cases.

- The minimum of the two foundation capacities and corresponding COVs were used in the sensitivity analysis. This was based on a review of the lateral and axial foundation capacities for the ST151H and ST130A platforms. In case of ST151H, the lateral load at pullout of first pile was calibrated. For ST130A, the lateral load level at hinging of first pile section was calibrated.

- The posterior likelihood functions for B'_j and B'_f (assumed equal to B'_{fl}) for the other seven platforms were assumed to be unchanged (i e , values as shown in Section 5.5.1).

- The posterior bias factors (B_j and B_f) were determined for both cases: foundation stronger than the jacket and foundation weaker than the jacket.

The joint likelihood functions for the two biases (jacket and foundation) for two cases (original interpretation as in Section 5.5.1 and alternative interpretation as in this section) are given in Figures 5-11(a) and 5-12(a) for platforms ST151H and ST130A, respectively. The marginal likelihood functions for two biases for both platforms are given in Figures 5-11(b) and 5-12(b).

The posterior distributions of the bias factors were obtained assuming normal prior distributions with mean values of 1.0 and COVs of 0.3. The posterior distributions were determined, for both B_j and B_f separately, for the following cases:

- Seven platforms (without ST151H and ST130A):

Jacket, B'_j	Mean = 1.15; COV = 0.13
Foundation, B'_f (=B'_{fl})	Mean = 1.24; COV = 0.18

- Nine platforms and calibration conditions for ST151H and ST130A as in Section 5.5.1 (i.e., foundation assumed to be stronger than the jacket):

Jacket, B_j	Mean = 1.10; COV = 0.13
Foundation, B_f (=B_{fl})	Mean = 1.32; COV = 0.17

- Nine platforms and calibration conditions for ST151H and ST130A as in this section (i e., foundation assumed to be weaker than the jacket):

Jacket, B_j	Mean = 1.17; COV = 0 12
Foundation, B_f	Mean = 1.15; COV = 0.17

This analysis indicated that a moderate change in the bias factors would occur if the foundation were assumed to fail. The jacket bias factor (B_j) would increase by 6 percent from 1.10 to 1.17 and the foundation bias factor (B_f) would reduce by 13 percent from 1.32 to 1.15

5.5.4 Sensitivity of Prior of B's

A sensitivity study performed during Phase I indicated that the posterior distribution of B is relatively insensitive to the COV of the prior.

In this study, the prior distributions of B_j and B_{fl} were assumed with a mean of 1.0 and a COV of 0.3. The prior of B_{fa} (for axial pile capacity) was assumed with a mean of 1.3 and a COV of 0.3. A sensitivity study was performed to assess the effect of change in the prior distribution on the posterior distribution of each bias factor. The mean and COV values of the prior distributions were varied individually.

The COVs of the priors were assigned values of 0.2, 0.3, and 0 4. The results given in Table 5-7 indicate that the mean and COV values of the posterior distributions are insensitive to variations in the COV except for B_{fl} in Case B. The mean of B_{fl} becomes 1.20 and 1.40 when COV of prior of B_{fl} is varied to 0.2 and 0 4, respectively.

The mean values of the priors of the three bias factors were varied individually. B_j was varied from 1.0 to 1.2. B_{fl} was varied from 1.0 to 1.3. B_{fa} was varied from 1.3 to 1.5. The mean and COV values of the posterior distributions of bias factors were found to be insensitive to the variations in the mean values of the priors, except for B_{fl} in Case B (see Table 5-7). The mean of posterior of B_{fl} changes form 1.32 to 1.45 due to variation in the mean of prior of B_{fl} from 1.0 to 1.3.

These results indicate that variations in prior distributions of bias factors have a minor effect on their posterior distributions.

5.5.5 Example Application of Bias Factors

The bias factors established in Section 5.5.1 represent biases in the estimate of the ratio of ultimate capacity to maximum environmental load (R_u/ S) and can be used to update the safety index or probability of failure for a platform. The distributions of the bias factors represent modeling errors, or Type-II uncertainties, due to various assumptions and simplifications in the analysis procedures followed.

The following steps describe the procedure used to incorporate these bias factors in the calculation of the annual probability of failure of a sample platform. Platform ST151K was used as the example with an assumed distribution of annual maximum seastate. The specific data and results of this example are provided to illustrate the process and are not intended to be used for other applications.

Step 1: Establish Annual Maximum Seastate Data

The distribution of annual maximum significant wave height, H_s, and associated current and wind magnitudes are needed for different directions that may be significant to the platform The example platform is located in the Gulf of Mexico in water depth of 137 ft. The annual maximum

significant wave height was assumed to have a log-normal distribution with a median of 17.5 ft. and a COV of 0.314. A 4 ft. storm tide was assumed. This distribution is assumed to be applicable to the omni-directional wave height. It is assumed that the storm duration is 3 hours which is equivalent to approximately 800 waves. The associated current was assumed to have a mean value of 2.1 knots with a COV of 0.15.

Platform specific seastate data was developed considering the orientation of the platform and storm approach directions based on the API RP 2A, Section 2.3.4 guidelines. Analysis was completed for only the diagonal direction as the capacity analysis results were not available for other directions. In a complete application it could be necessary to determine the failure probabilities for three or more directions. The median value of the current was determined as 0.88 kt for the diagonal direction The rate of storm occurrence in this direction was assumed as 1.0.

Step 2: Determine Base Shear Coefficients

The C_1, C_2, C_3, C_4 coefficients are required to define the base shear for a range of wave heights and currents. The coefficients determined for this platform (ST151K) in this study were used.

Step 3: Determine Ultimate Capacity of Platform

The ultimate capacity of the platform was defined for the Case-1, Case-2, and Case-3 variations. The ultimate capacities for this platform were 3,880 kips for jacket structure failure; 4,400 kips for the lateral foundation failure; and 4,000 kips for the axial foundation failure.

Step 4: Determine Failure Probability versus bias factors

The failure probability of the platform is determined for each condition where the assessment load level was found to be higher than the ultimate capacity for any of the three cases (Case-1, Case-2, or Case-3). The conditional probability of failure for given values of b_j, b_{fl}, and b_{fa} is obtained in the following way:

$$P_f = P[\{(S > b_j R_j) \cup (S > b_{fl} R_{fl}) \cup (S > b_{fl} R_{fl})\} \mid (b_j, b_{fl}, b_{fa})] \qquad [5\text{-}29]$$

The probabilities of failure were determined for a range of b values. The mean values of H_s and current noted in Step 1 were used. A log-normal distribution was assumed for the "error" in H_s with a mean of 1.0 and COV of 0.314 (based upon the previously noted Gulf of Mexico data). The Fornstall distribution was assumed for the individual wave heights. The distributions of capacity, error in base shear and error in current were used as given in Section 5 4.

Step 5: Determine Probabilities of Failure

The probability of failures (P_f) were determined for three cases to illustrate the variations in mean and COV values of P_f due to the updating process The three cases evaluated are identified as follows:

- The probability of failure, P_f, without including the modeling uncertainties
- The probability of failure, P_f', including the prior distributions of the Bs
- The posterior probability of failure, P_f'', including the posterior distributions of the Bs

The first case represents the probability of failure determined using the conventional procedure. The second case reflects the effect of including modeling uncertainties The third case reflects the effect of including the improvements in the modeling uncertainties obtained from the Andrew experience

The formulations for the three quantities for a specific direction of the platform are given as follows:

$$P_f = P[(S > R_j) \cup (S > R_{fl}) \cup (S > R_{fl})] \quad [5\text{-}30]$$

$$P'_f = \int P[\{(S > b_j R_j) \cup (S > b_{fl} R_{fl}) \cup (S > b_{fl} R_{fl})\} | (b_j, b_{fl}, b_{fa})] \; f'_B(b_j, b_{fl}, b_{fa})\, db_j\, db_{fl}\, db_{fa} \quad [5\text{-}31]$$

$$P''_f = \int P[\{(S > b_j R_j) \cup (S > b_{fl} R_{fl}) \cup (S > b_{fl} R_{fl})\} | (b_j, b_{fl}, b_{fa})] \; f''_B(b_j, b_{fl}, b_{fa})\, db_j\, db_{fl}\, db_{fa} \quad [5\text{-}32]$$

where

$P[S > R]$ represents the probability of failure for given S and R distributions.

$P[S > bR \mid b]$ represents the conditional probability of failure given b, (i.e , the variation of probabilities of failure for different fixed values of b).

$f_B'(b)$ represents the prior distributions of the Bs assumed in this study.

$f_B''(b)$ represents the posterior distribution of the Bs established in this study that reflect the updating of the modeling uncertainties in the capacity analysis recipe and procedures from Andrew experience.

The following annual probabilities of failure were obtained for the three cases using FORM analysis. Again, these results are based on a single wave direction.

P_f = 0.014 (without modeling uncertainties)

P_f' = 0 019 (with prior B)

P_f'' = 0.009 (with posterior B)

The following observations are made from these results:

- The probability of failure (P_f') defined with prior distribution of B (i.e., including (unbiased) modeling uncertainties) will always be higher than the "simple" probability of failure (P_f).

- In this case, the posterior value, P_f'', is lower than the simple value, P_f. The primary reason for this is that the posterior mean is greater than 1. The posterior COV of the Bs is small and has little effect compared to the random variabilities (e.g., in the annual H_s value or in the C_d coefficient).

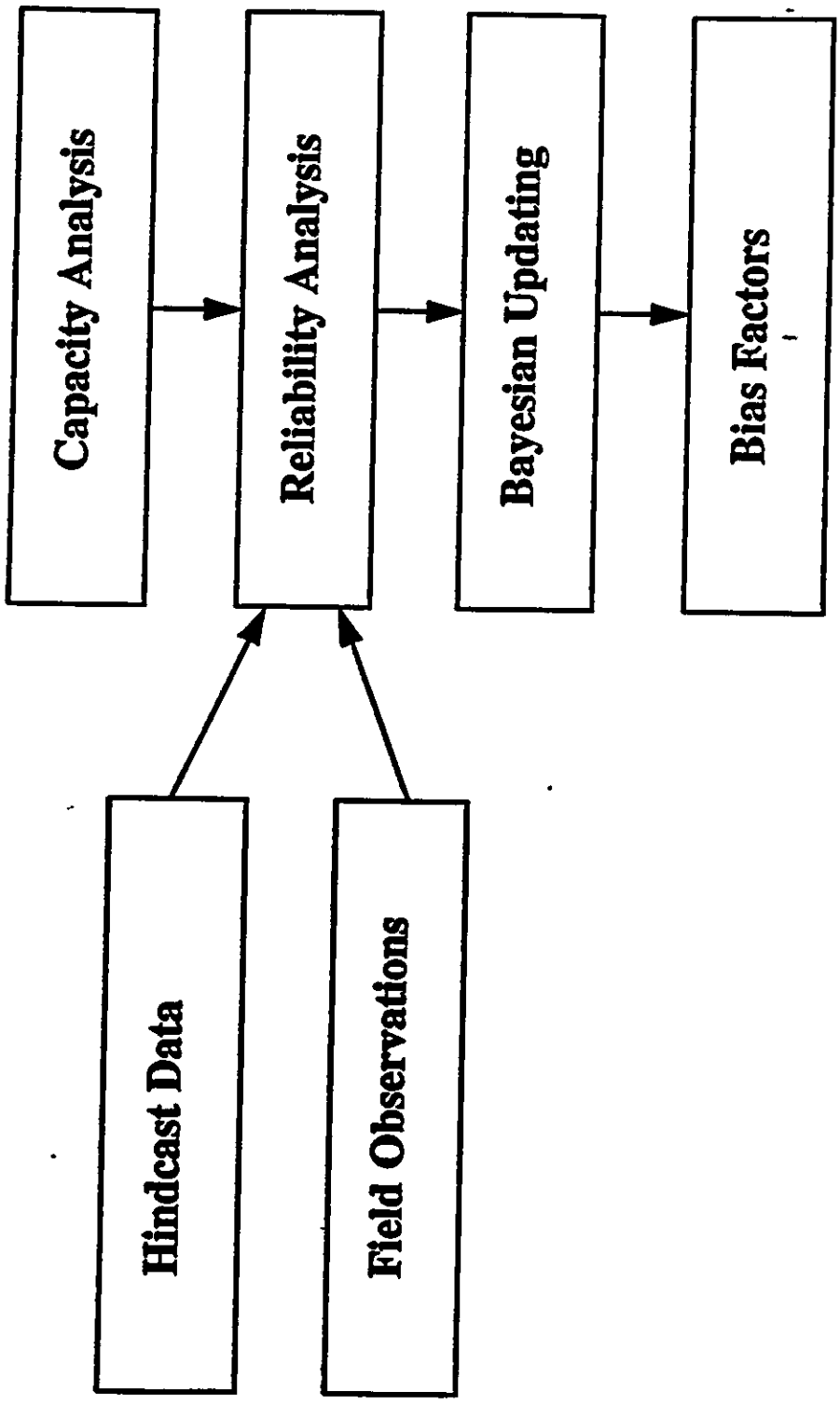

Figure 5-1: Calibration Methodology

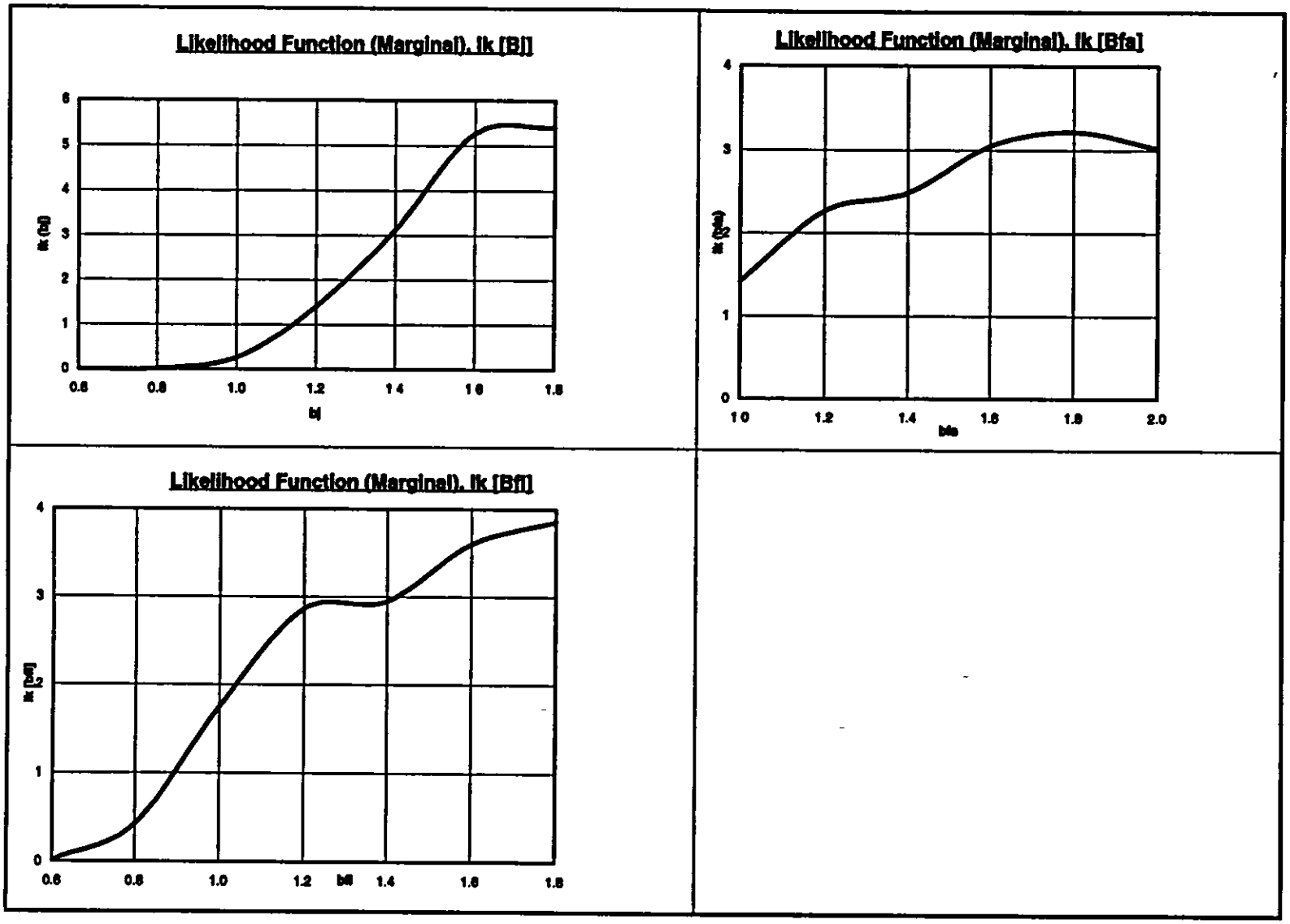

Figure 5-2(b): Marginal Likelihood Functions — All 3 Survival Platforms

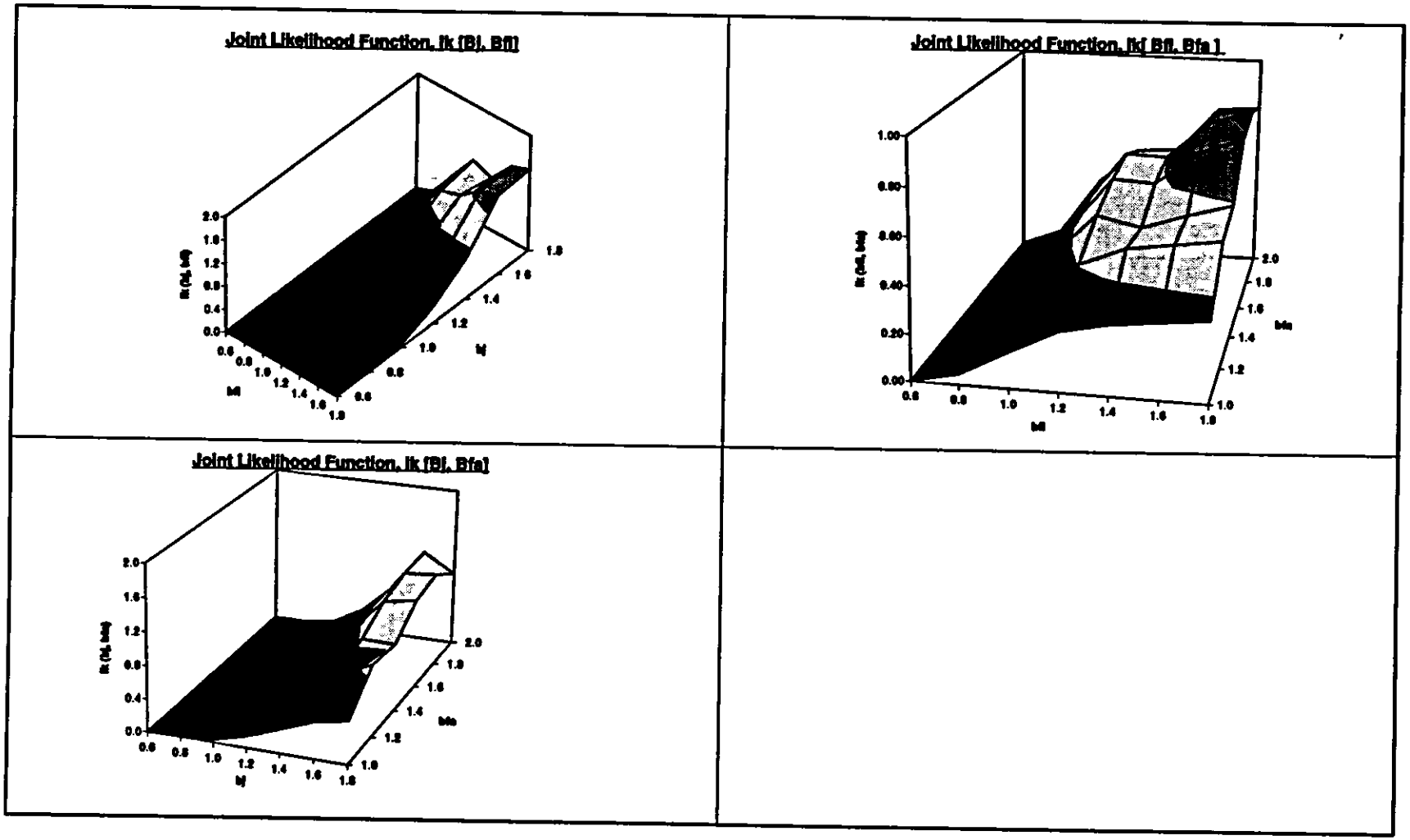

Figure 5-2(a): Joint Likelihood Functions — All 3 Survival Platforms

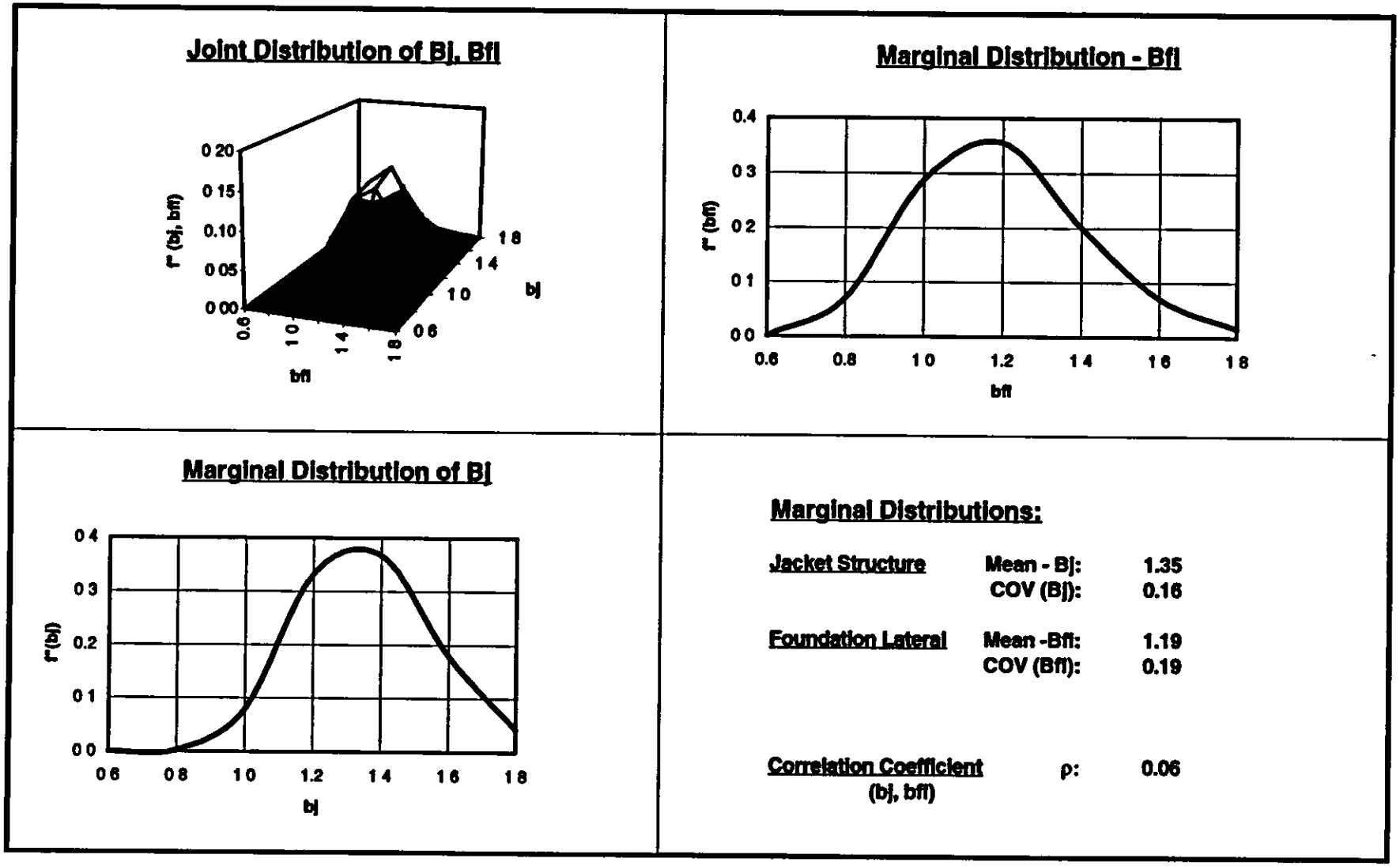

Figure 5-3(a): Posterior Distributions of Bias Factors (B_j, B_{fl}) — All 3 Survival Platforms

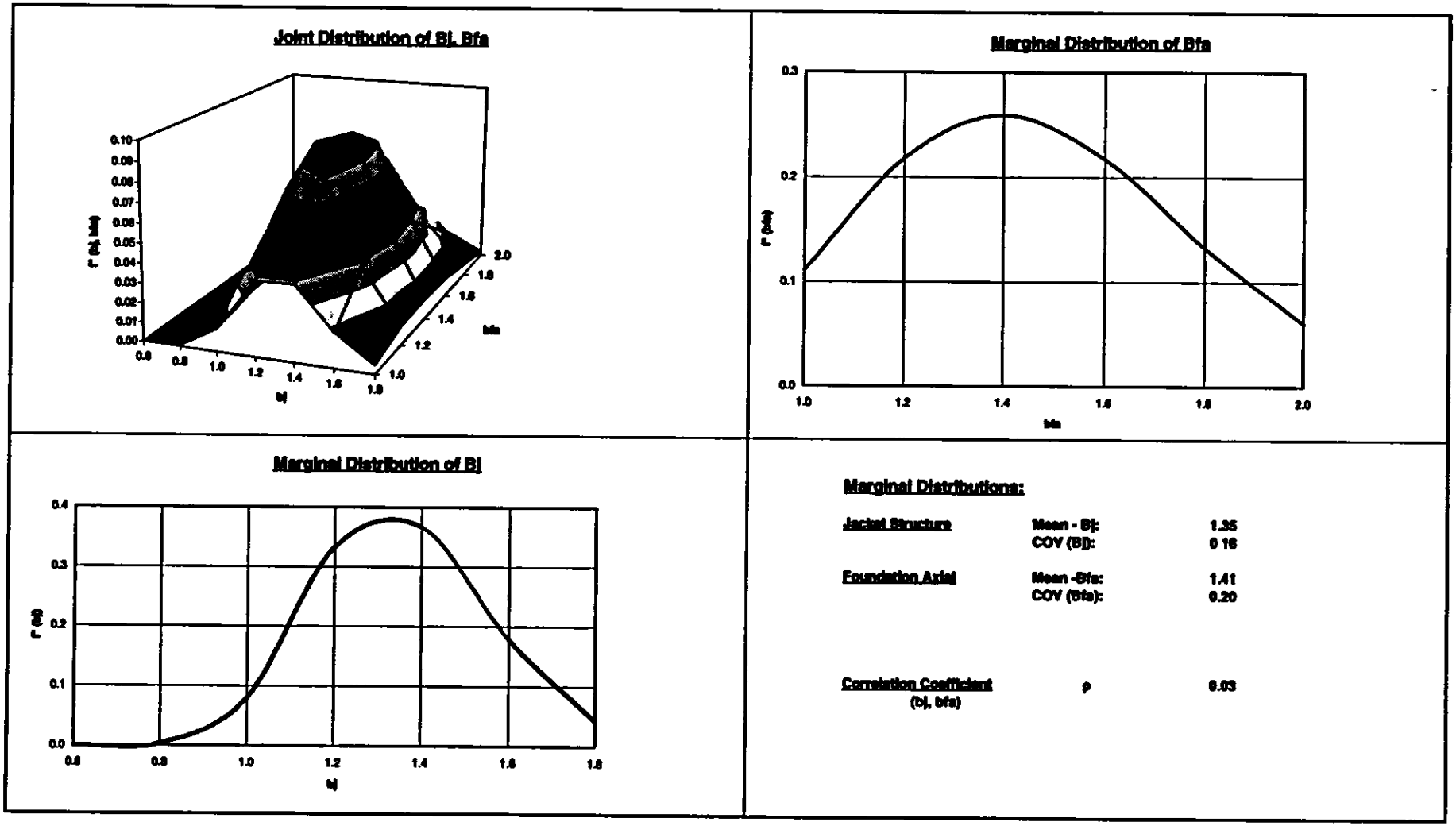

Figure 5-3(b): Posterior Distributions of Bias Factors (B_j, B_{fa}) — All 3 Survival Platforms

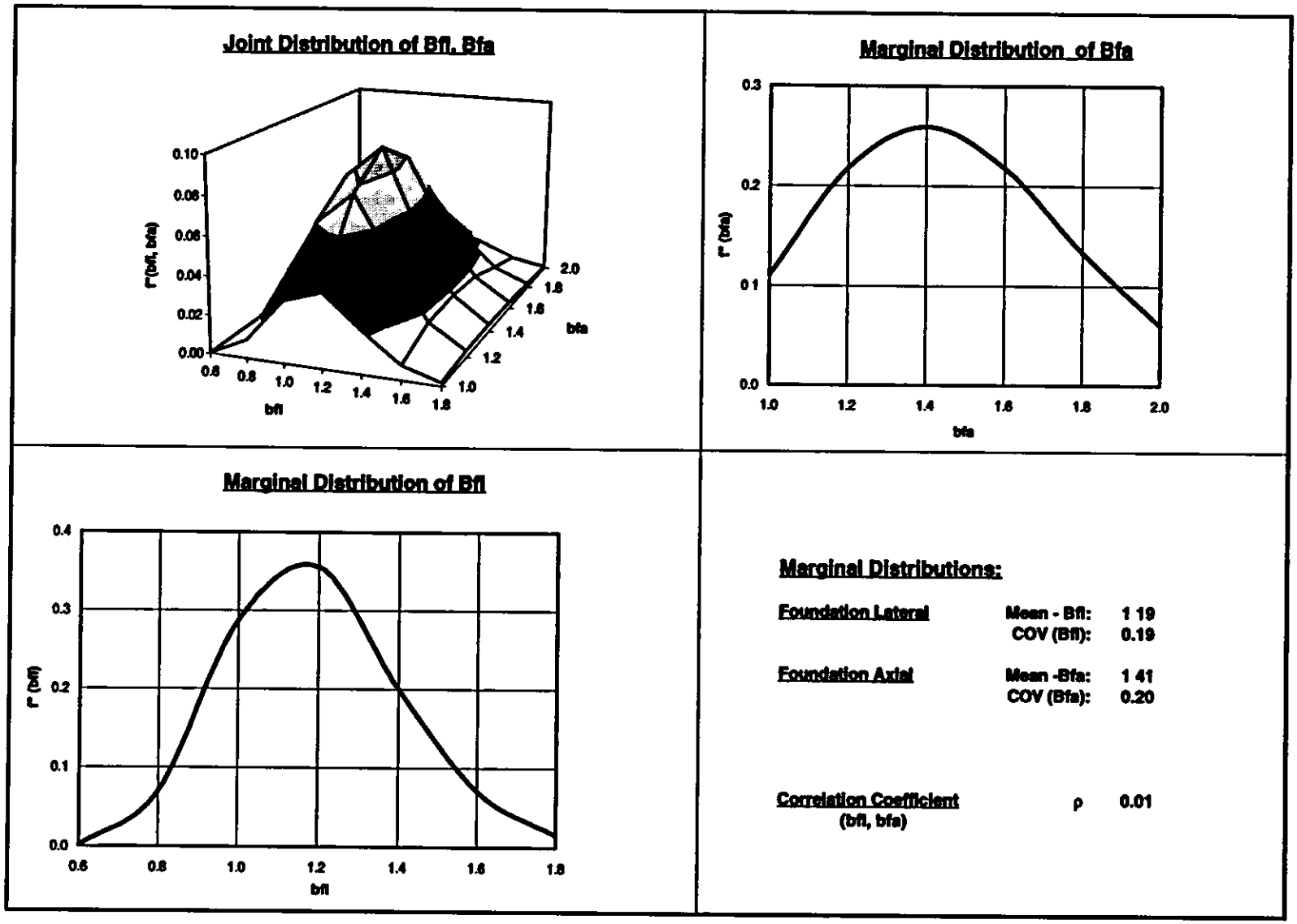

Figure 5-3(c): Posterior Distributions of Bias Factors (B_{fl}, B_{fa}) — All 3 Survival Platforms

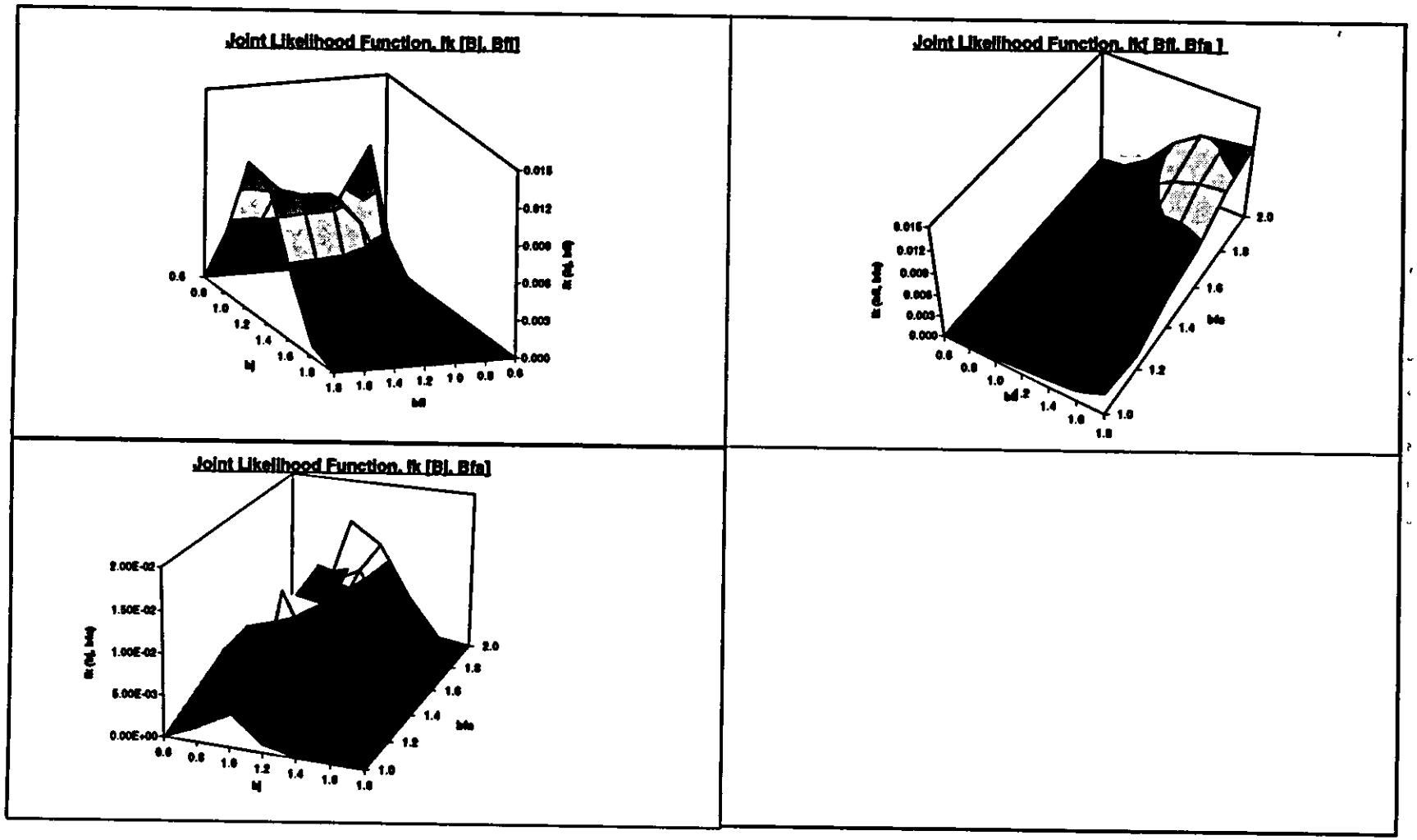

Figure 5-4(a): Joint Likelihood Functions — All 3 Damage Platforms

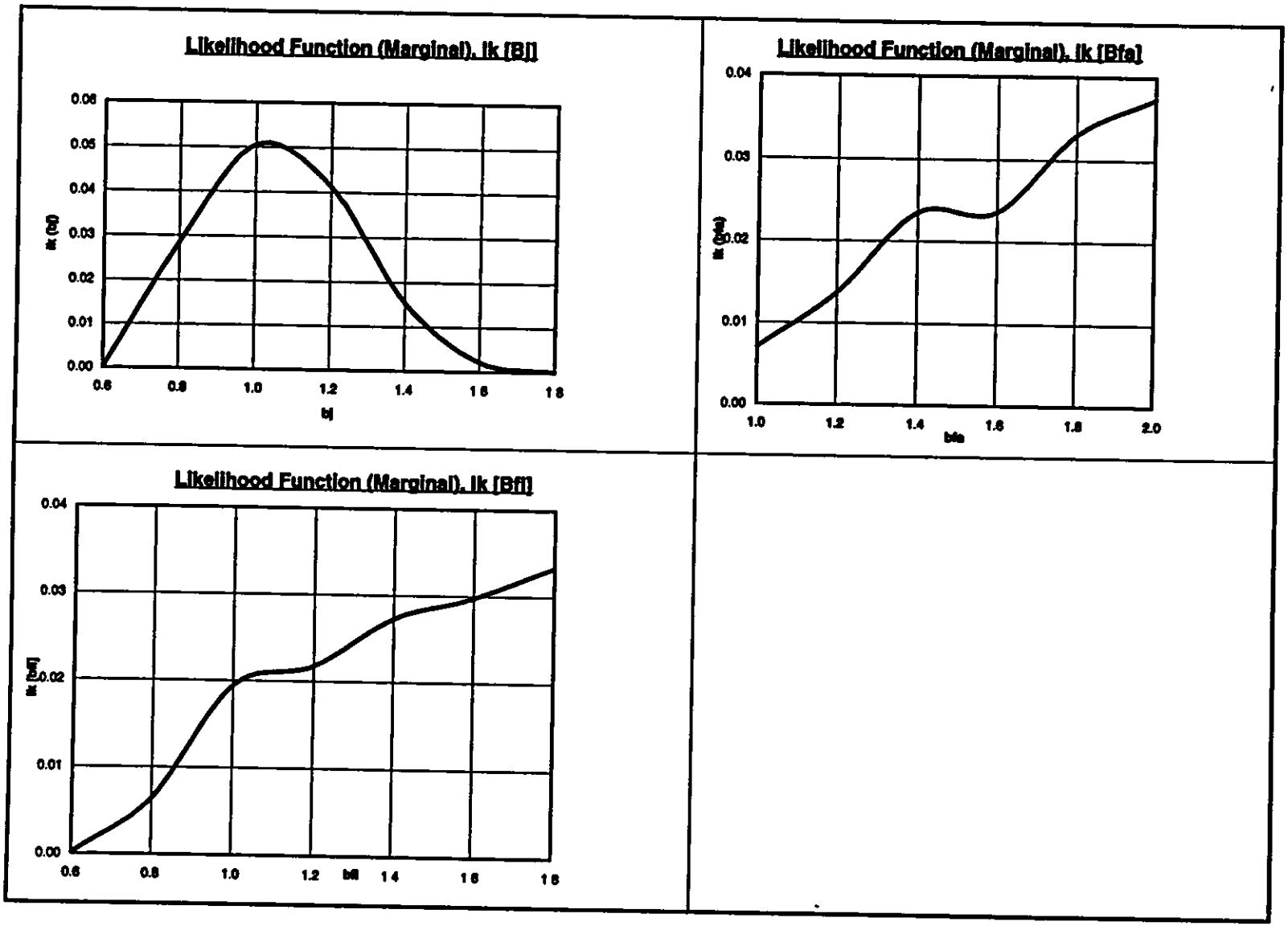

Figure 5-4(b): Marginal Likelihood Functions — All 3 Damage Platforms

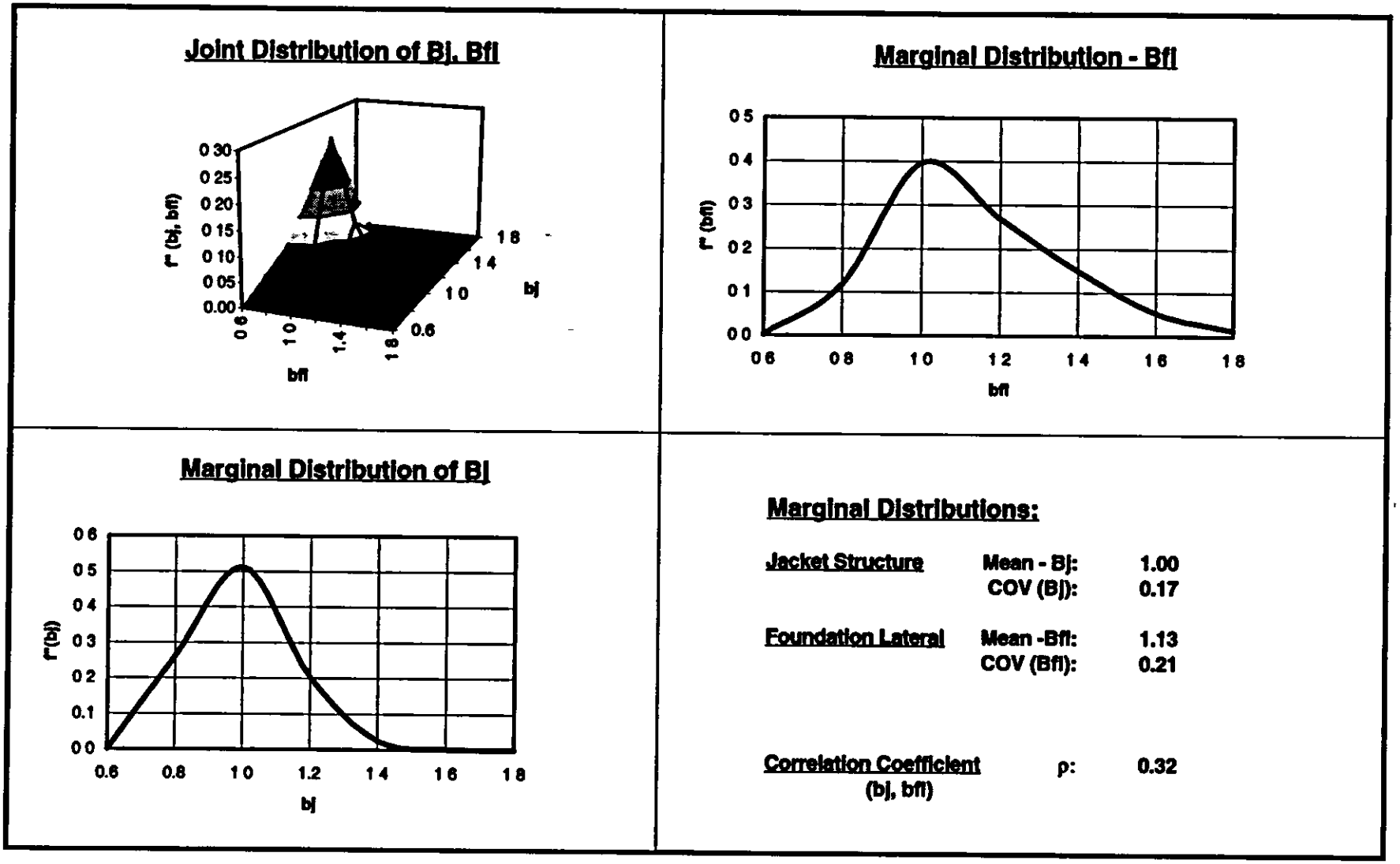

Figure 5-5(a): Posterior Distributions of Bias Factors (B_j, B_n) — All 3 Damage Platforms

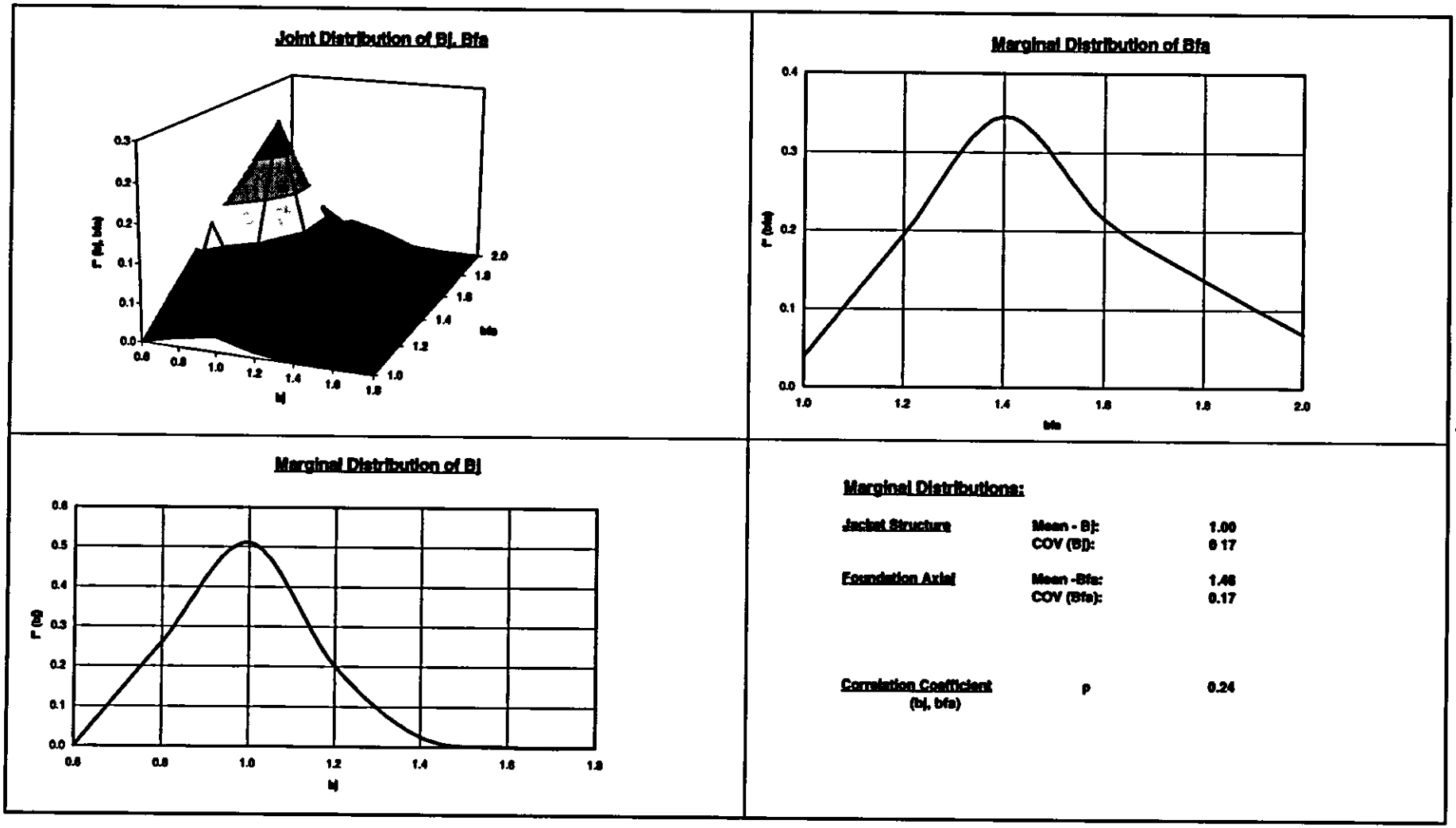

Figure 5-5(b): Posterior Distributions of Bias Factors (B_j, B_{fa}) — All 3 Damage Platforms

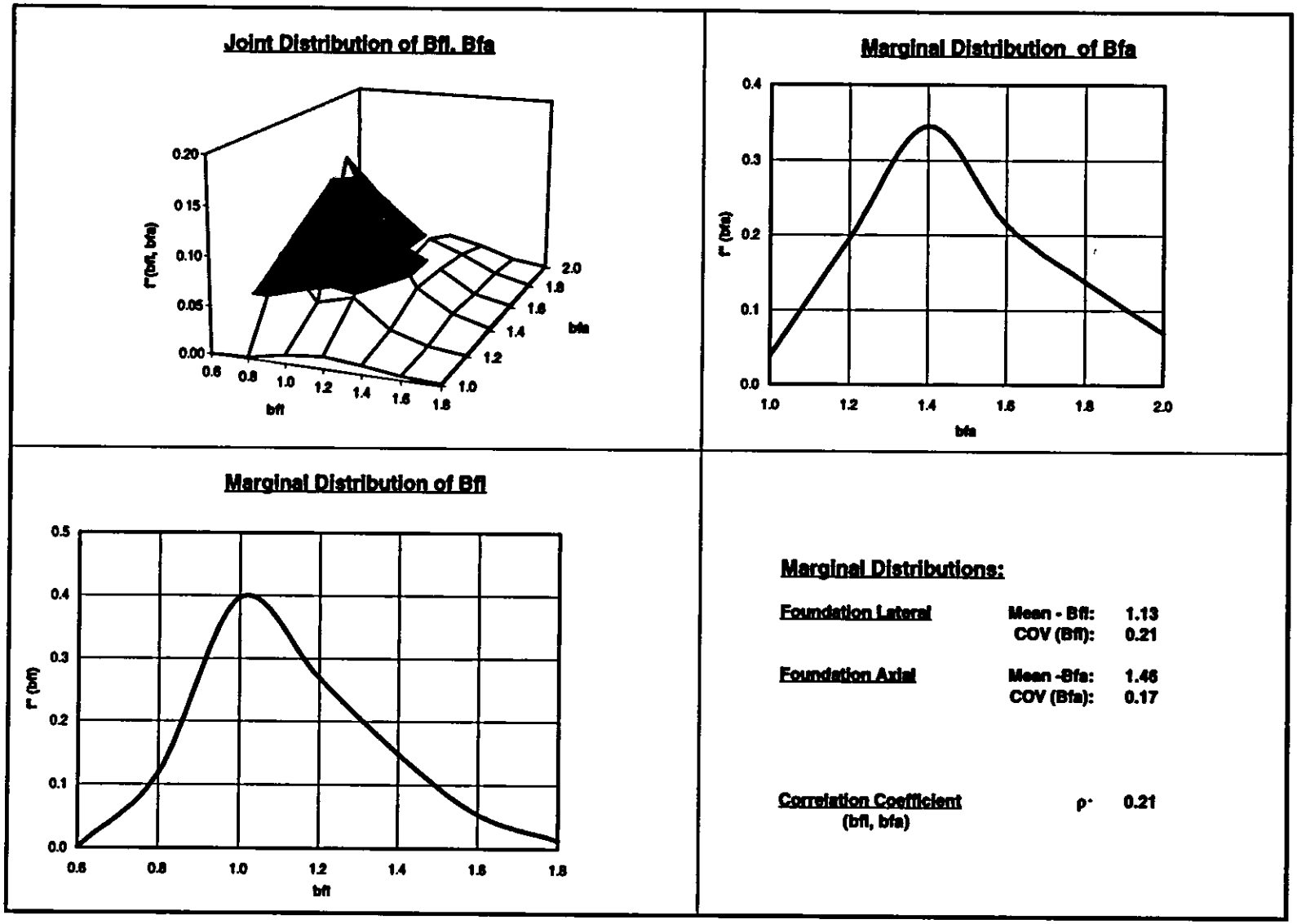

Figure 5-5(c): Posterior Distributions of Bias Factors (B_n, B_{fa}) — All 3 Damage Platforms

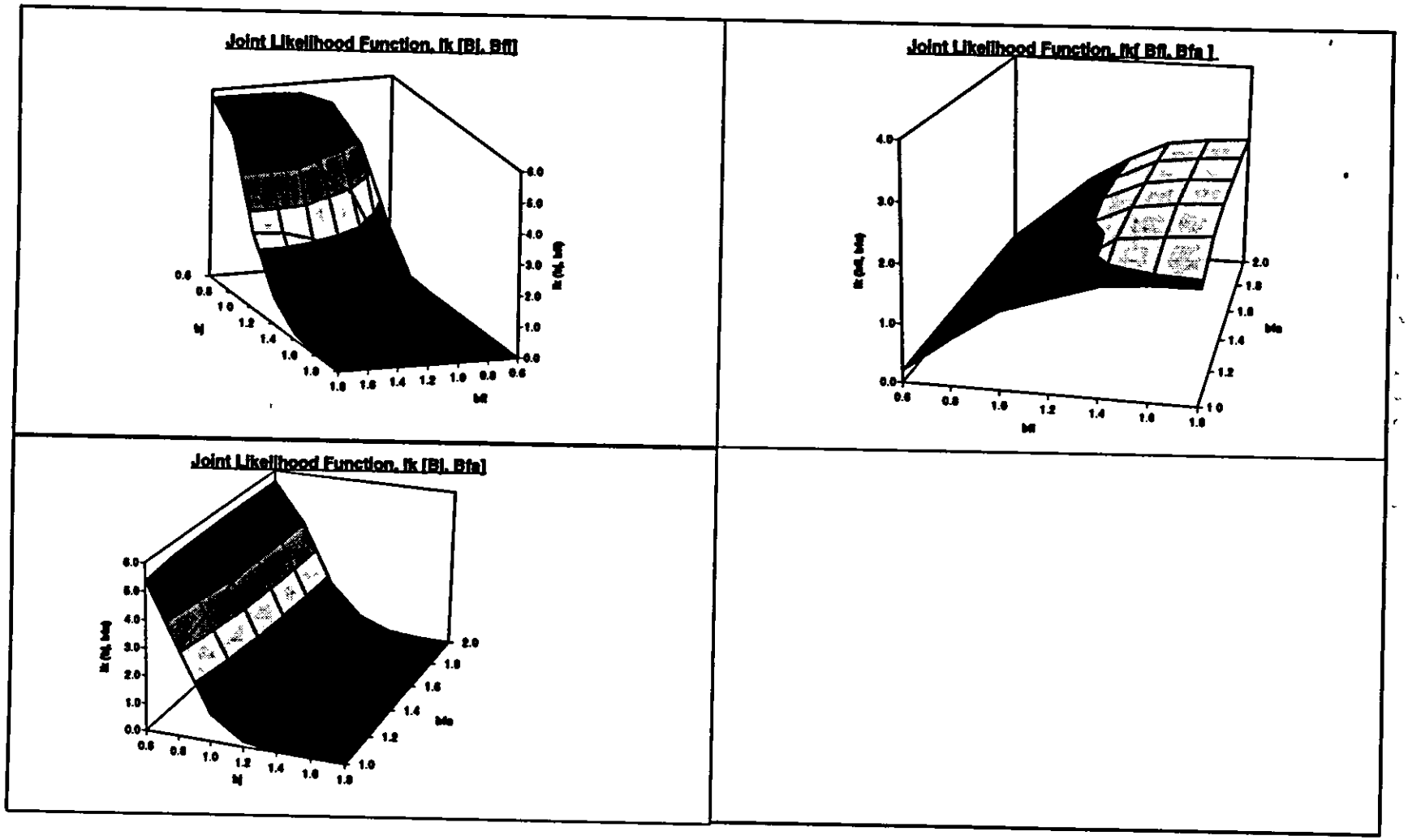

Figure 5-6(a): Joint Likelihood Functions — All 3 Failure Platforms

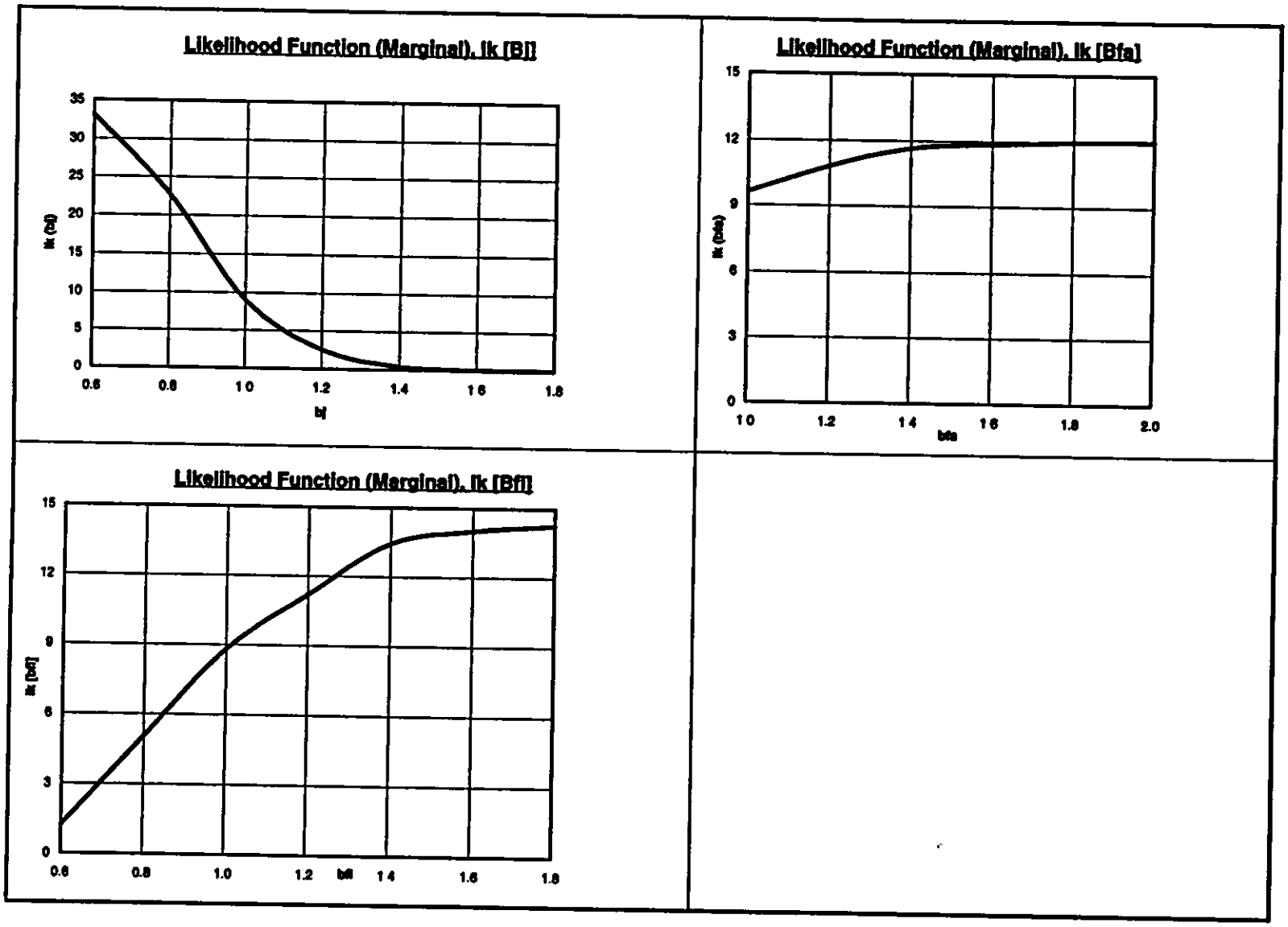

Figure 5-6(b): Marginal Likelihood Functions — All 3 Failure Platforms

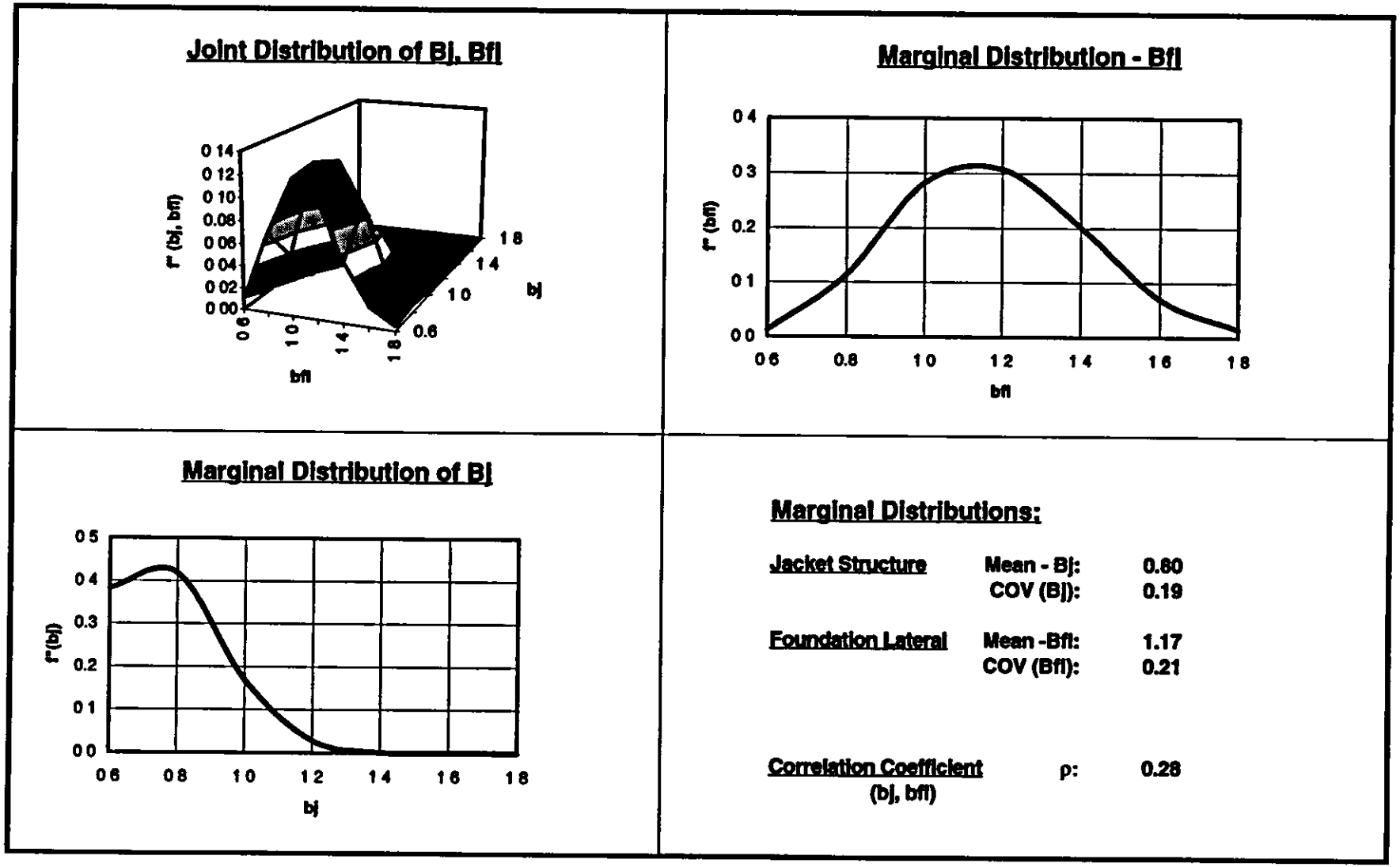

Figure 5-7(a): Posterior Distributions of Bias Factors (B_j, B_n) — All 3 Failure Platforms

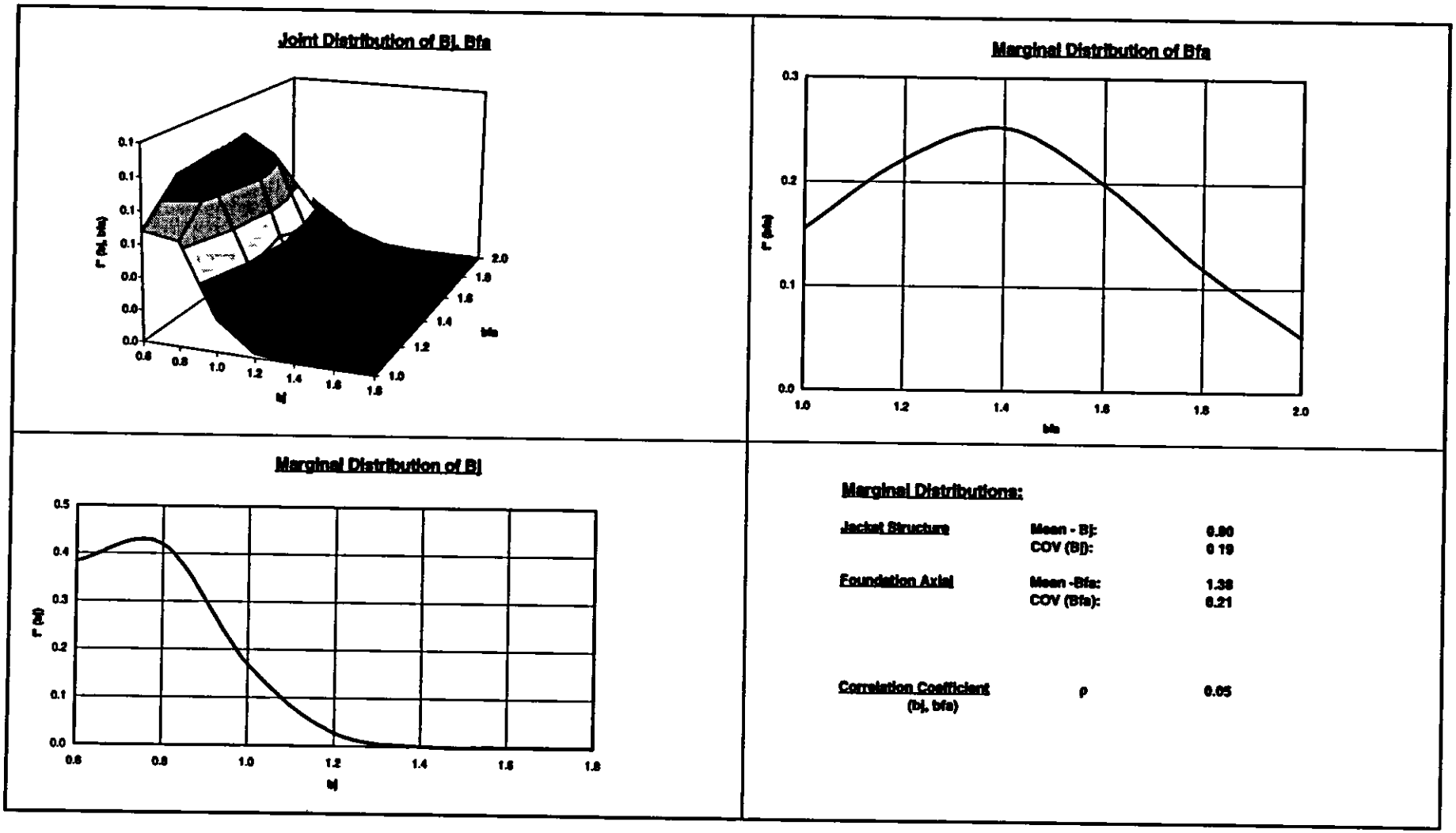

Figure 5-7(b): Posterior Distributions of Bias Factors (B_j, B_{fa}) — All 3 Failure Platforms

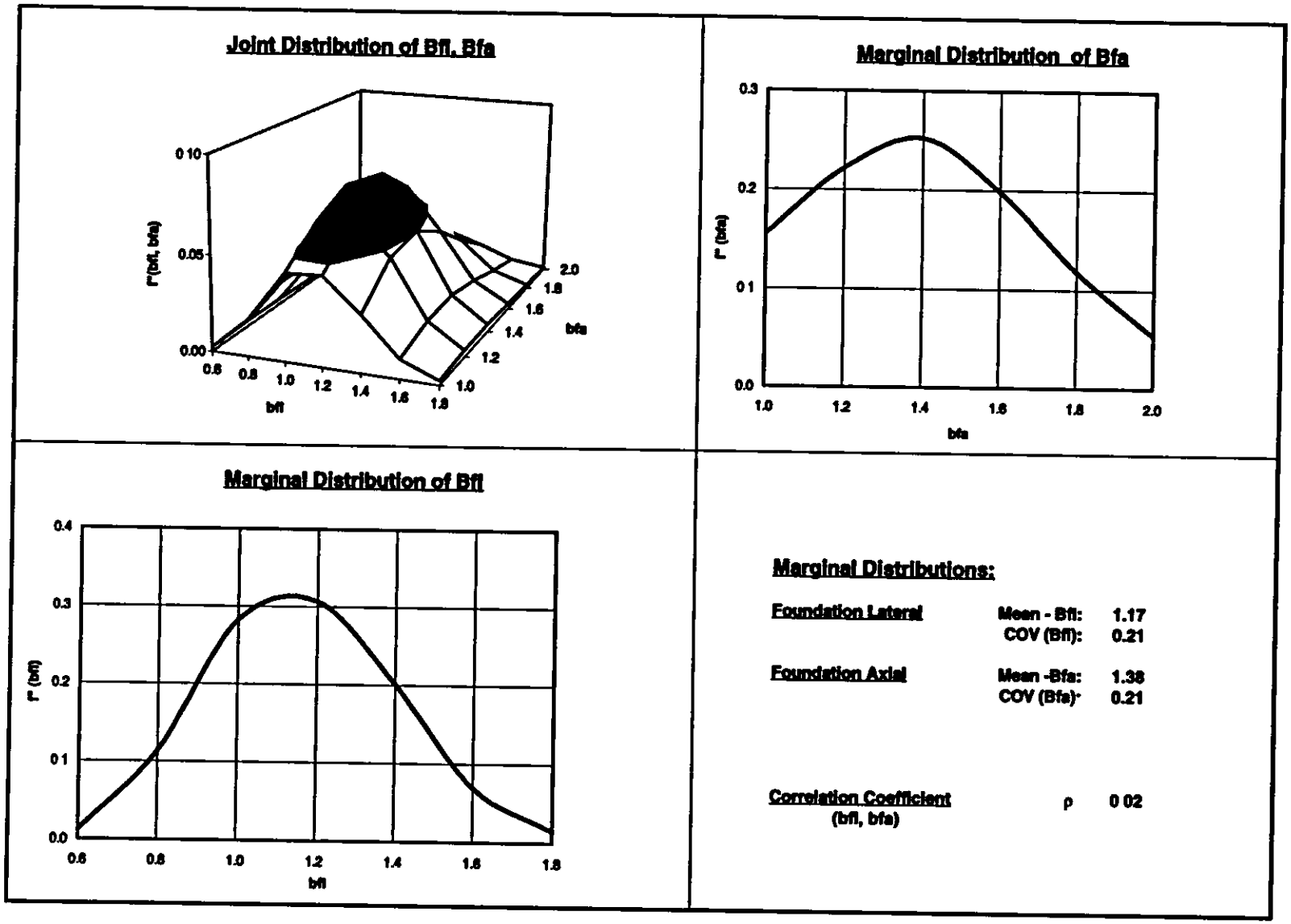

Figure 5-7(c): Posterior Distributions of Bias Factors (B_{fl}, B_{fa}) — All 3 Failure Platforms

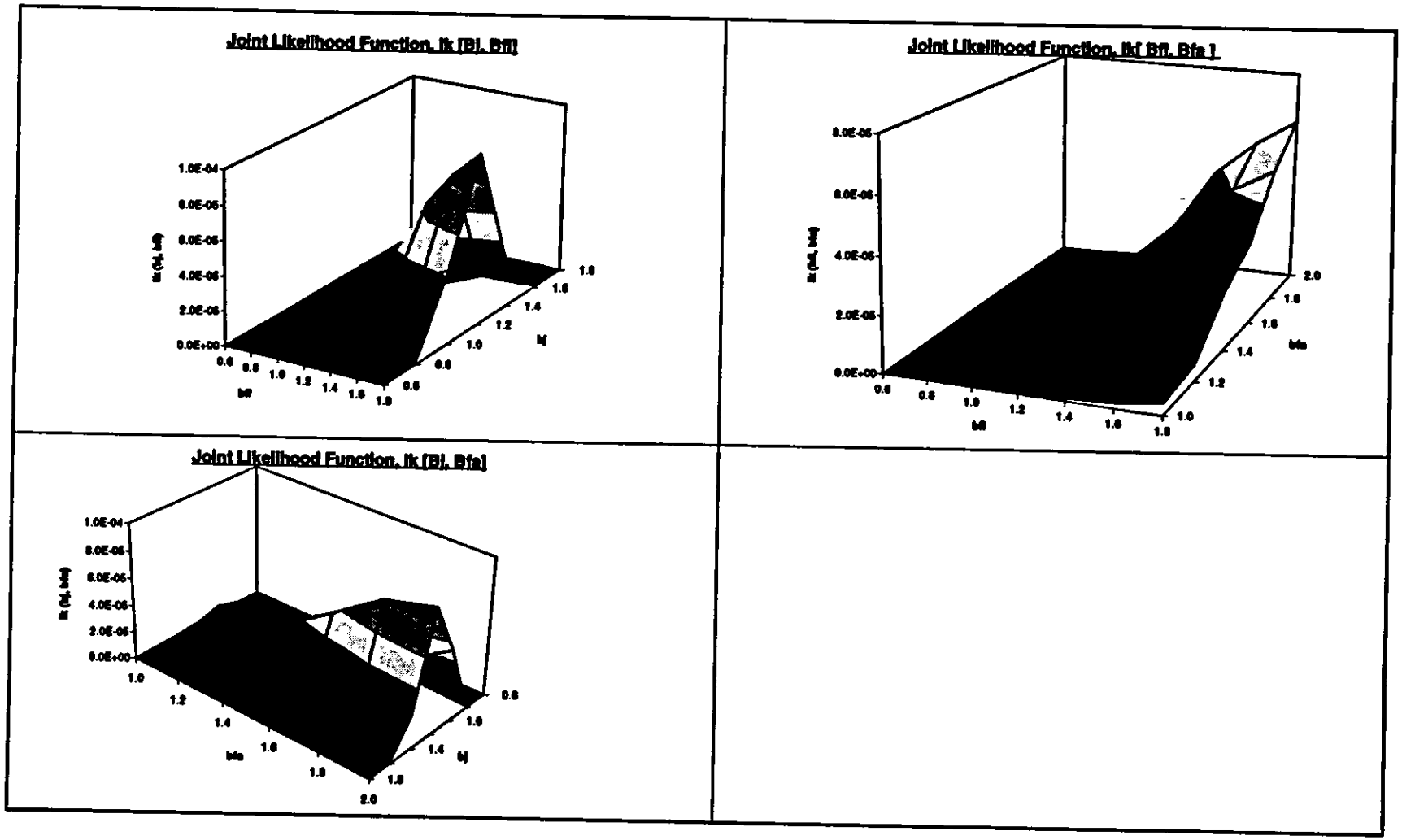

Figure 5-8(a): Joint Likelihood Functions — All 9 Jacket Platforms

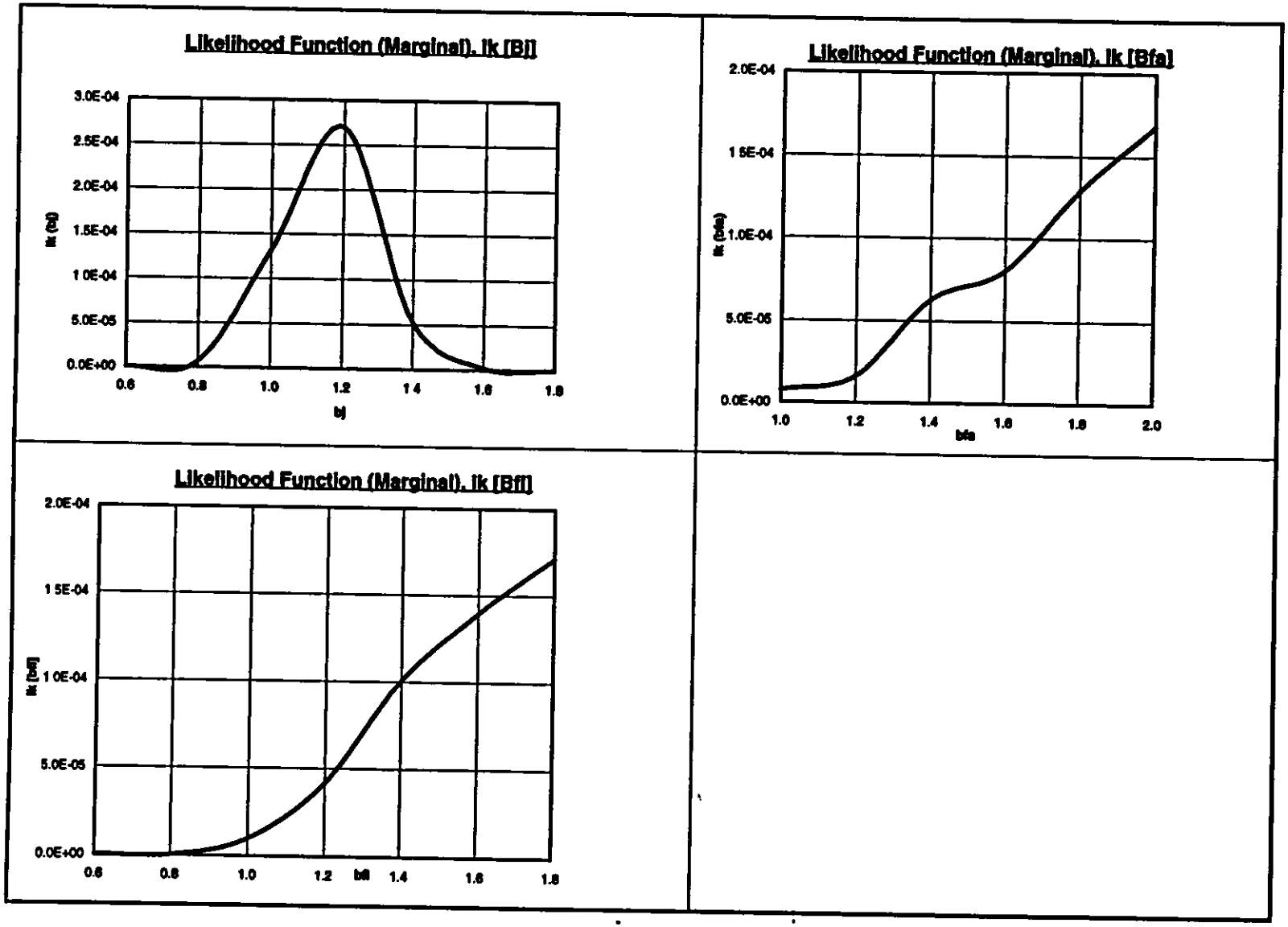

Figure 5-8(b): Marginal Likelihood Functions — All 9 Jacket Platforms

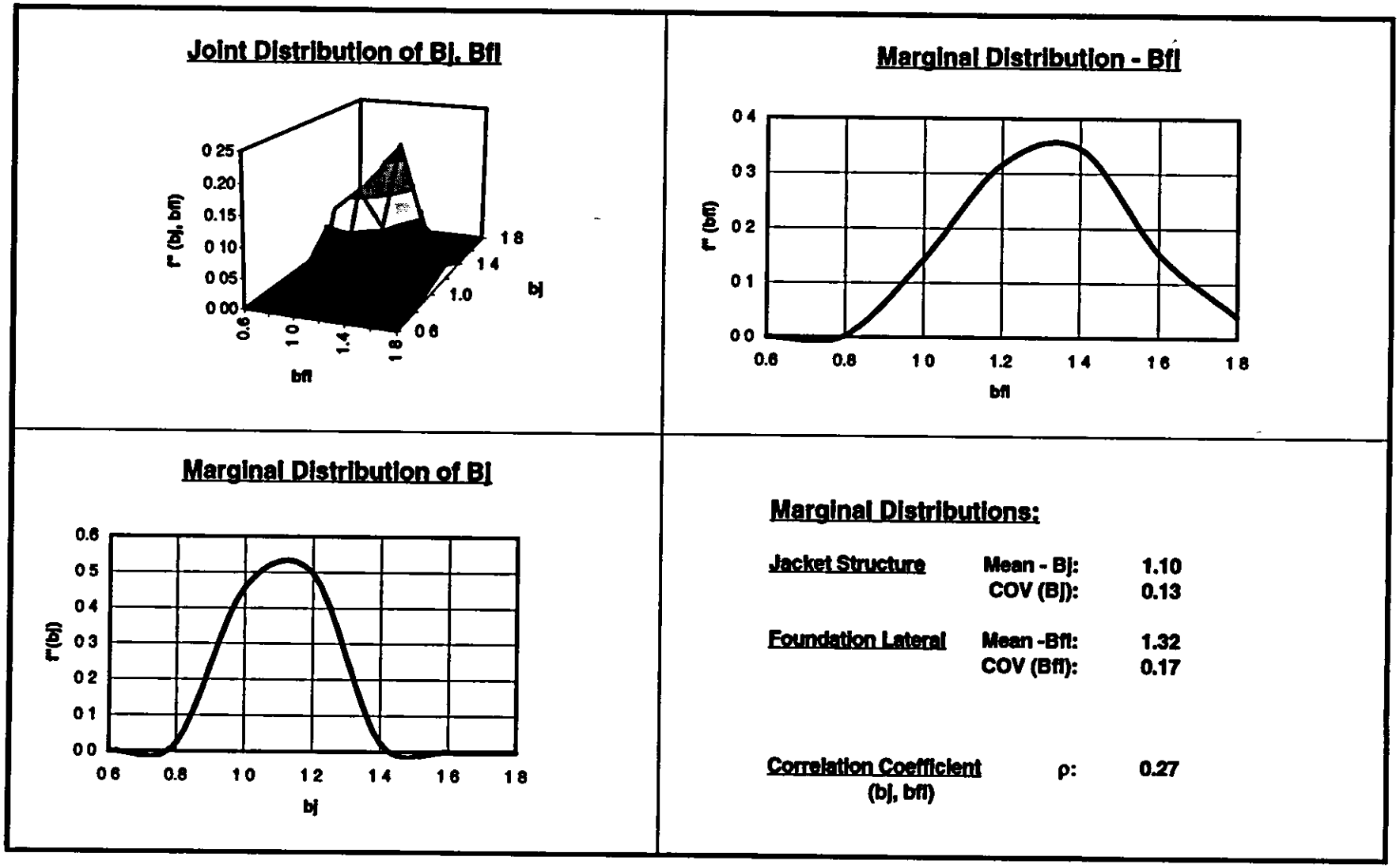

Figure 5-9(a): Posterior Distributions of Bias Factors (B_j, B_n) — All 9 Jacket Platforms

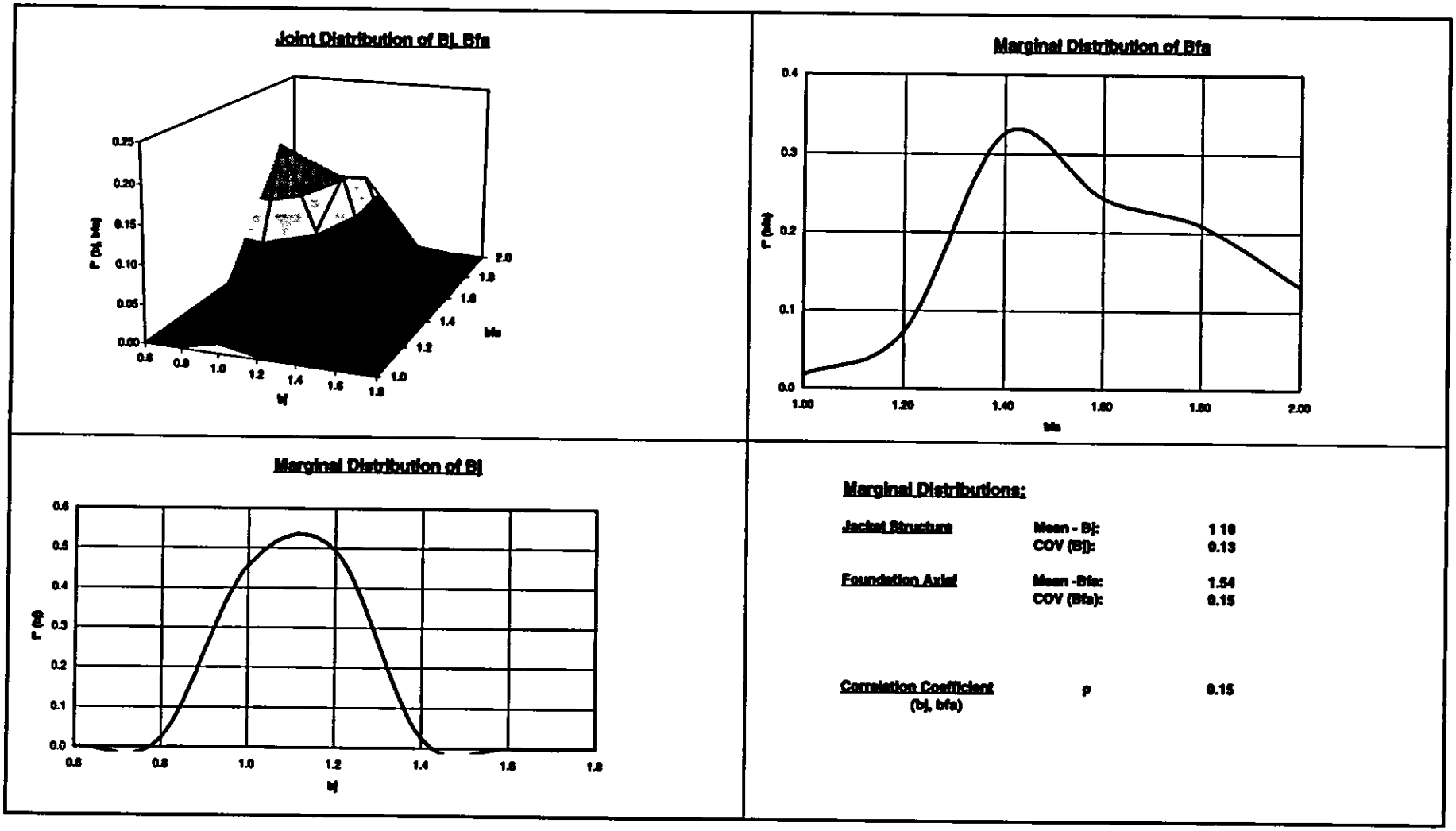

Figure 5-9(b): Posterior Distributions of Bias Factors (B_j, B_{fa}) — All 9 Jacket Platforms

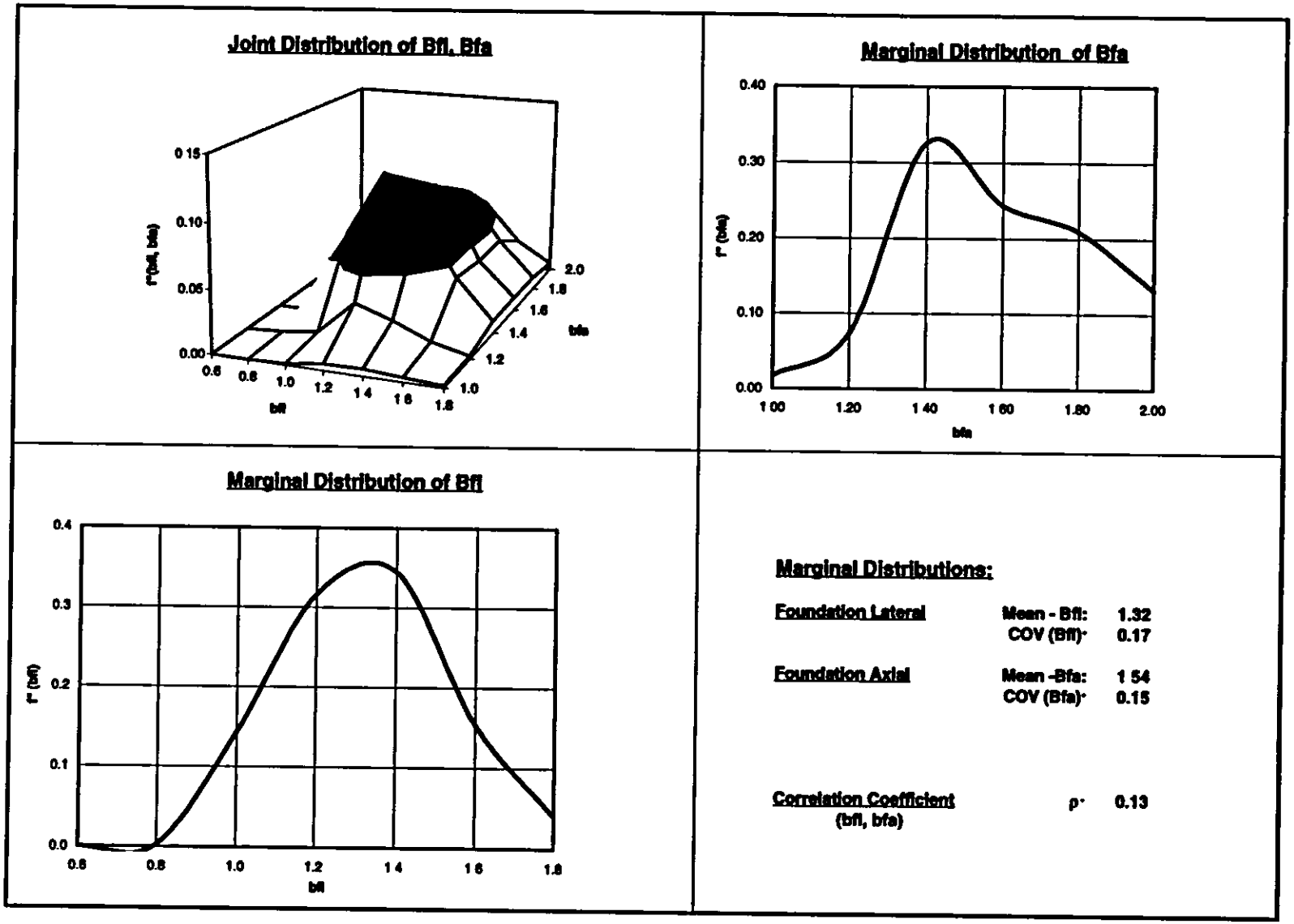

Figure 5-9(c): Posterior Distributions of Bias Factors (B_{fl}, B_{fa}) — All 9 Jacket Platforms

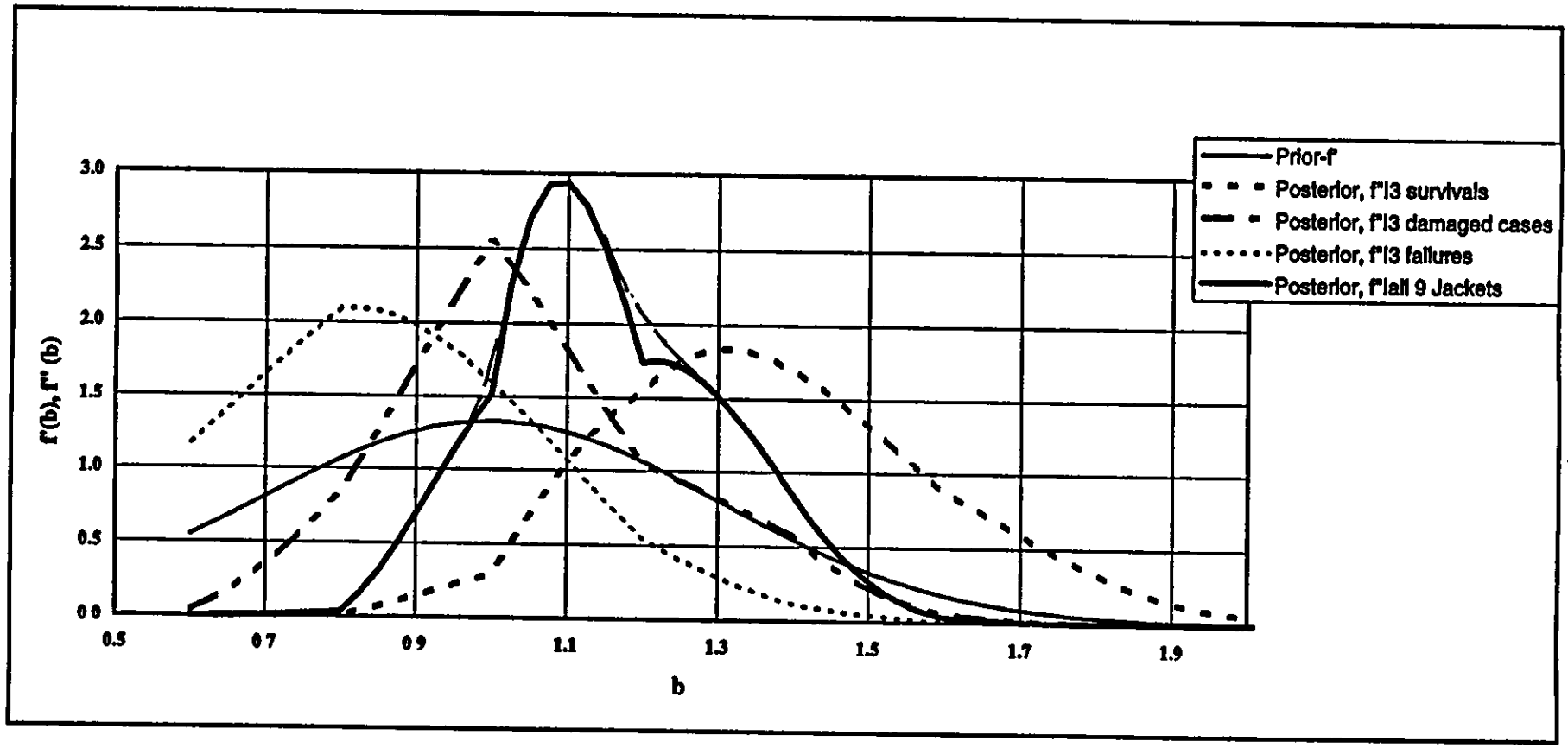

Figure 5-10: Prior and Posterior Distributions of Single Bias Factor, B — Base Case Analysis

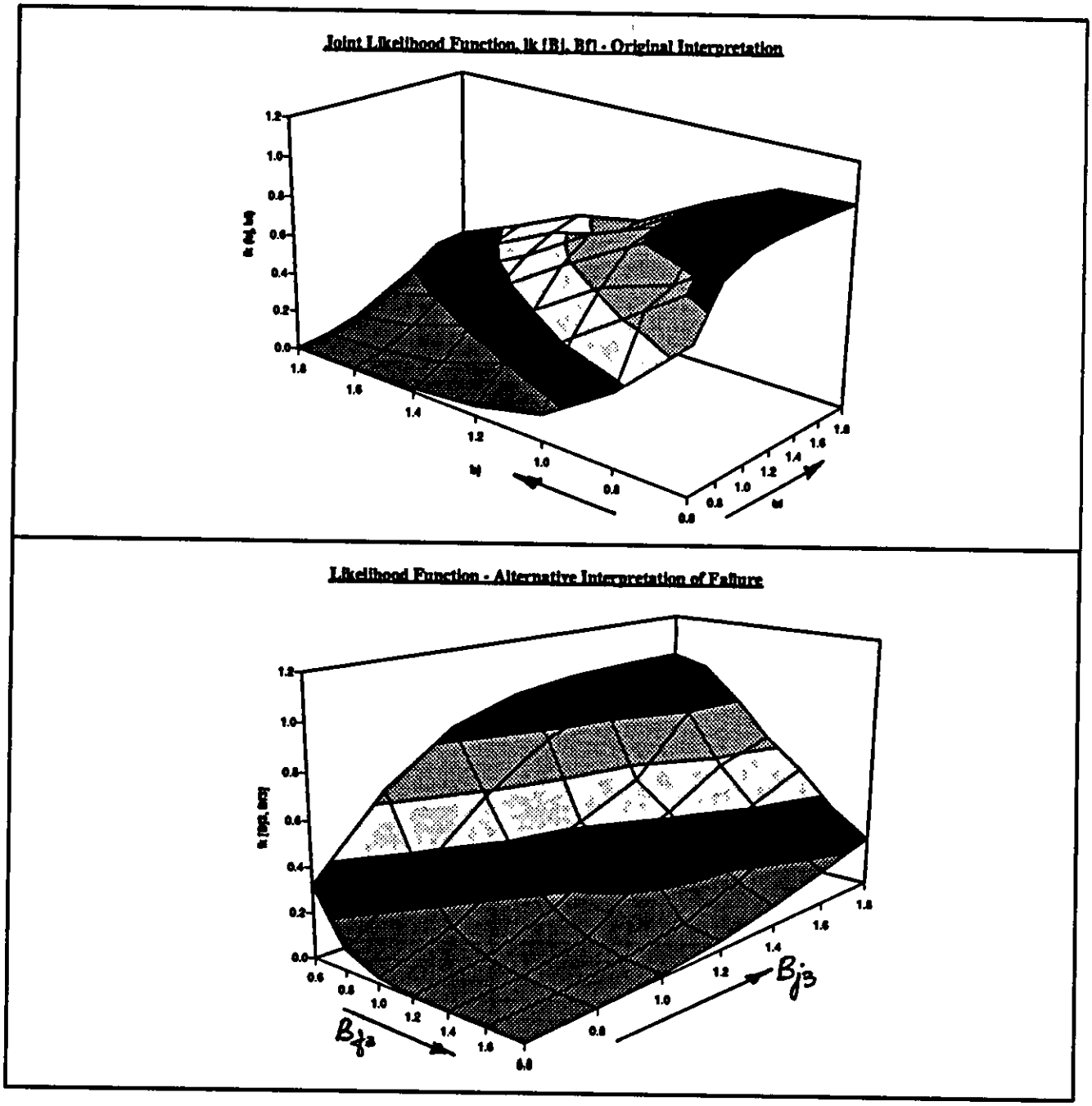

Figure 5-11(a): Joint Likelihood Functions (ST151H Platform) — Effect of Different Failure Interpretations

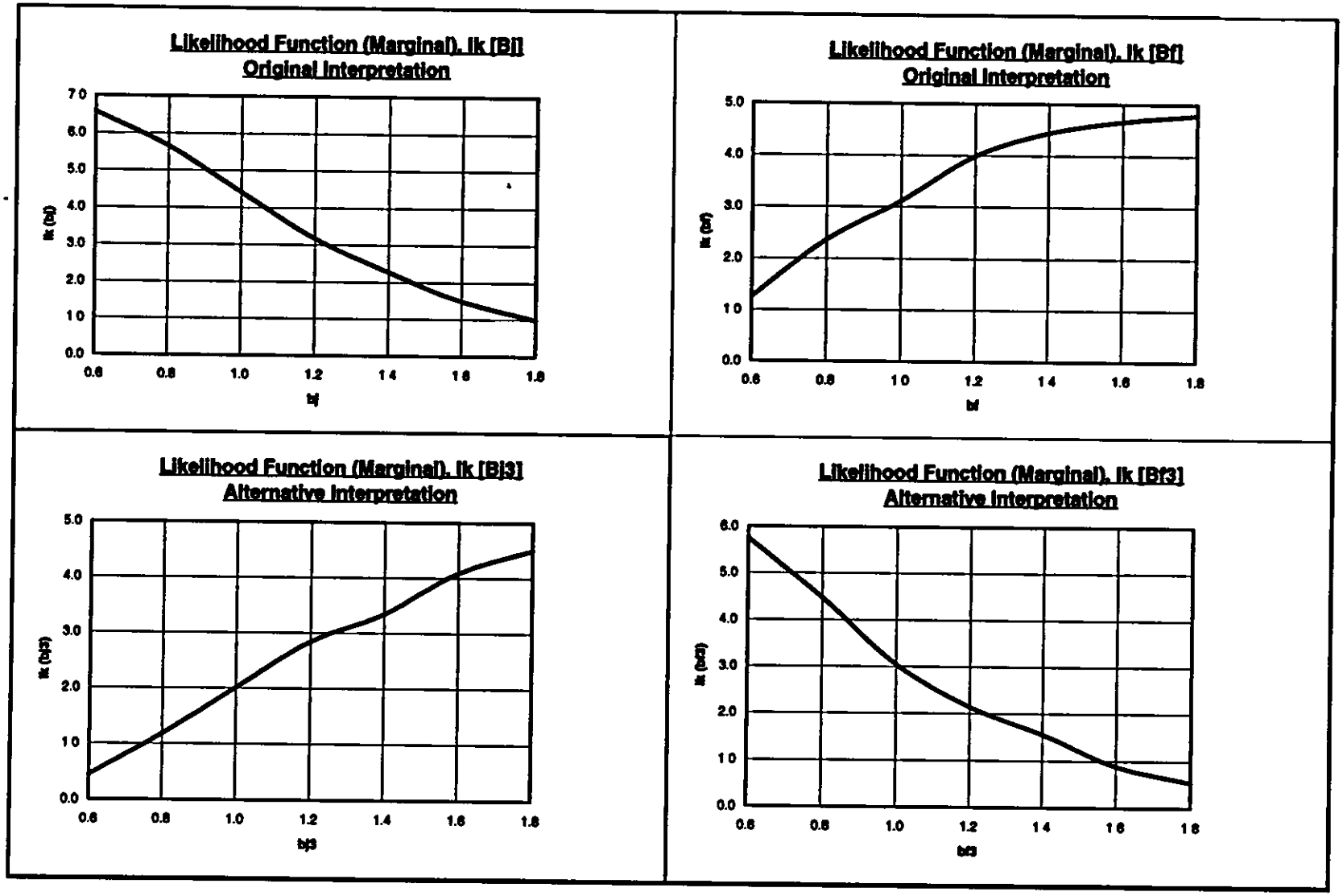

Figure 5-11(b): Marginal Likelihood Functions (ST151H Platform) — Effect of Different Failure Interpretations

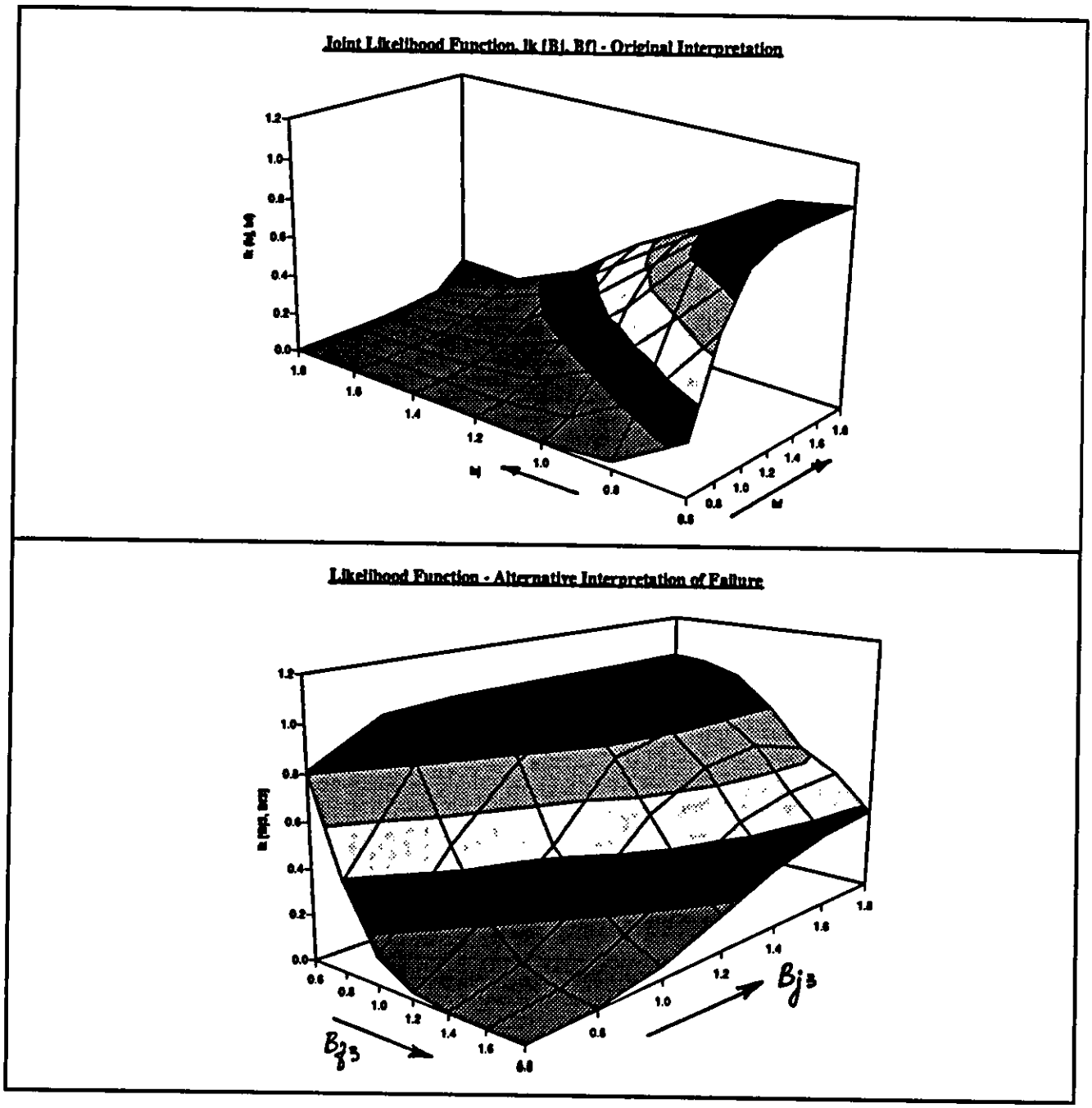

Figure 5-12(a): Joint Likelihood Functions (ST130A Platform) — Effect of Different Failure Interpretations

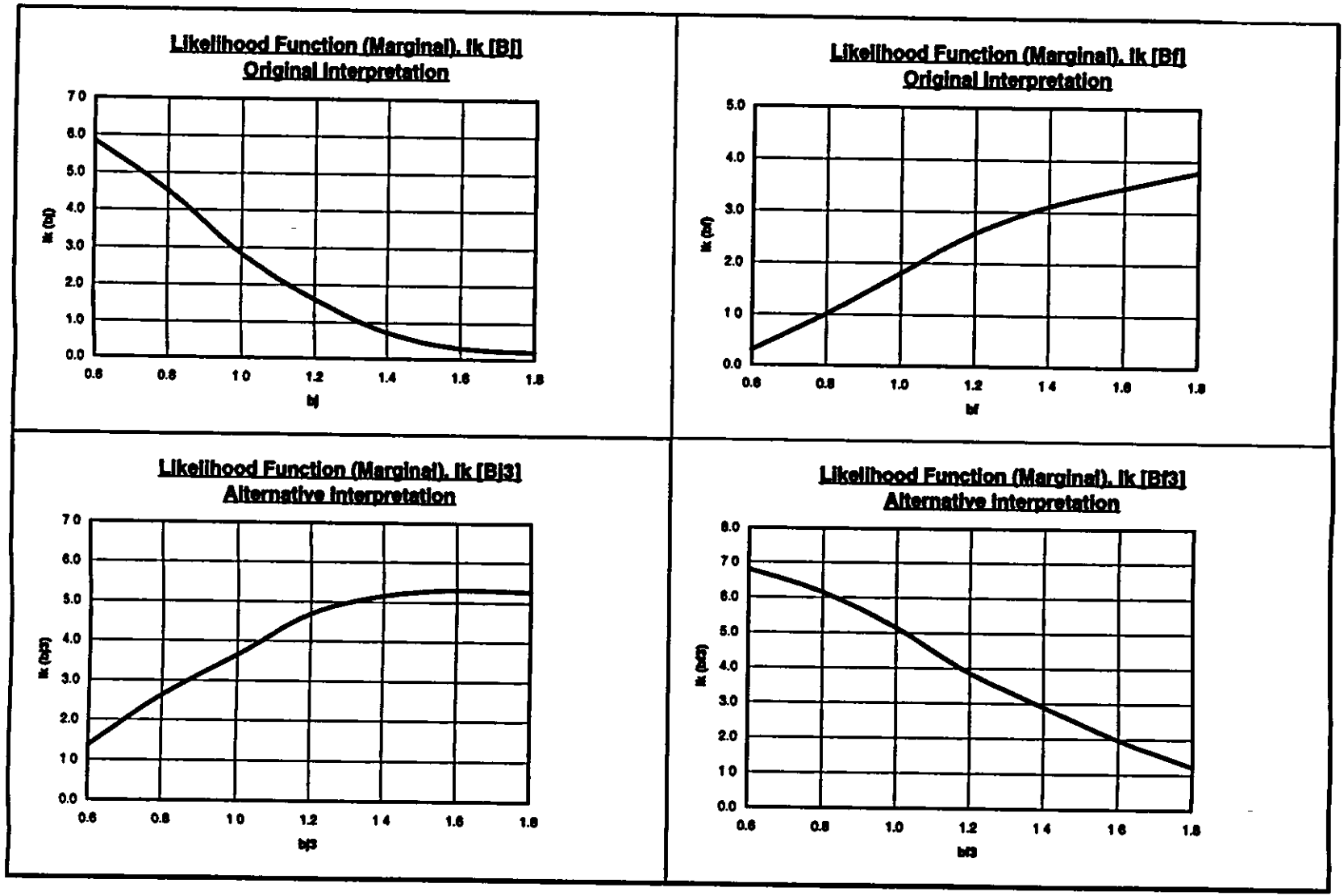

Figure 5-12(b): Marginal Likelihood Functions (ST130A Platform) — Effect of Different Failure Interpretations

Table 5-1: Summary of Calibration Conditions and Results - Survival Platforms

Capacity Analysis Case	Results from Capacity (Pushover) Analysis: Hindcast Base Shear (S-Andrew) (#1) S (kips)	Predicted Load Level at First Damage to the Jacket Structure (RJ1) (kips)	Predicted Load Level at Multiple Piles w/Fully Plastic Sections (Rff) (kips)	Predicted Load Level at Pullout/ Plunging of Several Piles (Rfa) (kips)	Calibration Conditions (#2)
Platform ST151K:					
Case-1 (Jacket)	3,700	2,900	-	-	S < 2,900 bj AND S < 4,230 bfl AND S < 4,000 bfa
Case-2 (Foundation Lateral)	3,700	-	4,230	-	
Case-3 (Foundation Axial)	3,700	-	-	4,000	
Platform ST130Q:					
Case-1 (Jacket)	990	1,380	-	-	S < 1,380 bj AND S < 1,470 bfl AND S < 1,860 bfa
Case-2 (Foundation Lateral)	990	-	1,470	-	
Case-3 (Foundation Axial)	990	-	-	1,860	
Platform WD103A:					
Case-1 (Jacket)	2,140	4,380	-	-	S < 4,380 bj AND S < 4,880 bfl AND S < 5,040 bfa
Case-2 (Foundation Lateral)	2,140	-	4,880	-	
Case-3 (Foundation Axial)	2,140	-	-	5,040	

Bias Factors (B's)	Mean and COV of Posteriors (Marginals) of B's for Individual Platforms(#3): Mean Value of B's (Bj, Bfl or Bfa)	COV of B's (Bj, Bfl or Bfa)	Mean and COV Values of Marginal Distributions of B's (Bj, Bfl or Bfa) for this Group
Bj	1 33	0 16	**Jacket Structure:** Mean, Bj = 1.35 COV, Bj = 0.16 **Foundation Lateral:** Mean, Bfl = 1 19 COV, Bfl = 0 19 **Foundation Axial:** Mean, Bfa = 1.41 COV, Bfa = 0.20
Bfl	1 15	0.21	
Bfa	1 40	0 20	
Bj	1 13	0.22	
Bfl	1 11	0.23	
Bfa	1 36	0.21	
Bj	1 09	0 23	
Bfl	1 08	0.24	
Bfa	1 36	0 21	

Notes:

(#1) - Expected Maximum Base Shear Given for "S" (a Random Variable)

(#2) - Mean Values of Predicted Capacity (a Random Variable) Given for Clarity

(#3) - Prior Distributions of Bj and Bfl Assumed with Mean of 1.0 and COV of 0.30

- Prior Distribution of Bfa Assumed with Mean of 1.3 and COV of 0.30

See Section 5.5 for Further Discussion

Table 5-2: Summary of Calibration Conditions and Results - Damaged Platforms

Capacity Analysis Case	Results from Capacity (Pushover) Analysis: Hindcast Base Shear (S-Andrew) (#1) S (kips)	Predicted Load Level at First Damage to the Jacket Structure (RJ1) (kips)	Predicted Load Level at Multiple Piles w/Fully Plastic Sections (Rfl) (kips)	Predicted Load Level at Pullout/ Plunging of Several Piles (Rfa) (kips)	Calibration Conditions (#2)
Platform ST151J:					
Case-1 (Jacket)	4,450	5,000 to 5,100	-	-	5,000 bj < S < 5,100 bj AND 5,000 bj < 6,000 bfl AND 5,000 bj < 5,785 bfa
Case-2 (Foundation Lateral)	4,450	-	6,000	-	
Case-3 (Foundation Axial)	4 450	-	-	5,785	
Platform ST177B:					
Case-1 (Jacket)	4,390	4,000 to 5,000	-	-	4,000 bj < S < 5,000 bj AND 4,000 bj < 4,700 bfl AND 4,000 bj < 3,700 bfa
Case-2 (Foundation Lateral)	4,390	-	4,700	-	
Case-3 (Foundation Axial)	4,390	-	-	3,700	
Platform SS139 (T25):					
Case-1 (Jacket)	1,060	2,100	-	-	S > 2,100 bj AND S > 2,240 bfl AND S > 2,665 bfa
Case-2 (Foundation Lateral)	1,060	-	2,240	-	
Case-3 (Foundation Axial)	1,060	-	-	2,665	

Bias Factors (B's)	Mean and COV of Posteriors (Marginals) of B's for Individual Platforms(#3): Mean Value of B's (Bj, Bfl or Bfa)	COV of B's (Bj, Bfl or Bfa)	Mean and COV Value of Marginal Distributions of B's (Bj, Bfl or Bfa) for this Group
Bj	1 02	0.20	**Jacket Structure:** Mean, Bj = 1.00 COV, Bj = 0.17
Bfl	1 12	0.22	**Foundation Lateral:** Mean, Bfl = 1 13 COV, Bfl = 0.21
Bfa	1 43	0 18	**Foundation Axial:** Mean, Bfa = 1.46 COV, Bfa = 0 17
Bj	1 03	0 20	
Bfl	1 14	0.21	
Bfa	1 40	0.21	
Bj	0 95	0.23	
Bfl	1 09	0.23	
Bfa	1 36	0 21	

Notes:

(#1) - Expected Maximum Base Shear Given for "S" (a Random Variable)

(#2) - Mean Values of Predicted Capacity (a Random Variable) Given for Clarity

(#3) - Prior Distributions of Bj and Bfl Assumed with Mean of 1.0 and COV of 0.30

- Prior Distribution of Bfa Assumed with Mean of 1.3 and COV of 0.30

See Section 5.5 for Further Discussion

Table 5-3: Summary of Calibration Conditions and Results - Failure Platforms

Capacity Analysis Case	Results from Capacity (Pushover) Analysis: Hindcast Base Shear (S-Andrew) (#1) S (kips)	Predicted Load Level at First Damage to the Jacket Structure (Rj1) (kips)	Predicted Load Level at Multiple Piles w/Fully Plastic Sections (Rfl) (kips)	Predicted Load Level at Pullout/ Plunging of Several Piles (Rfa) (kips)	Calibration Conditions (#2)
Platform ST151H:					
Case-1 (Jacket)	3,560	3,250	-	-	S > 3,250 bj AND 3,250 bj < 3,970 bfl AND 3,250 bj < 3,580 bfa
Case-2 (Foundation Lateral)	3,560	-	3,970	-	
Case-3 (Foundation Axial)	3,560	-	-	3,580	
Platform ST130A:					
Case-1 (Jacket)	1,990	2,100	-	-	S > 2,100 bj AND 2,100 bj < 1,800 bfl AND 2,100 bj < 2,860 bfa
Case-2 (Foundation Lateral)	1,990	-	1,800	-	
Case-3 (Foundation Axial)	1,990	-	-	2,860	
Platform ST52 (T21):					
Case-1 (Jacket)	1,380	1,610	-	-	S > 1,610 bj OR S > 3,250 bfl OR S > 2,700 bfa
Case-2 (Foundation Lateral)	1,380	-	3,250	-	
Case-3 (Foundation Axial)	1,380	-	-	2,700	

Bias Factors (B's)	Mean and COV of Posteriors (Marginals) of B's for Individual Platforms(#3): Mean Value of B's (Bj, Bfl or Bfa)	COV of B's (Bj, Bfl or Bfa)	Mean and COV Values of Marginal Distributions of B's (Bj, Bfl or Bfa) for this Group
Bj	0 92	0.23	**Jacket Structure:** Mean, Bj = 0.80 COV, Bj = 0.19
Bfl	1 11	0 23	
Bfa	1 39	0.20	**Foundation Lateral:** Mean, Bfl = 1.17 COV, Bfl = 0.21
Bj	0 86	0.22	**Foundation Axial:** Mean, Bfa = 1.38 COV, Bfa = 0.21
Bfl	1 18	0.21	
Bfa	1.37	0 21	
Bj	0 97	0.23	
Bfl	1 05	0 25	
Bfa	1 35	0 21	

Notes:

(#1) - Expected Maximum Base Shear Given for "S" (a Random Variable)

(#2) - Mean Values of Predicted Capacity (a Random Variable) Given for Clarity

(#3) - Prior Distributions of Bj and Bfl Assumed with Mean of 1.0 and COV of 0.30
- Prior Distribution of Bfa Assumed with Mean of 1.3 and COV of 0.30

See Section 5.5 for Further Discussion

Table 5-4: Summary of Calibration Results - All Platforms

Bias Factors (B's)	Mean and COV of Posterior Distributions of B's for Subsets of Platforms(#1)		Mean and COV Values of Posterior Distributions of B's (Bj, Bfl or Bfa) with all Platforms Included
	Mean Value of B's (Bj, Bfl or Bfa)	COV of B's (Bj, Bfl or Bfa)	
3 Survival Cases Only:			
Bj	1.35	0 16	**Jacket Structure:** Mean, Bj = 1.10 COV, Bj = 0.13 **Foundation Lateral:** Mean, Bfl = 1.32 COV, Bfl = 0.17 **Foundation Axial:** Mean, Bfa = 1.54 COV, Bfa = 0.15
Bfl	1.19	0 19	
Bfa	1 41	0 20	
3 Damage Cases Only:			
Bj	1 00	0 17	
Bfl	1 13	0 21	
Bfa	1 46	0 17	
3 Failure Cases Only:			
Bj	0 80	0 19	
Bfl	1 17	0 21	
Bfa	1.38	0 21	

Table 5-5: Summary of Calibration Conditions - Caissons (Lateral Capacity Case)

Platform	Results from Capacity (Pushover) Analysis			Calibration Conditions
	Hindcast Base Shear S-Andrew (#1) (kips)	Ultimate Capacity for Base Case Non-linear Model (Ru) (kips)	Load Level at Fully Plastic Section Event in Caisson Rp-1 (kips)	(#2), (#3)
SPelto 10	65	48	44	S > 44 bfl
SS135	132	148	128	S > 128 bfl
SS136	126	181	153	S > 153 bfl

Notes:
(#1) - Expected Maximum Base Shear Given for "S" (a Random Variable)
(#2) - Mean Values of Predicted Capacity (a Random Variable) Given for Clarity
(#3) - Calibration Condition that the Fully Plastic Section Event did not Occur

Table 5-6: Summary of Calibration Conditions and Results - Single Bias Factor - Base Case Analysis

Capacity Analysis Case	Results from Capacity (Pushover) Analysis: Hindcast Base Shear (S-Andrew) (#1) S (kips)	Predicted Load Level at First Damage to the Jacket Structure (RJ1) (#2) (kips)	Predicted Load Level at Multiple Piles w/Fully Plastic Sections (Rff) (kips)	Predicted Load Level at Pullout/ Plunging of Several Piles (Rfa) (kips)	Calibration Basis (#3)	Distribution of Posterior of B for Three Subsets of Platforms (#4)	Distribution of Posterior of B for All Platforms Included
Survival Platforms:							
ST151K	3,700	2,900	3,700	-	S < 2,900 b	Mean = 1.37 COV = 0.16	Mean = 1.15 COV = 0 13
ST130Q	990	-	1,380	-	S < 1,380 b		
WD103A	2,140	4,250	4,660	4,460	S < 4,250 b		
Damaged Platforms:							
ST151J	4,450	3,800 to 4,540	4,730	4,935	3,800 b < S < 4,540 b	Mean = 1.06 COV = 0.18	
ST177B	4,390	3,850	3,900	3,720	S > 3,850 b		
SS139 (T25)	1,060	1,640	-	-	S > 1,640 b		
Failed Platforms:							
ST151H	3,560	2,680 Ult. = 3,250	-	-	S > 3,250 b	Mean = 0 90 COV = 0.21	
ST130A	1,990	-	1,830	-	S > 1,830 b		
ST52 (T21)	1,380	1,610 Ult. = 1,610	-	-	S > 1,610 b		

Notes:

(#1) - Expected Maximum Base Shear Given for "S" (a Random Variable)

(#2) - Range of Predicted Load Level Given for ST151J During which the Observed Damage may have Occurred. The Ultimate Capacity for Failed Platforms Also Given.

(#3) - Mean Values of Predicted Capacity (a Random Variable) Given for Clarity

(#4) - Prior Distributions of B Assumed with Mean of 1.0 and COV of 0.30

Table 5-7: Summary of Sensitivity of Variations in the Priors of B's on their Posterior Distributions

Bias Factors, B's		Mean and COV of Posterior of B's			Mean and COV of Posterior of B's	
		Prior COV = 0.2	Prior COV = 0.3 (as in Table 5-4)	Prior COV = 0.4	(as in Table 5-4) Prior Mean (BJ) = 1.0 Prior Mean (Bfl) = 1.0 Prior Mean (Bfa) = 1.3	Variations of Prior Mean (BJ) = 1.2 Prior Mean (Bfl) = 1.3 Prior Mean (Bfa) = 1.5
Case A: Variation in Mean and COV of Prior of Bj Only (#1)						
BJ	Mean	1 09	1 10	1 11	1 10	1 13
	COV	0 13	0.13	0 14	0.13	0 13
Bfl	Mean	1.32	1.32	1.32	1.32	1.33
	COV	0 17	0.17	0.17	0.17	0 17
Bfa	Mean	1.54	1.54	1.54	1.54	1.55
	COV	0 15	0.15	0 15	0.15	0 15
Case B: Variation in Mean and COV of Prior of Bfl Only (#2)						
BJ	Mean	1.09	1.10	1 11	1 10	1 11
	COV	0 14	0.13	0 13	0.13	0 13
Bfl	Mean	1.20	1.32	1.40	1.32	1 45
	COV	0 16	0.17	0 17	0.17	0 16
Bfa	Mean	1.52	1.54	1.55	1.54	1.55
	COV	0 15	0.15	0 15	0.15	0 15
Case C: Variation in Mean and COV of Prior of Bfa Only (#3)						
BJ	Mean	1 09	1 10	1 11	1 10	1 11
	COV	0.13	0.13	0 13	0.13	0 13
Bfl	Mean	1 31	1.32	1.32	1.32	1.32
	COV	0.13	0.17	0 17	0.17	0 17
Bfa	Mean	1.48	1.54	1.57	1.54	1.59
	COV	0 14	0.15	0 15	0.15	0 15

Notes (#1) - Prior Distributions of Bfl (1.0, 0.3) and Bfa (1.3, 0.3) were kept same for all sensitivity analysis cases under Case A

(#2) - Prior Distributions of BJ (1.0, 0.3) and Bfa (1.3, 0.3) were kept same for all sensitivity analysis cases under Case B

(#3) - Prior Distributions of BJ (1.0, 0.3) and Bfl (1.0, 0.3) were kept same for all sensitivity analysis cases under Case C

Section 6
Conclusion and Recommendations

This study provides information that improves the understanding of biases that are inherent in the current state-of-the-practice platform assessment process. These results can be used to improve the definition of failure probability of specific platforms as part of fitness-for-pupose evaluations. The primary conclusions relating to each of the major elements of the study are presented in the following sections.

6.1 CAPACITY ASSESSMENT

An improved capacity analysis procedure was developed through case studies and was tested on nine steel jacket platforms. In addition to general improvements in the recipe, specific improvements in the analyses of the selected platforms (as compared to the Phase I study) were gained through additional information (such as new hindcast data, site-specific soil information, confirmation of platform damage from new inspections and salvage of platforms). This improvement reduced the uncertainties in the predictions of platform behavior during Andrew. The resulting structural analyses were found to match very closely with the post Andrew inspections.

The improved predictions of the platforms behavior during Andrew were realized due to the following key factors:

- General reduction in the Andrew load level estimates using the new hindcast
- Explicit joint strength and stiffness modeling
- Realization of significant differences in the biases in the strength characterizations for the pile/soil and jacket elements

A set of four analyses were completed for each platform to determine the uncoupled estimates of capacity based on possible failures of the jacket and foundation (lateral and axial). These analyses were performed to eliminate the effects of uncertainties associated with the complement parts of the platform (e.g., the effect of foundation uncertainty on the estimate of jacket strength). This set of capacity analyses improved the understanding of the platform behavior specifically with respect to the interaction of damage predictions in one part of the platform on the other parts. It also improved the understanding of the effects of various parameters on ultimate capacity.

In some cases these estimates provided reasons for the differences between predictions and observations. For example, the Case-2 (lateral foundation) analysis predicted pile hinging for only two platforms The Case-3 (axial foundation) analysis predicted pullout/plunging of multiple piles for only two platforms. This is a significant change from the predictions in Phase I where much more foundation damage was predicted.

The analysis predicted very small lateral and axial pilehead displacements even after full plasticity of several piles or following pile/soil axial failure. This amount of deformation is considered to be too small to be observable by conventional inspection methods. This implies that some modification to some of the platform observation classifications could be made if more detailed

information were available regarding pile response. These results indicate that the predictions of pile lateral capacity may not be overly conservative.

Analysis to determine "failure mode specific" capacity estimates help to identify areas of strengths and weaknesses which is beneficial in developing cost effective mitigation measures that may be required to meet the new API RP 2A, Section 17 guidelines. In some cases, mitigation measures based on minimal, or simplistic, analysis could be too costly or even counter productive.

The number of analyses could be further increased to more accurately define behavior and differentiate the effects of biases within the various elements of a jacket, (e.g , braces, joints, jacket legs). In many cases, information on the state of a platform is limited and gross assumptions are necessary which may influence the analytical results and recommendation. Further investigation of the effects of such assumptions could have a dramatic effect on the results of the assessment.

6.2 CALIBRATION

A calibration process was developed to determine multiple bias factors, applicable to both the jacket structure and its foundation, using mode specific capacity predictions.

Bias Factors

Bias factors were computed for the jacket structure (B_j), foundation lateral (B_{fl}), and foundation axial (B_{fa}) as 1.1, 1.3 and 1.5, respectively. These results confirm the expectation that the formulation of foundation capacity is more conservative than that of the jacket structure. The estimate of the mean value of B_j (1.1) is lower than the overall (system) bias factor determined during the Phase I [1, 4]. The Phase I bias factor was not applicable to a specific failure mode (jacket structure or foundation). The mean value of B_{fl} is the same as the uncoupled bias factor of 1.3 determined in the API/MMS Foundation Study [5]. The mean of B_{fa} (1.5) is lower than the uncoupled bias factor of 1.7 determined in the API/MMS Foundation Study. These results indicate a level of consistency in the evolution of the calibration through the three studies and a confirmation of a level of conservatism in the assessment process

Uncertainties Model

The bias factors determined are related to the capacity analysis procedures and the reliability analysis model followed. Studies were performed that indicated that the final bias factors are generally insensitive to variations in the random variables (e.g., COVs of R, U, T_p) and prior bias distributions. Variation of these quantities may have a more prominent effect on the likelihood functions but the effect on bias factor is diminished due to multiplication of the prior distributions and due to the combination of platforms.

The reliability model is consistent with the current industry practice in wave force formulation, however, new information regarding wave force variability suggests the possibility of a new model. The data gathered for Exxon's ocean test structure [40] indicated variability in the

relationship between individual wave height and base shear. This variability was found to be significant (20 to 25 percent), which is generally treated as the drag coefficient (force) variability. More recently some researchers have suggested that the variability in the maximum base shear in a seastate may be consistent with the variability in maximum wave height. An alternative reliability model could be developed to consider the different approach for wave force variability.

The effects of the assumptions regarding correlation among various random variables was not evaluated in this study. Further work is needed to address this issue.

Application of Bias Factors

The bias factors represent errors associated with modeling of the loading and response. These factors are applicable to the overall safety factor (resistance divided by loading effects) for platforms during extreme hurricane loading The fact that all of the bias factors exceed unity indicates that the procedures used in this study for the sample of structures, are somewhat conservative. The analysis has predicted more damage and failure than was actually observed. The results should be considered as evidence supporting the use of the analysis procedures developed by industry in that they appear to be somewhat conservative overall. It is not recommended that the calculated bias factors be applied to individual platforms in any assessment since they were derived from a small sample of platforms. Also, the individual platform bias factors ranged from 0.86 to 1.32 for jacket structure capacity, from 1.05 to 1.18 for foundation lateral capacity, and from 1.35 to 1.44 for foundation axial capacity indicating that the application of a single average bias factor on an individual platform may not be appropriate.

These bias factors have provided a better appreciation of the uncertainties and biases that affect reliability analysis. The API and the regulatory bodies can use the results in the development of guidelines and criteria for platform assessment. With good engineering judgment, the results can be applied in probability based requalification of steel jacket platforms that are similar to the sample investigated. These factors may be considered in determination of the average failure probability estimates and in the economic risk and cost-benefit studies for a fleet of platforms. The proper use of this data could help in establishing more appropriate mitigation needs for a platform for its survivability against large storms. It is recommended that these results not be used as the basis for new design, however, they may be useful in sensitivity studies.

However, these results should not be used for new construction because the cost penalties for not using it are small.

6.3 RECOMMENDATIONS

Now that the procedure for analysis, calibration, and Bayesian updating is set-up, it will be relatively easy to include additional data as they become available. The definition of these bias factors can be further improved as additional cases are included in the calibration. In particular, structures that have experienced extreme loading provide very useful information to support the

calibration. This improvement can come both in the form of refinement to the current bias factors and in the development of bias factors that can be used more directly within the analysis. This could include, for example, bias factors specifically for joints, braces, and piles.

Further improvement in the process can be achieved through the following specific recommendations:

1) Further Improvement of Capacity Analysis Procedures

- Investigate additional platforms to determine the differences in the uncoupled capacity estimates for the jacket structure and its foundation. It would be preferable to include platforms with structural configurations different than those used in this study.
- Additional information is needed regarding the strength and stiffness of joints specifically with physical properties characteristic of those on older platforms.

2) Further Improvement of the Bias Factors

- Include additional platforms in the sample such as those loaded by more recent (i.e. Opal) and future hurricanes. Platforms experiencing foundation damage would be most useful
- Performing a similar study using platforms from another region For example, a large number of platforms affected by Hurricane Roxanne in the Bay of Campeche could provide significant information useful to the calibration.
- Investigate the sensitivity of bias factors due to differences in the consideration of uncertainties.
  * The effect of considering the wave force variability associated with only the largest wave in a storm, instead of the wave-to-wave wave force variability considered in this phase.
  * The effect of considering correlations (dependence) in wave-to-wave variabilities in H and ε_o, hour-to-hour uncertainties in H_s and U, site-to-site uncertainties in H_s and U, and platform-to-platform uncertainties in capacities.

3) Further Improvement of the Reliability Analysis Procedures

- Estimate the annual probability of failure for all platforms investigated in this study to get a better understanding of the implication of the process on platform safety decisions.
- Develop a white paper on various approaches used by the offshore industry to determine the annual failure probability. A study comparing the different approaches for selected platforms may lead to an improved procedure.

Appendix A
Platform Details

The following platform specific information is provided:

- Platform orientation and storm approach direction
- Structural details
  - vertical framing and sizes
  - key pile information
- Structural damage information, where applicable
- Soil shear strength profiles
- Hindcast data at platform locations

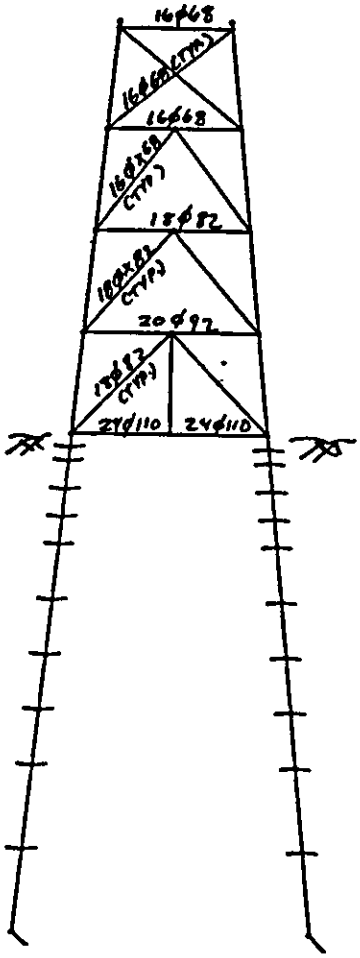

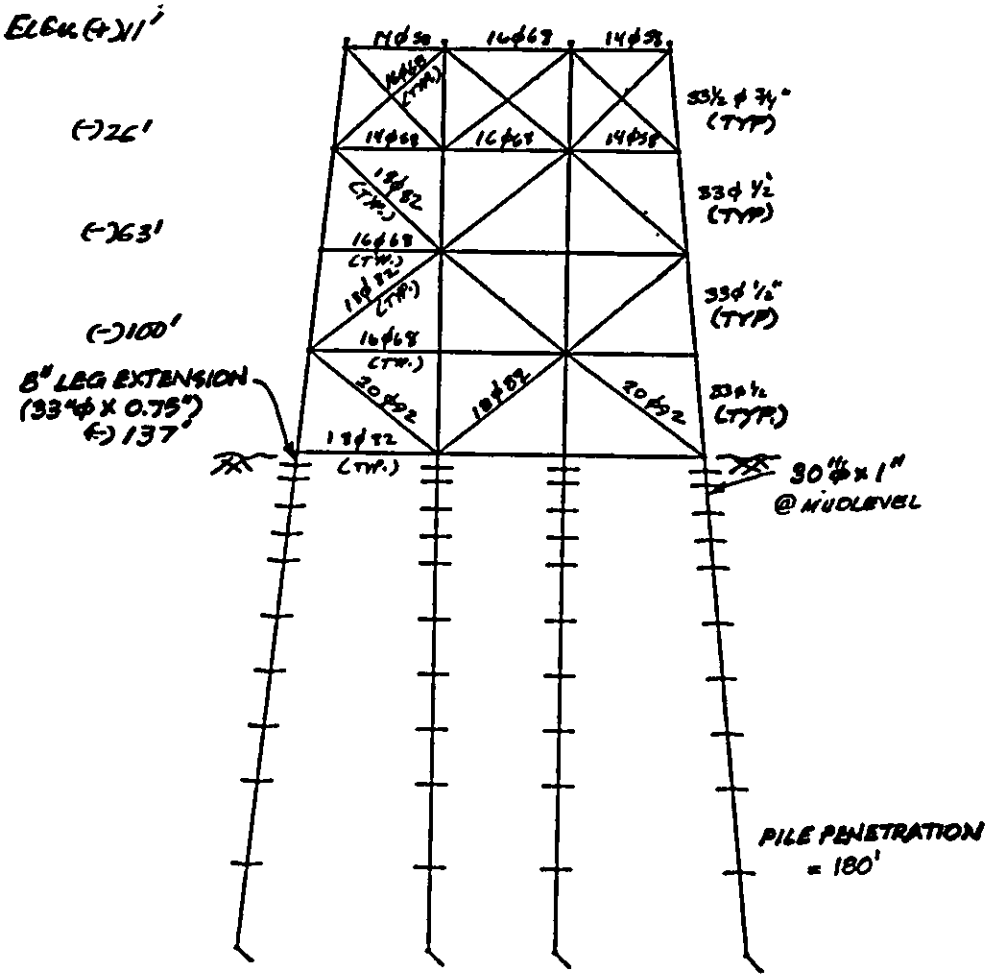

Rows 1 to 4

Rows A & B

Notes:
- Brace sizes indicate diameter and unit weight in lb/ft.
- Thickness of braces is 0.438" unless noted.
- Thickness is 0.406" for 16φ68 and 14φ58

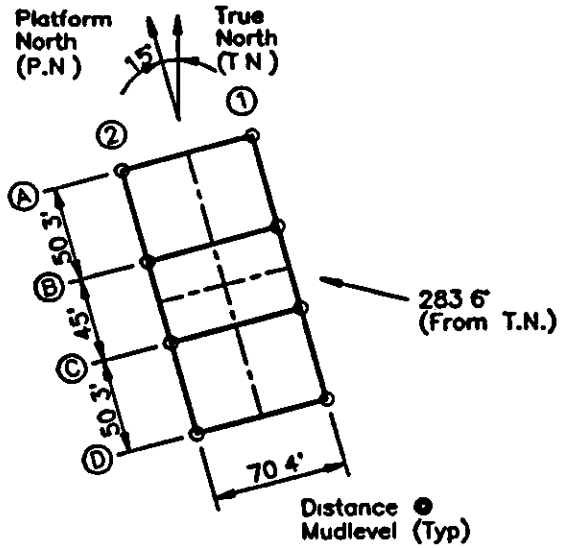

ST151K - Structural Configuration

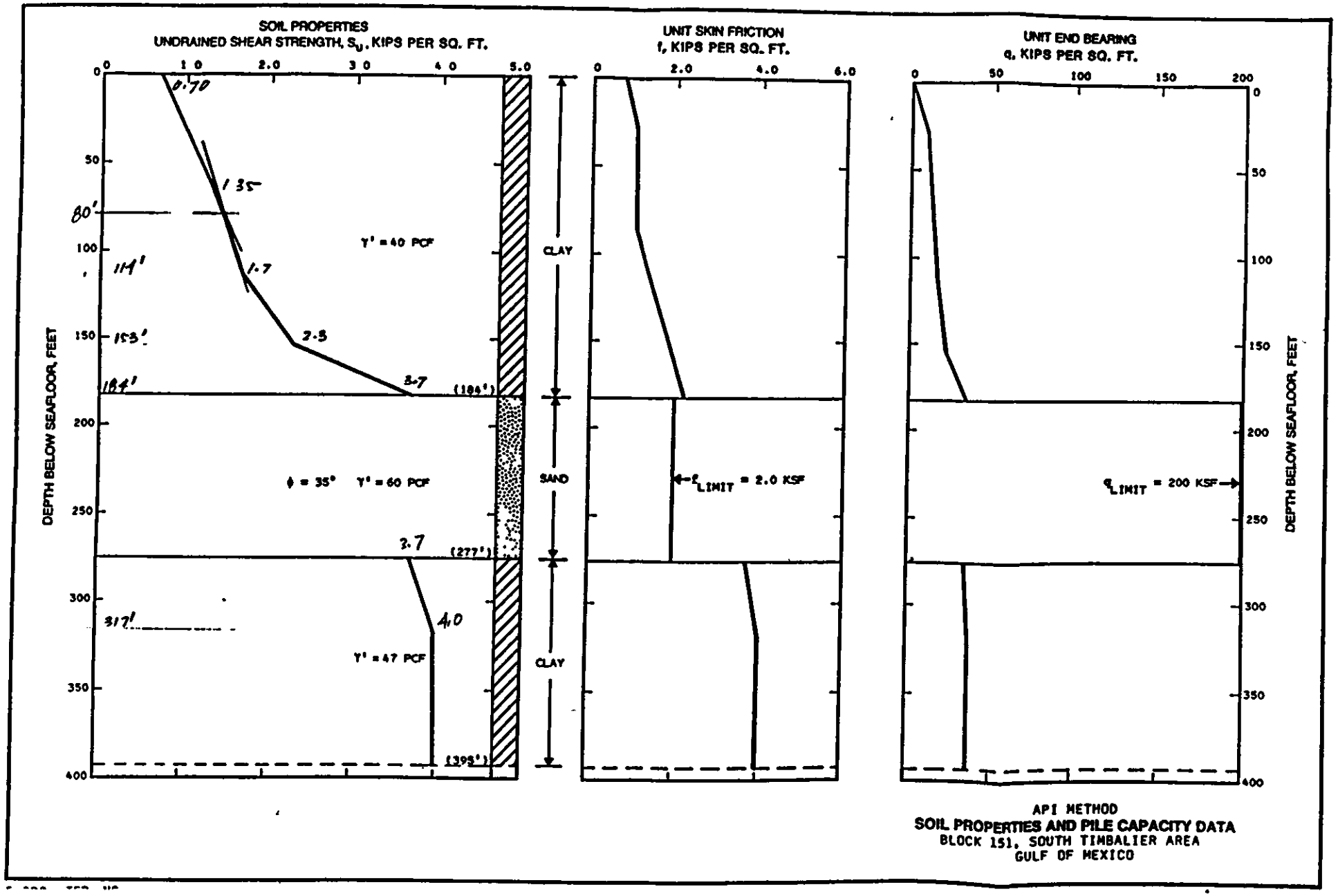

ST151K - Soil Properties

DAY	HOUR	HS	HMAX	TP	TZ	DIRDOM	CSPEED	CDIRN	CRES	WINDD	WINDS
25	16	15.07	25.61	14.48	10.72	273.6	1.40	275.0	1.39	26.01	65.37
25	17	17.60	29.91	14.34	10.61	273.8	1.82	274.7	1.82	26.10	73.83
25	18	20.35	34.60	14.27	10.56	274.1	2.19	273.9	2.19	28.39	84.97
25	19	23.46	39.88	14.17	10.49	275.0	2.51	272.7	2.51	30.83	99.04
25	20	26.86	45.66	14.06	10.41	276.7	2.84	271.3	2.83	32.46	116.93
25	21	30.41	51.70	13.49	9.98	278.8	3.19	270.5	3.15	39.38	136.70
25	22	34.74	59.05	13.11	9.70	283.6	3.39	270.1	3.30	69.81	159.15
25	23	34.58	58.78	12.98	9.61	288.2	3.31	270.5	3.15	121.70	151.57
26	00	31.75	53.97	12.76	9.44	293.6	2.95	270.9	2.72	144.12	139.64
26	01	28.66	48.72	11.68	8.65	297.6	2.52	271.4	2.26	152.53	124.25
26	02	24.96	42.44	11.21	8.30	307.0	2.11	272.3	1.73	152.42	109.84
26	03	23.39	39.77	9.51	7.04	317.6	1.77	274.2	1.28	159.13	100.47
26	04	21.86	37.16	9.47	7.01	330.3	1.48	277.1	0.89	157.76	93.21
26	05	20.52	34.88	9.15	6.77	17.9	1.22	280.2	-0.16	166.48	85.95
26	06	19.19	32.63	8.98	6.65	38.8	0.97	284.4	-0.40	172.04	81.15

FACTOR HMAX/HS USED IS 1.70000

ST151K - Hindcast Data

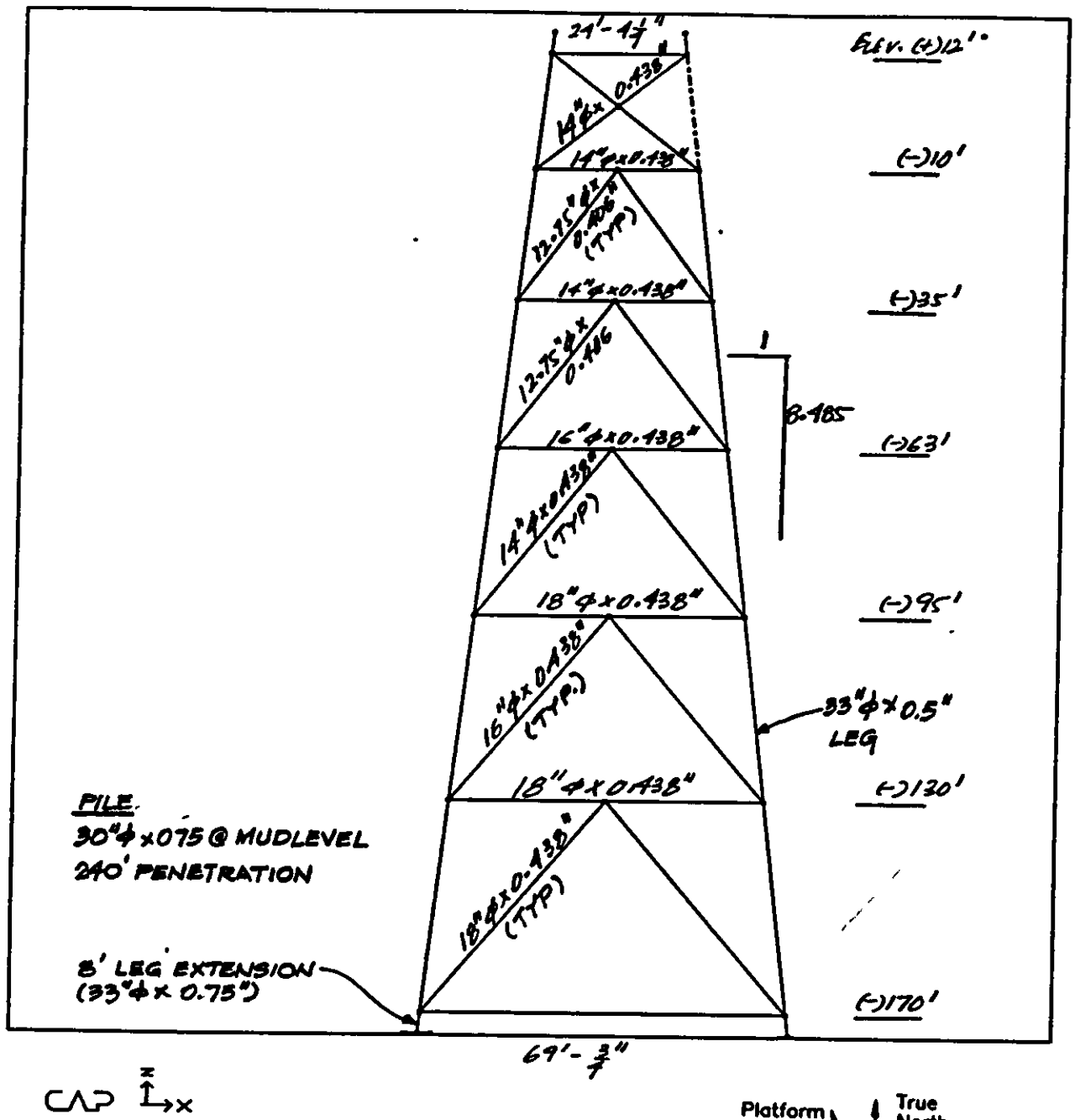

ST1300 -Typical Framing

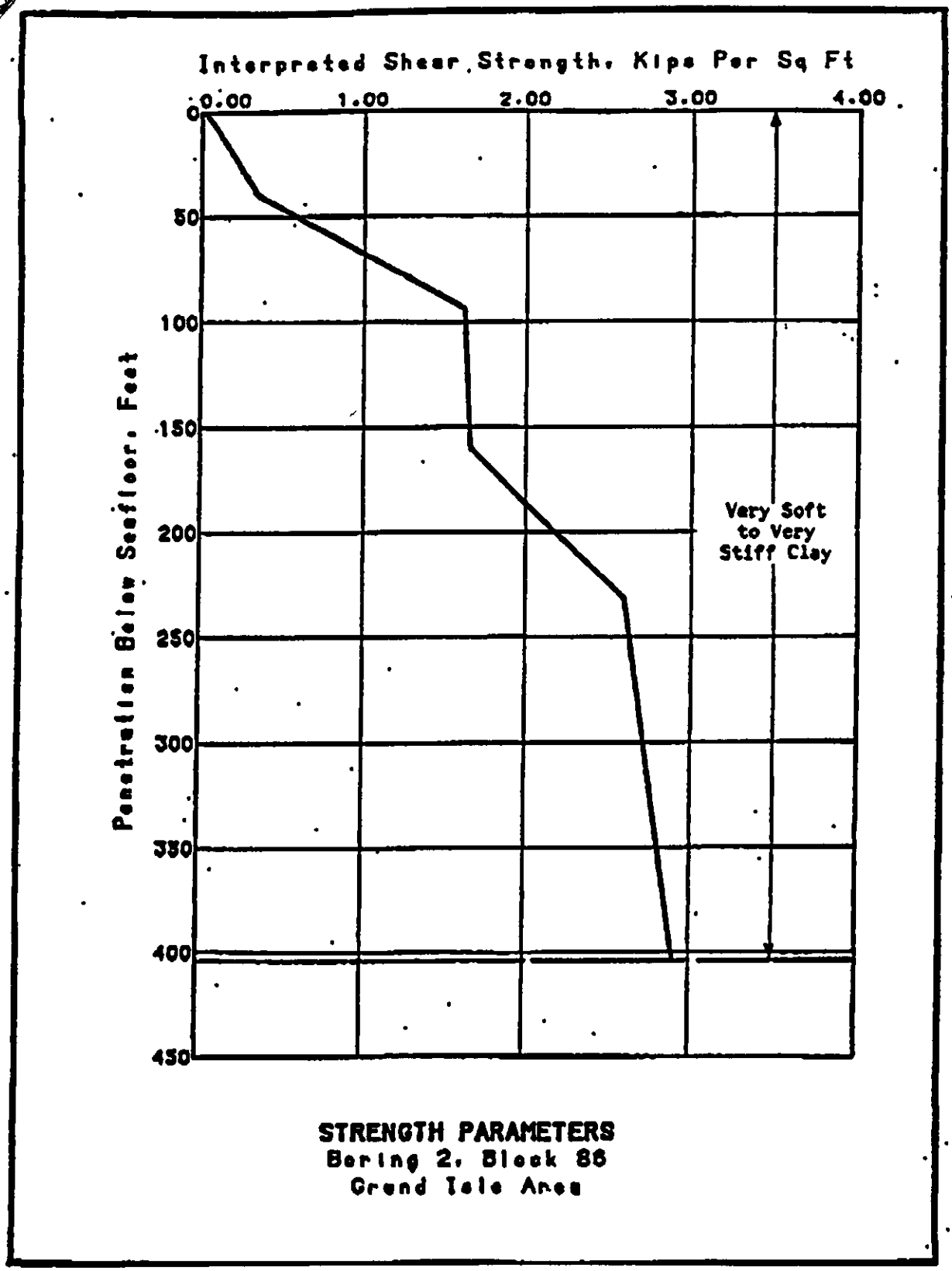

ST130Q - Soil Shear Strength Profile

DAY	HOUR	HS	HMAX	TP	TZ	DIRDOM	CSPEED	CDIRN	CRES	WINDD	WINDS
25	16	15.24	26.37	14.61	10.81	272.5	1.24	273.9	1.24	29.34	66.27
25	17	17.73	30.67	14.35	10.62	272.6	1.62	272.9	1.62	30.29	74.46
25	18	20.46	35.39	14.26	10.55	273.3	1.97	272.7	1.97	33.74	84.86
25	19	23.47	40.61	14.10	10.43	274.9	2.29	272.9	2.28	37.33	97.86
25	20	26.69	46.17	12.78	9.46	277.4	2.61	272.9	2.60	40.53	114.05
25	21	29.81	51.58	13.14	9.72	280.5	2.93	273.0	2.91	48.89	130.80
25	22	33.27	57.56	12.99	9.61	285.2	3.12	273.7	3.05	74.94	149.13
25	23	33.69	58.29	12.94	9.57	291.6	3.03	275.2	2.91	113.38	145.00
26	00	32.01	55.38	12.11	8.96	297.5	2.71	276.4	2.53	132.25	133.82
26	01	29.26	50.62	11.60	8.58	301.8	2.32	277.1	2.10	142.04	118.62
26	02	25.59	44.27	11.22	8.30	309.4	1.93	277.6	1.64	144.37	105.00
26	03	24.39	42.20	9.72	7.19	317.6	1.61	279.1	1.26	151.84	96.99
26	04	22.52	38.96	9.70	7.18	325.1	1.35	282.4	0.99	151.81	90.54
26	05	20.83	36.04	9.41	6.97	338.5	1.13	286.9	0.70	160.63	84.26
26	06	19.36	33.49	9.10	6.74	351.6	0.92	293.2	0.48	166.23	80.11

FACTOR HMAX/HS USED IS 1.73000

ST130Q - Hindcast Data

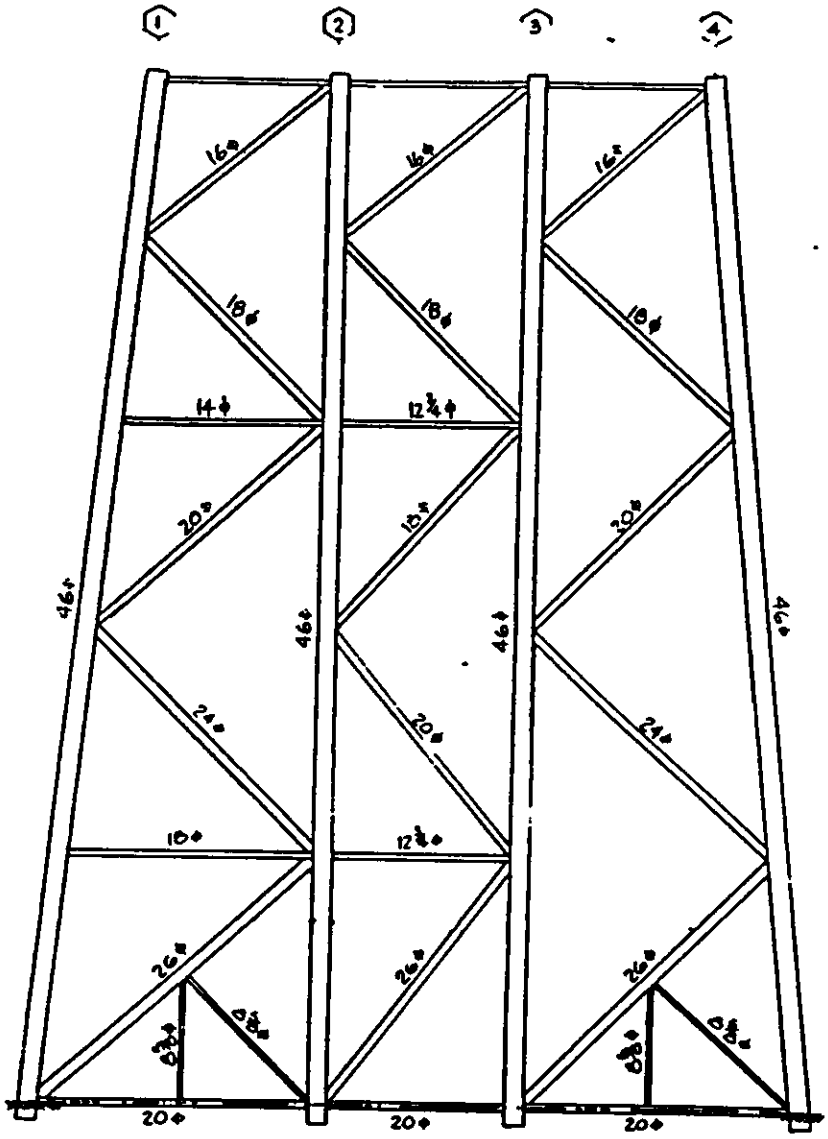

Row A

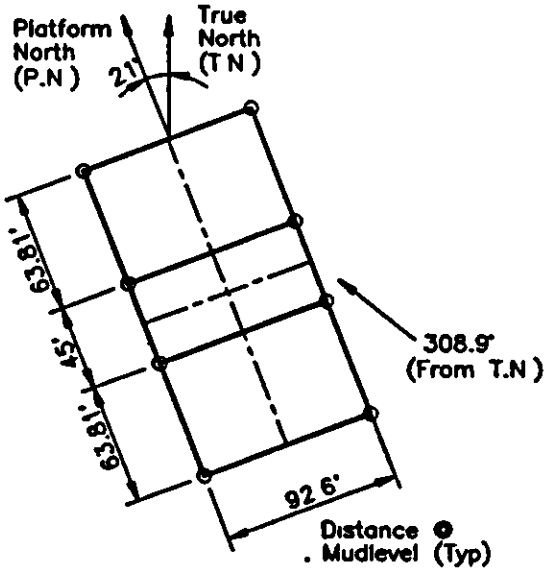

WD103 - Structural Configuration

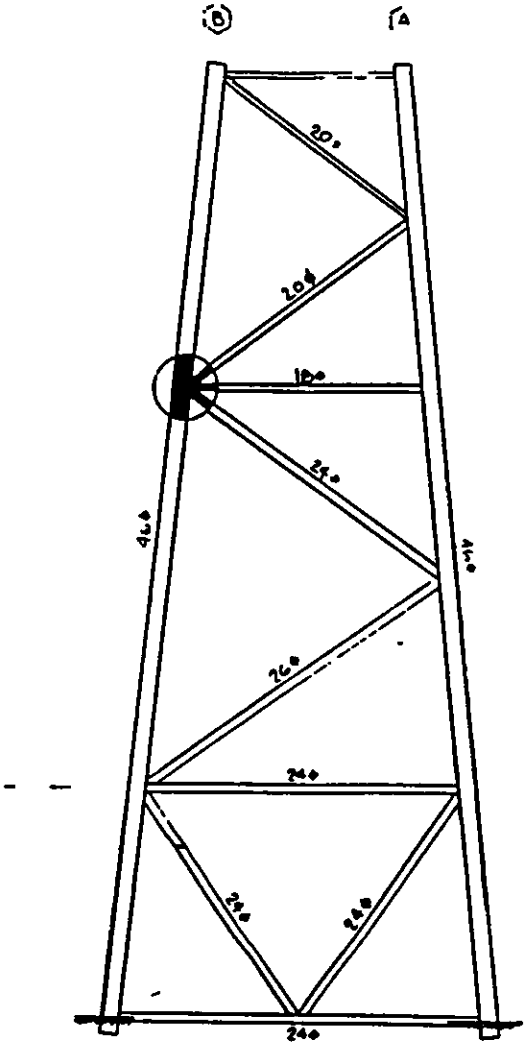

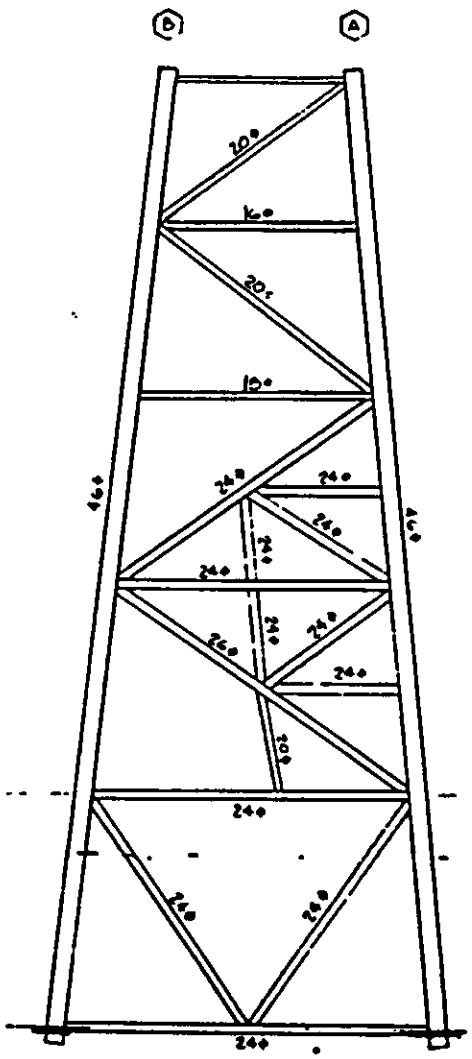

Row 1
(Row 4 - Opposite)

Row 2
(Row 3 - Opposite)

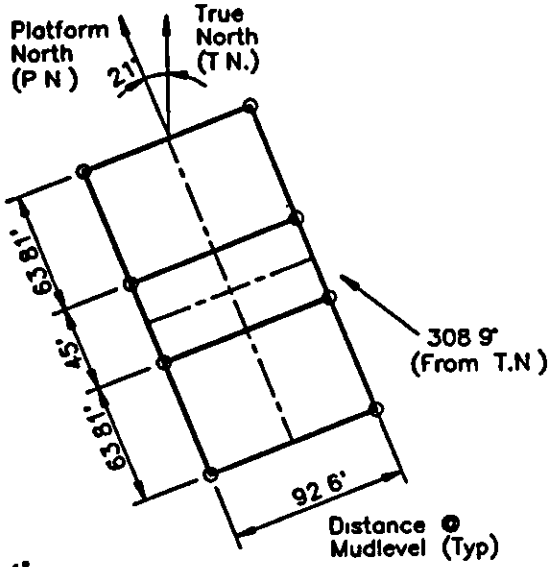

WD103 - Structural Configuration

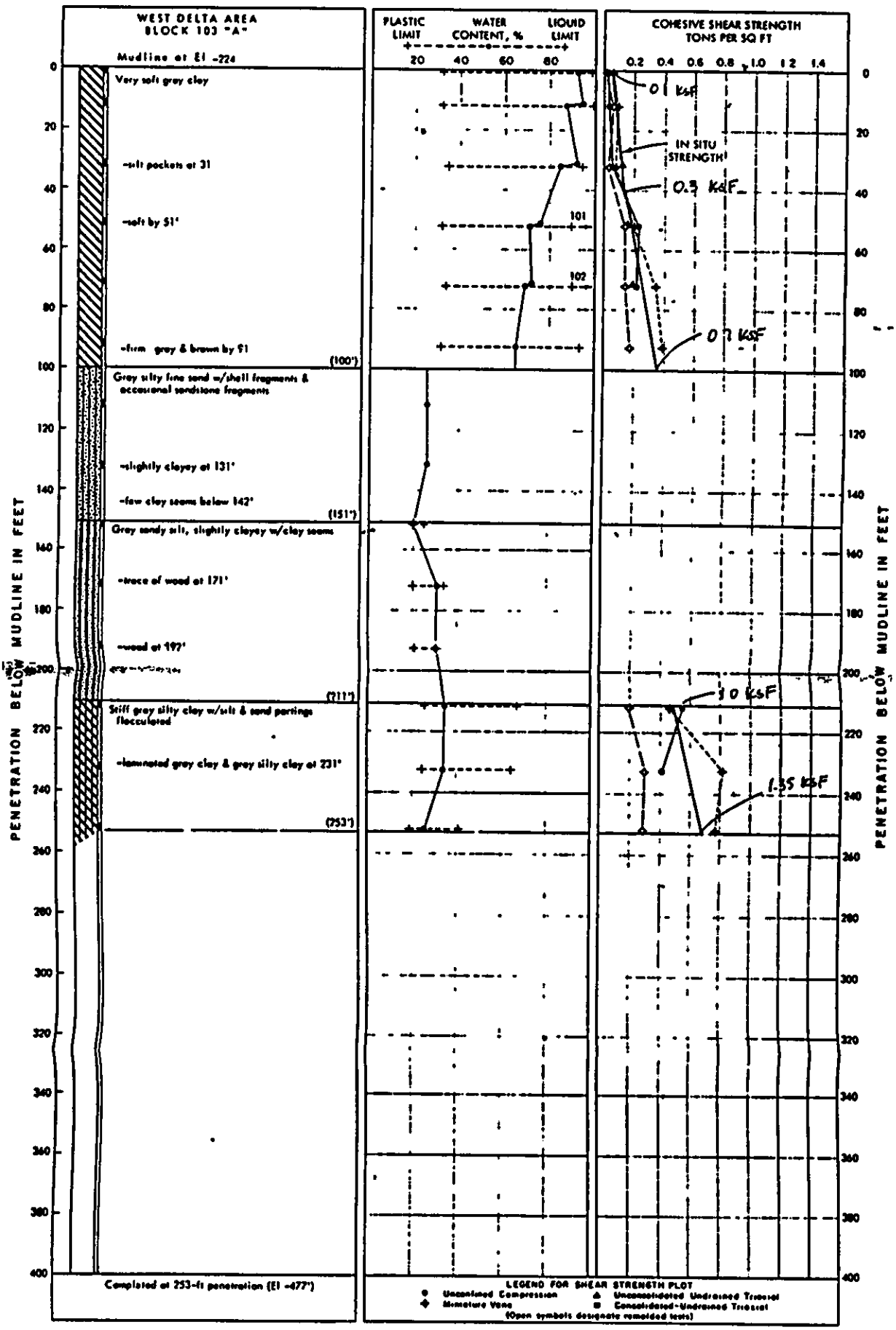

LOG OF BORING AND TEST RESULTS

WD103 - Soil Properties

DAY	HOUR	HS	HMAX	TP	TZ	DIRDOM	CSPEED	CDIRN	CRES	WINDD	WINDS
25	16	16.59	28.87	13.79	10.20	289.2	0.72	270.2	0.68	45.22	69.89
25	17	18.60	32.37	13.59	10.06	290.2	0.91	269.9	0.86	49.80	76.04
25	18	20.71	36.03	13.42	9.93	291.7	1.08	270.7	1.01	57.49	81.97
25	19	22.74	39.57	12.97	9.60	293.7	1.23	272.2	1.15	65.24	88.84
25	20	24.56	42.74	12.71	9.41	296.0	1.42	274.2	1.32	71.94	96.82
25	21	26.20	45.59	12.66	9.37	298.8	1.61	276.6	1.49	80.28	102.68
25	22	27.99	48.70	12.64	9.35	303.0	1.73	279.6	1.58	94.69	104.69
25	23	28.86	50.21	11.75	8.70	308.9	1.69	282.5	1.51	109.20	101.60
26	00	27.85	48.46	11.47	8.49	313.8	1.50	283.9	1.30	118.33	97.36
26	01	25.66	44.64	11.12	8.23	316.3	1.26	283.2	1.06	126.10	89.59
26	02	25.04	43.57	10.57	7.82	319.9	1.01	281.2	0.79	130.42	82.33
26	03	23.40	40.72	10.28	7.61	324.6	0.78	277.8	0.54	136.15	78.85
26	04	20.96	36.47	9.96	7.37	328.4	0.62	274.0	0.36	137.67	74.28
26	05	18.95	32.97	9.67	7.16	332.7	0.50	270.7	0.23	144.62	71.12
26	06	17.50	30.46	9.38	6.94	338.8	0.40	270.1	0.14	149.27	69.24

FACTOR HMAX/HS USED IS 1.74000

WD103 - Hindcast Data

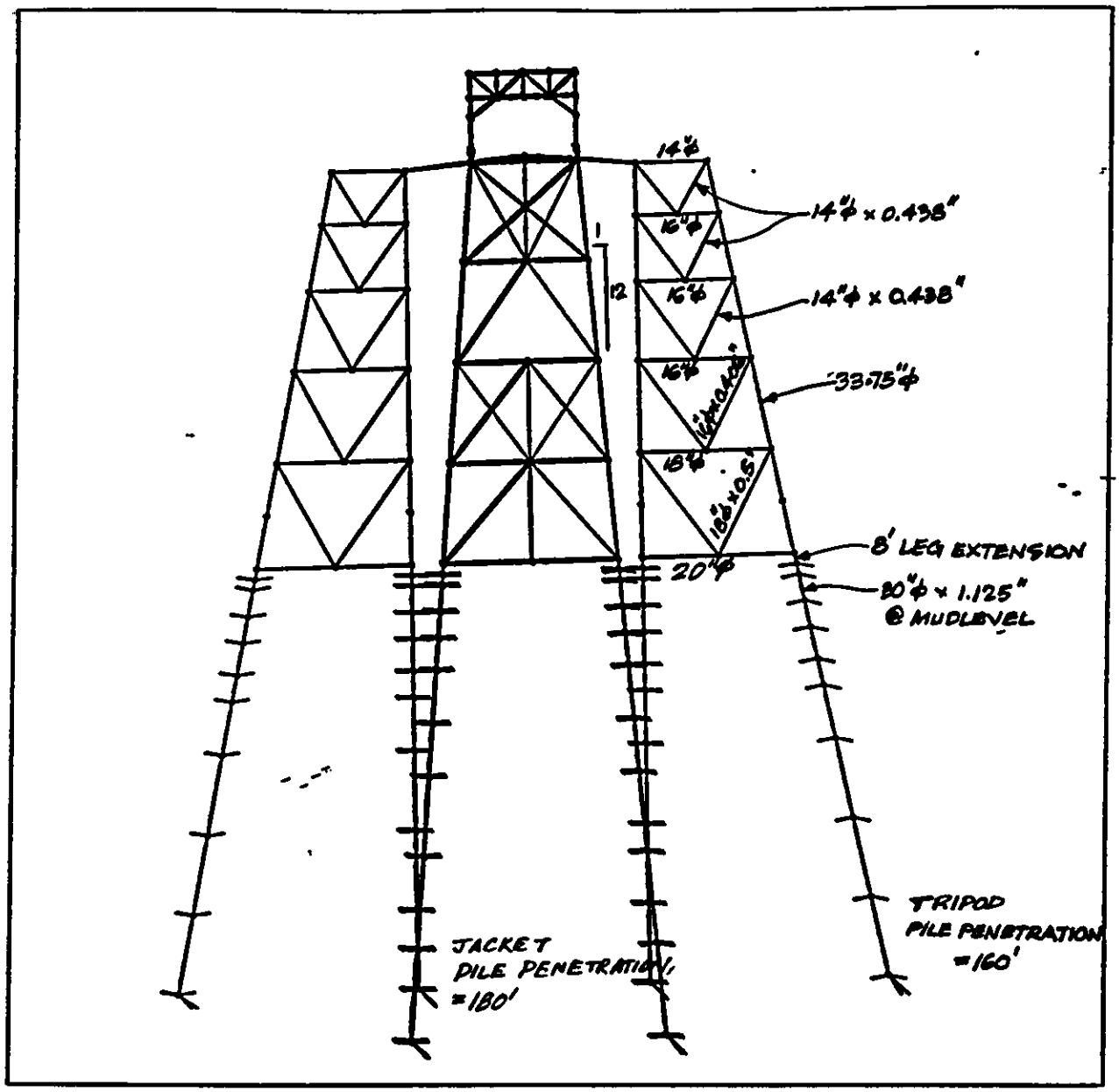

CAP -i

Platform North (P.N) 35° True North (T.N)

STEEL JACKET CONFIGURATION SAME AS PER ST151H

SOIL DATA SAME AS FOR PLATFORM ST151K

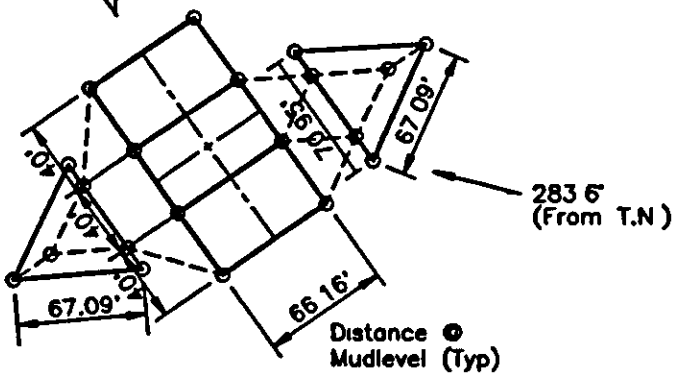

Platform ST151J with Two Tripods

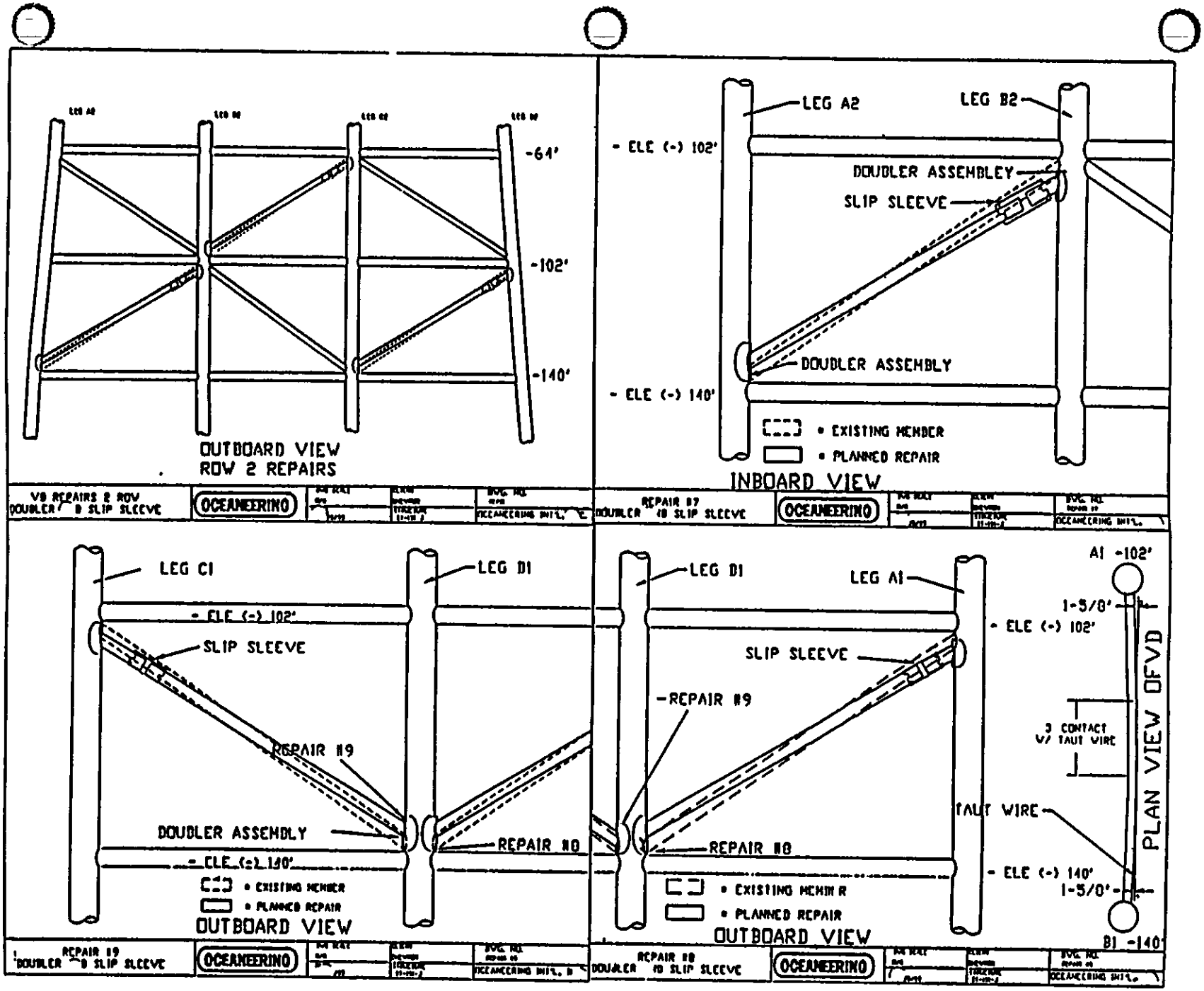

South Timbalier ST151J Platform Repairs

DAY	HOUR	HS	HMAX	TP	TZ	DIRDOM	CSPEED	CDIRN	CRES	WINDD	WINDS
25	16	14.94	25.40	14.48	10.72	273.7	1.41	275.0	1.41	25.98	65.16
25	17	17.45	29.67	14.34	10.61	273.9	1.83	274.7	1.83	26.00	73.58
25	18	20.19	34.32	14.28	10.57	274.3	2.20	273.9	2.20	28.23	84.67
25	19	23.27	39.56	14.18	10.49	275.2	2.52	272.7	2.52	30.54	98.66
25	20	26.64	45.29	14.07	10.41	276.9	2.85	271.3	2.84	32.02	116.45
25	21	30.17	51.29	13.53	10.01	279.0	3.20	270.5	3.16	38.67	136.17
→ 25	22	34.57	58.77	13.12	9.71	283.6	3.41	270.0	3.31	68.43	159.21
25	23	34.53	58.71	12.98	9.61	288.2	3.33	270.3	3.17	120.97	151.83
26	00	31.66	53.83	12.77	9.45	293.6	2.98	270.7	2.75	144.20	140.09
26	01	28.59	48.60	11.69	8.65	297.6	2.55	271.2	2.29	152.76	124.74
26	02	24.90	42.32	11.23	8.31	306.9	2.14	272.1	1.76	152.63	110.36
26	03	23.31	39.63	9.50	7.03	317.6	1.80	274.1	1.30	159.38	100.96
26	04	21.80	37.06	9.47	7.00	330.5	1.51	277.0	0.90	157.88	93.57
26	05	20.49	34.83	9.15	6.77	14.0	1.25	280.1	-0.08	166.69	86.24
26	06	19.17	32.59	8.98	6.64	48.7	0.99	284.2	-0.56	172.26	81.38

FACTOR HMAX/HS USED IS 1.70000

ST151J - Hindcast Data

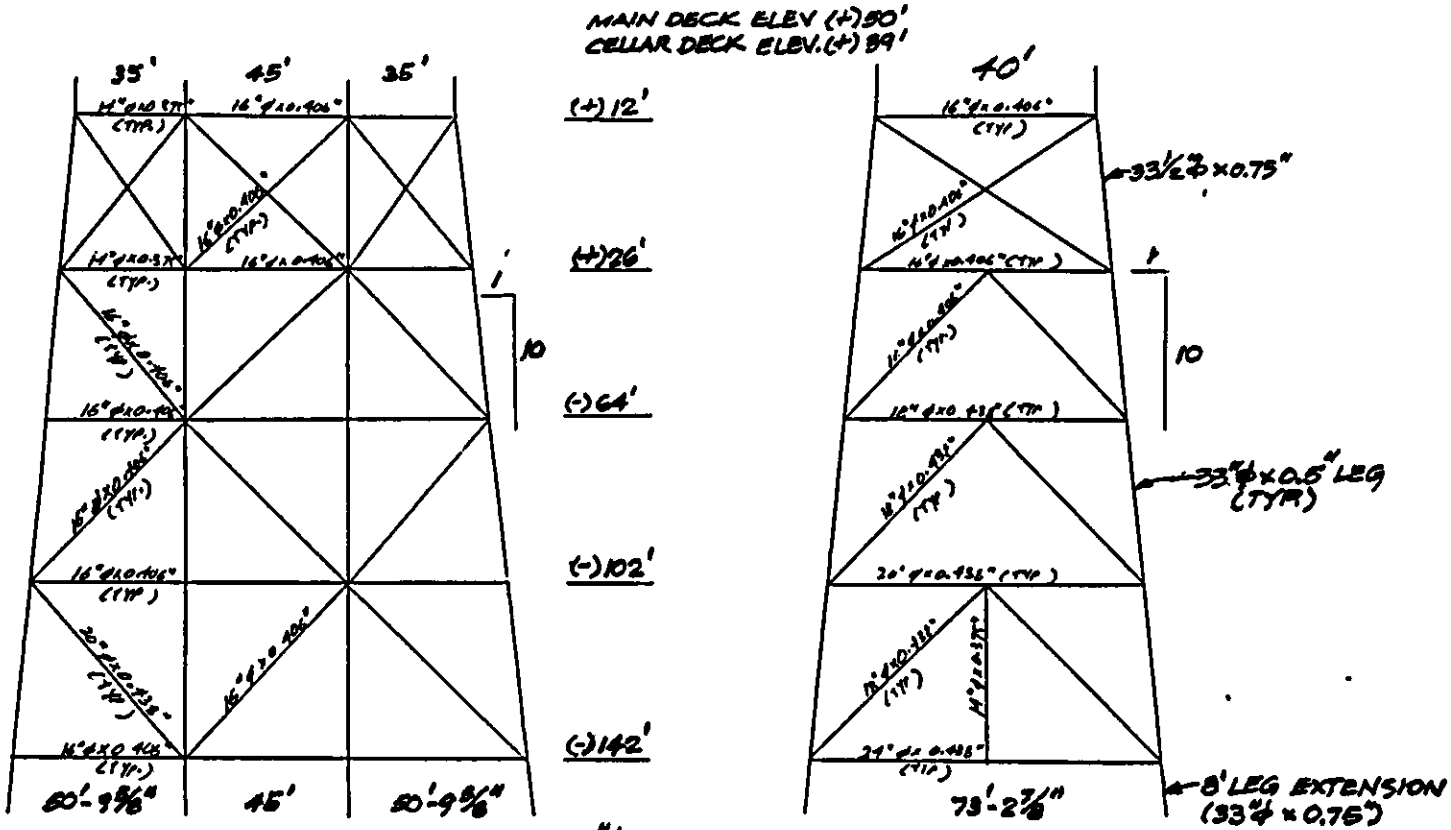

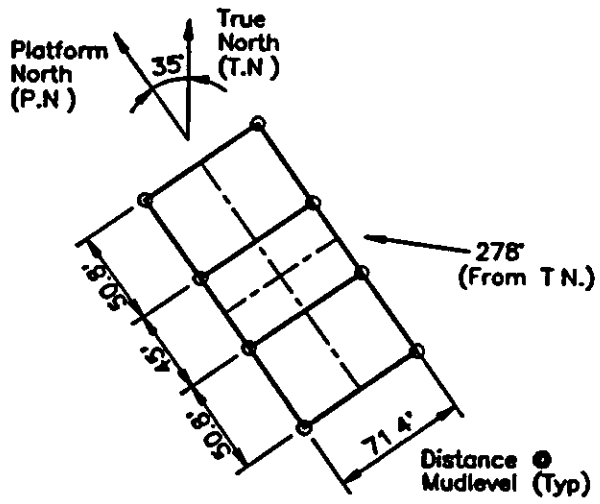

ST177B - Structural Configuration

DAY	HOUR	HS	HMAX	TP	TZ	DIRDOM	CSPEED	CDIRN	CRES	WINDD	WINDS
25	16	14.84	24.63	14.54	10.76	271.9	1.42	275.4	1.41	21.00	64.53
25	17	17.44	28.95	14.40	10.66	271.9	1.91	275.4	1.91	19.86	73.37
25	18	20.32	33.73	14.34	10.61	271.9	2.39	275.5	2.38	20.73	85.42
25	19	23.65	39.27	14.28	10.57	272.7	2.85	275.0	2.84	21.31	101.22
25	20	27.30	45.32	14.23	10.53	274.3	3.35	274.1	3.35	20.16	120.87
25	21	31.10	51.62	13.98	10.35	275.4	3.84	273.0	3.84	24.24	143.82
25	22	35.90	59.59	13.25	9.80	278.3	4.18	271.7	4.15	61.62	159.58
25	23	32.20	53.45	12.98	9.60	281.4	4.03	270.8	3.97	147.28	123.46
26	00	28.02	46.51	12.73	9.42	286.6	3.60	271.0	3.46	172.99	137.35
26	01	24.77	41.12	11.65	8.62	290.5	3.09	272.0	2.93	174.49	127.20
26	02	22.59	37.50	9.94	7.36	297.6	2.60	274.1	2.39	168.75	113.18
26	03	21.55	35.78	9.02	6.67	259.7	2.17	277.7	2.06	173.12	102.73
26	04	20.96	34.80	9.06	6.70	202.1	1.79	282.8	0.29	168.93	94.99
26	05	20.21	33.55	8.93	6.61	13.8	1.46	289.0	0.13	176.70	85.96
26	06	19.03	31.59	8.86	6.56	20.5	1.17	296.5	0.12	181.69	80.34

FACTOR HMAX/HS USED IS 1.66000

ST177B - Hindcast Data

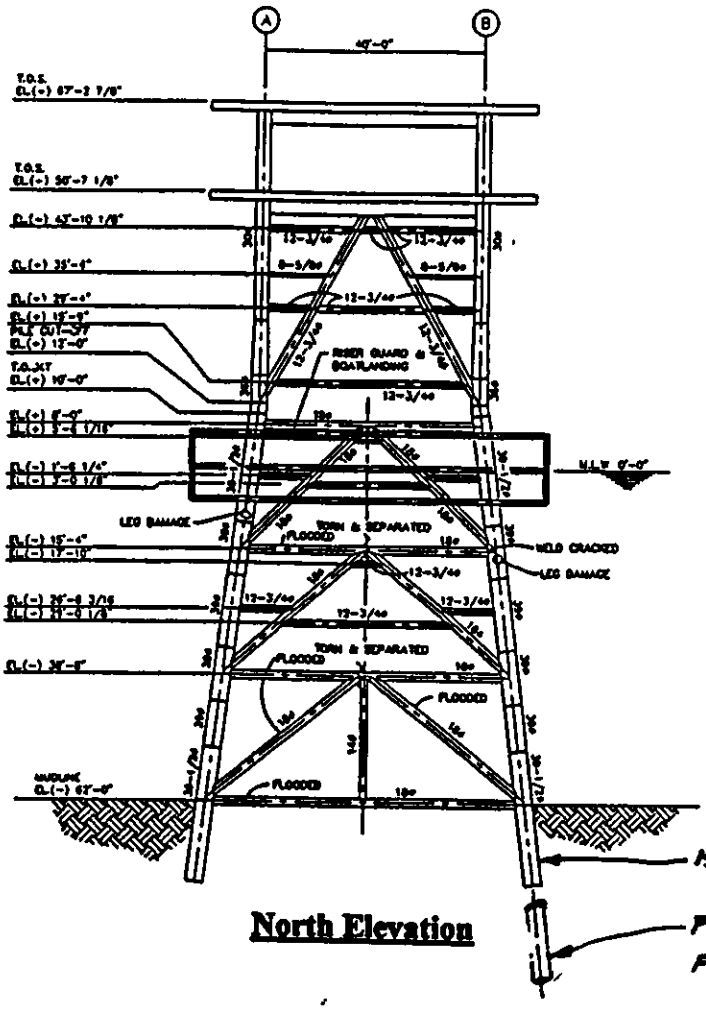

15' LEG EXTENSION

PILE - 36"ϕ x 1" @ MUDLEVEL

PILE PENETRATION = 162.5'

North Elevation

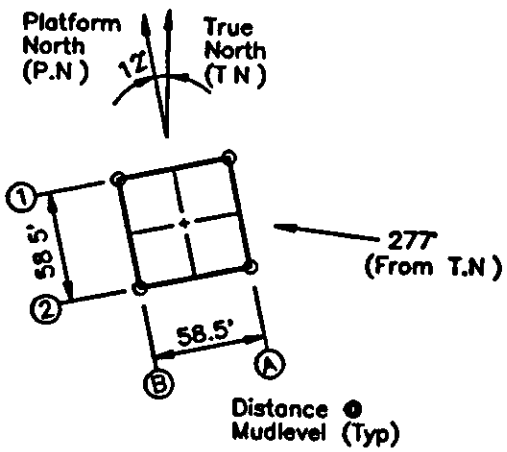

SS139 (T25) - Structural Configuration

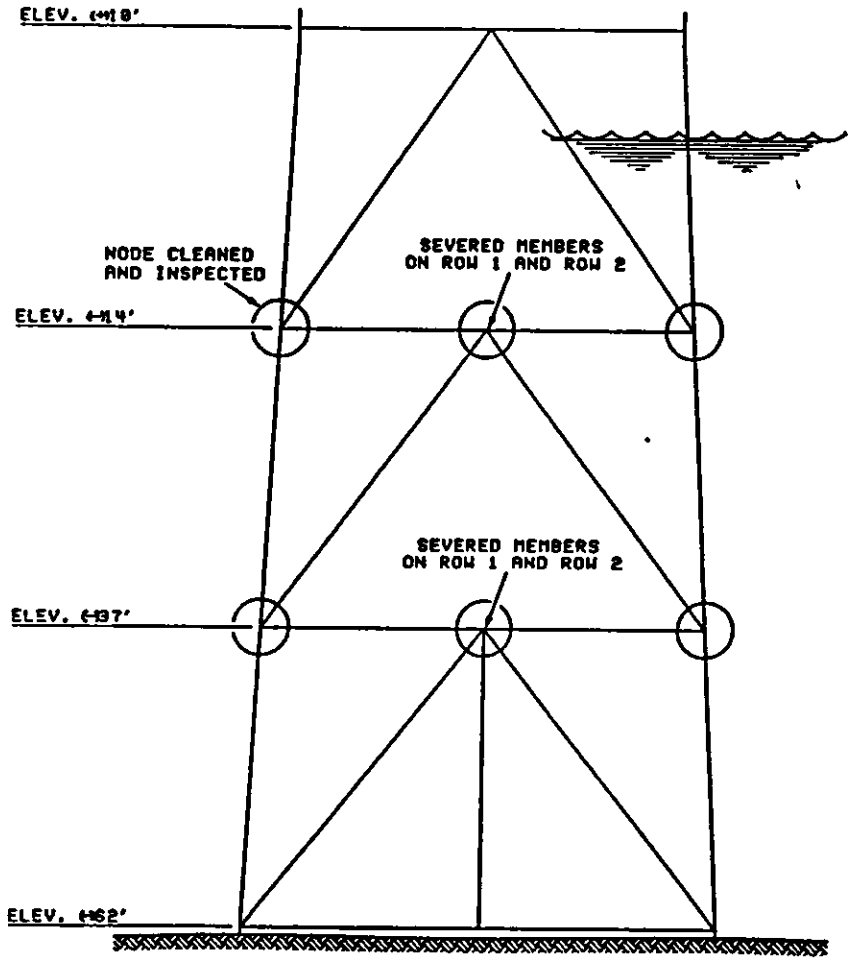

TYPICAL ELEVATION FOR ROWS A, B, 1, AND 2

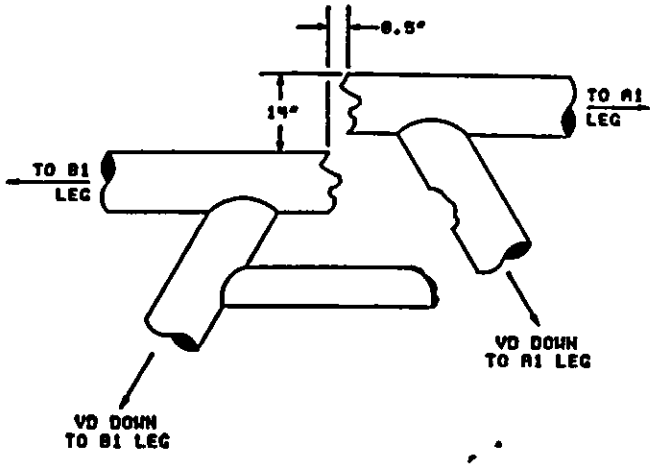

-14' A1/B1 HORIZONTAL (BREAK)

NOTE: 1. THIS DRAWING IS NOT DRAWN TO ANY SCALE.

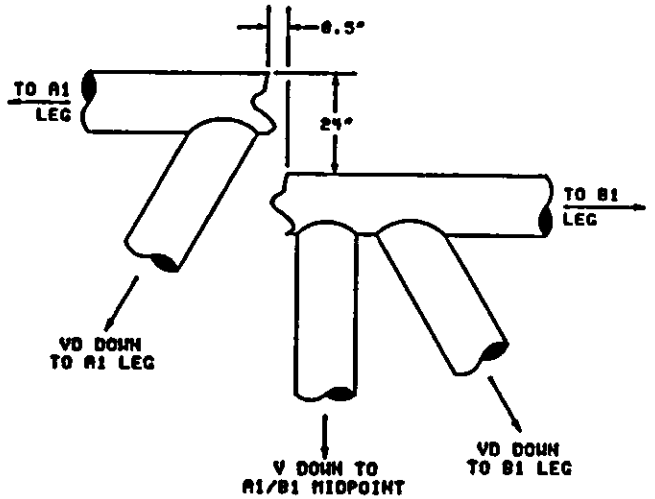

-37' A1/B1 HORIZONTAL (BREAK)

Platform SS139 - Damage Details

DAY	HOUR	HS ft	HMAX ft	TP sec	TZ sec	DIRDOM °	CSPEED ft/sec	CDIRN °	CRES ft/sec	WINDD °	WINDS ft/sec
25	16	7.87	13.14	14.81	10.96	254.8	1.38	290.1	1.12	27.13	52.65
25	17	9.45	15.77	14.69	10.87	264.4	1.77	286.9	1.64	24.79	58.25
25	18	10.78	18.00	14.54	10.76	269.3	2.21	284.8	2.13	23.34	65.71
25	19	12.22	20.41	14.55	10.77	273.1	2.69	282.8	2.65	20.84	74.63
25	20	13.85	23.13	14.50	10.73	277.5	3.23	280.9	3.22	16.71	84.42
25	21	15.56	25.98	14.47	10.71	281.6	3.76	280.7	3.76	14.17	96.25
25	22	17.48	29.19	14.32	10.60	279.9	4.21	280.6	4.21	13.24	118.41
25	23	21.05	35.15	13.89	10.28	275.0	4.47	279.6	4.45	18.59	150.74
26	00	26.02	43.46	13.04	9.65	276.6	4.46	278.5	4.45	48.30	161.63
26	01	24.47	40.86	12.83	9.50	283.6	4.26	279.6	4.25	117.20	81.79
26	02	20.55	34.32	11.69	8.65	291.7	3.92	283.6	3.88	162.38	128.00
26	03	17.40	29.05	10.83	8.02	299.7	3.53	289.2	3.47	184.23	127.43
26	04	17.45	29.14	8.12	6.01	336.5	3.14	294.5	2.33	177.11	124.64
26	05	17.89	29.88	8.40	6.22	21.8	2.81	299.4	0.37	189.23	112.02
26	06	17.73	29.61	8.58	6.35	28.4	2.42	304.6	0.26	195.66	103.30

SS139 (T25) - Hindcast Data

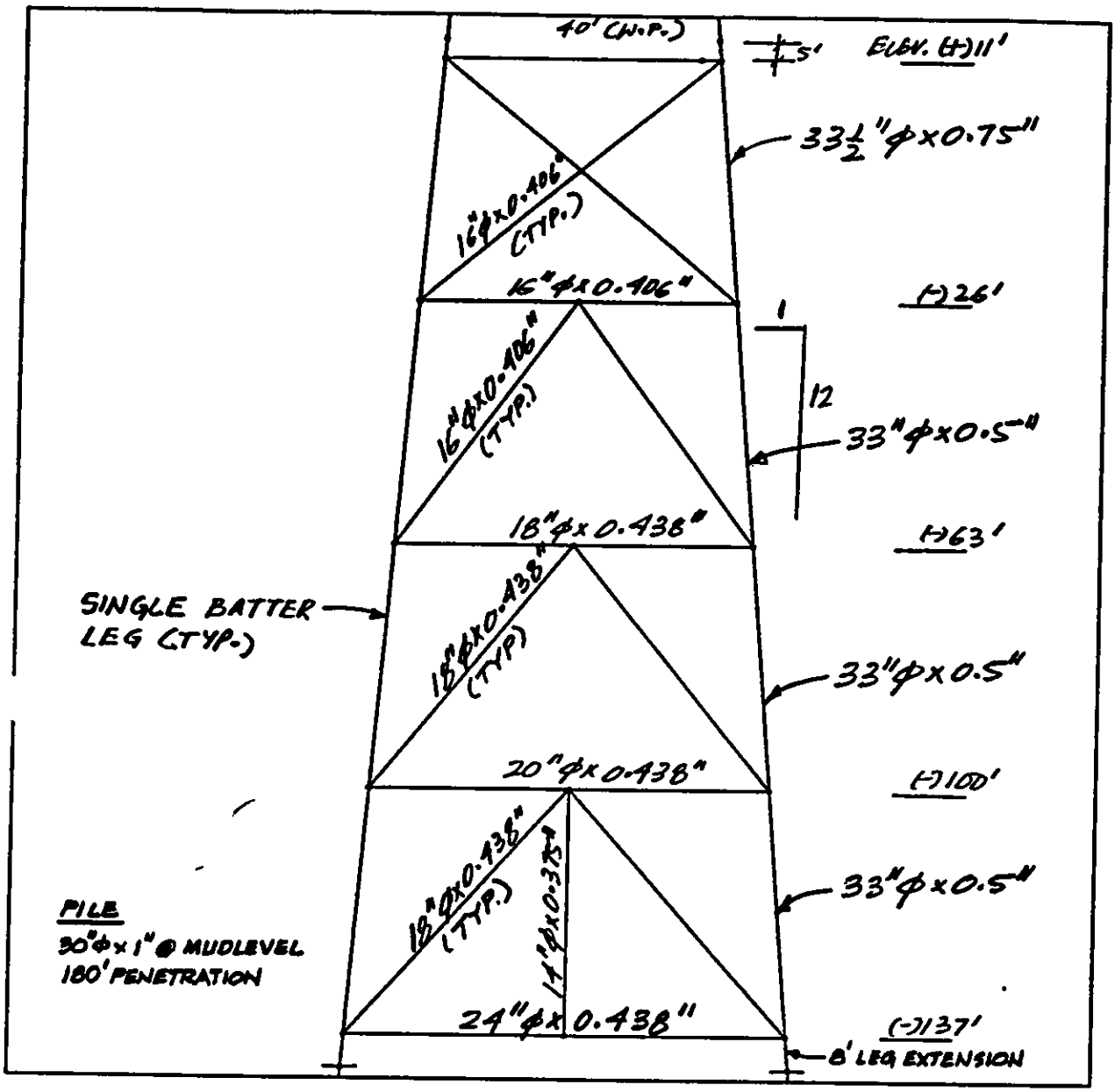

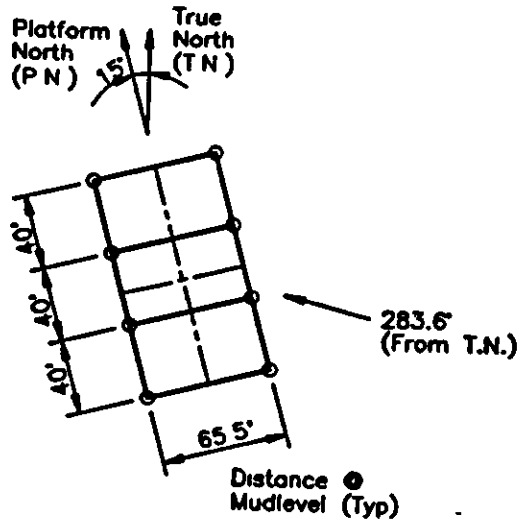

NOTE: SOIL DATA SAME AS FOR PLATFORM ST151K

ST151H - Typical End-on Framing

DAY	HOUR	HS	HMAX	TP	TZ	DIRDOM	CSPEED	CDIRN	CRES	WINDD	WINDS
25	16	15.07	25.61	14.48	10.72	273.6	1.40	275.0	1.39	26.01	65.37
25	17	17.60	29.91	14.34	10.61	273.8	1.82	274.7	1.82	26.10	73.83
25	18	20.35	34.60	14.27	10.56	274.1	2.19	273.9	2.19	28.39	84.97
25	19	23.46	39.88	14.17	10.49	275.0	2.51	272.7	2.51	30.83	99.04
25	20	26.86	45.66	14.06	10.41	276.7	2.84	271.3	2.83	32.46	116.93
25	21	30.41	51.70	13.49	9.98	278.8	3.19	270.5	3.15	39.38	136.70
25	22	34.74	59.05	13.11	9.70	283.6	3.39	270.1	3.30	69.81	159.15
25	23	34.58	58.78	12.98	9.61	288.2	3.31	270.5	3.15	121.70	151.57
26	00	31.75	53.97	12.76	9.44	293.6	2.95	270.9	2.72	144.12	139.64
26	01	28.66	48.72	11.68	8.65	297.6	2.52	271.4	2.26	152.53	124.25
26	02	24.96	42.44	11.21	8.30	307.0	2.11	272.3	1.73	152.42	109.84
26	03	23.39	39.77	9.51	7.04	317.6	1.77	274.2	1.28	159.13	100.47
26	04	21.86	37.16	9.47	7.01	330.3	1.48	277.1	0.89	157.76	93.21
26	05	20.52	34.88	9.15	6.77	17.9	1.22	280.2	-0.16	166.48	85.95
26	06	19.19	32.63	8.98	6.65	38.8	0.97	284.4	-0.40	172.04	81.15

FACTOR HMAX/HS USED IS 1.70000

ST151H - Hindcast Data

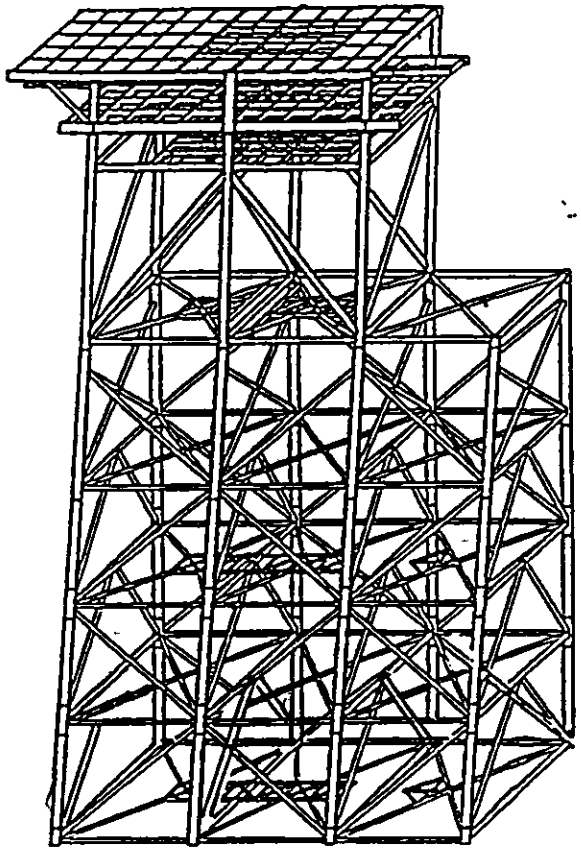

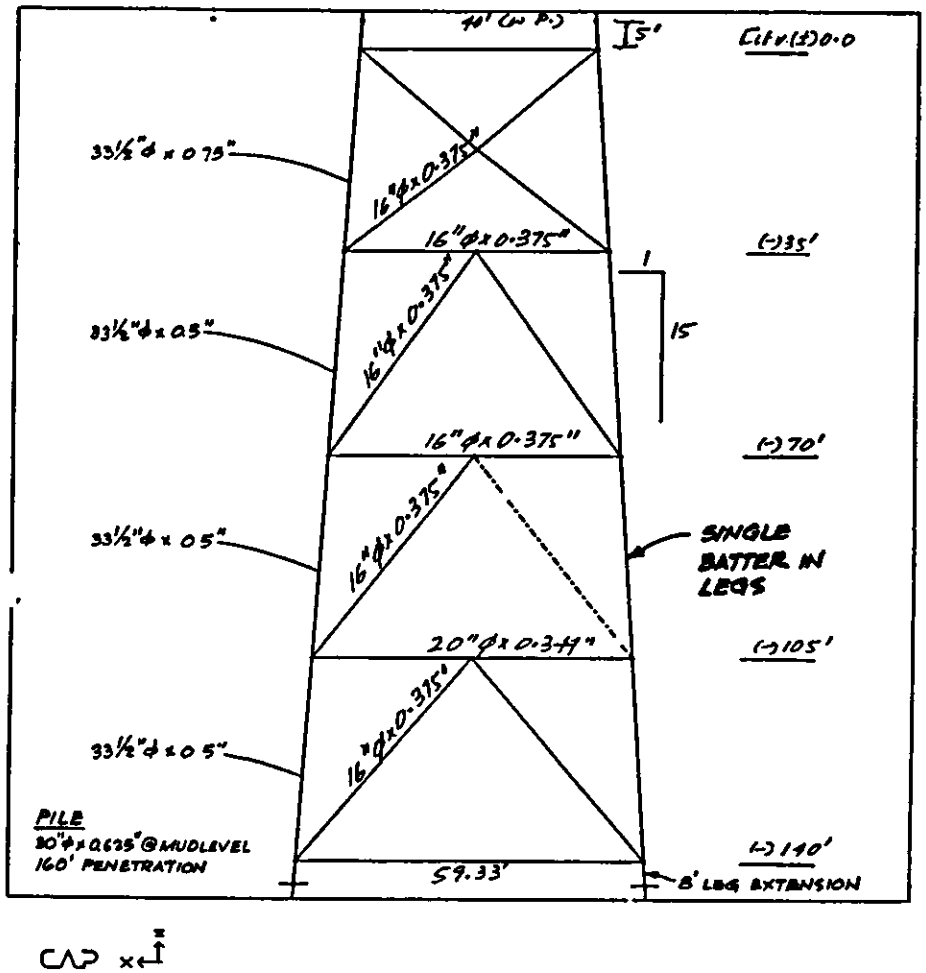

CAP x

Platform ST130A - Toppled in Andrew

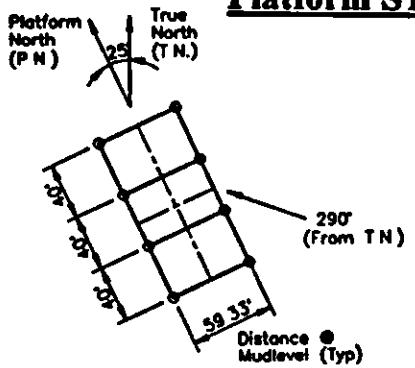

Platform ST130A - Typical End-on Framing

NOTE: USBP SOIL DATA SAME AS FOR PLATFORM ST130Q

DAY	HOUR	HS	HMAX	TP	TZ	DIRDOM	CSPEED	CDIRN	CRES	WINDD	WINDS
25	16	14.59	24.94	14.59	10.80	268.9	1.22	273.6	1.21	29.80	65.24
25	17	16.95	28.98	14.28	10.57	269.2	1.58	272.7	1.57	30.77	73.16
25	18	19.53	33.40	14.17	10.49	270.2	1.92	272.5	1.92	34.20	83.16
25	19	22.38	38.27	13.99	10.35	272.0	2.24	272.6	2.24	37.75	95.62
25	20	25.41	43.46	12.05	8.92	274.9	2.58	272.6	2.58	40.82	110.96
25	21	28.35	48.48	12.99	9.61	278.1	2.88	272.7	2.87	48.71	126.99
25	22	31.71	54.22	12.84	9.50	282.8	3.06	273.5	3.02	72.99	144.88
25	23	32.41	55.43	12.79	9.47	289.5	2.98	275.1	2.88	109.22	142.50
26	00	30.94	52.90	11.72	8.67	295.7	2.66	276.5	2.52	128.04	131.94
26	01	28.36	48.49	11.44	8.46	300.2	2.28	277.3	2.10	138.29	117.34
26	02	24.94	42.64	11.06	8.18	307.1	1.91	277.9	1.66	141.16	104.04
26	03	23.90	40.87	9.61	7.11	314.9	1.59	279.5	1.30	148.79	96.20
26	04	22.09	37.78	9.61	7.11	321.9	1.33	282.9	1.03	148.95	89.85
26	05	20.48	35.02	9.35	6.92	334.0	1.11	287.5	0.76	157.83	83.71
26	06	19.07	32.62	9.02	6.68	346.1	0.89	294.1	0.55	163.48	79.68

FACTOR HMAX/HS USED IS 1.71000

ST130A - Hindcast Data

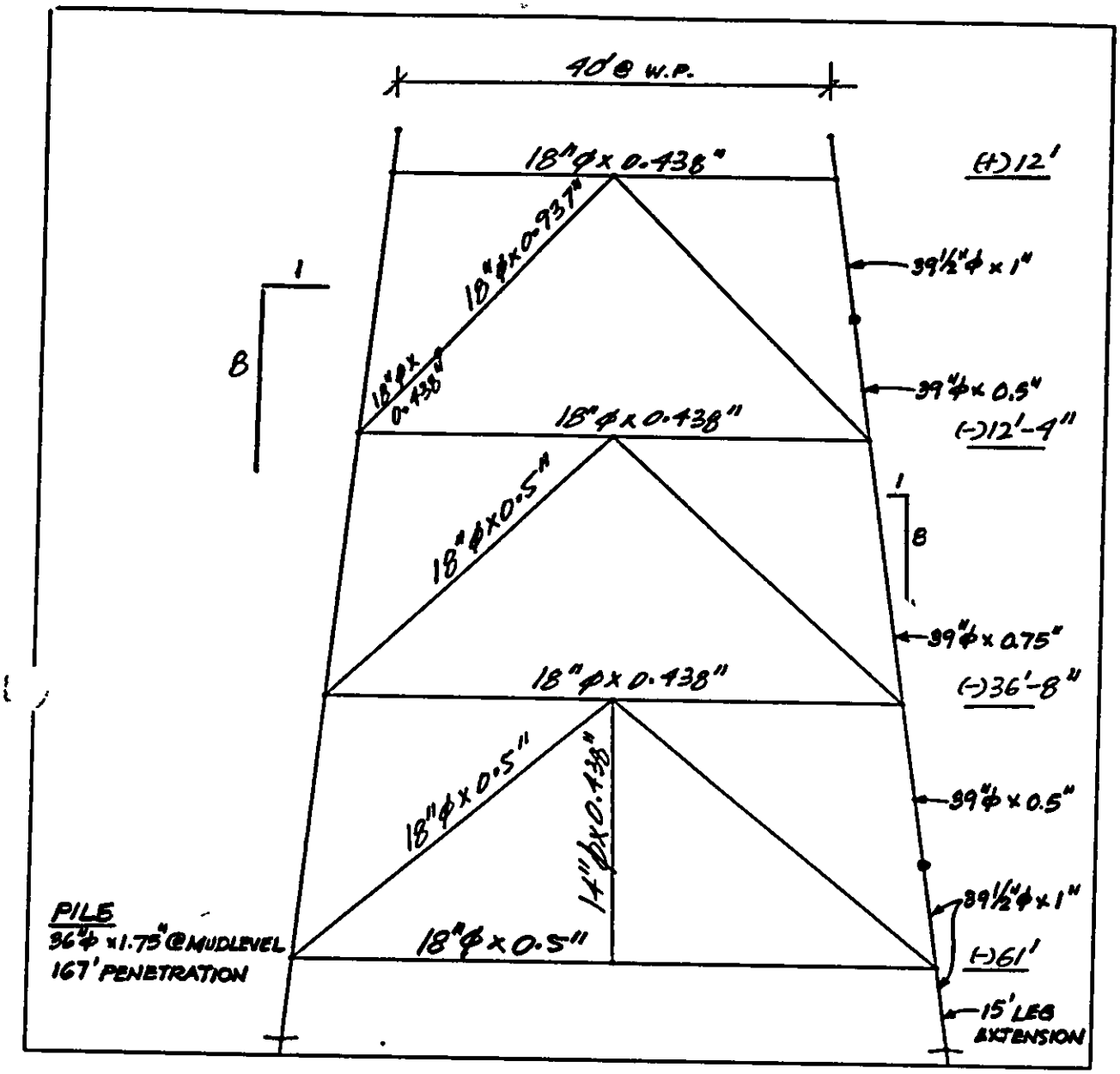

CAP x

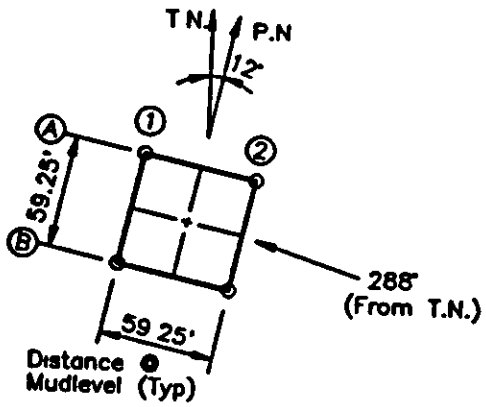

ST72 (T21) - Typical Framing

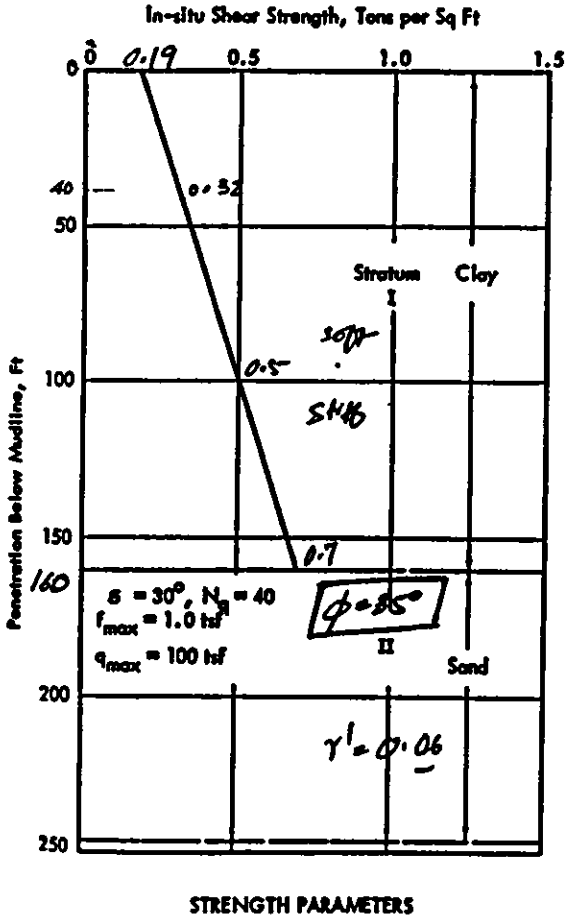

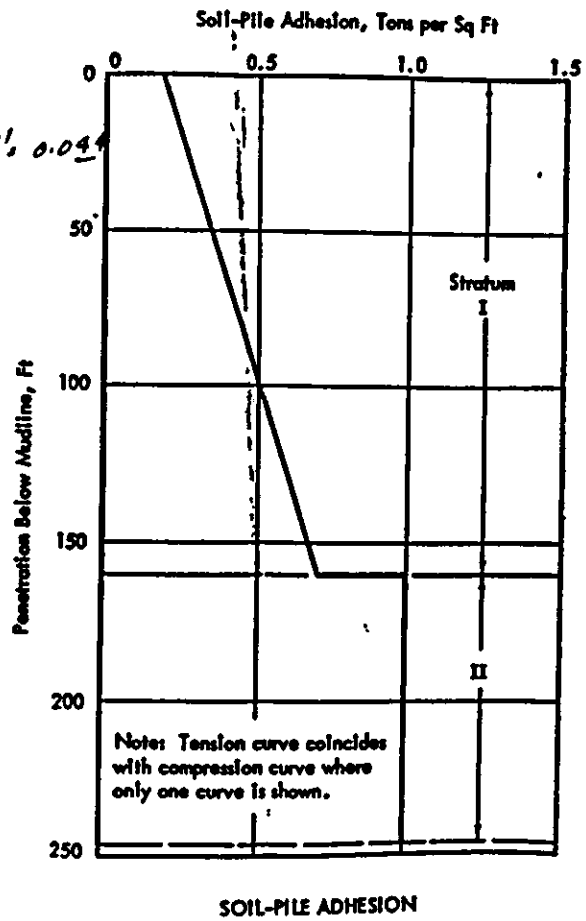

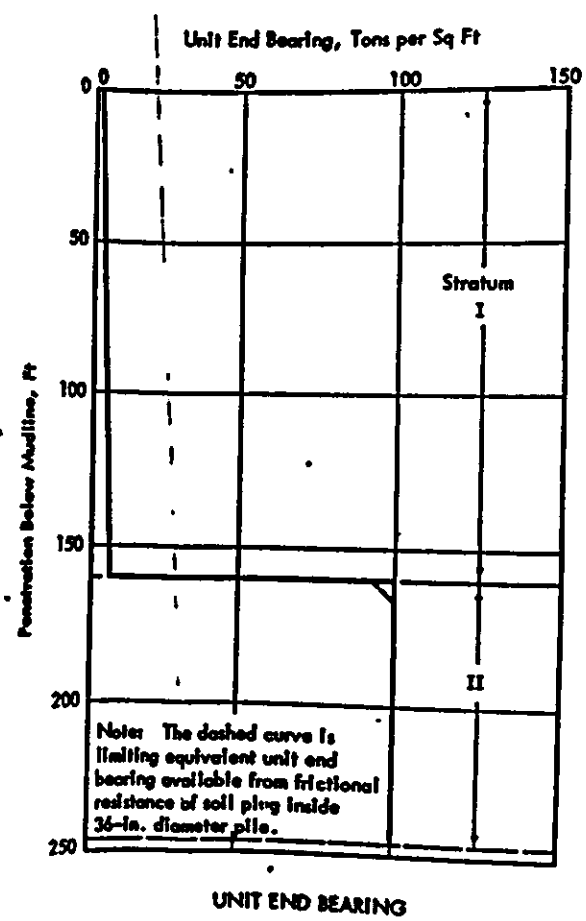

Platform ST72 (T21) - Soil Information

DAY	HOUR	HS	HMAX	TP	TZ	DIRDOM	CSPEED	CDIRN	CRES	WINDD	WINDS
25	16	8.27	13.90	14.78	10.94	261.1	1.30	284.4	1.19	29.40	54.36
25	17	9.82	16.50	14.62	10.82	269.5	1.69	284.3	1.63	27.68	60.10
25	18	11.11	18.66	14.50	10.73	272.8	2.10	283.7	2.07	27.02	67.66
25	19	12.57	21.11	14.52	10.74	275.4	2.53	282.6	2.51	25.57	76.85
25	20	14.16	23.78	14.46	10.70	277.7	3.00	282.5	2.99	22.57	87.23
25	21	15.87	26.66	14.39	10.65	279.8	3.45	283.6	3.44	21.58	99.51
25	22	18.07	30.36	14.11	10.44	278.6	3.81	284.8	3.79	24.17	122.38
25	23	22.78	38.26	13.56	10.04	281.0	3.99	285.0	3.98	37.60	152.67
26	00	27.90	46.87	13.11	9.70	287.8	3.97	284.7	3.96	73.38	158.64
26	01	27.49	46.18	12.82	9.49	293.6	3.80	285.6	3.76	122.00	143.52
26	02	24.79	41.64	11.66	8.63	298.5	3.49	288.1	3.43	141.85	137.66
26	03	21.14	35.51	10.26	7.59	307.2	3.12	291.4	3.01	160.86	128.95
26	04	20.23	33.99	9.27	6.86	320.7	2.76	294.6	2.47	157.50	120.54
26	05	19.19	32.23	9.23	6.83	-16.1	2.41	297.6	1.66	172.65	110.02
26	06	18.51	31.10	8.92	6.60	3.9	2.01	301.7	0.94	180.86	102.34

FACTOR HMAX/HS USED IS 1.68000

Platform ST72 (T21) - Hindcast Data

DAY	HOUR	HS	HMAX	TP	TZ	DIRDOM	CSPEED	CDIRN	CRES	WINDD	WINDS
25	16	4.97	8.45	4.79	3.54	255.5	0.56	312.1	0.31	33.53	51.03
25	17	5.73	9.73	14.81	10.96	267.8	0.67	312.2	0.48	31.80	55.87
25	18	6.36	10.82	14.58	10.79	275.5	0.80	310.7	0.65	30.94	62.09
25	19	7.16	12.16	14.60	10.80	279.5	0.95	306.3	0.85	29.28	69.53
25	20	8.09	13.75	14.56	10.78	283.4	1.18	300.0	1.13	26.26	77.75
25	21	9.06	15.41	14.51	10.74	286.4	1.50	295.8	1.48	24.46	87.37
25	22	10.33	17.56	14.37	10.63	285.6	1.82	293.4	1.81	25.30	104.52
25	23	12.55	21.33	13.97	10.34	284.9	2.16	289.2	2.15	30.69	128.29
26	00	16.36	27.81	13.29	9.83	292.8	2.49	284.4	2.46	44.66	147.73
26	01	19.97	33.94	13.00	9.62	300.9	2.81	281.4	2.65	74.71	156.55
26	02	21.04	35.77	11.87	8.78	307.5	3.01	282.2	2.72	105.12	147.39
26	03	19.08	32.44	11.46	8.48	313.6	2.96	284.6	2.59	134.88	138.87
26	04	18.07	30.72	9.59	7.10	319.7	2.75	287.5	2.32	139.13	131.44
26	05	16.65	28.30	9.64	7.13	330.8	2.48	290.0	1.87	163.80	121.15
26	06	15.83	26.91	9.11	6.74	-9.1	2.12	293.3	1.13	176.82	114.24

FACTOR HMAX/HS USED IS 1.70000

Caisson SP #10 - Hindcast Data

DAY	HOUR	HS	HMAX	TP	TZ	DIRDOM	CSPEED	CDIRN	CRES	WINDD	WINDS
25	16	5.75	9.60	5.45	4.03	245.2	0.64	280.6	0.52	27.29	48.24
25	17	6.90	11.53	14.93	11.05	249.9	0.75	281.5	0.64	24.03	52.89
25	18	8.09	13.51	14.63	10.82	259.0	0.86	282.4	0.79	21.44	59.27
25	19	9.35	15.62	14.49	10.72	266.7	0.97	283.3	0.93	17.70	66.57
25	20	10.76	17.98	14.51	10.73	307.6	1.10	283.0	1.00	12.41	73.99
25	21	12.05	20.12	14.48	10.72	322.8	1.25	282.6	0.95	8.26	83.03
25	22	13.60	22.71	14.42	10.67	328.8	1.45	280.9	0.97	3.40	99.62
25	23	15.51	25.90	14.18	10.49	148.5	1.80	277.0	-1.12	358.85	122.63
26	00	17.81	29.75	7.32	5.42	298.1	2.28	272.6	2.06	359.17	147.12
26	01	19.70	32.90	7.57	5.60	268.4	2.80	270.4	2.80	15.55	147.52
26	02	14.67	24.50	7.74	5.73	279.7	3.19	269.8	3.14	43.13	27.43
26	03	11.80	19.70	8.01	5.93	288.3	3.40	269.9	3.23	247.15	87.38
26	04	11.90	19.87	8.22	6.08	88.2	3.50	270.7	-3.50	212.03	117.33
26	05	13.70	22.88	8.38	6.20	67.5	3.45	271.6	-3.15	224.12	115.74
26	06	14.90	24.88	8.73	6.46	61.2	3.24	272.4	-2.77	224.96	108.46

FACTOR HMAX/HS USED IS 1.67000

SS135 #10 - Hindcast Data

The key item of the recipe used in this project were discussed in Section 2.1. The additional details of the recipe followed in the project are primarily based on the API RP 2A, 20th Edition A summary of the criteria used for evaluation of loads on and resistance of platforms is presented in the following sub-sections

B-1: LOAD ESTIMATE

Loads on the platform were evaluated using the guidelines in the 20th Edition of API-RP-2A [3].

Gravity

a. Structural Framing

Material Weight:	Steel: 0.4905 kips/ft^3 Grout: 0.137 kips/ft^3 (dry weight)
Flooded Members:	All main legs, skirt legs and casings were considered flooded, unless otherwise identified for a platform.
Buoyant Members:	All jacket members except legs, skirt legs, casings, conductors considered buoyant, unless noted otherwise.
Marine Growth:	0.075 kips/ ft^3 (dry weight of hard marine growth)

b. Deck Loads

Specific equipment weight:	Dead loads
Distributed loading:	25 % of live load during hurricane. Equipment loads which are applicable during hurricane loading were considered. No detailed distribution of equipment loads were considered.

Wind

a. Wind associated with the hurricane wave height during specific hour were considered in evaluation of the total wind loads on the deck equipment and structure.

b. Wind speed: per 1994 hindcast [13].

c. Wind loads: per API RP 2A formulation, Eqn. 2.3.2.8

d. Shape coefficients: per API RP 2A Section 2.3.2 (e)

e. Shielding coefficient: per API Section 2.3.2 (f)

Waves

a. Wave height: per 1994 hindcast [13].

b. Wave period: per 1994 hindcast [13]

The *wave periods* associated with the individual wave heights were computed based on a wave steepness of 1/13.

c. Storm surge plus tide: per 1992 hindcast [12], as advised by Oceanweather.

d. Wave directions: per 1994 hindcast [13].

e. Wave loads per Morrison equation w/ API RP 2A corrections

Stream function profile and kinematics: Stream function wave theory [26] of 3rd order was used for intermediate and deep water locations. In case of shallower water depths, higher order of Stream Function theory was used in accordance with Fig. 2.3.1-3 of API RP 2A, 20th Edition.

Wave kinematics correction factor: Wave kinematics correction factor of 0.88 was used to account for wave directional spreading and irregular sea effects

Combined wave/current kinematics: Wave kinematics adjusted for directional spreading and irregular seas were combined vectorially with the stretched current profile.

Marine Growth: In cases where actual marine growth profiles were not available from inspections, the general profile given in Section 2.3.4.d of API RP 2A, 20th Edition for the Gulf of Mexico was used.

Elevation	Marine growth (inch)
Above MHHW	none
MHHW to (-)150'	1.5 inch thick
Below (-)150'	none

Drag (Cd) and Inertia (Cm) Coefficients: For unshielded circular cylinders with K-C number (=UT/D) more than 30, the following coefficients were used

Type	Cd	Cm
smooth	0.65	1.6

rough	1.05	1.2

Conductor Shielding Factor: Wave force reduction factor in accordance with Figure. 2.3.1.4 of API RP 2A, 20th Edition were applied to the drag and inertia coefficients for closely spaced conductor arrays.

Appurtenances: Jacket appurtenances include boat landings, fenders or bumpers, walkways, stairways, grout lines, and anodes. The hydrodynamic loads on only major appurtenances in the wave zone such as boat landings, fenders and bumpers was determined

Currents (with waves)

a. Surface velocity

Hindcast:	per 1994 hindcast [13].
Variation with depth:	per API RP 2A, 20th Edition
Current Profile:	the "free field" current profile was used.

b. Current direction: per 1994 hindcast [13].

The *current speed* inline with the maximum wave was used.

c. Current blockage factor: The blockage factor in the direction analyzed was obtained from Section 2.3.1.b-4 of API RP 2A, 20th Edition. The effective local current profile was determined by multiplying the free field current profile with the current blockage factor.

d. Current profile stretching: The current profile was stretched to the local wave surface by vertical stretching in case of slab current or by linear stretching for other current profiles, as per Section 2.3.1.b-5 of API RP 2A, 20th Edition.

Wave in Deck

a. In cases where waves impact the deck, the simplified procedure developed by API Task Group 92-5, given in the Draft Section 17 (April 20, 1994 version) was used.

b Variable pushover load patterns were used for cases where deck inundation occurred.

B-2: RESISTANCE ESTIMATE

Deck

a. Material classification per operator

Most of the platforms were fabricated using steel with a 36 ksi nominal yield strength Participants voted on using a yield strength of 42 ksi for these cases to account for the difference between nominal and mean yield strength and to account for the increase in strength due to strain rate effects (rapid loading in storms) [14]. The mill certificate or field test data was used, when available.

b. Primary members only: The primary members (deck legs, deck girders and deck trusses) were modeled in detail and the secondary members were represented by equivalent sections to simulate load paths. Secondary members such as deck beams and stringers, plating or grating, and cantilever support framing were represented by X-braces to transfer load between deck legs and deck girders.

c. Nonlinear elements: Deck legs were modeled as non-linear beam columns.

d. Linear elements: Deck braces, deck girders, and deck trusses were modeled as linear beam elements, unless their failure were apparent. Equivalent braces for secondary members were modeled as linear beam elements.

Jacket

a. Material classification per operator

Mean yield strength used (42 ksi for 36 ksi steel), see discussion under Deck (a). Mill certificates or field test data were used, where available

b. Legs/Piles

Element Type: Modeled as nonlinear beam/columns

Effective length factor (k) per API-RP-2A. k = 1.0

Leg/pile annulus grouted: Composite leg/ pile section properties were used. Equivalent section properties (A, I) were evaluated to account for steel sections of leg and pile, as well as the marginal effect of leg can sections (if provided). The material properties were based on the main leg sections and piles. In case leg and pile actual yield strengths differed, the lower values were used or an equivalent value was determined.

Leg/pile annulus ungrouted: Explicit leg and pile with shims were used. Equivalent section properties (A, I) for the legs were evaluated to account for the marginal increase in leg properties due to leg can sections (if deemed appropriate).

c. Braces

Element Type: The braces were modeled using Struts, Beam Columns or with a new "Fiber Element." The diagonal braces (leg-to-leg) were modeled as Marshall Struts. The K-braces (or K-joints braces) were modeled using a Fiber Element (a modified beam column element to include the joint capacity/stiffness information) in all instances where the joint capacity governed joint/brace strength. The horizontal braces near the mudline and waterline were checked for the axial vs. flexural behavior dominance and, in general, were modeled with beam columns.

Allowable Capacity: The brace capacity was defined by Equation D.2.2-2 of API RP 2A, LRFD [15].

Effective length factor, (k) Section 17 does not recommend values of k (the effective length factor) for use in ultimate capacity analysis. Recent tests and analytical studies [16,17,18] have indicated the appropriate values of "k", without factors of safety, are 0.5 for X- braces, 0.55 to 0.65 for diagonal braces (depending upon end fixity) and 0.65 for K- braces.

An effective length factor of 0.65 was used for "k" and "diagonal" braces. The length was taken as node-to-node distance (not face-to-face of the leg) An effective length factor of 0.55 was used for "X" braces with the member length taken as one-half the longest segment length(i.e. out-of-plane buckling is not considered due to the compensating effect of the tension brace).

d. Joints: The capacity of braces and their connections were evaluated based on conservative joint capacity formula (i.e., API RP 2A) and prior experience. An explicit joint model was developed in all instances where the joint strength was determined to control. Joint strength and load-deformation formulations, (P-δ) and (M-θ), were developed for these joints by MSL Engineering Section 2 2 includes further details on joint modeling These formulas were used to define the properties of the corresponding beam-column and fiber element models.

Grouted joint: The API RP 2A equations for joint capacity were used, without safety factors, and with an equivalent thickness for the leg representing strength of the composite section (leg/pile) [19]

e. Secondary Members

The primary members of jacket launch trusses were modeled. The conductor guide framings were modeled by equivalent members to represent load path for load transfer between primary jacket frame members. The strengths of other secondary members and appurtenances were ignored

Foundation

a. *Soil Shear Strength.* Shear strength profiles were developed based on comparison of the following profiles:

* Based on Strength Ratio (S_u/σ_v') of 0.23 and assuming an over consolidation ratio (OCR) of 1.0
* Miniature Vane (MV) tests on undisturbed samples
* Interpreted or Design shear strength profile from soil reports

In case of driven samples a modification factor of 1.2 was used to account for the effect of sample disturbance if it was not already included in the soil report. In case of pushed samples no modification factor was used

The soil shear strength data were based on available geotechnical reports in the same or nearby blocks of platform locations

b. Explicit non-linear pile-soil interaction: Non-linear pile-soil interaction curves per API RP 2A.

c. *Lateral Soil Capacity:* The AIM projects [20] and other assessment-type studies have typically used degraded soil-pile capacity to develop p-y nonlinear soil springs for pushover analysis. This is based upon the assumption that the soil strength is degraded at the time of the peak wave due to cyclic action of other large waves during storm build-up. However, recent laboratory tests by Exxon [21] indicated that, for pushover type analysis, the static lateral soil strength is a better measure. Therefore, static p-y soil strength was used and was defined by the API RP 2A formula.

d. *Arial "t-z" Springs:* Static soil strength (no degradation) per API RP2A were used.

Pile axial capacity estimates per API RP 2A are affected by loading (or strain) rate, cyclic loading, reconsolidation (time effect), compressibility (pile length effect) and pile aging effects The influence of these factors reported in the literature was summarized in the API/MMS foundation study [5]. The contribution of these factors to the pile axial capacity is uncertain and thus, in Phase II, a correction factor was not applied to the pile axial capacities The cumulative effect of all of these factors will be reflected in the resulting foundation axial bias factor

e. Mudmat effect. Mudmat effect was not included.

Conductors

a. Conductors were modeled with linear beam elements. Conductors were modeled to move freely in the vertical direction and to transfer lateral wave loads in orthogonal directions to the jacket structure.

b. Conductors were always modeled to capture their wave load contribution. The structural resistance of the conductors, which increase the lateral load carrying capacity of the foundation, were modeled only in instances where the conductors were guided at the mudline and initial analysis predicted a pile yield/hinge failure mode. The conductors were guided at the mudlevel horizontal framing for only two platforms (WD103A, ST130A) and were modeled for structural resistance in only ST130A.

Appendix C
Joint Information

The following information is provided:

- Summary tables with joint parameters
- Structural configuration of jacket frames
- Basic joint strengths provided by MSL
- P-δ and M-θ plots for platform ST177B provided by MSL

Table C-1: Joint Data

Joint Location	Joint Type	Chord D inch	Chord T inch	Brace d inch	Brace t inch	Theta degree	Eccentricity e inch	Gap g inch	Work-point offset inch	Beta β	Gamma γ	Length L ft.	Length l ft.
Platform ST 151K (A):													
Top bay	X	16	0 406	16	0 406	79 87	-	-	-	1 00	19 70	57 64	26.41/31 23
2nd bay	K	16	0 406	16	0 406	53 2	10 01	2 00	9 99	1 00	19 70	47 90	46 34
3rd bay	K	18	0 438	18	0 438	49 73	10 34	2 00	11 80	1 00	20 55	55 30	48 64
Bottom bay	KT	20	0 438	18	0 438	46 55	7 85	2 00	13 77	0 90	22 83	62 70	51 10
				14	0 375	90	-	overlap	-	-	-	-	-
Platform ST130Q (B):													
Top bay	X	14	0 438	14	0 438	84 19	-	-	-	1 00	15 98	35 61	16 15/19 46
2nd bay	K	14	0 438	12.75	0 406	54	7 59	2 00	8 65	0 91	15 98	30 48	31 06
3rd bay	K	14	0 438	12 75	0 406	52.5	7 33	2 00	8 82	0 91	15 98	36.38	35 45
4th bay	K	16	0 438	14	0 438	51 7	7 20	2 00	10 19	0 88	18 26	42 98	40 94
5th bay	K	18	0 438	16	0 438	50	7 78	2 00	11 75	0 89	20 55	50 52	45 89
Bottom bay	K	18	0 438	18	0 438	49 6	10 32	2 00	11 82	1 00	20.55	58 77	52 77
Platform ST151H (D):													
Top bay	X	16	0 406	16	0 406	79 93	-	-	-	1 00	19 70	57 68	26 83/30 85
2nd bay	K	16	0 406	16	0.406	54 1	10 17	2 00	9 88	1 00	19 70	42 98	40 94
3rd bay	K	18	0.438	18	0 438	51 1	10 60	2 00	11 56	1 00	20.55	50 52	45 89
Bottom bay	KT	20	0 438	18	0 438	48 3	8 29	2 00	13 39	0 90	22 83	58 77	52 77
				14	0 375	90	-	overlap	-	-	-	-	-

Table C-2: Joint Data

Joint Location	Joint Type	Chord D inch	Chord T inch	Brace d inch	Brace t inch	Theta degree	Eccentricity e inch	Gap g inch	Work-point offset inch	Beta β	Gamma γ	Length L ft.	Length l ft.
Platform ST 130A (E):													
Top bay	X	16	0 375	16	0 375	78 39	-	-	-	1 00	21 33	55 46	26 83
2nd bay	K	16	0 375	16	0 375	54.5	10 24	2 00	9 83	1 00	21 33	45 33	43 01
3rd bay	K	16	0 375	16	0 375	52	9 80	2 00	10 15	1 00	21 33	50 00	44 41
Bottom bay	K	20	0 344	16	0 375	49 7	6 02	2 00	13 11	0 80	29 07	54 67	45 88
Platform ST72-T21 (F):													
Top bay	K	18	0.438	18	0 937	45 9	12	4 38	12.53	1 00	20.55	41	33 99
Middle bay	K	18	0 438	18	0.5	42.5	9.5	2.50	13 32	1 00	20 55	47 08	36 17
Bottom bay	KT	18	0.438	18	0.5	39 4	24	17.56	14 18	1 00	20.55	53 17	38 46
				14	0.438	90	12	-	-	-	-	-	-
Platform SS139 - T25 (H):													
Top bay	K	18	0 438	18	0 937	45 43	12	4 46	12 63	1 00	20 55	41	33 25
Middle bay	K	18	0.438	18	0 5	42	12	5 09	13.45	1 00	20.55	47	35 3
Bottom bay	KT (#3)	18	0 438	18	0 5	39 265	24	17.58	14 22	1 00	20 55	52 7	37 53
		Vertical brace (#1)		14	0.438	90	12	-	-	-	-	-	-
Platform ST177B (J):													
Top bay	X	16	0 406	16	0.406	80 86	-	-	-	1 00	19 70	58 72	26 86/31 86
2nd bay	K	16	0 406	16	0 406	53 6	10 08	2 00	9 94	1 00	19 70	48 4	47 36
3rd bay	K	18	0.438	18	0 438	50 17	10.43	2 00	11 72	1 00	20 55	56	49 55
Bottom bay	KT (#3)	20	0 438	18	0 438	48	8 21	2 00	13 46	0 90	22 83	63 6	53 83
		Vertical brace (#2)		14	0 375	90	-	-	-	-	-	-	-

Notes: **#1: Does not overlap K-braces**

#2: Overlaps K-brace

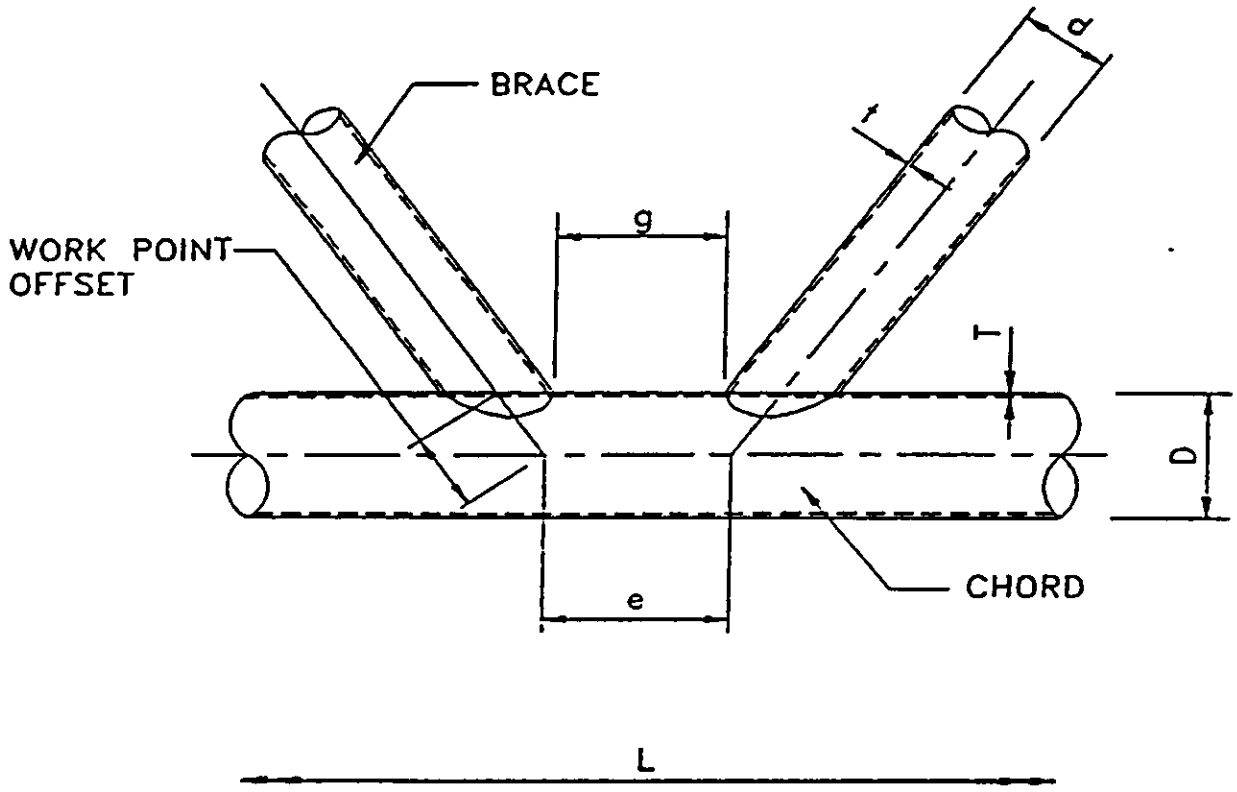

Notation for Tubular Joints

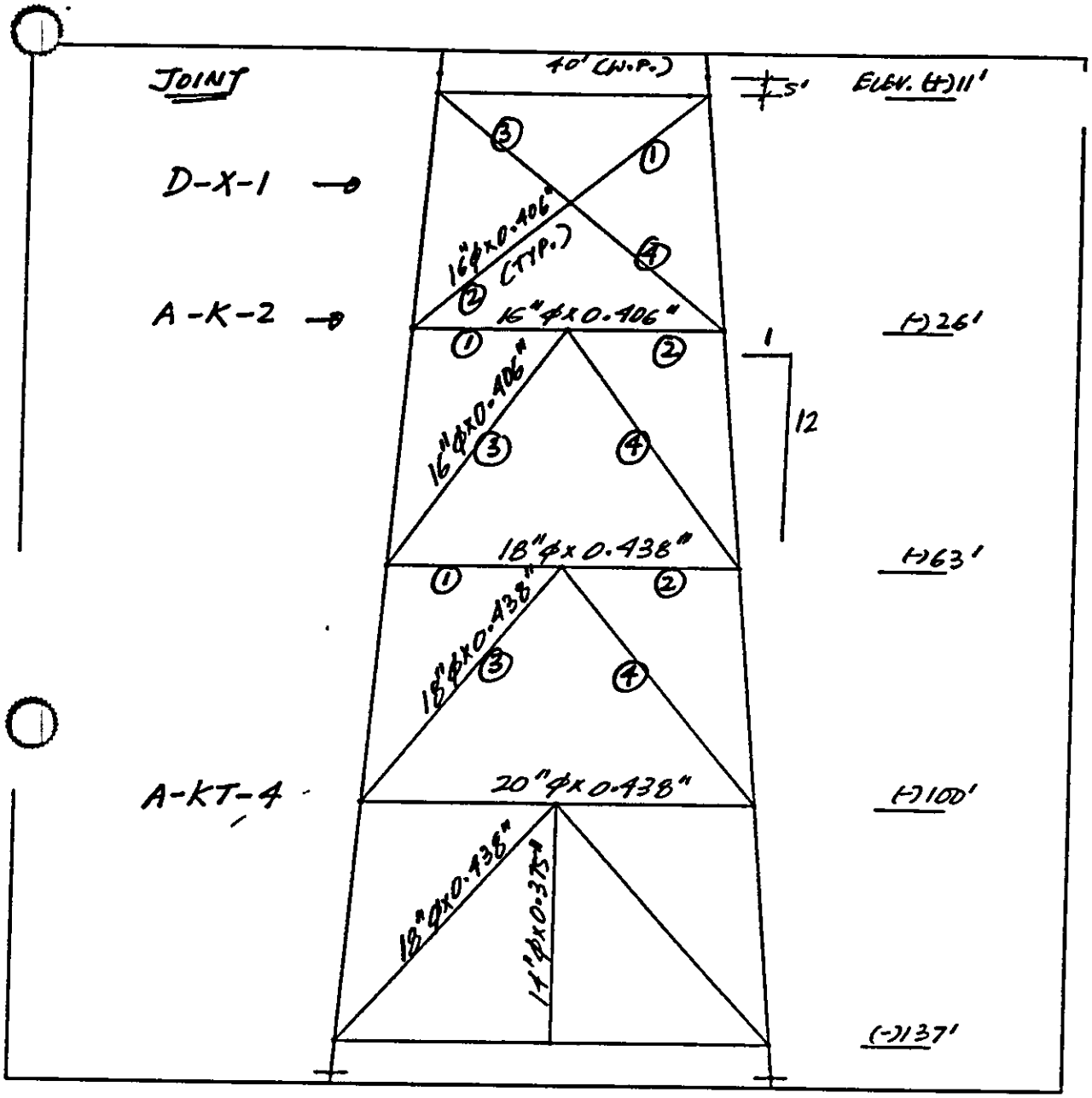

CAP

PLATFORM – A (STIS-1K)

(SIMILAR TO PLATFORM-D)

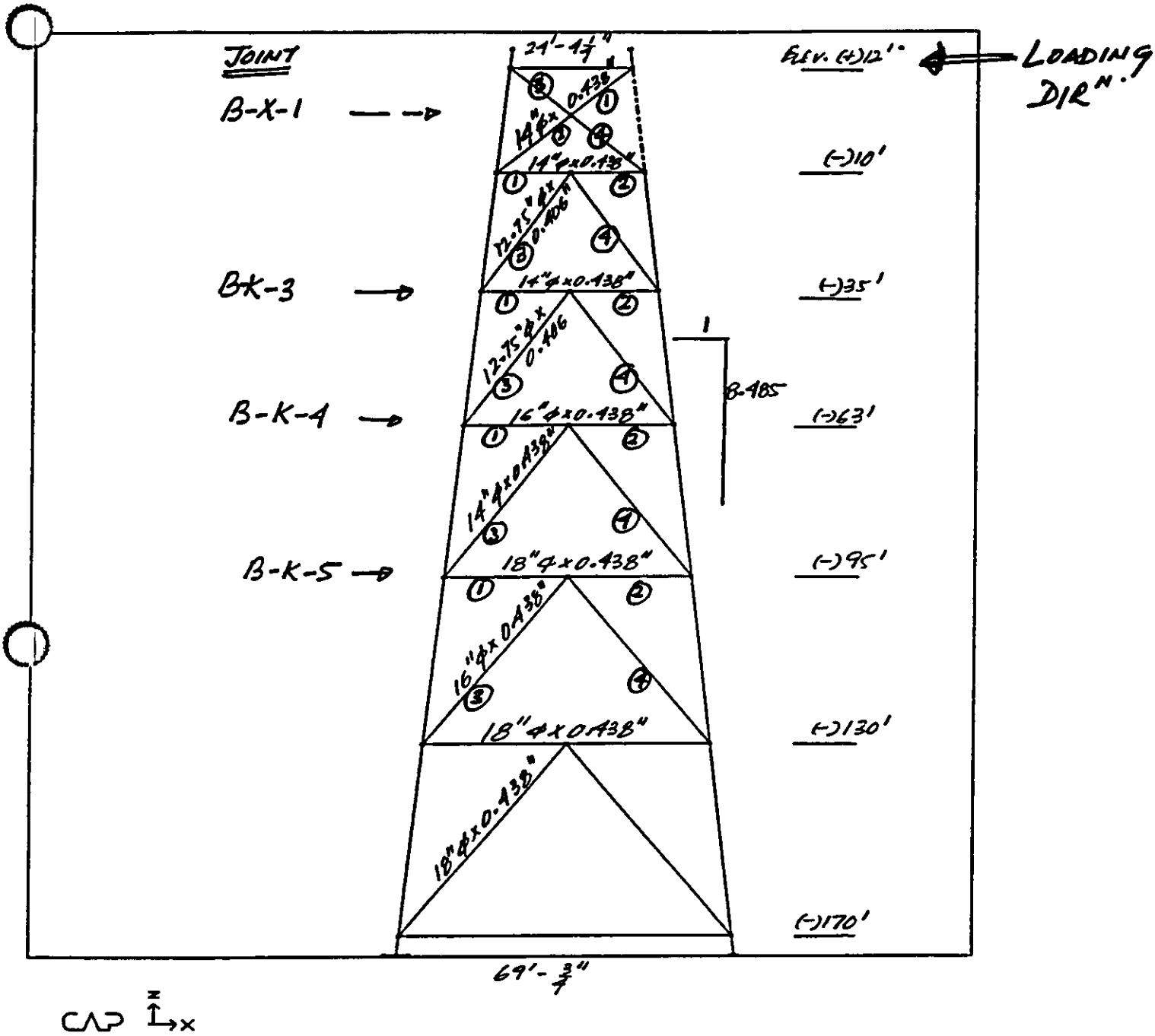

CAP $\hat{I}_{zx}$

PLATFORM B (ST130Q)

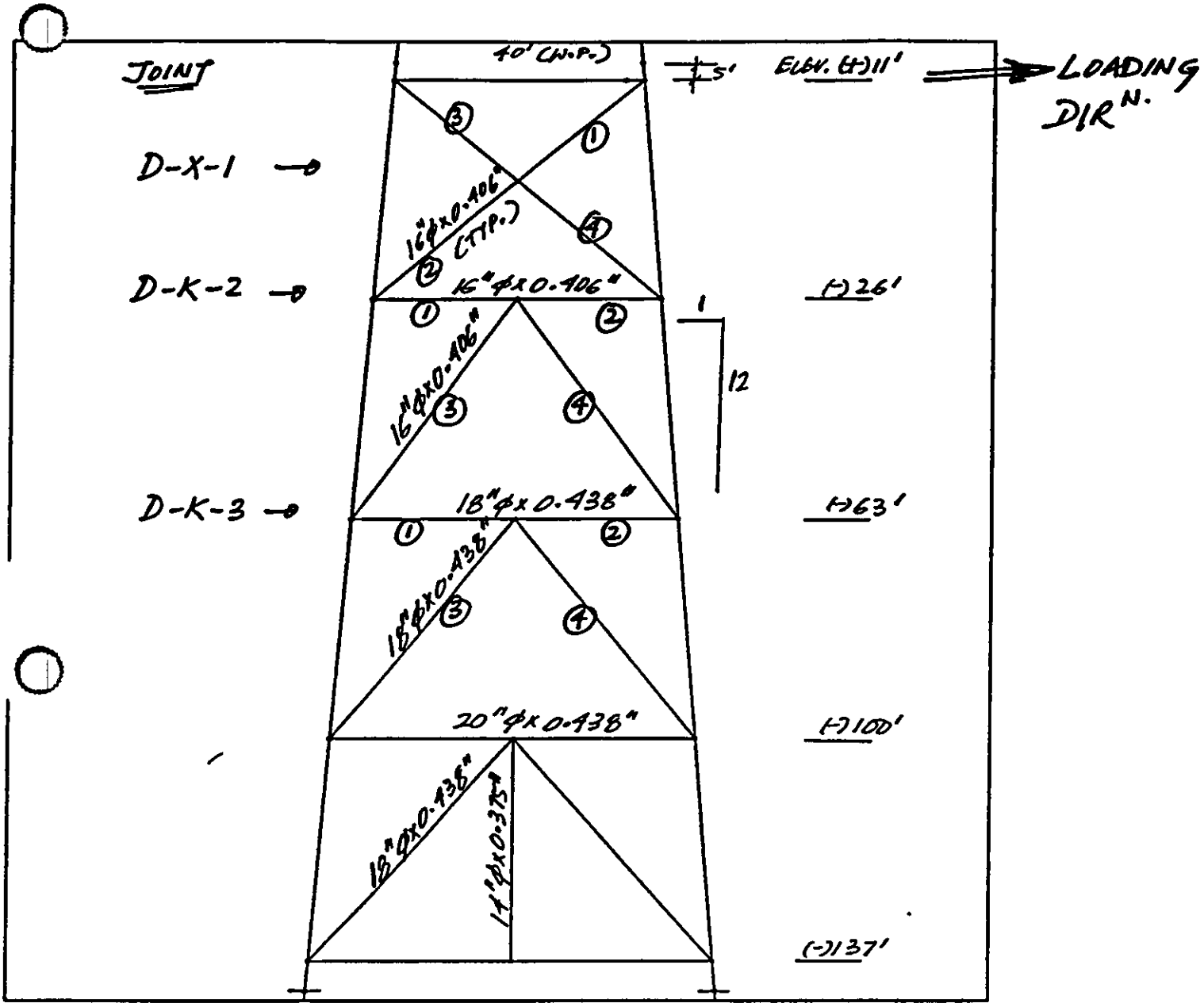

CAP -- i

PLATFORM – D (STISIH)

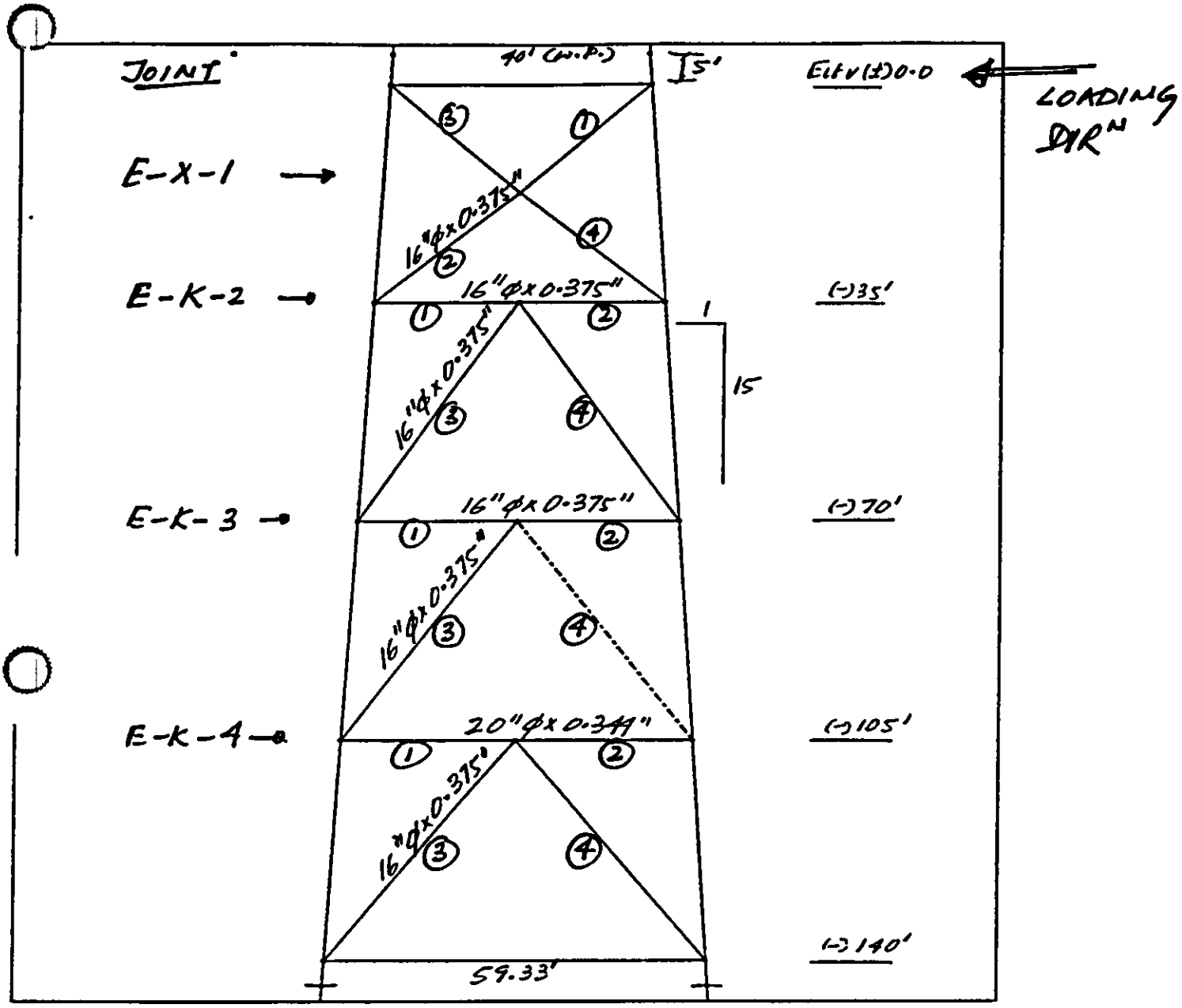

PLATFORM - E (ST130A)

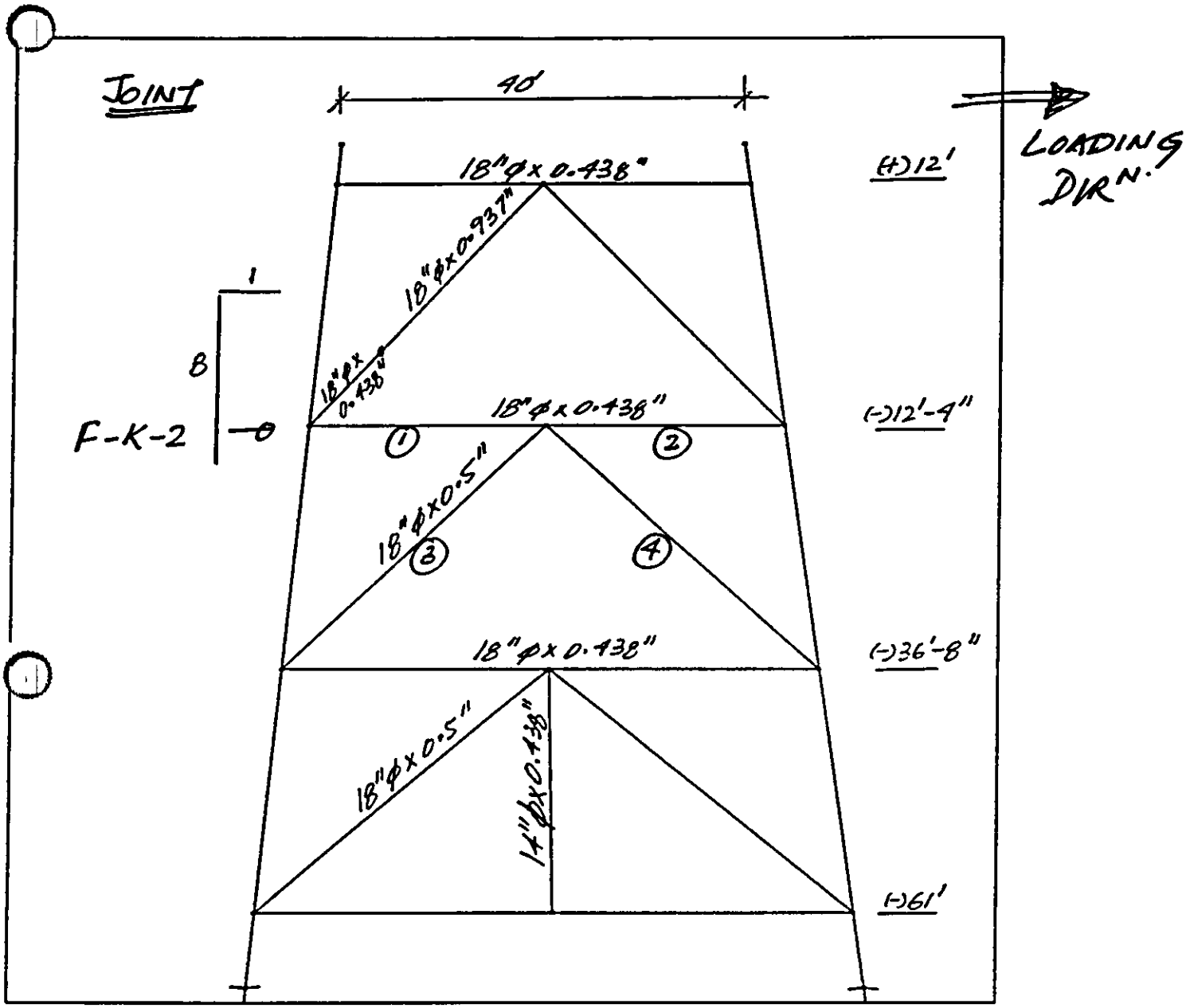

CAP x

PLATFORM - F (ST72 - T21)

JOINT

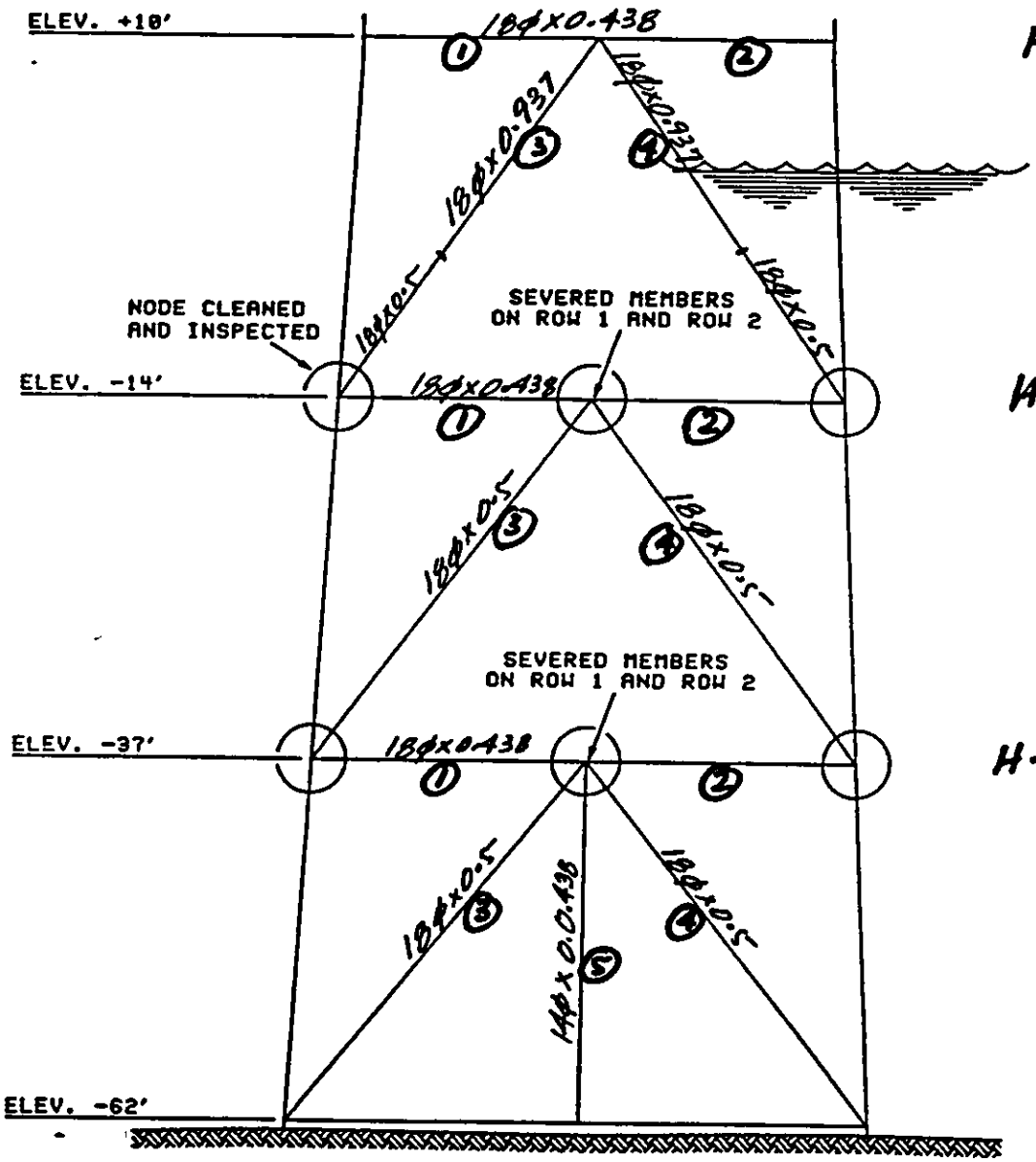

PLATFORM - H (SS-139-T25)

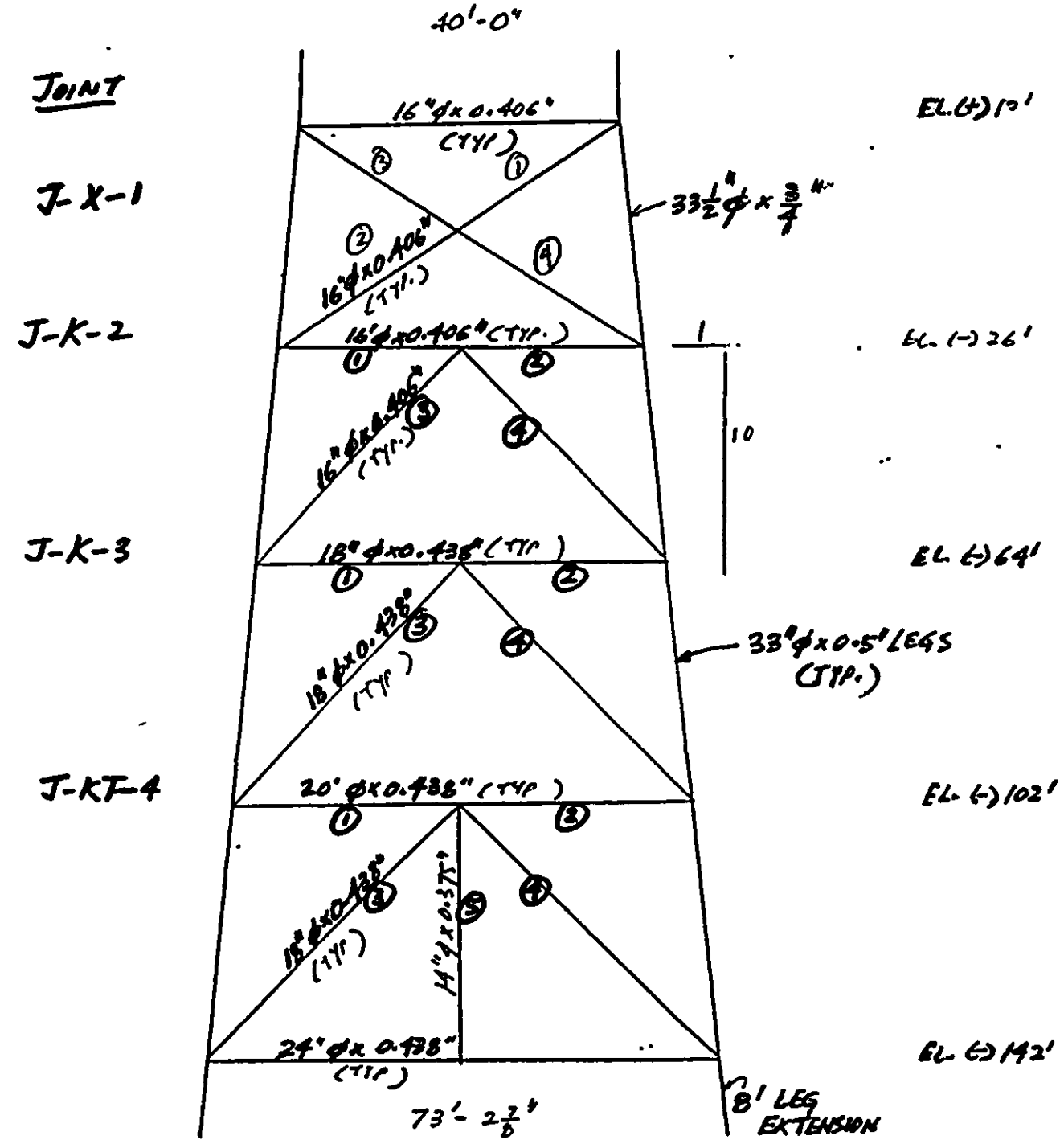

PLATFORM-J (ST177B)

BASIC JOINT STRENGTHS [1]

Joint Identification	Brace No	Comp P_u K-joint	Comp P_u X/Y-joint	Tension P_u K-joint	Tension P_u X/Y-joint	$M_{u\,IPB}$	$M_{u\,OPB}$
PLATFORM A (ST151K)							
A-X-1	3 & 4	-	6.15	-	-	5 41	4 16
A-K-2	3	11.68	7 91	-	-	6 65	5 12
	4	-	-	12 85	13 48	6 65	5 12
A-K-3	3	14 83	9 66	-	-	9 34	7 18
	4	-	-	16 31	16 47	9 34	7 18
A-KT-4	3	-	-	13 95	15 78	9 31	5 91
	4	12 68	8 54	-	-	9 31	5 91
	5[2]	8 71	-	-	-	4 09	2.02
PLATFORM B (ST130Q)							
B-X-1	3 & 4	-	6 08	-	-	5 35	4 12
B-K-3	3	9 34	6.83	-	-	4 06	3 34
	4	-	-	10 27	12 52	4 06	3 34
B-K-4	3	10 54	7 62	-	-	5 89	4 17
	4	-	-	11 59	14 31	5 89	4 17
B-K-5	3	11 30	7 95	-	-	7 37	5 17
	4	-	-	12 43	14 81	7 37	5 17
B-K-6	3	15 02	9 68	-	-	9 36	7 99
	4	-	-	16 52	16 50	9 36	7 99

Basic Joint Strengths (Continued)

Joint Identification	Brace No	Comp P_a K-joint	Comp P_a X/Y-joint	Tension P_a K-joint	Tension P_a X/Y-joint	M_{aIPB}	M_{aOPB}
PLATFORM D (ST151H)							
D-X-1	3 & 4	-	-	-	10 97	5 41	4 16
D-K-2	3	-	-	12 62	13 33	6 58	5 06
	4	11 47	7 82	-	-	6 58	5 06
D-K-3	3	-	-	15 82	16 15	9 16	7 04
	4	14 38	9 47	-	-	9 16	7 04
D-KT-4	3	-	-	13 34	15 34	9 05	5 75
	4	12 13	8 30	-	-	9 05	5 75
	5[2]	8 71	-	-	-	4 09	1 42
PLATFORM E (ST130A)							
E-X-1	3 & 4	-	-	-	11 02	-	-
E-K-2	3	13.25	9 05	-	-	-	-
	4	-	-	14 57	15 43	-	-
E-K-3	3	11 97	8 04	-	-	-	-
	4	-	-	13 17	13 70	-	-
E-K-4	3	14 99	9 66	-	-	-	-
	4	-	-	16 49	16 48	-	-
PLATFORM F (ST 72-T21)							
F-K-1	3	-	-	13 99	15 03	7 90	5 83
	4	12 72	8 82	-	-	7 90	5 83
F-K-2	3	-	-	16.60	15 98	8 40	6 19
	4	15 09	9 37	-	-	8 40	6.19
F-KT-3	3	-	-	18.04	18 04	9 09	5 83
	4	9 77	9 77	-	-	9 09	5 83
	5[2]	9 38	-	-	-	4 31	2.35

Basic Joint Strengths (Continued)

Joint Identification	Brace No	Comp P_u K-joint	Comp P_u X/Y-joint	Tension P_u K-joint	Tension P_u X/Y-joint	$M_{u\,IPB}$	$M_{u\,OPB}$
PLATFORM E (REVISED) ST 130A-							
E-X-1	3 & 4	-	-	-	11 02	6 13	4 35
E-K-2	3	13 25	9 05	-	-	9 26	7 62
	4	-	-	14 57	15 43	9 26	7 62
E-K-3	3	11 97	8 04	-	-	7 62	5 41
	4	-	-	13 17	13 70	7 62	5 41
E-K-4	3	14 99	9 66	-	-	15 72	8 54
	4	-	-	16 49	16 48	15.72	8 54

Basic Joint Strengths (Continued)

Joint Identification	Brace No	Comp P_a K-joint	Comp P_a X/Y-joint	Tension P_a K-joint	Tension P_a X/Y-joint	$M_{a\,IPB}$	$M_{a\,OPB}$
PLATFORM H (SS139 - T21)							
H-K-1	3	14 93	10 34	-	-	10 00	7.69
	4	-	-	16 42	17 64	10 00	7 69
H-K-2	3	16 15	11 01	-	-	10 65	8 19
	4	-	-	17 77	18.78	10 65	8 19
H-KT-3	3	12.35	11 64	-	-	11.25	8.65
	4	-	-	13 59	19 84	11.25	8 65
	5	6 19	4 96	-	-	4 34	2.36
PLATFORM J (ST177 B)							
J-X-1	3 & 4	-	6 13	-	-	5 39	4 15
J-K-2	3	-	-	13 71	14 06	6 94	5 34
	4	12 47	8.25	-	-	6.94	5 34
J-K-3	3	-	-	16 15	16.36	9.28	7.13
	4	14 68	9 60	-	-	9.28	7 13
J-KT-4	3	-	-	13 44	15.41	9 09	5 77
	4	12.22	8.34	-	-	9 09	5 77
	5(2)	8.71	-	-	-	4 09	2.02

Notes:

(1) All values to be multiplied by Fy (chord yield strength in ksi) to give strengths in terms of kips or kips-ft.

(2) The overlapping T brace of the KT joint is now assumed to have the strength of the brace of an overlapping K joint.

Notes on Curve Information

1: Pu information for the overlapping T braces of KT joints (e.g. brace 5 of joint J-KT-4) have been changed.
2: Platforms A,D and J joints are of very similar geometry (differences in angle of 2-3° make a very small difference to Pδ behaviour). The same curves may be used for the platforms with very little loss of accuracy. Hence only Pδ information for platform D is presented to add to the existing information on platform J.
3: Only K joint information is presented for the very large gapped KT joint of platform F (F-KT-3). Very large gapped K joints behave like Y joints so there is no difference between the two curves.

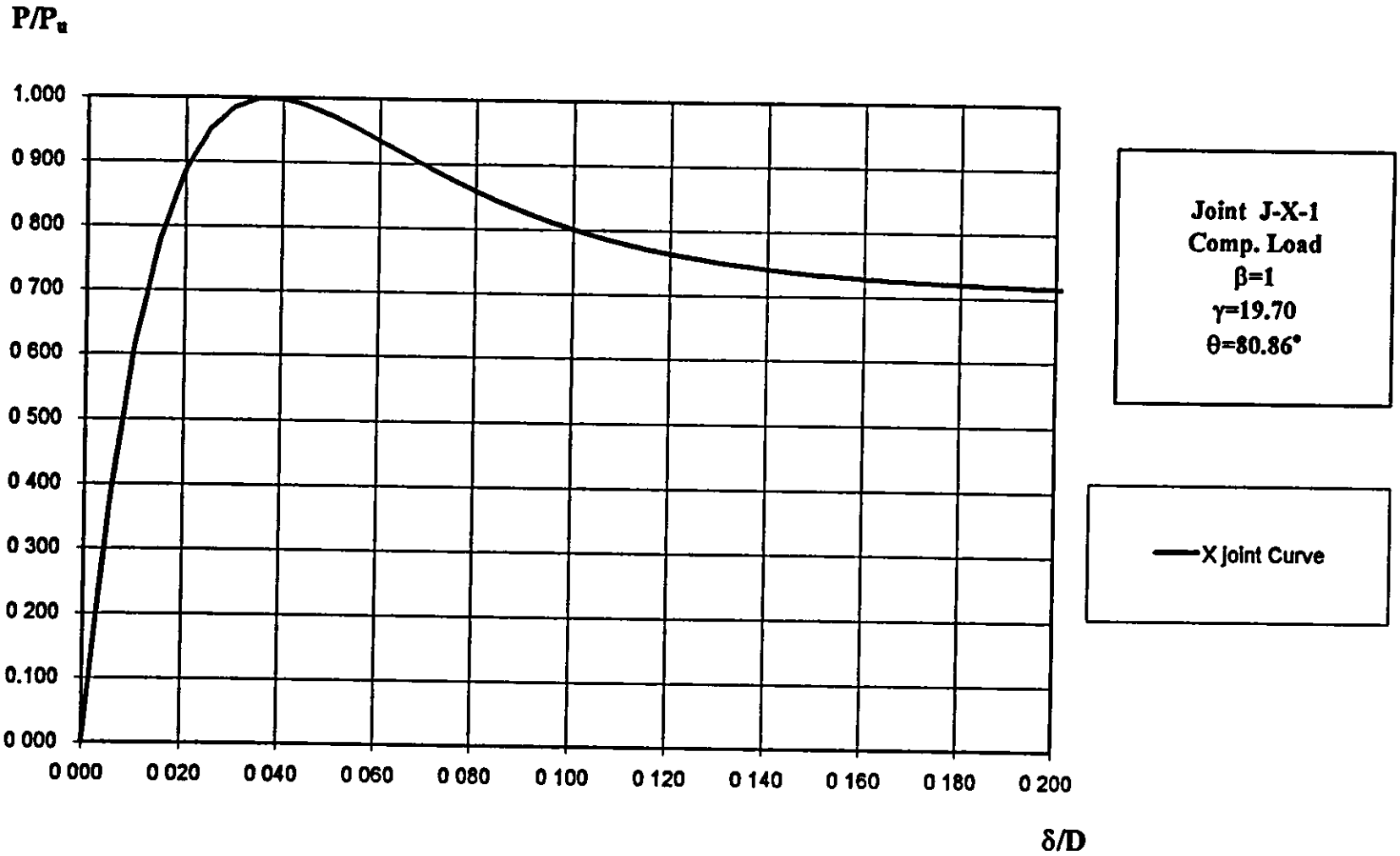
P/Pu
1.000
0 900
0 800
0 700
0 600
0 500
0 400
0 300
0 200
0.100
0 000
0 000
0 020
0 040
0 060
0 080
0 100
0 120
0 140
0 160
0 180
0 200
δ/D
Joint J-X-1
Comp. Load
β=1
γ=19.70
θ=80.86°
X joint Curve

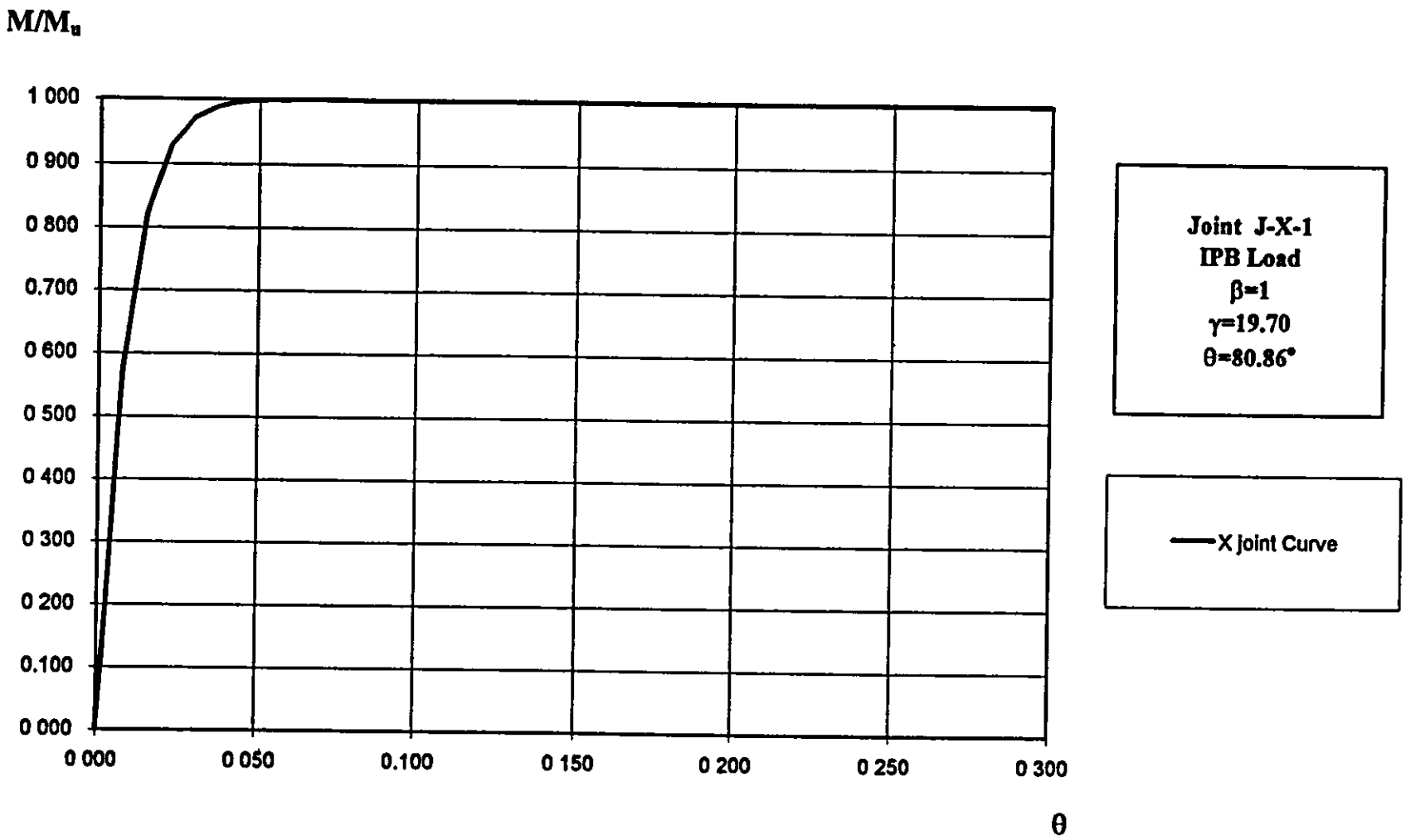
M/Mu
1 000
0 900
0 800
0.700
0 600
0 500
0 400
0 300
0 200
0.100
0 000
0 000
0 050
0.100
0 150
0 200
0 250
0 300
θ
Joint J-X-1
IPB Load
β=1
γ=19.70
θ=80.86°
X joint Curve

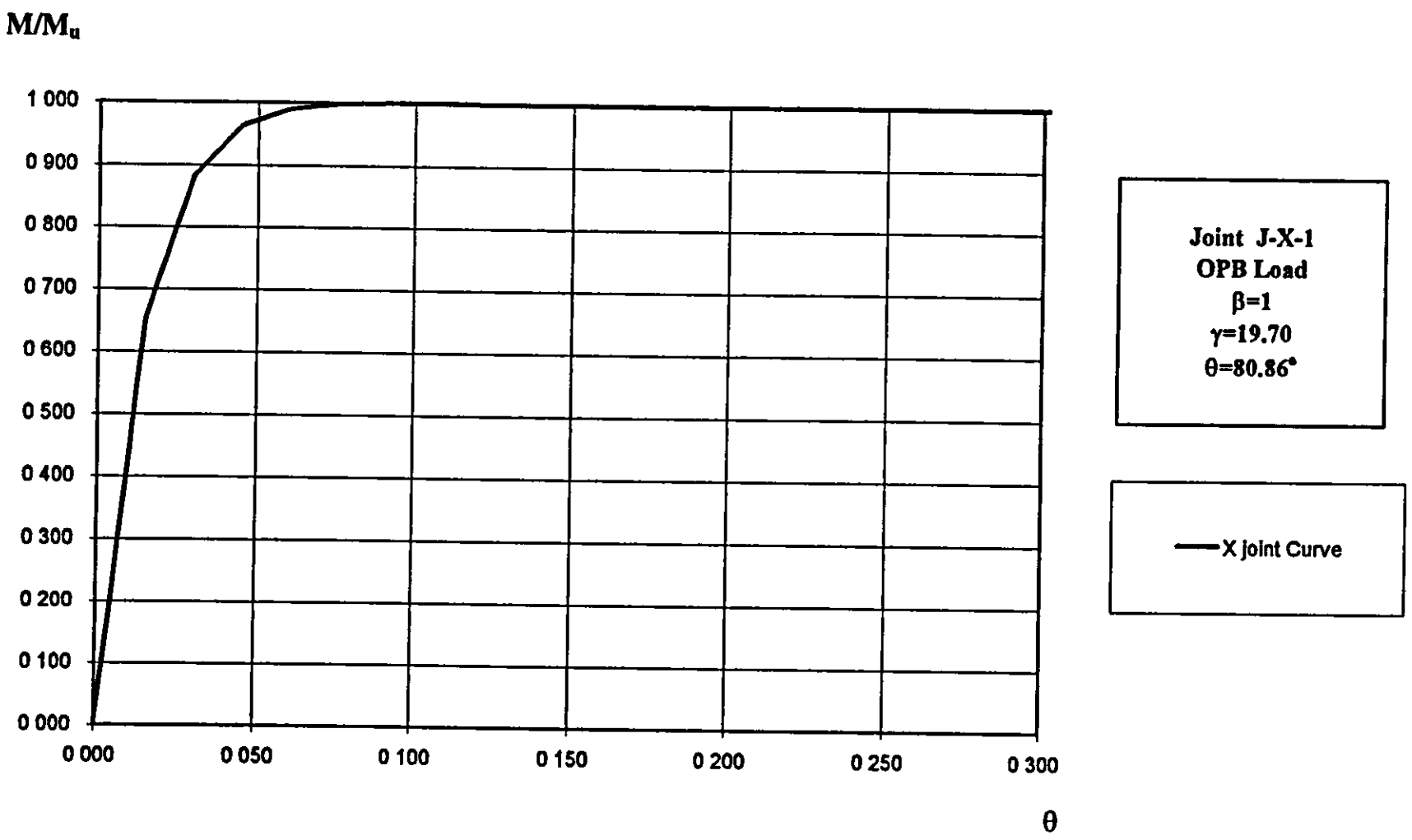
M/Mu
1 000
0 900
0 800
0 700
0 600
0 500
0 400
0 300
0 200
0 100
0 000
0 000
0 050
0 100
0 150
0 200
0 250
0 300
θ
Joint J-X-1
OPB Load
β=1
γ=19.70
θ=80.86°
X joint Curve

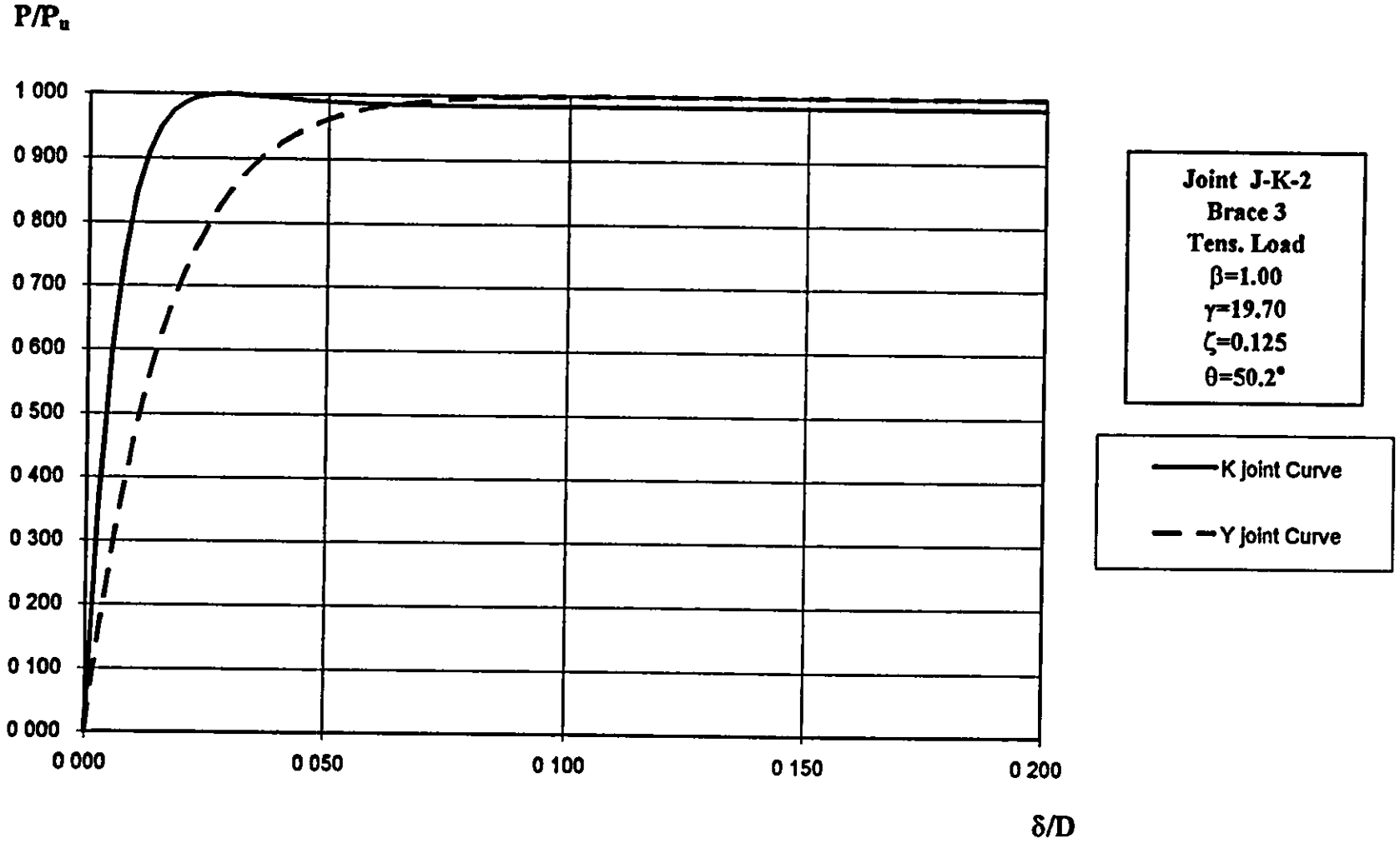
P/Pu
1 000
0 900
0 800
0 700
0 600
0 500
0 400
0 300
0 200
0 100
0 000
0 000
0 050
0 100
0 150
0 200
δ/D
Joint J-K-2
Brace 3
Tens. Load
β=1.00
γ=19.70
ζ=0.125
θ=50.2°
K joint Curve
Y joint Curve

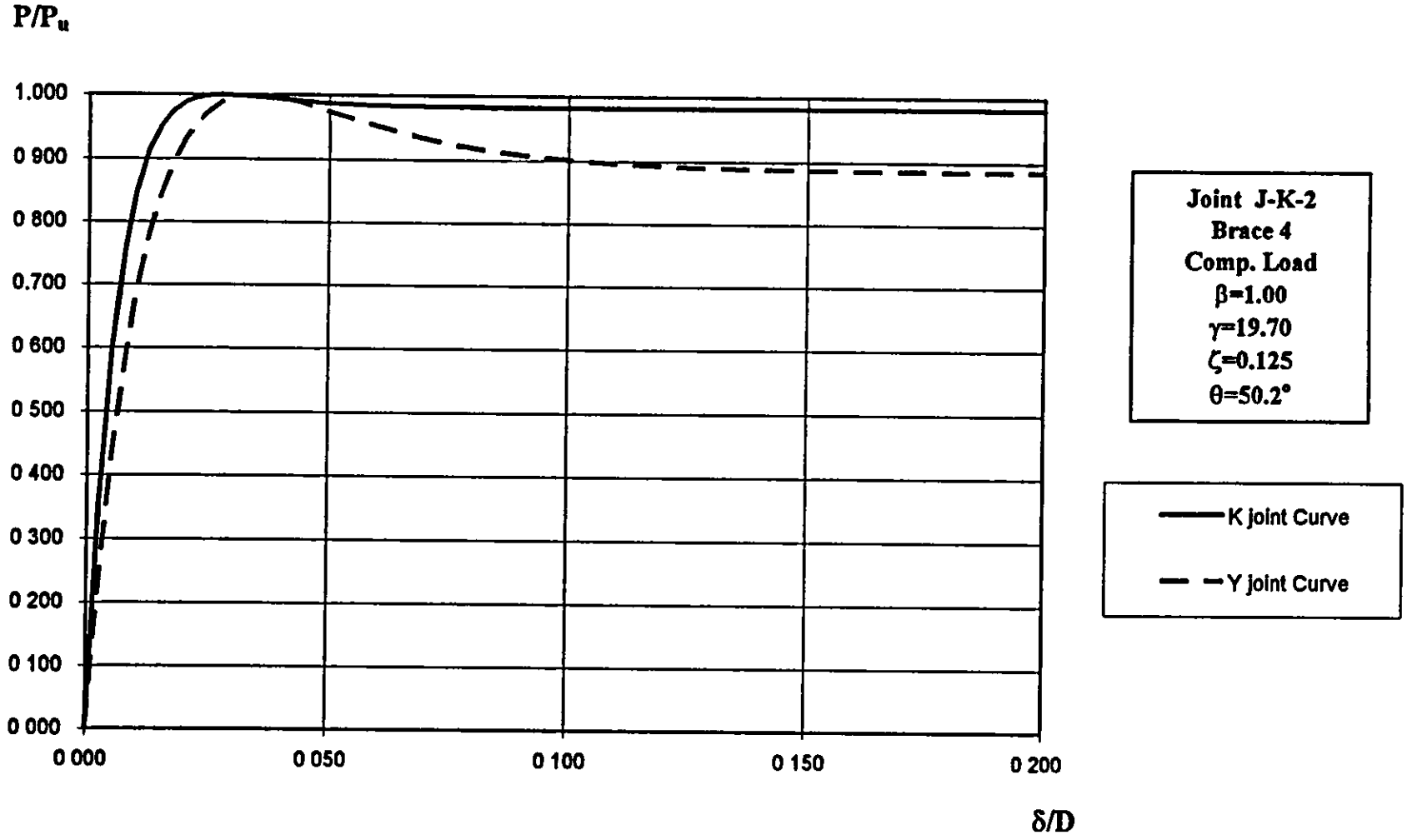
P/Pu
1.000
0 900
0 800
0.700
0 600
0 500
0 400
0 300
0 200
0 100
0 000
0 000
0 050
0 100
0 150
0 200
δ/D
Joint J-K-2
Brace 4
Comp. Load
β=1.00
γ=19.70
ζ=0.125
θ=50.2°
K joint Curve
Y joint Curve

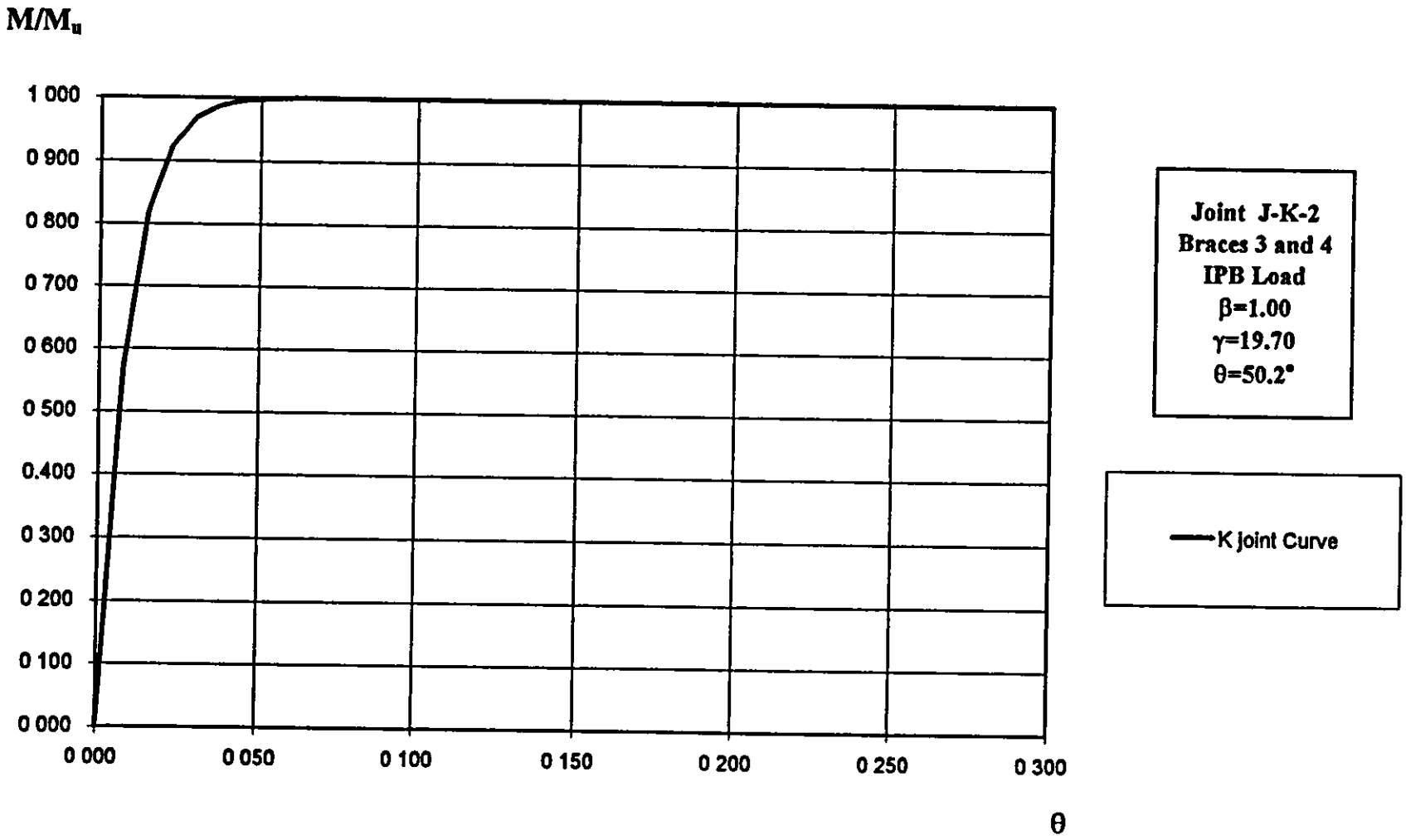
M/Mu
1 000
0 900
0 800
0 700
0 600
0 500
0.400
0 300
0 200
0 100
0 000
0 000
0 050
0 100
0 150
0 200
0 250
0 300
θ
Joint J-K-2
Braces 3 and 4
IPB Load
β=1.00
γ=19.70
θ=50.2°
K joint Curve

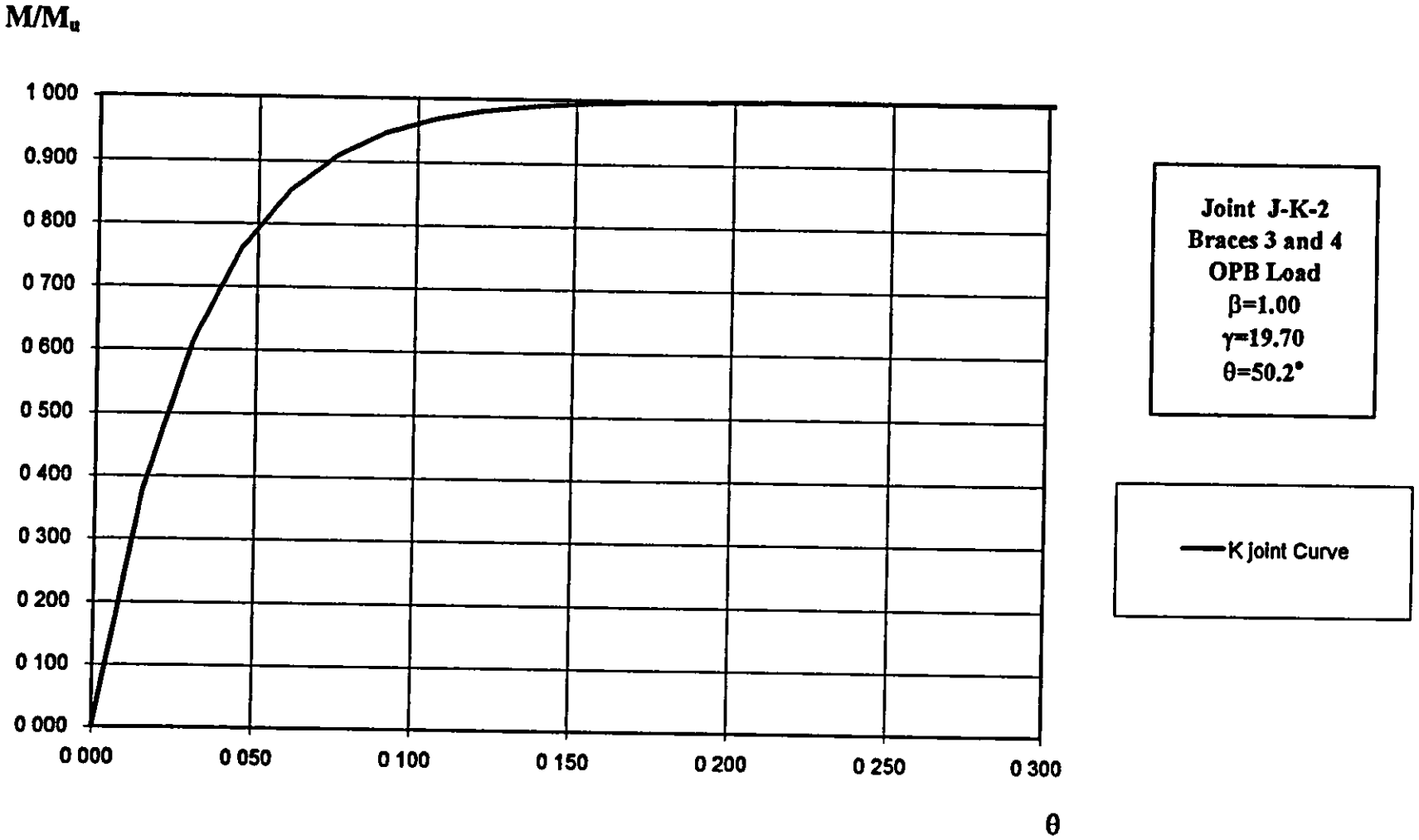
M/Mu
1 000
0.900
0 800
0 700
0 600
0 500
0 400
0 300
0 200
0 100
0 000
0 000
0 050
0 100
0 150
0 200
0 250
0 300
θ
Joint J-K-2
Braces 3 and 4
OPB Load
β=1.00
γ=19.70
θ=50.2°
K joint Curve

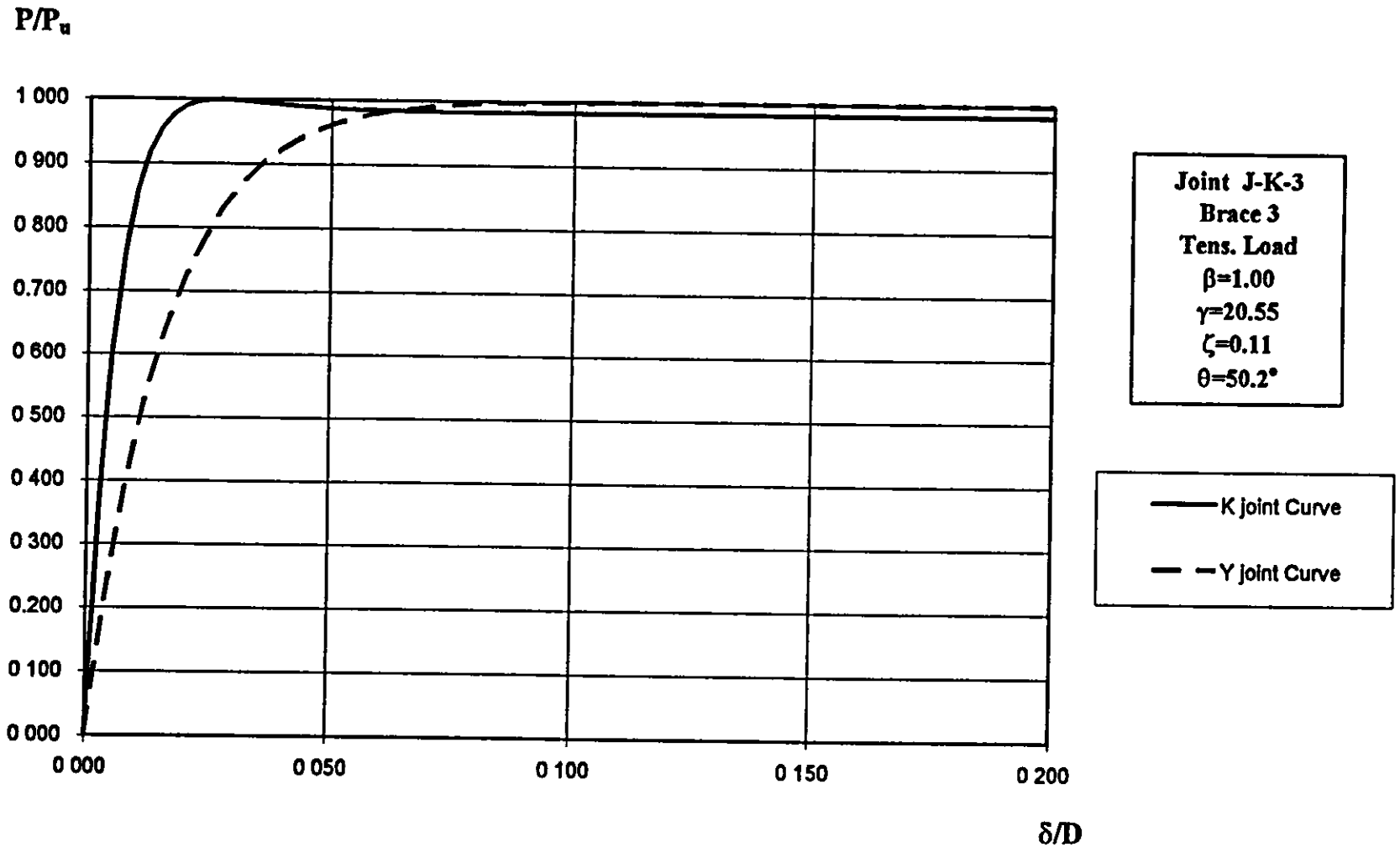
P/Pu
1 000
0 900
0 800
0.700
0 600
0 500
0 400
0 300
0.200
0 100
0 000
0 000
0 050
0 100
0 150
0 200
δ/D
Joint J-K-3
Brace 3
Tens. Load
β=1.00
γ=20.55
ζ=0.11
θ=50.2°
K joint Curve
Y joint Curve

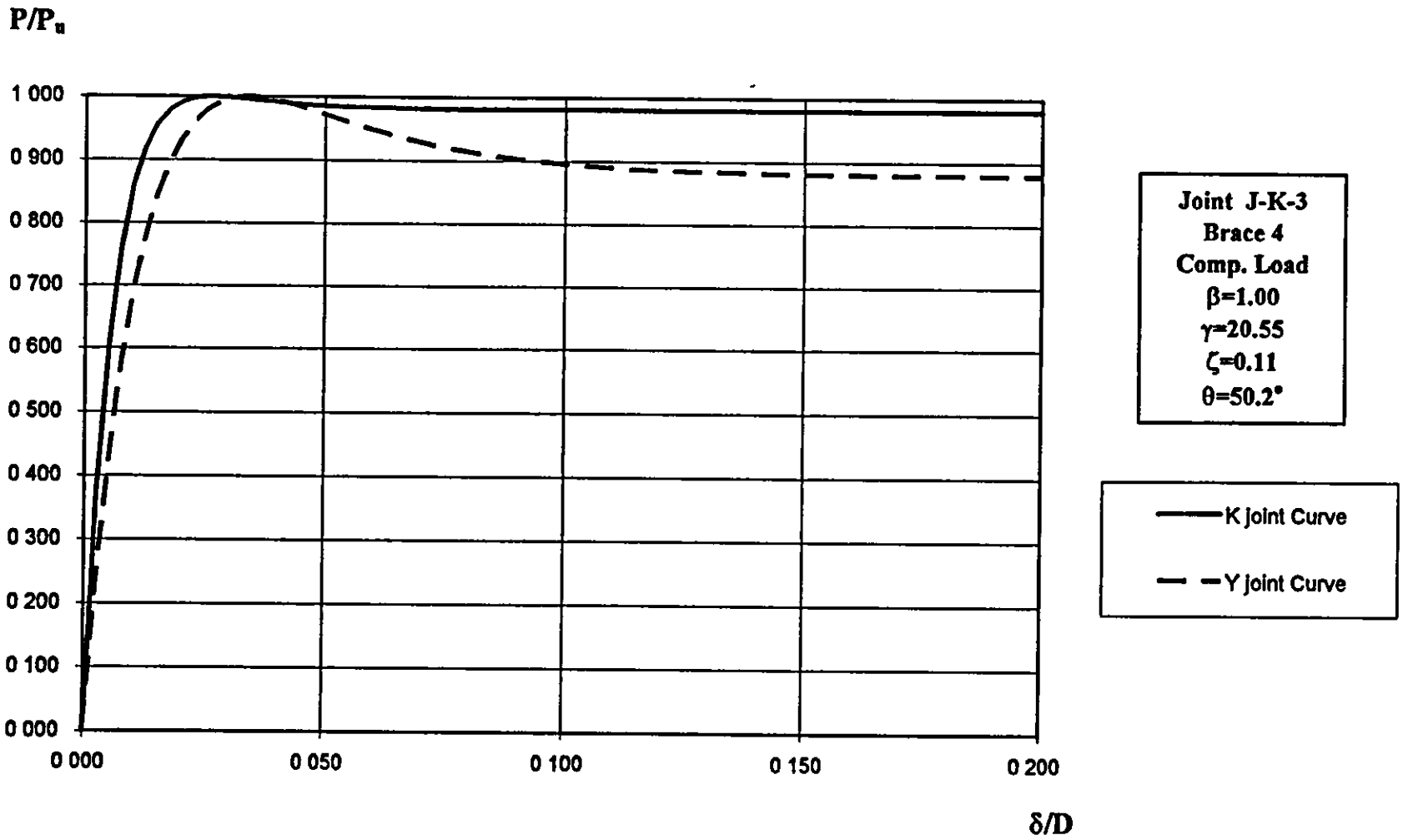
P/Pu
1 000
0 900
0 800
0 700
0 600
0 500
0 400
0 300
0 200
0 100
0 000
0 000
0 050
0 100
0 150
0 200
δ/D
Joint J-K-3
Brace 4
Comp. Load
β=1.00
γ=20.55
ζ=0.11
θ=50.2°
K joint Curve
Y joint Curve

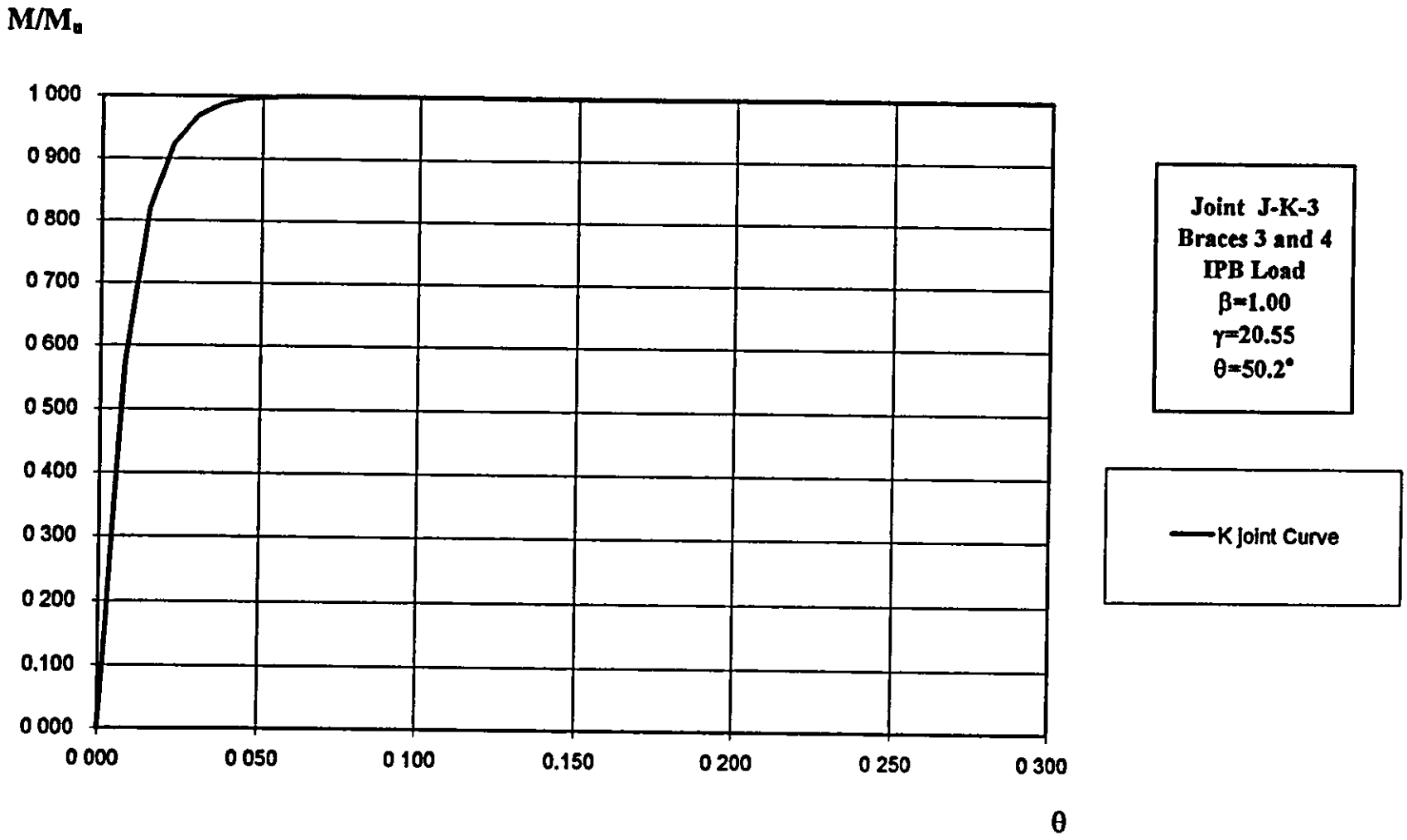
M/Mu
1 000
0 900
0 800
0 700
0 600
0 500
0 400
0 300
0 200
0.100
0 000
0 000
0 050
0 100
0.150
0 200
0 250
0 300
θ
Joint J-K-3
Braces 3 and 4
IPB Load
β=1.00
γ=20.55
θ=50.2°
K Joint Curve

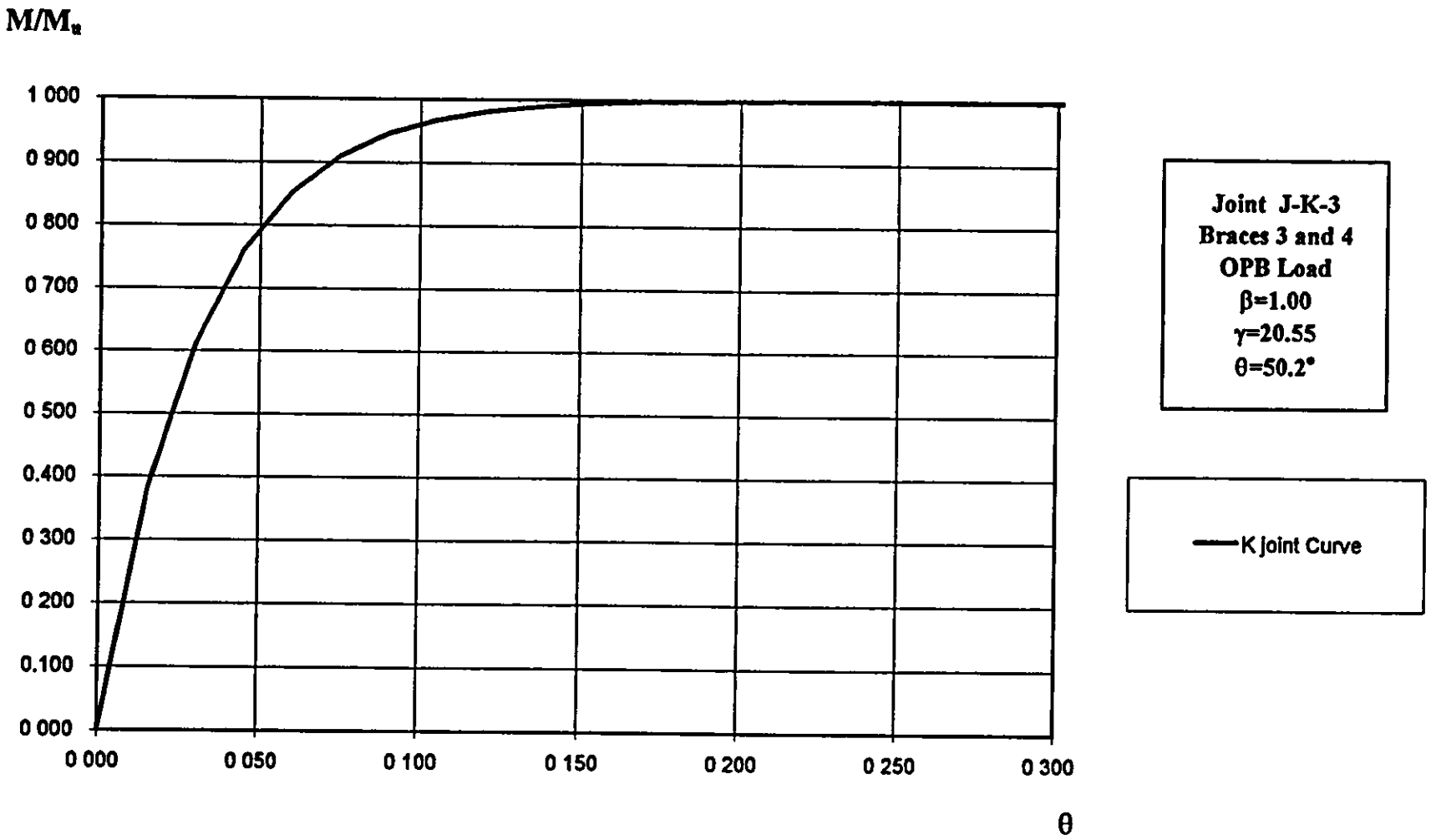
M/Mu
1 000
0 900
0 800
0 700
0 600
0 500
0.400
0 300
0 200
0.100
0 000
0 000
0 050
0 100
0 150
0 200
0 250
0 300
θ
Joint J-K-3
Braces 3 and 4
OPB Load
β=1.00
γ=20.55
θ=50.2°
K Joint Curve

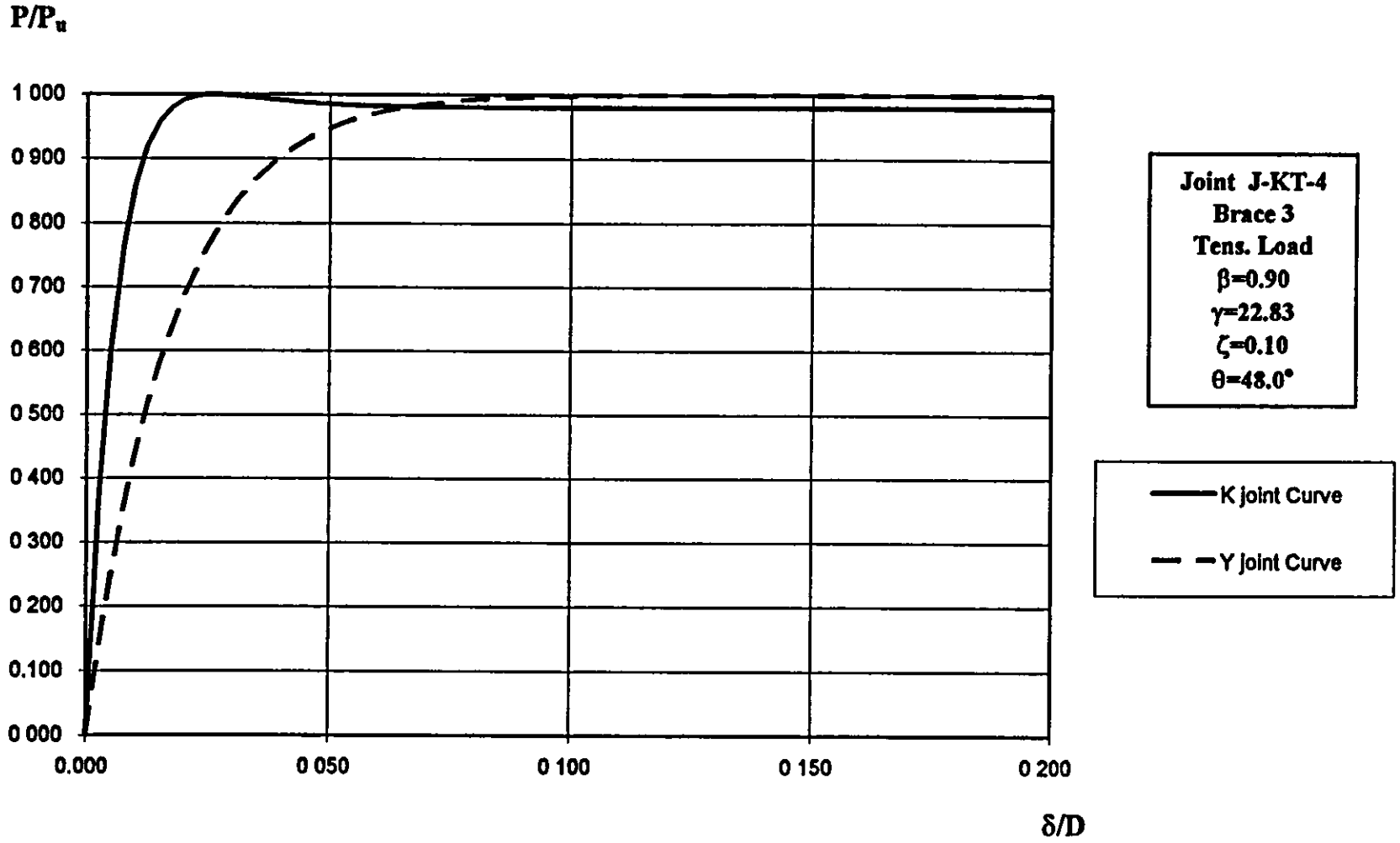
P/Pu
1 000
0 900
0 800
0 700
0 600
0 500
0 400
0 300
0 200
0.100
0 000
0.000
0 050
0 100
0 150
0 200
δ/D
Joint J-KT-4
Brace 3
Tens. Load
β=0.90
γ=22.83
ζ=0.10
θ=48.0°
K joint Curve
Y joint Curve

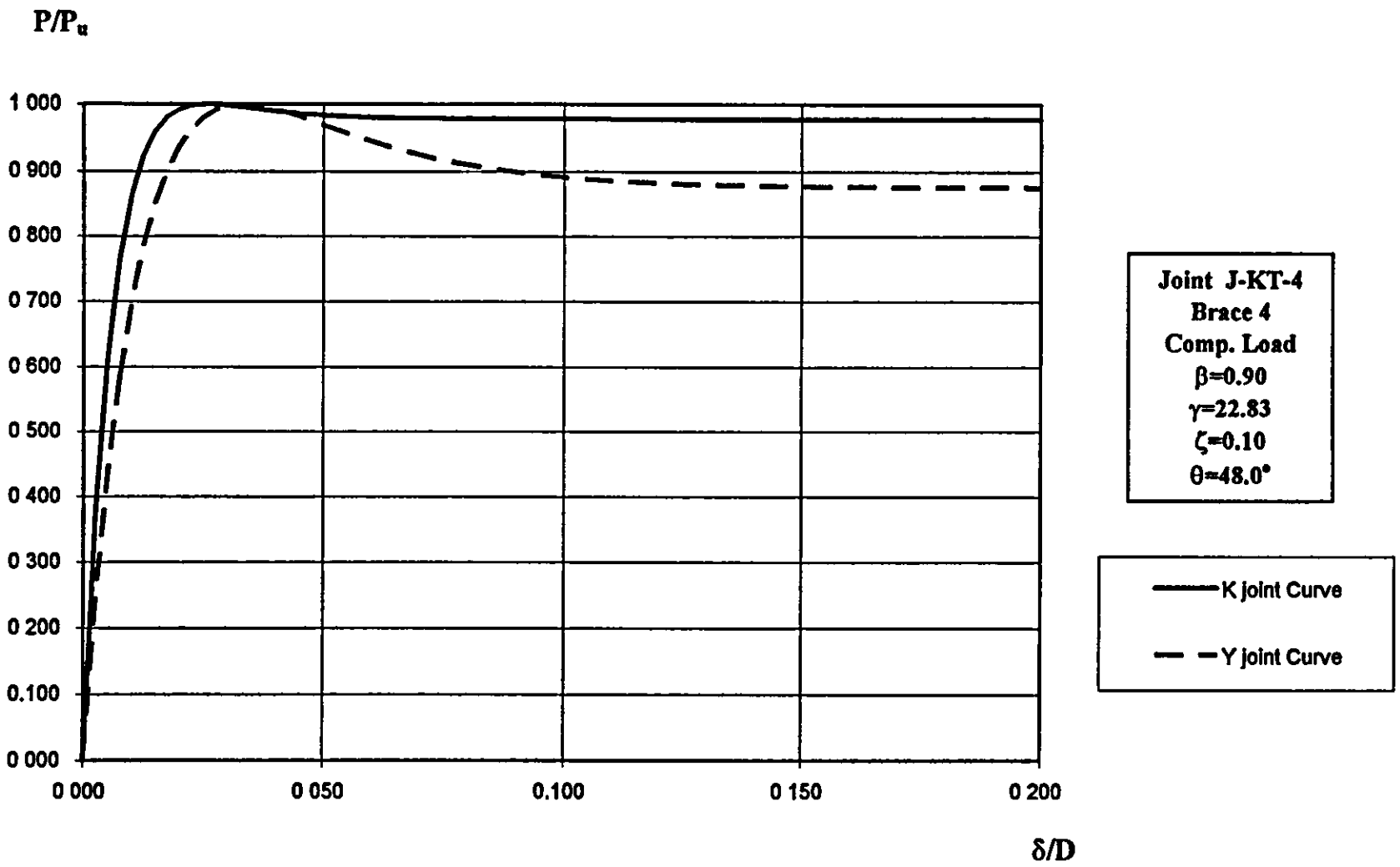
P/Pu
1 000
0 900
0 800
0 700
0 600
0 500
0 400
0 300
0 200
0.100
0 000
0 000
0 050
0.100
0 150
0 200
δ/D
Joint J-KT-4
Brace 4
Comp. Load
β=0.90
γ=22.83
ζ=0.10
θ=48.0°
K joint Curve
Y joint Curve

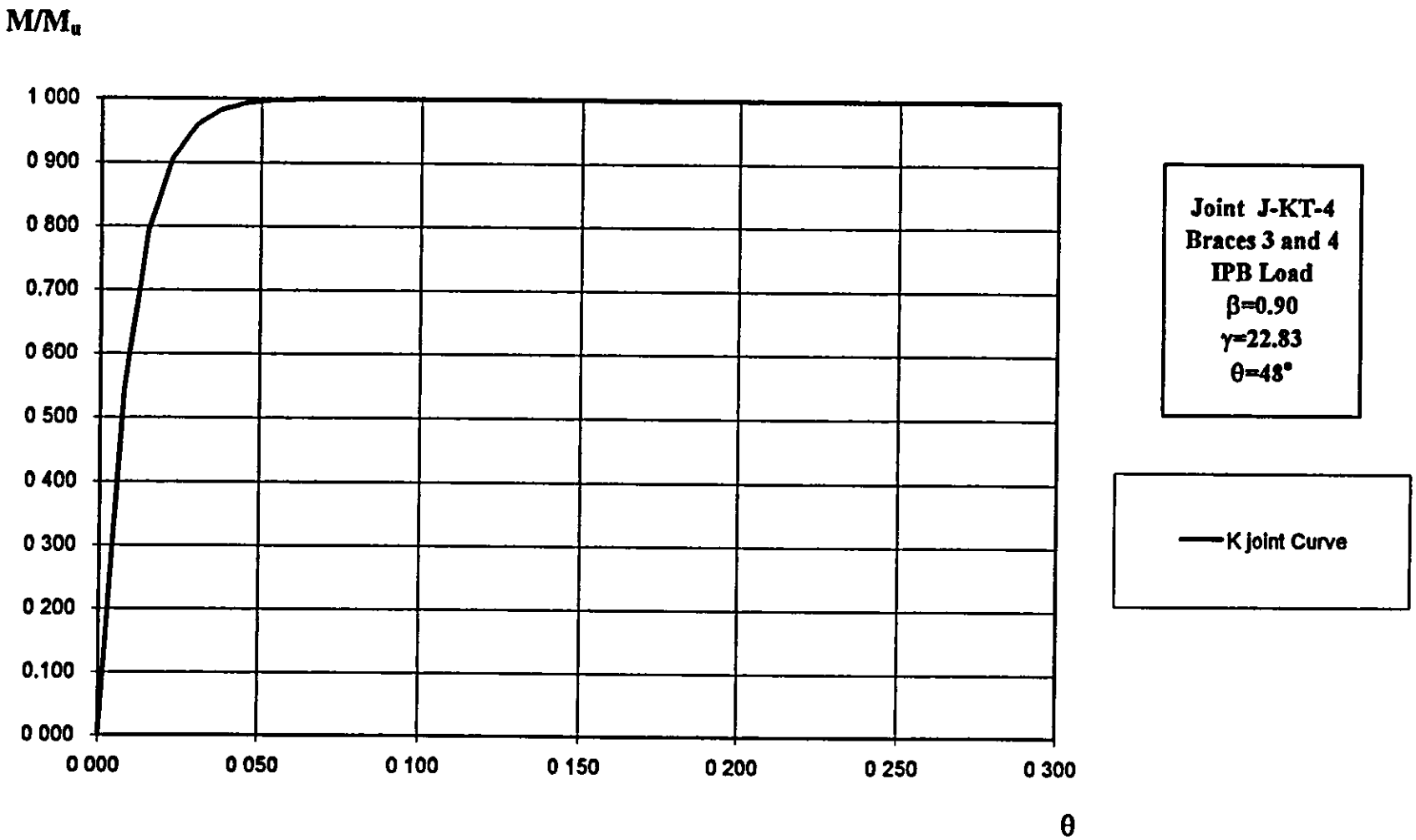
M/Mu
1 000
0 900
0 800
0.700
0 600
0 500
0 400
0 300
0 200
0.100
0 000
0 000
0 050
0 100
0 150
0 200
0 250
0 300
θ
Joint J-KT-4
Braces 3 and 4
IPB Load
β=0.90
γ=22.83
θ=48°
K joint Curve

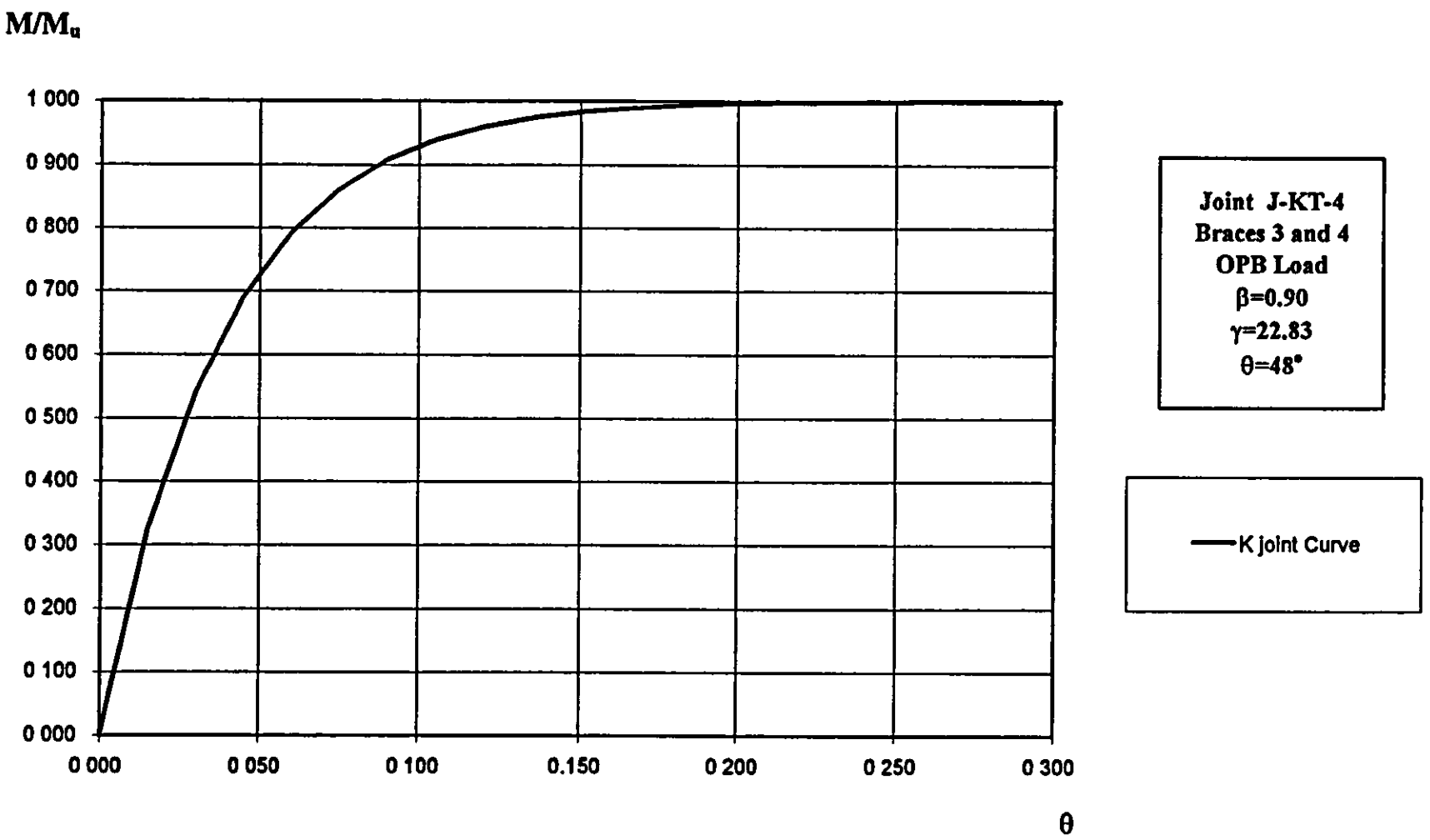
M/Mu
1 000
0 900
0 800
0 700
0 600
0 500
0 400
0 300
0 200
0 100
0 000
0 000
0 050
0 100
0.150
0 200
0 250
0 300
θ
Joint J-KT-4
Braces 3 and 4
OPB Load
β=0.90
γ=22.83
θ=48°
K joint Curve

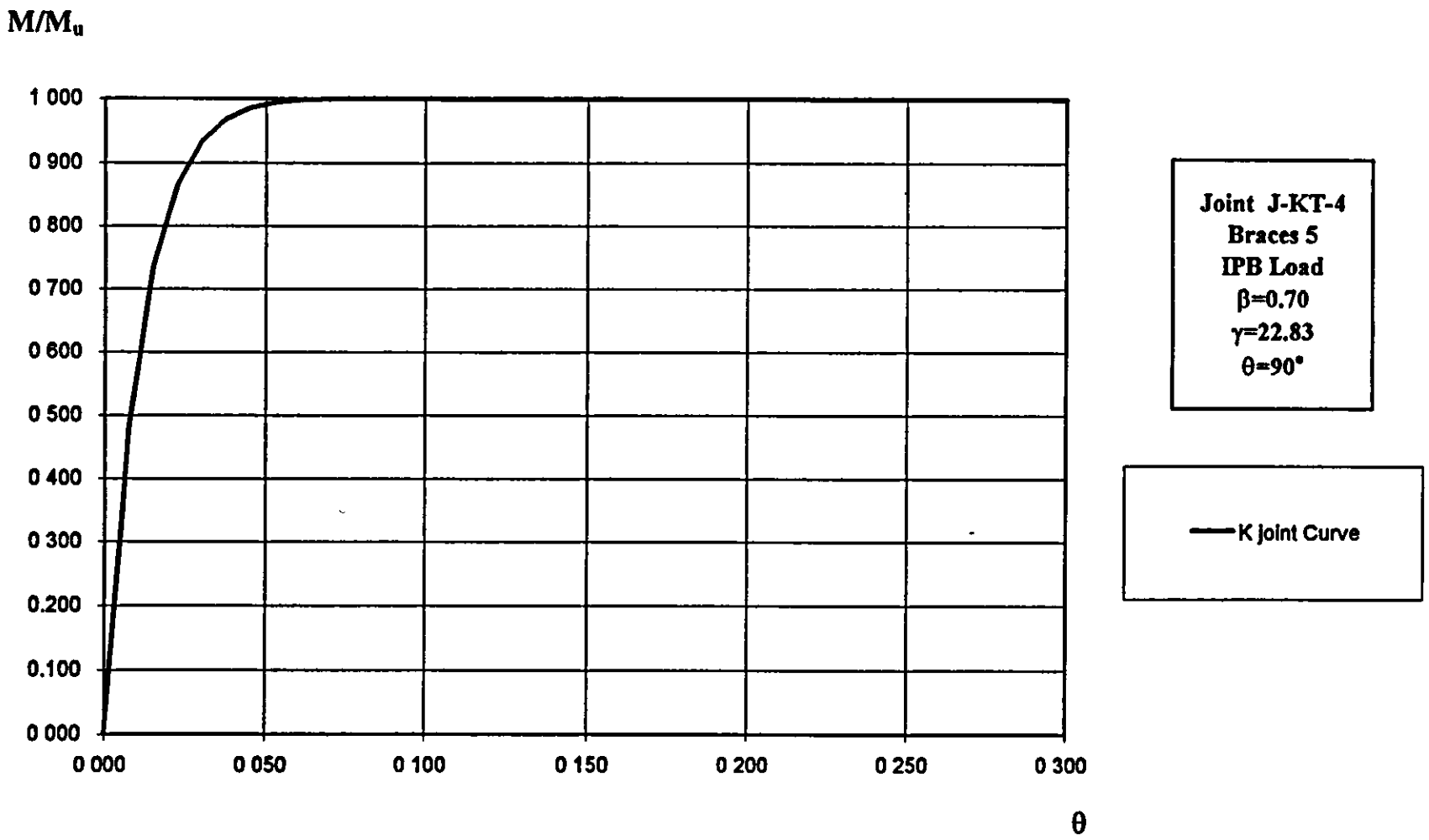
M/Mu
1 000
0 900
0 800
0 700
0 600
0 500
0 400
0 300
0.200
0.100
0 000
0 000
0 050
0 100
0 150
0 200
0 250
0 300
θ
Joint J-KT-4
Braces 5
IPB Load
β=0.70
γ=22.83
θ=90°
K joint Curve

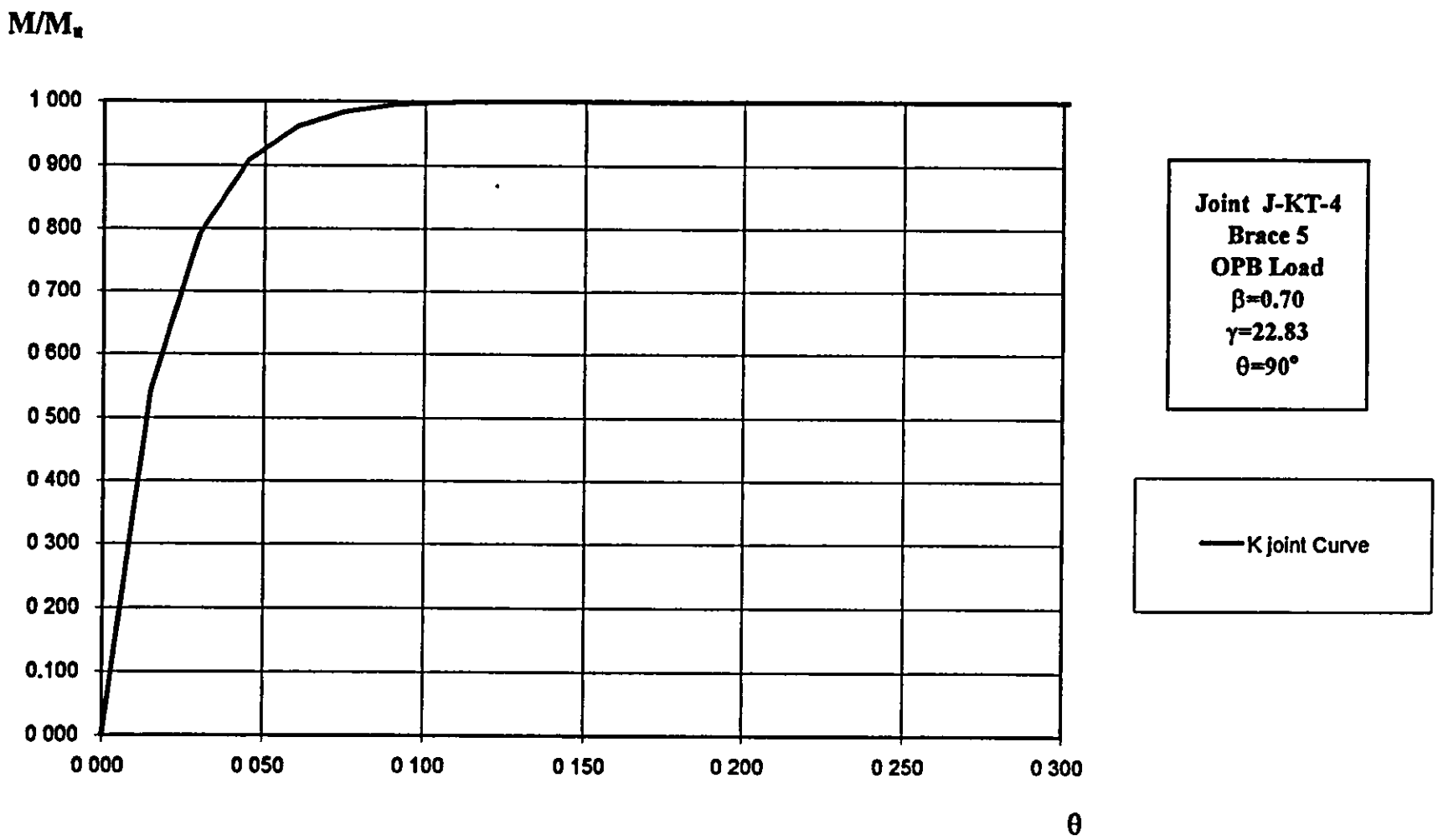
M/Mu
1 000
0 900
0 800
0 700
0 600
0 500
0 400
0 300
0 200
0.100
0 000
0 000
0 050
0 100
0 150
0 200
0 250
0 300
θ
Joint J-KT-4
Brace 5
OPB Load
β=0.70
γ=22.83
θ=90°
K joint Curve

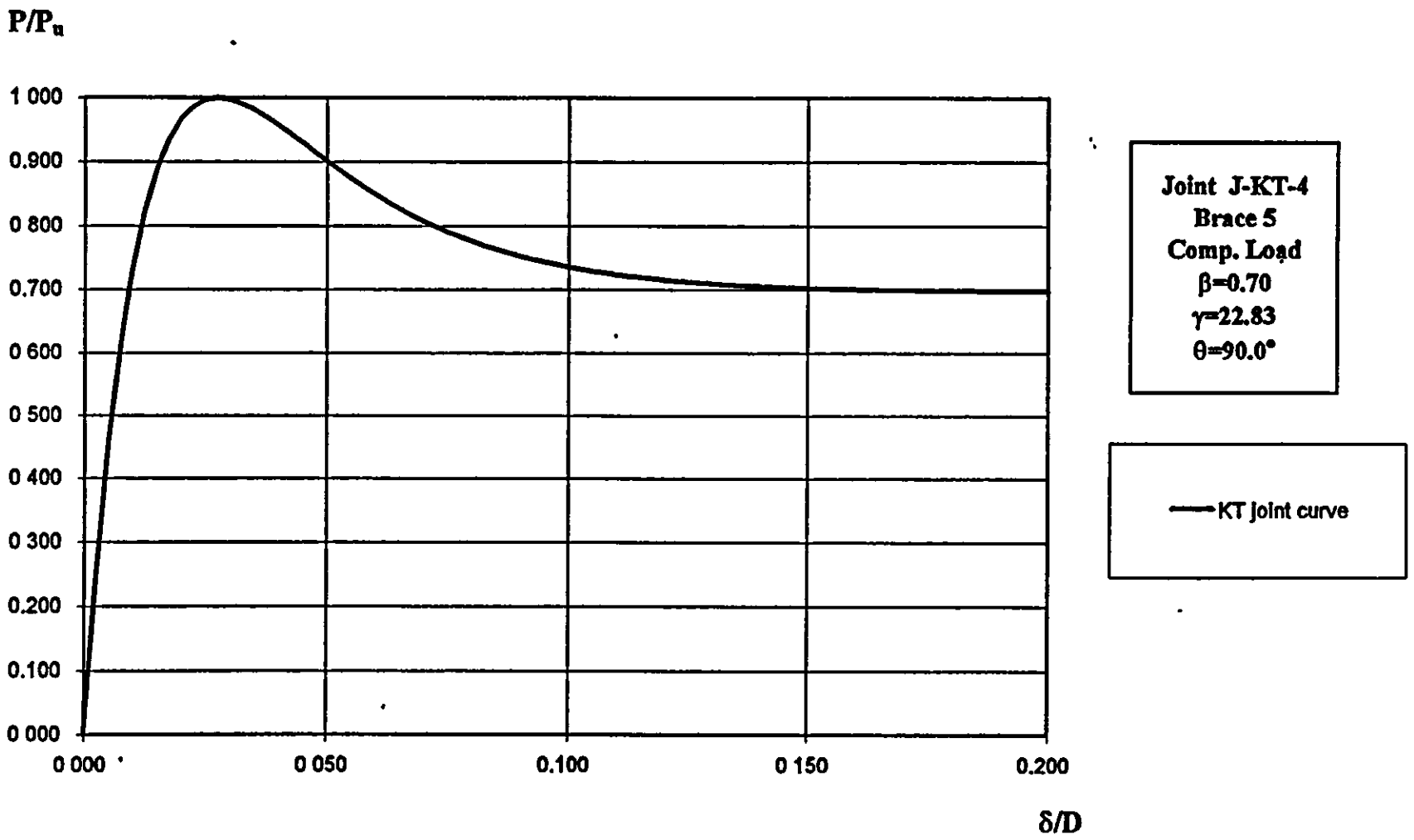
P/Pu
1 000
0.900
0 800
0.700
0 600
0 500
0 400
0 300
0.200
0.100
0 000
0 000
0 050
0.100
0 150
0.200
δ/D
Joint J-KT-4
Brace 5
Comp. Load
β=0.70
γ=22.83
θ=90.0°
KT joint curve

Appendix D
Hindcast Data

The following information is provided.

- Summary from new hindcast (from Oceanweather)
- Extraction and interpolation of hindcast data
- Comparison of Depth vs. Distance Based Interpolation

[Refer to Appendix A for platform specific seastate data]

FINAL REPORT

HINDCAST STUDY OF WIND WAVE AND CURRENT FIELDS IN HURRICANE ANDREW - GULF OF MEXICO

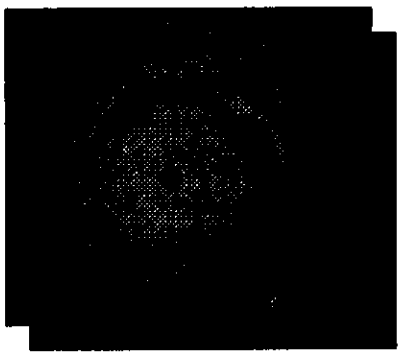

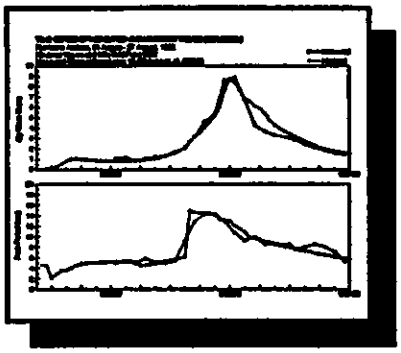

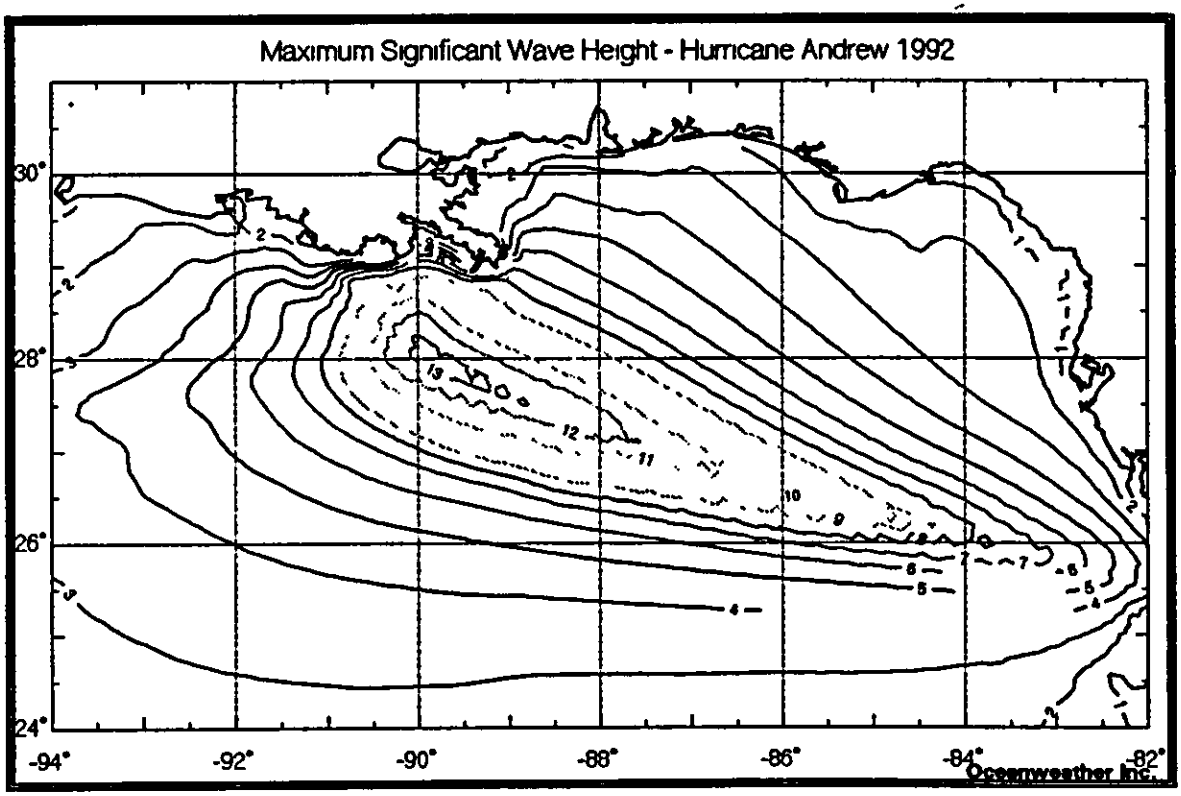

About the Cover

The upper left panel shows a GOES satellite visible image of Andrew in the Gulf of Mexico near maximum intensity (936 mb). The upper right panel shows the comparisons of hindcast (dashed) and measured (solid line) time series of significant wave height (upper graph) and spectral peak period (lower graph) at LATEX Station 16, located in 19 meters water depth at 28 degrees 52.024 minutes North latitude, 90 degrees 29.572 West longitude. The lower panel shows the envelope of maximum hindcast significant wave height (contours at 1 meter intervals). The wave hindcast was made with Oceanweather's third-generation spectral wave model.

FINAL REPORT

HINDCAST STUDY OF WIND WAVE AND CURRENT FIELDS IN HURRICANE ANDREW - GULF OF MEXICO

by

Vincent J. Cardone, Andrew T. Cox and J. A. Greenwood
Oceanweather Inc
Cos Cob, CT

Douglas J. Evans and Harriett Feldman
Evans - Hamilton Inc
Rockville, Maryland

Scott. M. Glenn
Rutgers University
New Brunswick, New Jersey

Timothy R. Keen
Naval Naval Research Laboratory
Stennis Space Center, MS

submitted to

Minerals Management Service
Department of Interior
Procurement Operations Branch, MS 2510
381 Elden Street
Herndon, VA 22070-4817
Contracting Officer: James E. MacKay

November, 1994

Abstract

The evolution of the surface wind field and ocean response in the northern Gulf of Mexico in hurricane Andrew (1992) is described through the application of advanced numerical wind, ocean surface wave and three-dimensional current hindcast models adapted to the basin at high spatial resolution (grid spacing of 10 km). The models adopted have been previously applied to model historical Gulf of Mexico hurricanes; in this study, the models were carefully validated against all available data acquired in Andrew.

The study included a substantial data assembly and processing component to ensure that all public domain measurements from government, institutional and offshore industry sources of surface wind, surface waves, storm surge and currents were identified, acquired and made available in forms most useful for model calibration and validation.

Surface wind fields were developed using an improved version of a numerical model of the vortex planetary boundary layer model. The parameters of the model relied heavily on the extensive suite of meteorological data acquired by US Air Force and NOAA reconnaissance aircraft. Surface waves were modeled using a third-generation model which included shallow water physics. Surface and sub-surface currents were modelled using a three-dimensional hydrodynamic model which resolves the vertical coordinate in 13 layers and includes prognostic equations for temperature, salinity and turbulent energy as well as surface height and velocity.

The study provides a data base not only of scientific interest, but also of use in engineering studies, such as analyses of post-mortem platform response and failure, investigations of pipeline failure modes, and assessment of various types of environmental loading on offshore structures. The modeling capability demonstrated and validated through this study establishes an analysis tool for reassessment of extreme environmental criteria especially for water depths in which alternative existing criteria may conflict (approximately the range 15-50 m).

Table of Contents

6. Summary and Conclusions

This study may be viewed within the context of a series of industry and government sponsored measurement programs conducted within the past 20 years or so in the Gulf of Mexico to study the ocean response to the passage of hurricanes, including the Ocean Data Gathering Program (ODGP) for winds and waves, the Ocean Current Measurement Program (OCMP) for continental shelf currents, the Ocean Test Structure (OTS) program for platform response, and a number of Ocean Response to a Hurricane (ORH) programs which utilized air-dropped current meters to measure mixed-layer storm driven currents. Data acquired in these programs have been used extensively to develop, refine and validate numerical models. The data acquired in the ODGP provided a basis for the development and calibration of numerical models for the accurate specification of surface wind and wave fields in historical Gulf of Mexico hurricanes (Cardone et al., 1976). The ocean current data acquired in the OCMP and ORH have used by several current modelers to adapt and calibrate current response models (e.g. Forristall et al, 1977, Keen and Slingerland, 1993a).

The models applied in this study may be considered logical evolutions and refinements of the these modeling capabilities. The surface wind field was specified with an improved version of the method and model used in the ODGP to specify surface winds. The almost continuous monitoring of Hurricane Andrew by aircraft, satellite and shore based radars allowed the specification of storm track to the maximum possible accuracy, within about +/- 10 km, or about one grid spacing of the grids used for ocean response models applied. The hindcast windfields are compared to available measurements sites, none of which experienced hurricane force winds because the eye of the storm passed more than 50 km from the closest measurement site. Based upon these data comparisons and prior validation studies carried out with the same hindcast methodology we estimate that the wind fields are specified to an accuracy within +/- 2.5 m/s in wind speed and +/-25 degrees in wind direction (rms). However, we can not state unequivocally that these errors are randomly distributed about negligible means. If they are not, then the systematic part of the error is probably distributed by storm quadrant (e.g. wind speeds slightly too high with too much inflow in one quadrant and vice versa in another). We estimate the magnitude of systematic errors to be less than half the magnitude of the errors quoted above.

The hindcast wave fields are verified against waves which in deep water were measured at sites which again were never closer than about 50 km from the storm center. The maximum waves in deep water were measured at Bullwinkle

platform, which was located 74 km southwest of the center at closest approach. The maximum measured HS at this site was 7.9 m, which may be compared to the maximum hindcast HS of 8.7 m at the model grid point closest to the platform. The peak hindcast HS was within 1 m of the peak measured HS at the other deep water sites as well. At the shallow water site, LATEX station 16, the most recent analysis of the measured data yields a peak HS of 8.9 m in 20 m water depth, compared to the hindcast peak of 8.7 m. This excellent agreement, however, must be conditioned on the continuing investigation of the validity of the measurements at this site after the instrument mount overturned just before peak conditions were experienced.

The maximum hindcast HS in deep water of 13.5 m ranks Hurricane Andrew very highly in terms of wave generation. If we use the ODGP suite of historical hindcasts as a reference (Ward et al., 1979) the maximum deep water hindcast HS in Andrew at the shelf break south of the Mississippi Delta of 13.5 m (44.3 ft) was exceeded in only 6 storms this century anywhere in the Gulf. This ranking is consistent with the basic meteorological characteristics of Andrew in the Gulf. Only four hurricanes this century attained central pressure of lower than 936 mb in the Gulf. In the absence of any compelling evidence to the contrary we estimate that the hindcast of peak HS and associated TP has achieved an accuracy consistent with a scatter index of about 10%.

The hydrodynamic modeling of Andrew was most successful at simulating the spatial distribution and magnitude of the primary forced ocean response at intermediate water depths. Runs completed to date appear to slightly underpredict peak currents in very deep water and to slightly overpredict peak current speeds in very shallow water. These "asymptotic" response regimes are often modeled fairly accurately with simpler mixed-layer (deep water) and barotropic vertically integrated formulations (shallow water), but such models can not provide a complete three-dimensional picture of the ocean current response on the whole of the continental shelf. It is expected that with some further refinement and tuning of the vertical mixing parameterization of the model and inclusion of wave enhanced bottom stresses, better absolute agreement between the modeled and measured peak currents may be achieved. Additional improvement in the overall time history of agreement would appear to benefit from a more complete specification of the initial current and density distributions throughout the model domain than was possible in this study.

EXTRACTION AND INTERPOLATION OF DATA FROM FILES

Grid Point Data

The data came on a CDROM from Oceanweather, Inc., in two sets. The first set was from a wave hindcast model. The second was from a current model. In each case each file contained all the data for a given time, the time being included in the name of the file. Each line of these files gives data at a particular grid point.

In addition, for each data set there was a file giving the peak values of all variables.

The wave hindcast file data was for every hour, with 63 hours included. The data included:

WINDD	Wind direction, degrees from which, clockwise from north.
WINDS	Wind speed, m/sec
TPTOT	Peak spectral period, sec
HS	Significant wave height, m
DIRDOM	Dominant wave direction, degrees to which, clockwise from north

The current hindcast file was for every half hour, covering the same period. The data consisted of:

U	Surface current velocity, positive to east, cm/sec
V	Surface current velocity, positive to north, cm/sec
SURGE	Surface elevation above still water level, cm

Surge

Vince Cardone of Oceanweather, Inc. advised PMB that the surge in this hindcast did not include barometric pressure effects. Because of this, the surge from the new (1994) hindcast was ignored, and surge from the 1992 hindcast was used.

Interpolation of Wave Data

The data was given at grid points spaced approximately 6 miles apart. Data at platform coordinates was estimated from grid points data by interpolation. There is typically considerable difference between values of the significant wave height, H_s, at adjacent grid points, frequently rather more than 10 percent. The following shows the maximum H_s at the four grid points surrounding each platform. (The maxima shown in this table for a given platform occur, in general, at different times, but in the processing described below, the values at a given time are extracted from the grid values.)

Platform	Maximum Hs at Surrounding Grid Points (m)				Max Diff, as % of smaller
SS139 (T25)	7.67	8.68	7.70	8 48	11
ST72 (T21)	8.68	9.42	8.48	8.60	11
ST177B	10.90	11.39	10.21	11.10	11
ST151H	11.10	11.52	10.44	10.60	10
ST151K	11.10	11.52	10.44	10.60	10
ST130Q	10.60	11.11	8.94	9.40	24
ST130A	10.60	11.11	8.94	9.40	24
ST151J	11.10	11.52	10.44	10 60	10
SS209A	7.87	8.55	7.61	8.03	12
SS135#10	6.01	6.59	4.92	6.15	34
SP10#18	7.70	8.48	6.12	6.67	39
SP9#9	7.70	8.48	6 12	6.67	39
WD103A	9.28	9.04	8.24	7.64	21

It is seen that Hs at surrounding grid points for most platforms vary significantly, frequently by more than 20 percent. Since wave forces vary as at least the second power of the wave heights, care must be taken in the interpolation of grid point data.

Two possible general ways of interpolating data are:

(1) With respect to location, requiring two-dimensional interpolation

(2) With respect to depth, requiring only one-dimensional interpolation.

If the seafloor varied smoothly between grid points, there would be no difference in these two methodologies. In fact, more often than not the platform depths (supplied by the operators) are not closely the same as the depths that would be found by interpolating from surrounding grid point depths (which were obtained from ocean charts). Some of the discrepancies may be from measurements, some may be from the unevenness of the seafloor. The following table shows the depth at the platform and at the surrounding four grid points

Platform	Depth at Surrounding Grid Points (m)				Depth at Platform (m)
SS139 (T25)	17.4	17.7	12.1	15.8	19.8
ST72 (T21)	17.7	17.4	15.3	17.8	19.5
ST177B	45.2	49.6	36.4	42.7	43.9
ST151H	42.7	50.6	27.9	39.9	42.4
ST151K	42.7	50.6	27.9	39.9	42.4
ST130Q	39.9	97.7	30.7	40.8	52.4
ST130A	39.9	97.7	30.7	40.8	43.3
ST151J	42.7	50 6	27.9	39.9	43.3
SS209A	37.5	88.9	27.1	25.0	29.7
SS135#10	12.0	15.4	7.8	10 3	16 8
SP10#18	12.1	15.8	8.2	8.8	11.6
SP9#9	12.1	15.8	8.2	8.8	11.6
WD103A	59.5	69.8	50.4	53.2	68.0

It is seen that in many cases the depth at platform is considerably more than the deepest of the surrounding grid points. Further, although not shown in this table, frequently the grid point with the nearest depth, is not the grid point nearest the platform.

In shallow water, the wave heights will vary with depth, even if there would otherwise be no spatial variations Similarly, close to the track of the hurricane, even with no differences in depth, the wave heights will vary from place to place at any time. In general, both effects are present, and it causes considerable difficulty in defining an interpolation procedure. Dr. Vince Cardone of Oceanweather, Inc. and Dr. Chuck Petrauskas of Chevron were consulted to discuss the preferred interpolation procedure.

Interpolation by location gives a unique result (if linear variation in longitude and latitude is assumed). Interpolation by depth does not, and there may be considerable subjectivism in using this procedure. There are many ways of drawing lines through the grid point data.

However, examination of the significant wave height maxima over a 3x3 set of grid points generally shows variations of H_s with both depth and position, as would of course be expected in a realistic hindcast model. A joint depth- and position-related interpolation would be needed to do an adequate job. This was particularly difficult in the situations where the depth of the platform was considerably more than the depth at the surrounding grid points.

The 16 grid points around each platform were laid out, with the depth and H_s shown at each grid point. The rate at which the significant wave heights and water depths varied between grid points was examined. For all platforms it appeared that depth at the surrounding grid points was not the principal parameter affecting H_s, due, presumably, to the closeness of the storm track and the resulting rapid variation of H_s with location. In the end, position-related interpolation was used, sometimes using the four surrounding grid points, and sometimes using only two or three.

Attached are figures showing the time history of significant wave heights for seven platforms, using four point location-interpolation, and a depth-interpolation procedure. It is apparent that for some platforms there is a significant difference in the wave heights based on these two procedures.

Interpolation of Current Data

Since current data was considered to vary more with location than depth, interpolation was based on the position of the platform within the four surrounding grid points, using linear interpolation in longitude and latitude (which is equivalent to assuming the data forms a hyperbolic paraboloid between the grid lines.)

Final Output

After extracting the data from the hindcast files, it was processed to produce the following items:

HS	Significant wave height, ft
HMAX	Maximum wave height, ft
TZ	Mean zero-crossing period, sec
DIRDOM	Dominant wave direction (degrees to which, clockwise from north)
CSPEED	Current speed, ft/sec
CDIR	Current direction (degrees to which, clockwise from north)
VCRES	Current speed resolved in direction DIRDOM, ft/sec
SURGE	Surge, ft. (as mentioned above, these values were not used in the project)
WINDD	Wind direction (degrees to which, clockwise from north)
WINDS	Wind speed, ft/sec

Maximum Wave Height, H_{max}

The maximum wave height, H_{max}, was determined by Oceanweather, Inc. from the significant wave height, H_s, by assuming the Forristal distribution of wave heights, and integrating over the hour to obtain a uniform probability of occurrence of this maximum wave in this hour. The multiplier from H_s to H_{max} was thus dependent on the wave period history over the hour. In the file of maximum values provided by Oceanweather, Inc., the ratio H_{max}/H_s varied from about 1.65 to 1.74 for the grid points surrounding the platforms considered. While not causing as large a variation as that arising from interpolation of the more fundamental hindcast data, the interpolation of the wave height factor H_{max}/H_s from the values at the surrounding grid points will affect the final H_{max} value at the platform.

The same weights at the four surrounding grid points were chosen as were used for extracting the fundamental hindcast data.

This factor will not influence the probability of failure computation, because the H_s values and their distributions are used in the failure probability analysis. Its correctness is of importance for comparison of the mean maximum expected load level with the platform mean capacity.

Mean Zero-crossing Period T_z

This was computed from the peak period, T_p, from the relation:

$$T_z = 0.74 \times T_p$$

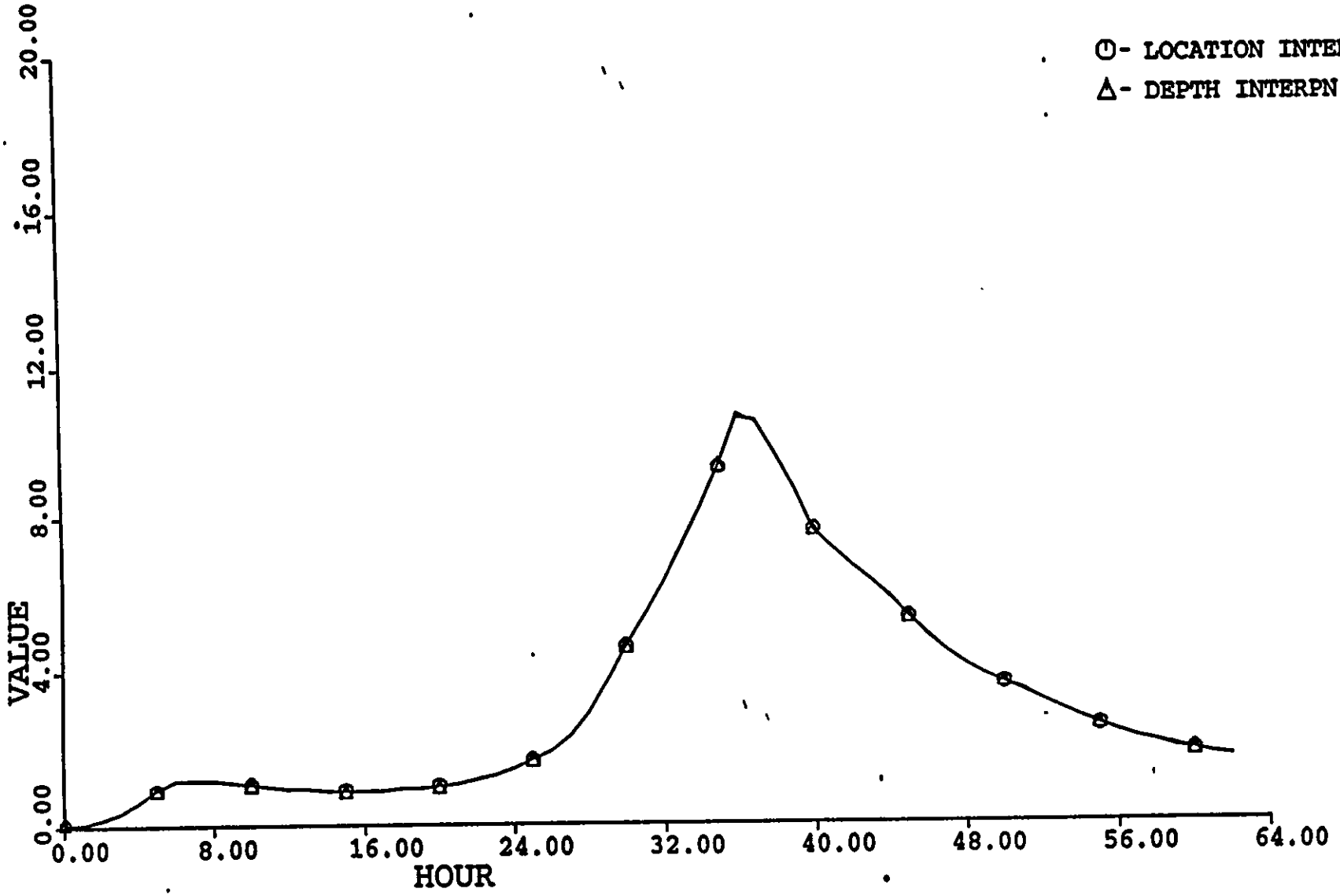
⊙- LOCATION INTERPN.
Δ- DEPTH INTERPN.
VALUE
0.00
4.00
8.00
12.00
16.00
20.00
0.00
8.00
16.00
24.00
32.00
40.00
48.00
56.00
64.00
HOUR

ST151K Hs

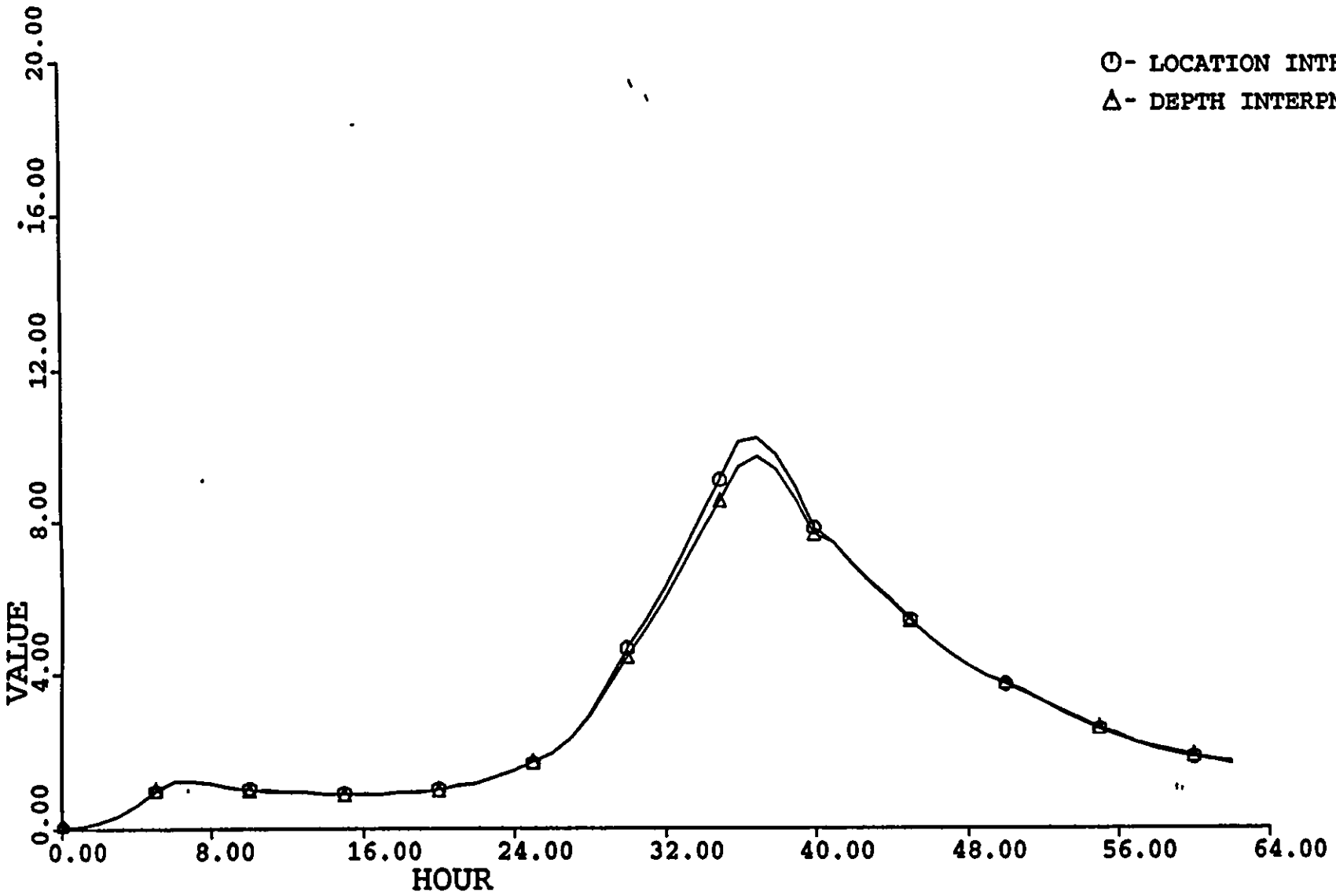
O- LOCATION INTERPN.
Δ- DEPTH INTERPN.
VALUE
0.00
4.00
8.00
12.00
16.00
20.00
0.00
8.00
16.00
24.00
32.00
40.00
48.00
56.00
64.00
HOUR

ST130Q Hs

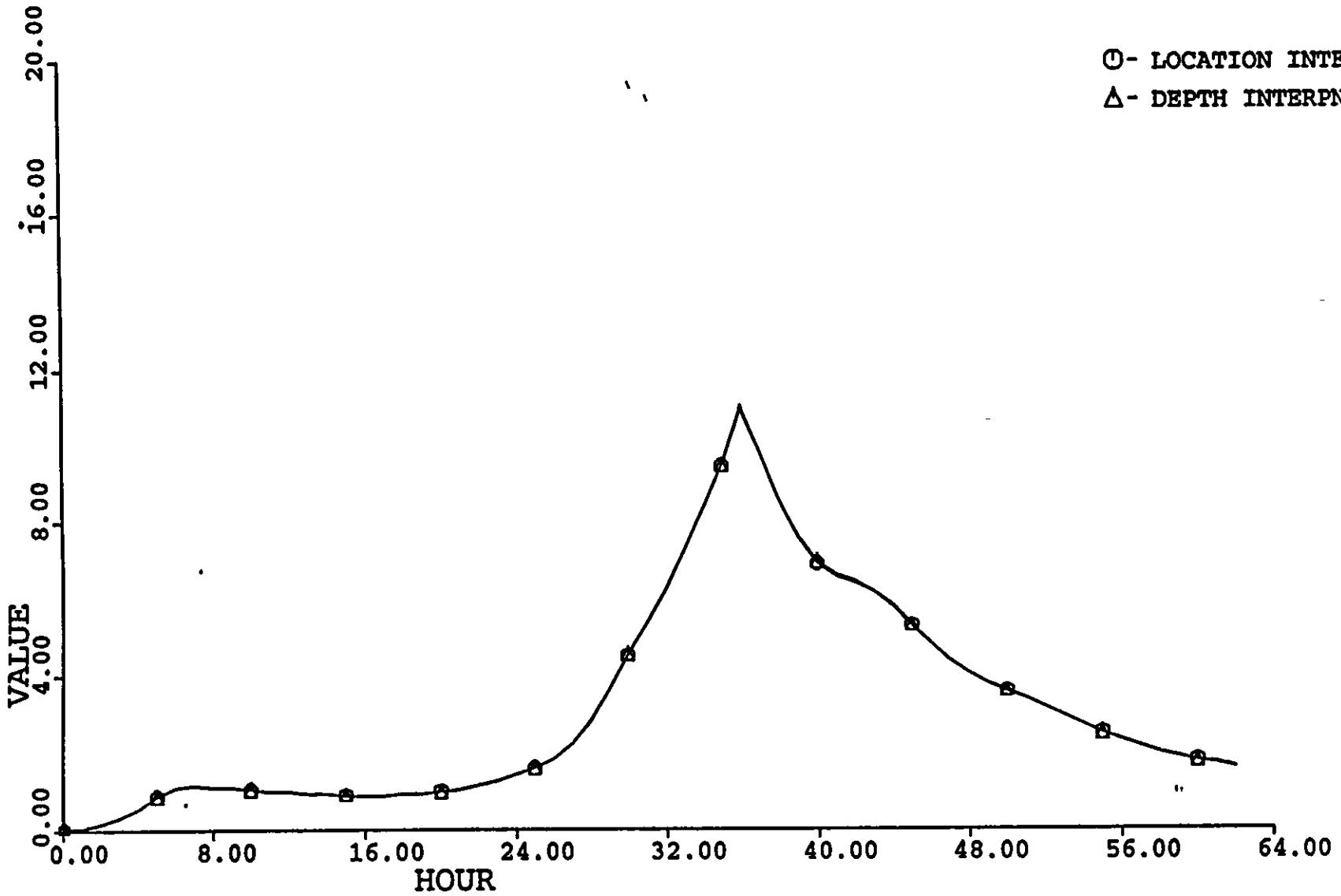
⊙- LOCATION INTERPN.
△- DEPTH INTERPN.
VALUE
0.00
4.00
8.00
12.00
16.00
20.00
0.00
8.00
16.00
24.00
32.00
40.00
48.00
56.00
64.00
HOUR

ST177B Hs

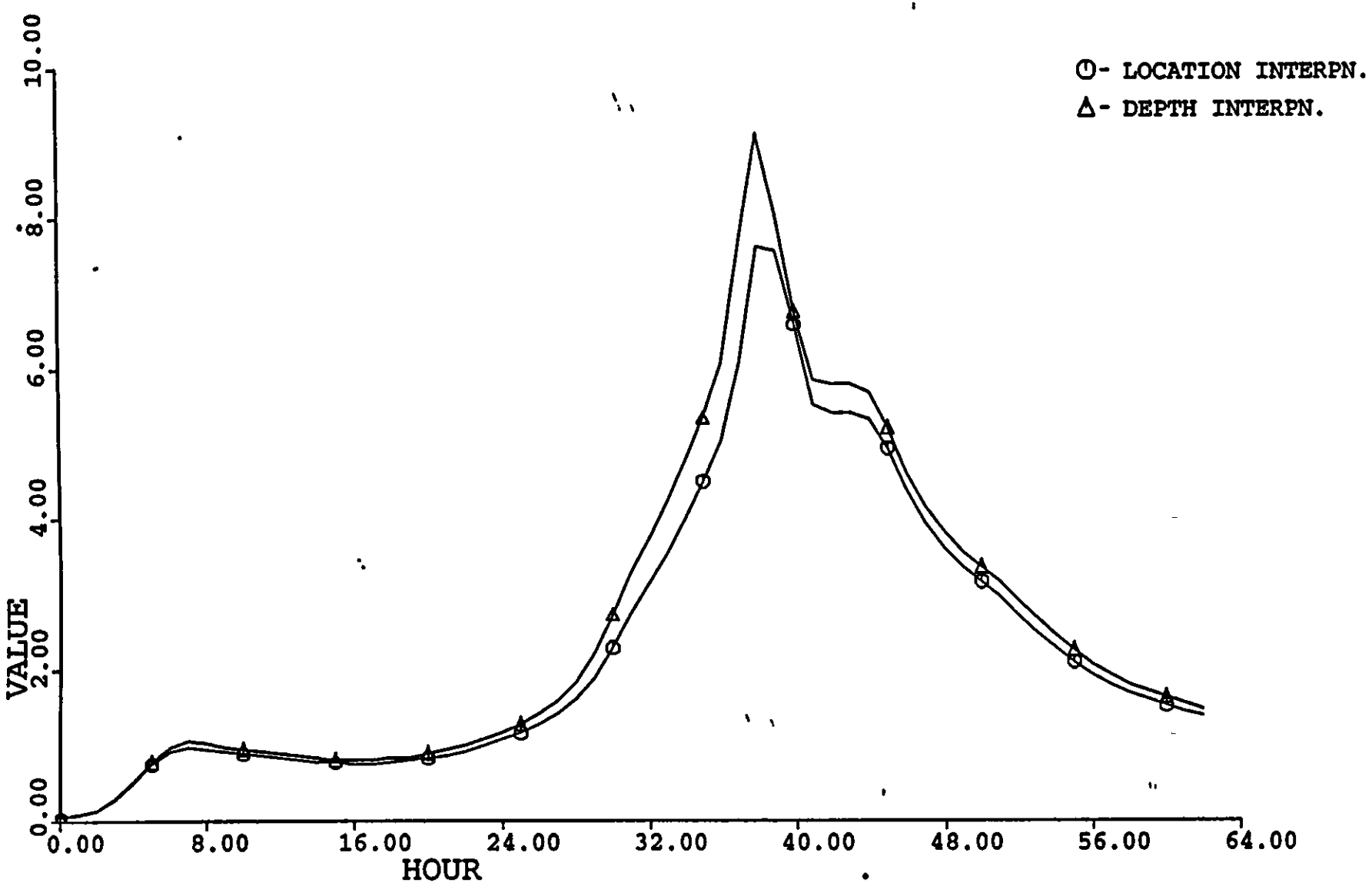
O- LOCATION INTERPN.
Δ- DEPTH INTERPN.
VALUE
HOUR
0.00
2.00
4.00
6.00
8.00
10.00
0.00
8.00
16.00
24.00
32.00
40.00
48.00
56.00
64.00

T25 Hs

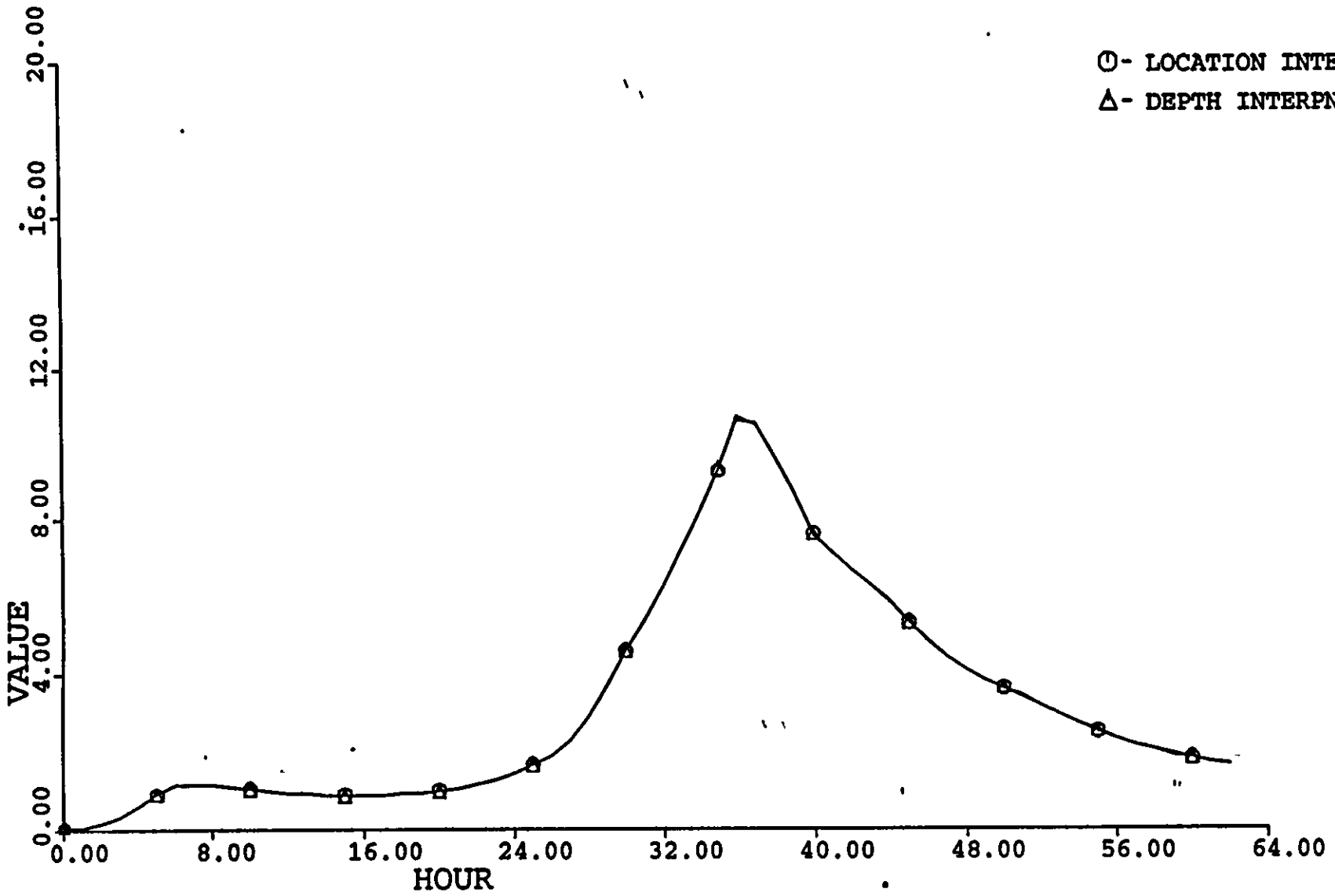
⊙- LOCATION INTERPN.
Δ- DEPTH INTERPN.
VALUE
0.00
4.00
8.00
12.00
16.00
20.00
0.00
8.00
16.00
24.00
32.00
40.00
48.00
56.00
64.00
HOUR

ST151H Hs

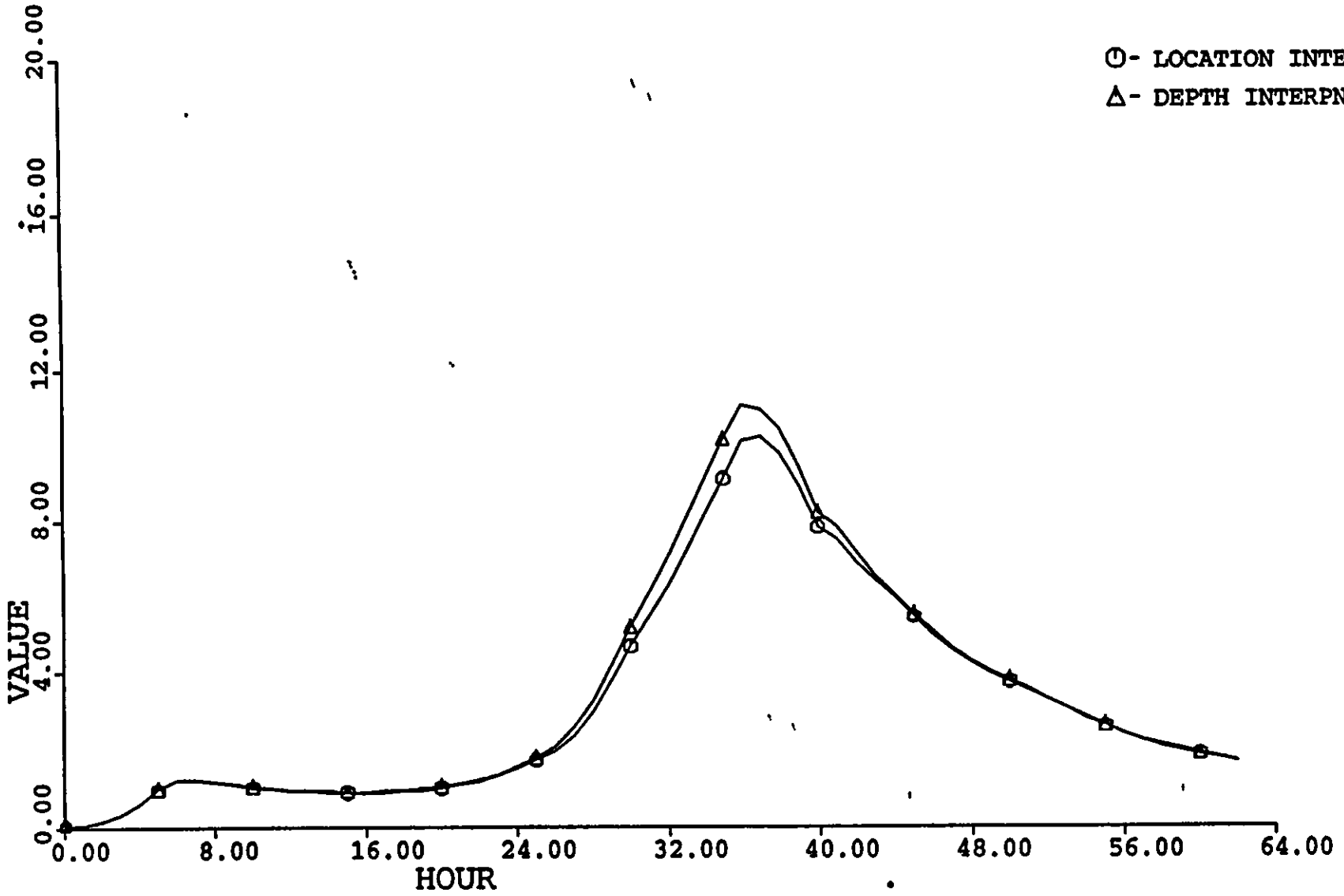
O- LOCATION INTERPN.
Δ- DEPTH INTERPN.
VALUE
0.00
4.00
8.00
12.00
16.00
20.00
0.00
8.00
16.00
24.00
32.00
40.00
48.00
56.00
64.00
HOUR

ST130A Hs

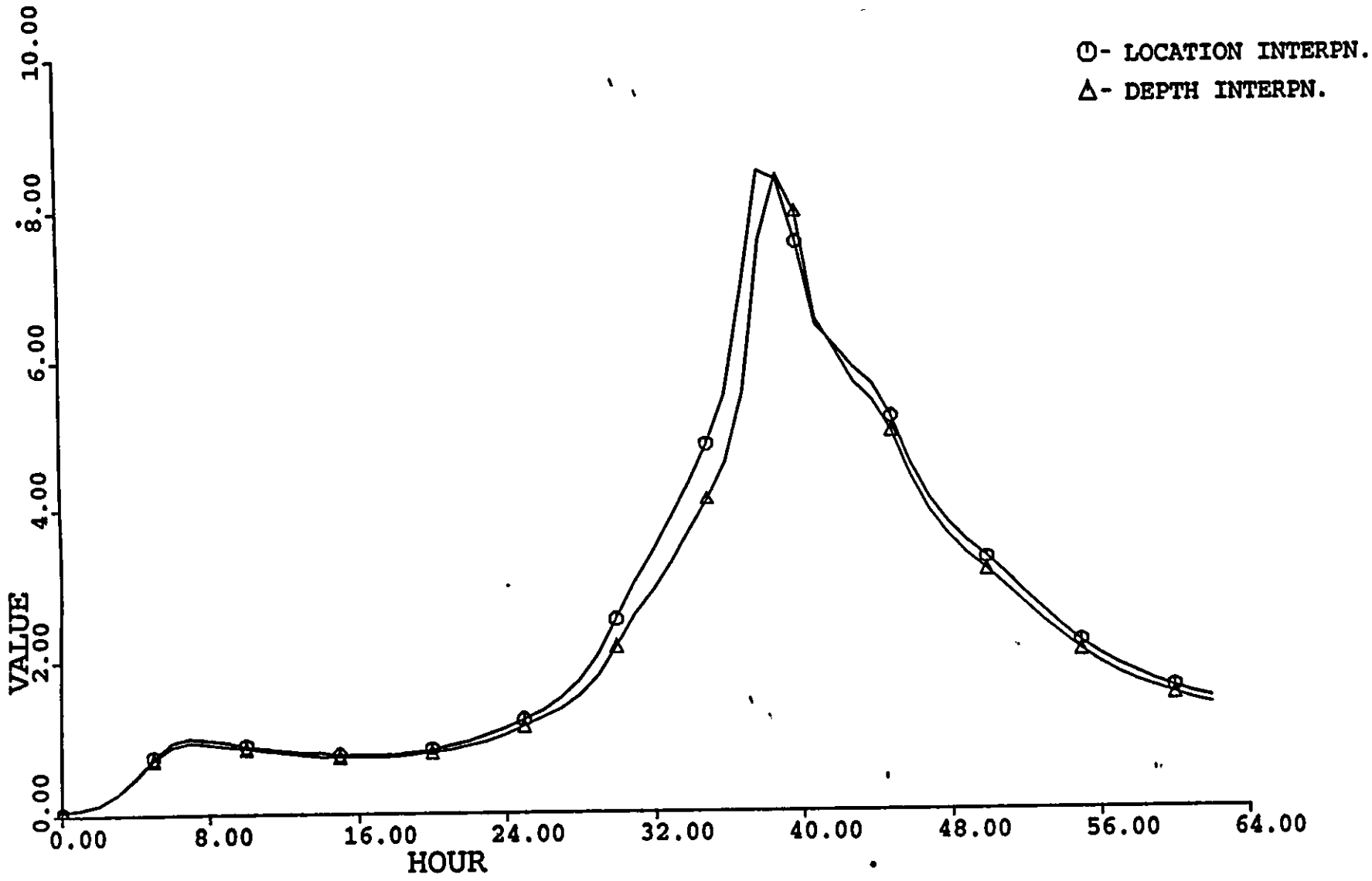
O- LOCATION INTERPN.
Δ- DEPTH INTERPN.
VALUE
0.00
2.00
4.00
6.00
8.00
10.00
0.00
8.00
16.00
24.00
32.00
40.00
48.00
56.00
64.00
HOUR

T21 Hs

Appendix E
Additional Calibration Results

The following calibration results are provided:

- Joint and Marginal Likelihood Functions for Individual Platforms
- Joint and Marginal Posterior Distributions of Bias Factors for
  - Platform ST151K
  - Platform ST151J
  - Platform ST130A

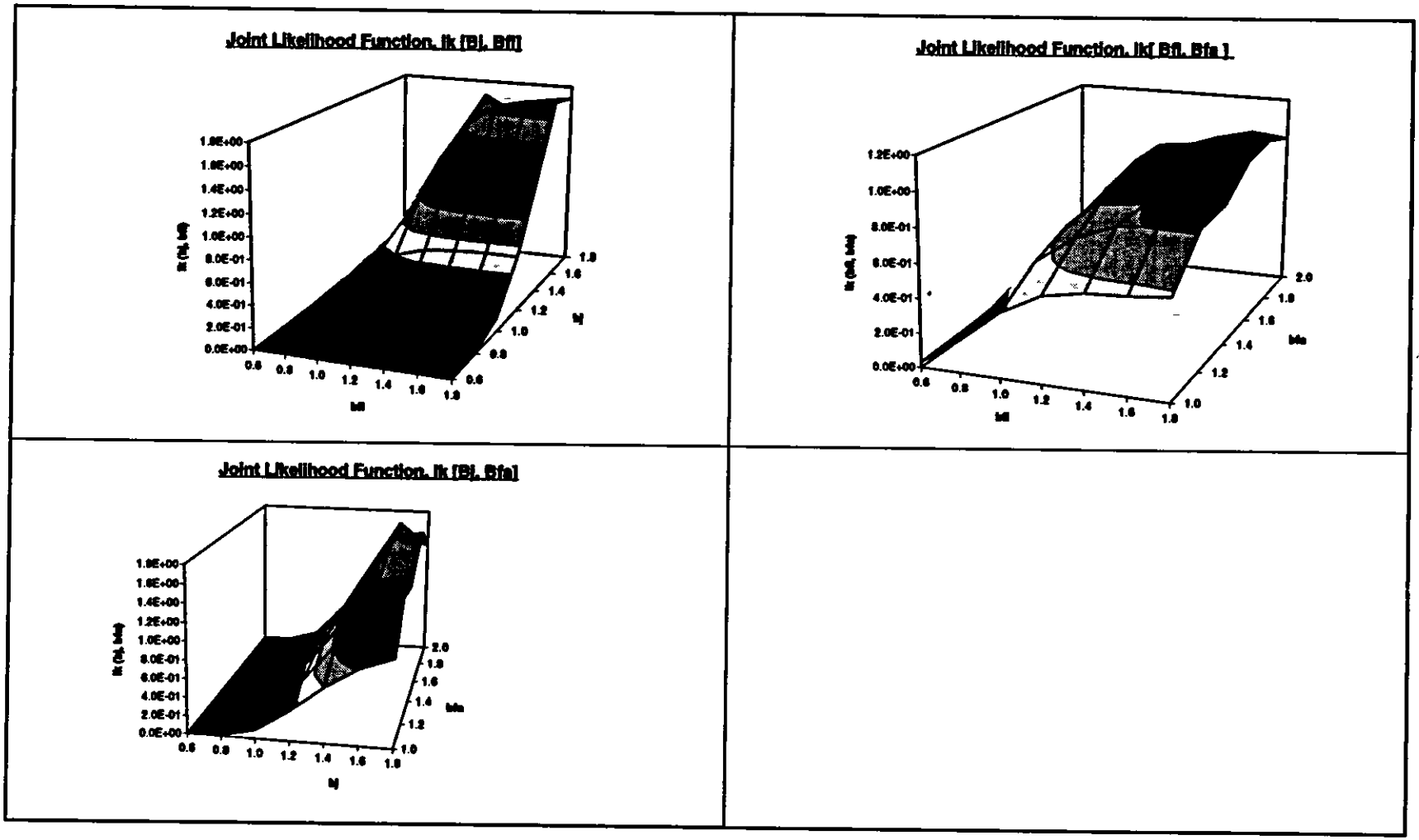

Figure E-1(a): Joint Likelihood Functions — Survival Platform ST151K

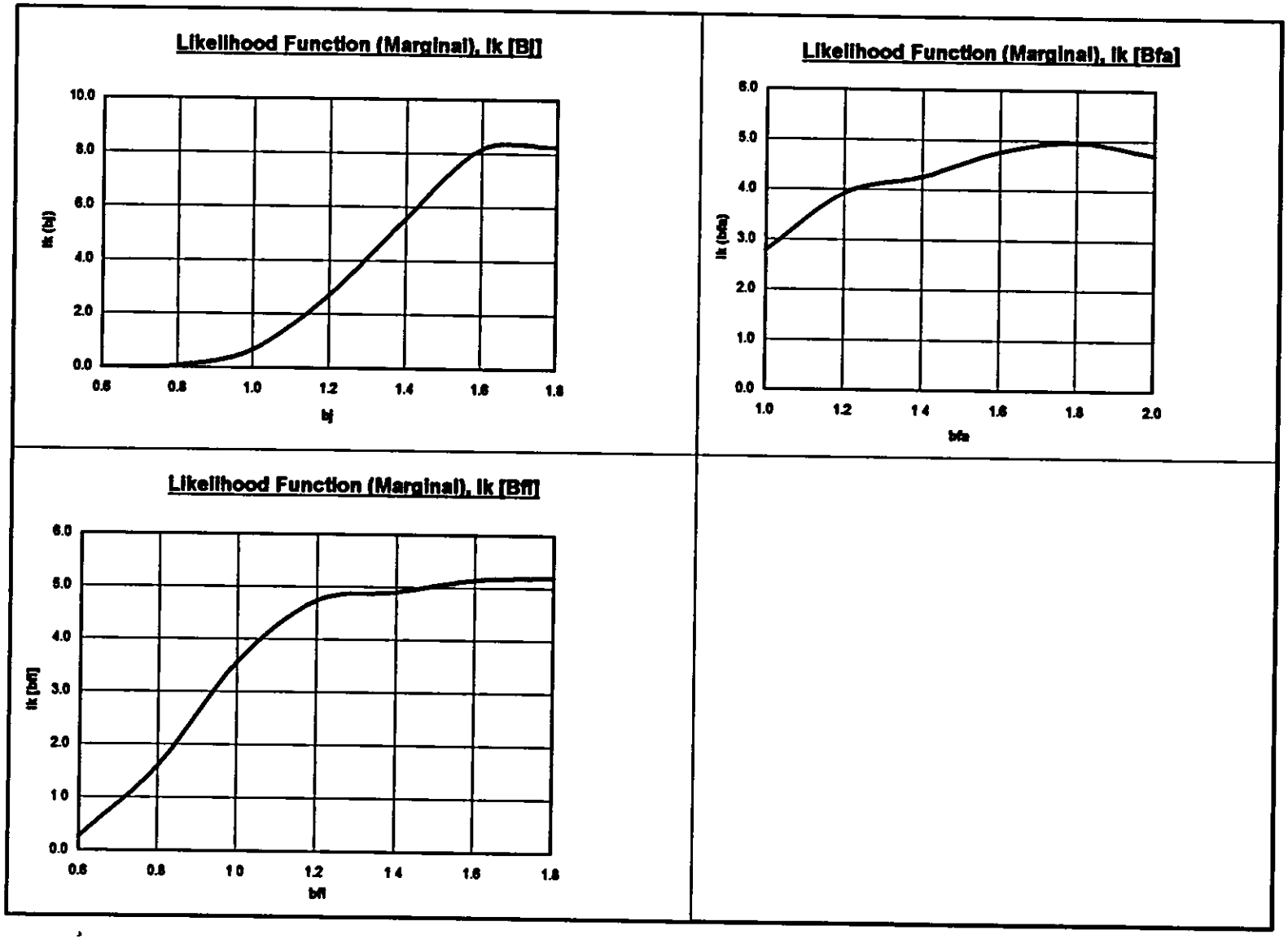

Figure E-1(b): Marginal Likelihood Functions — Survival Platform ST151K

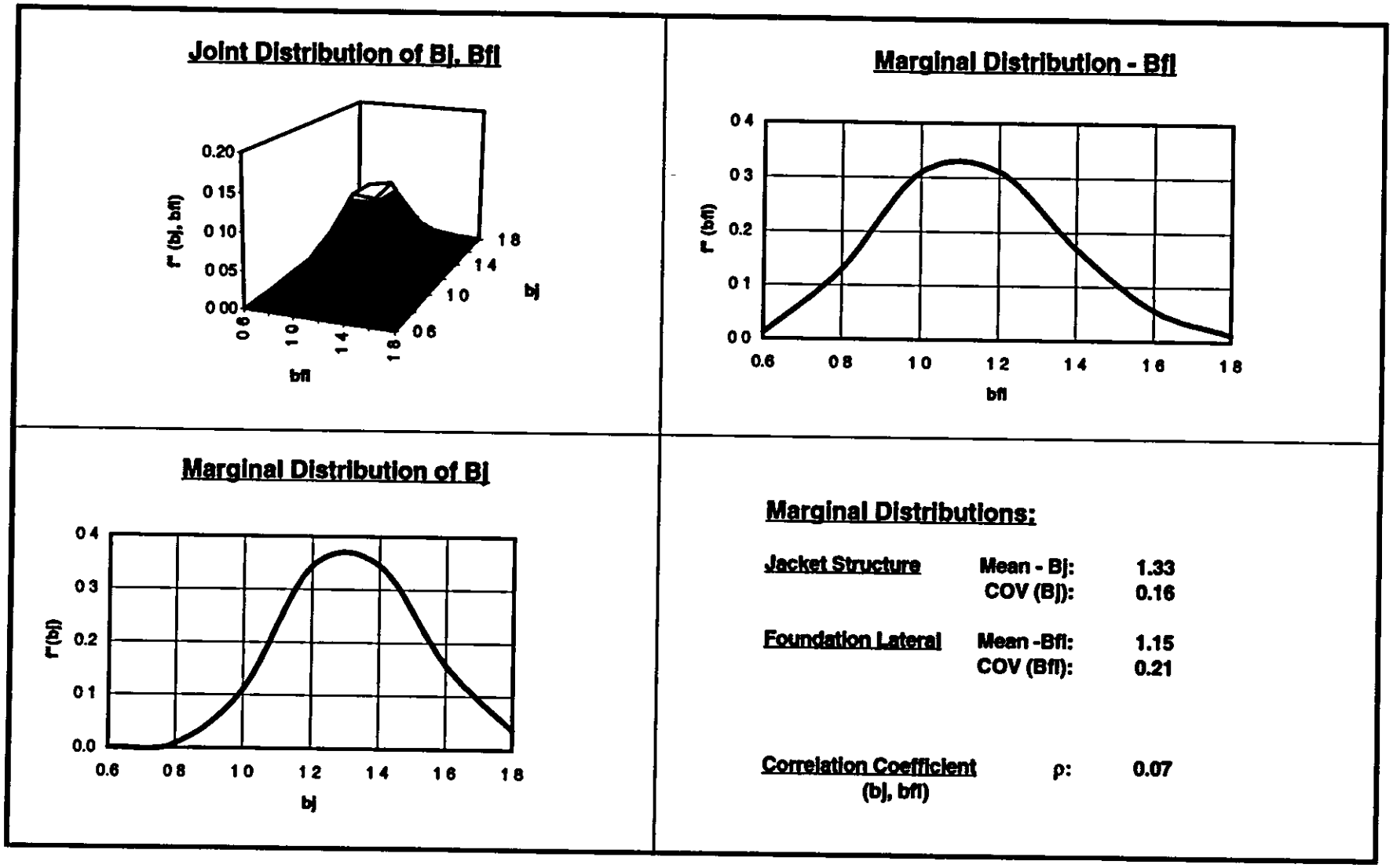

Figure E-2 (a): Posterior Distributions of Bias Factors (B_j, B_n) — Survival Platform ST151K

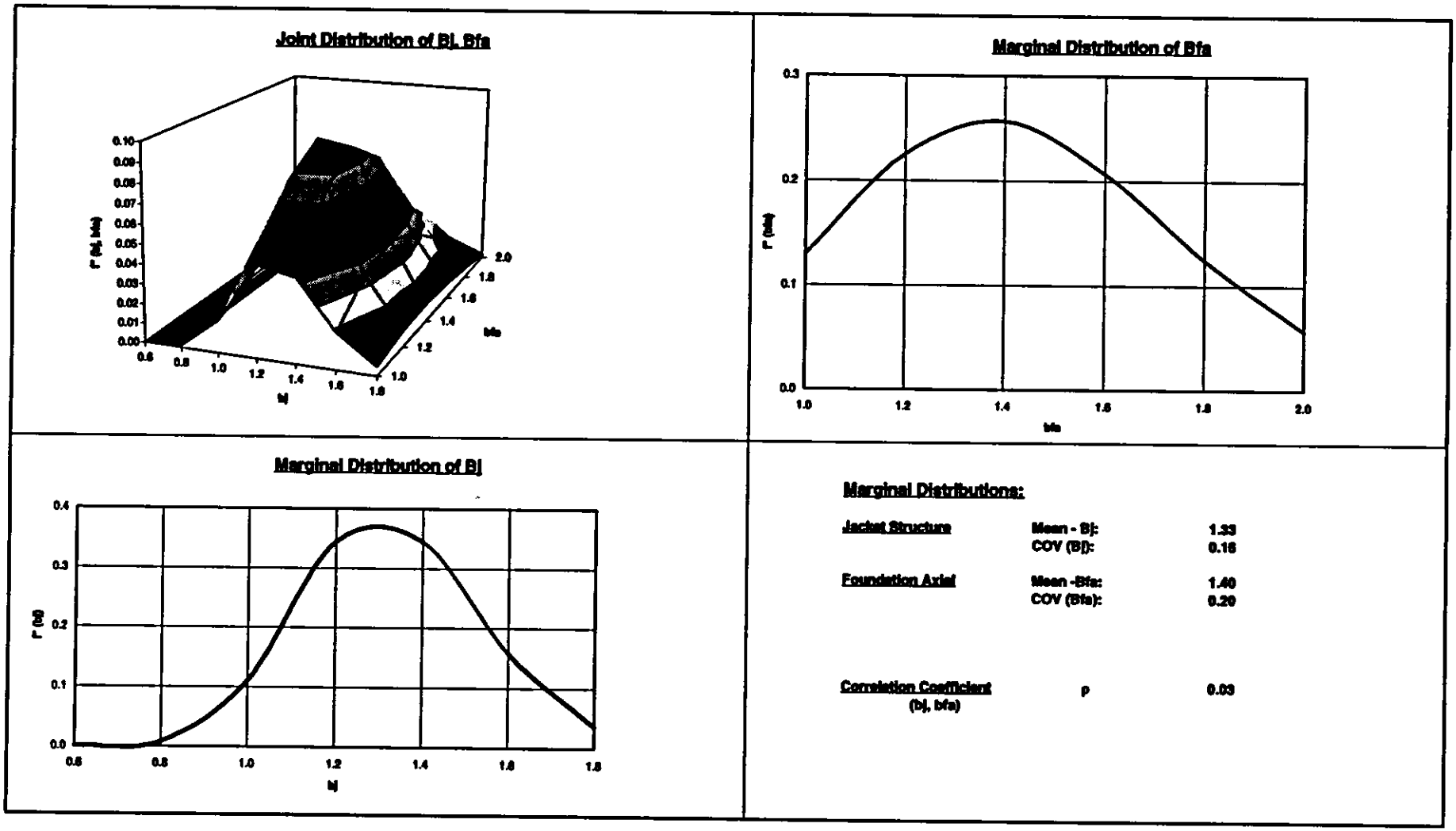

Figure E-2(b): Posterior Distributions of Bias Factors (B_j, B_{fa}) — Survival Platform ST151K

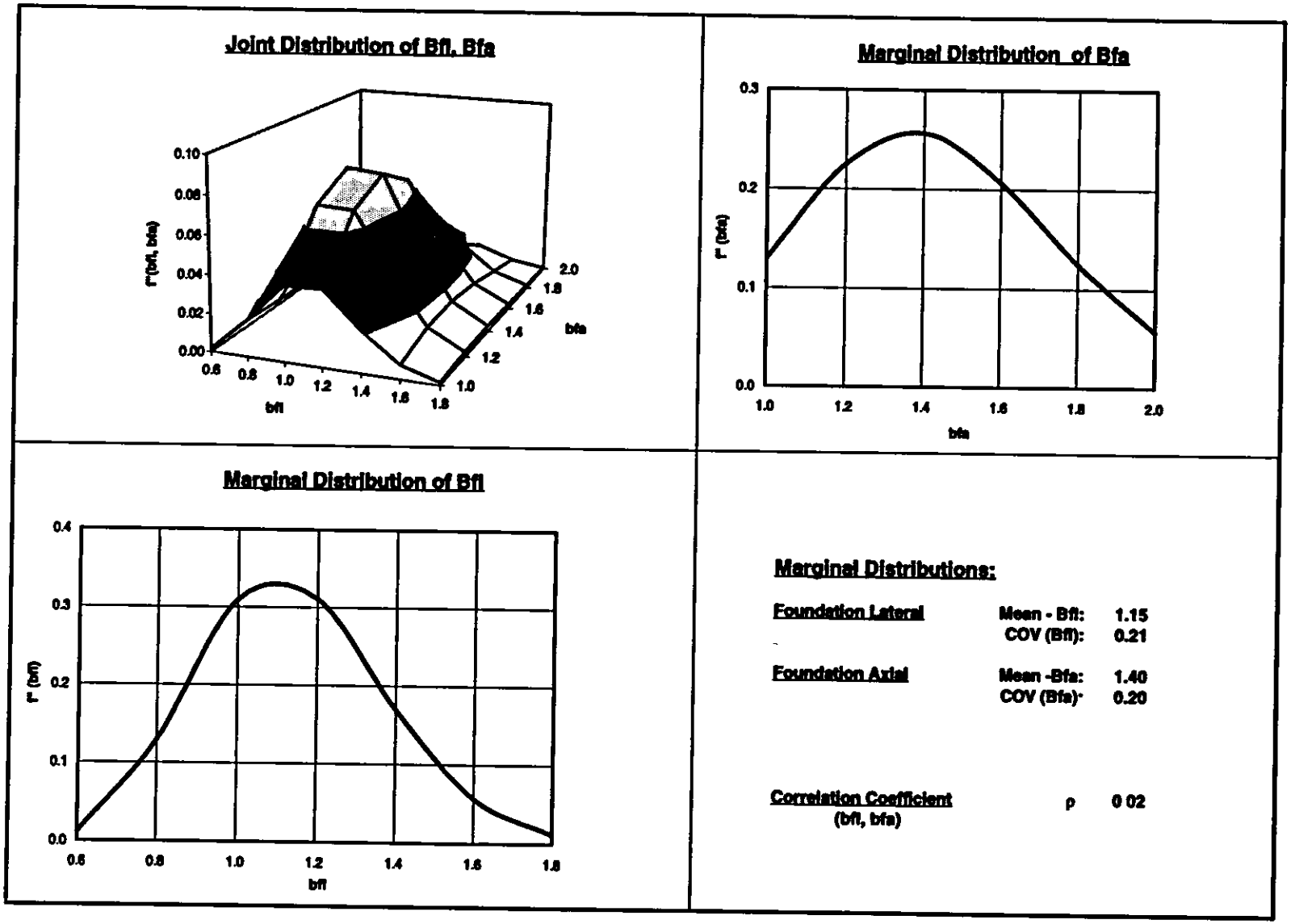

Figure E-2(c): Posterior Distributions of Bias Factors (B_{fl}, B_{fa}) — Survival Platform ST151K

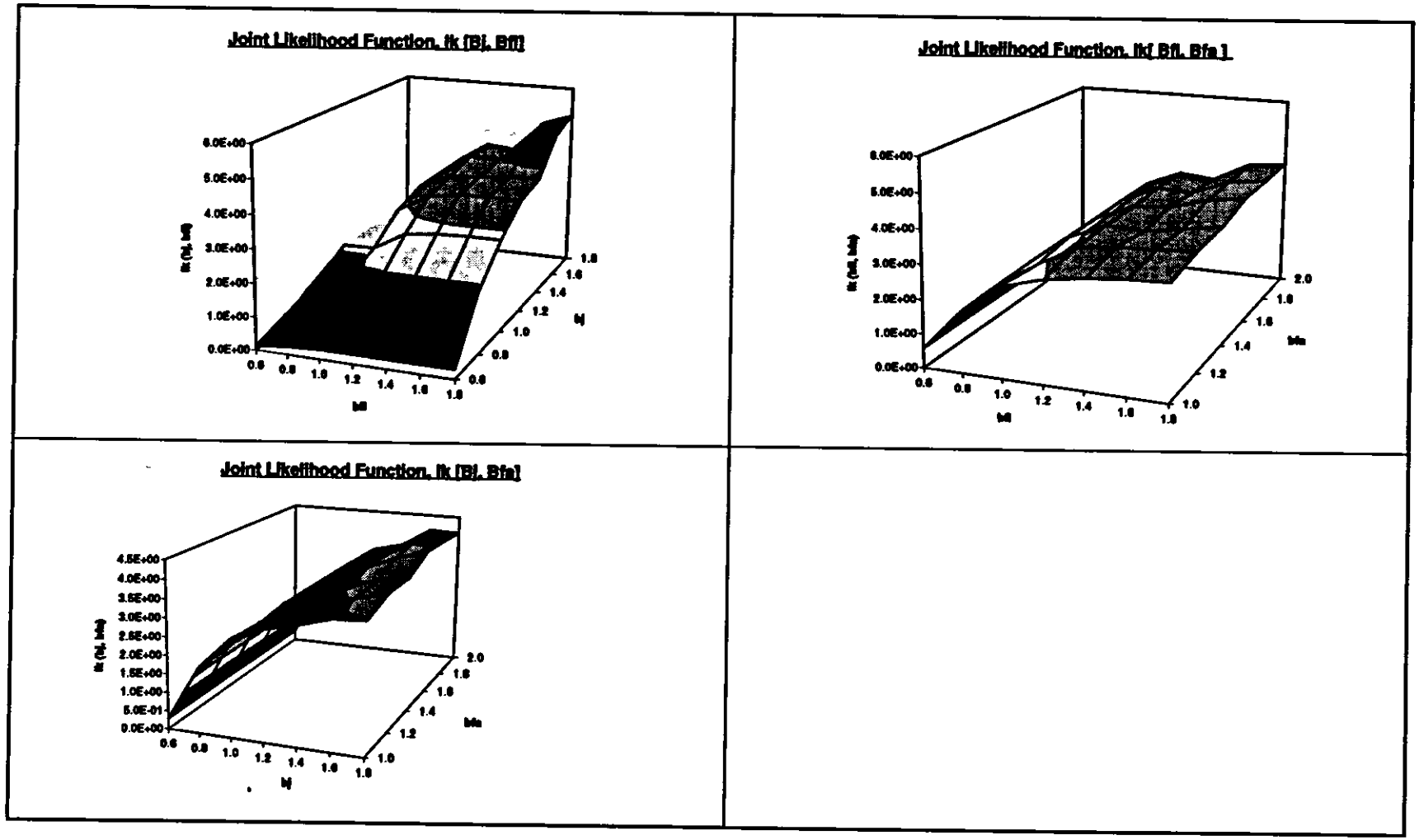

Figure E-3(a): Joint Likelihood Functions — Survival Platform ST130Q

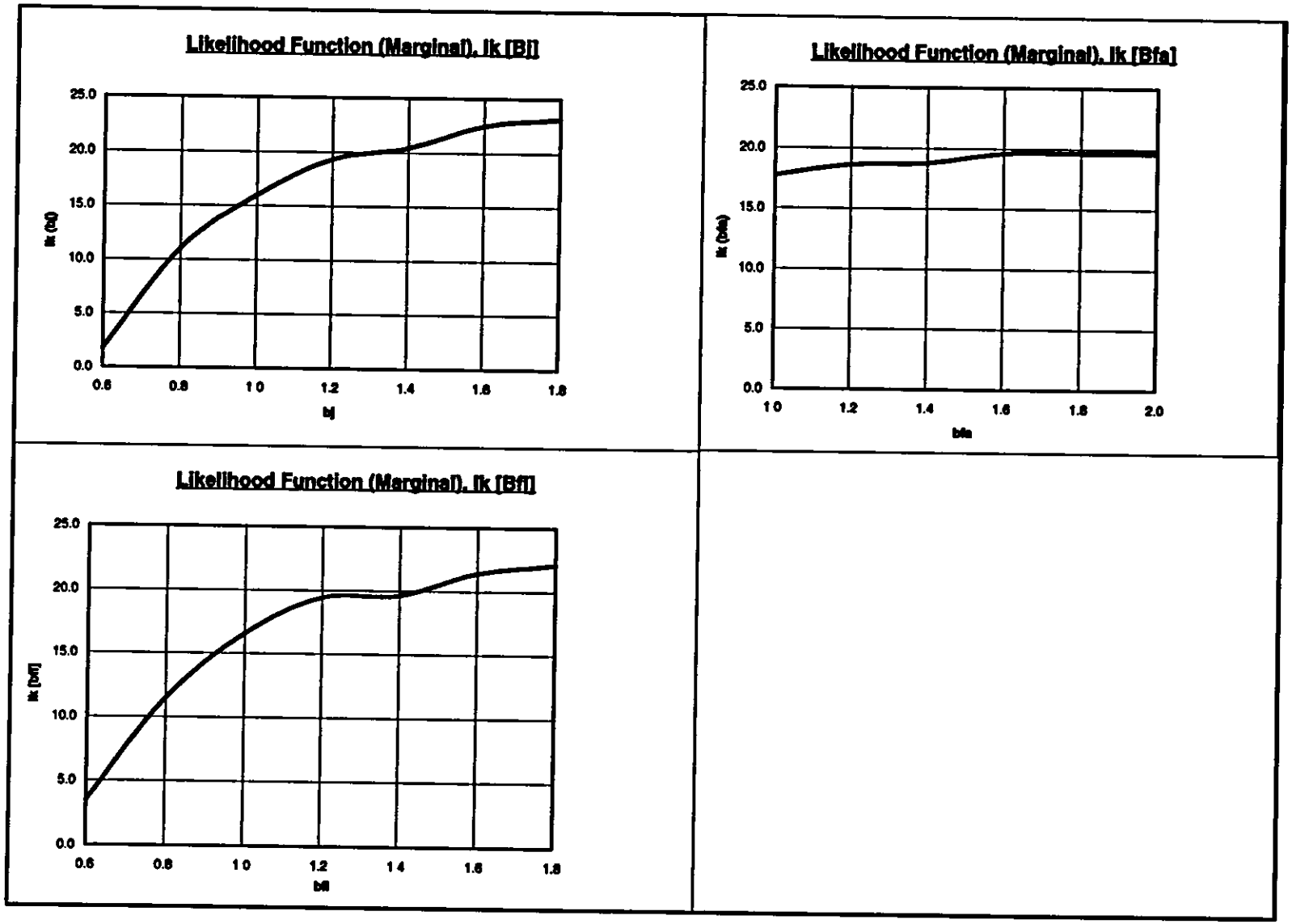

Figure E-3(b): Marginal Likelihood Functions — Survival Platform ST130Q

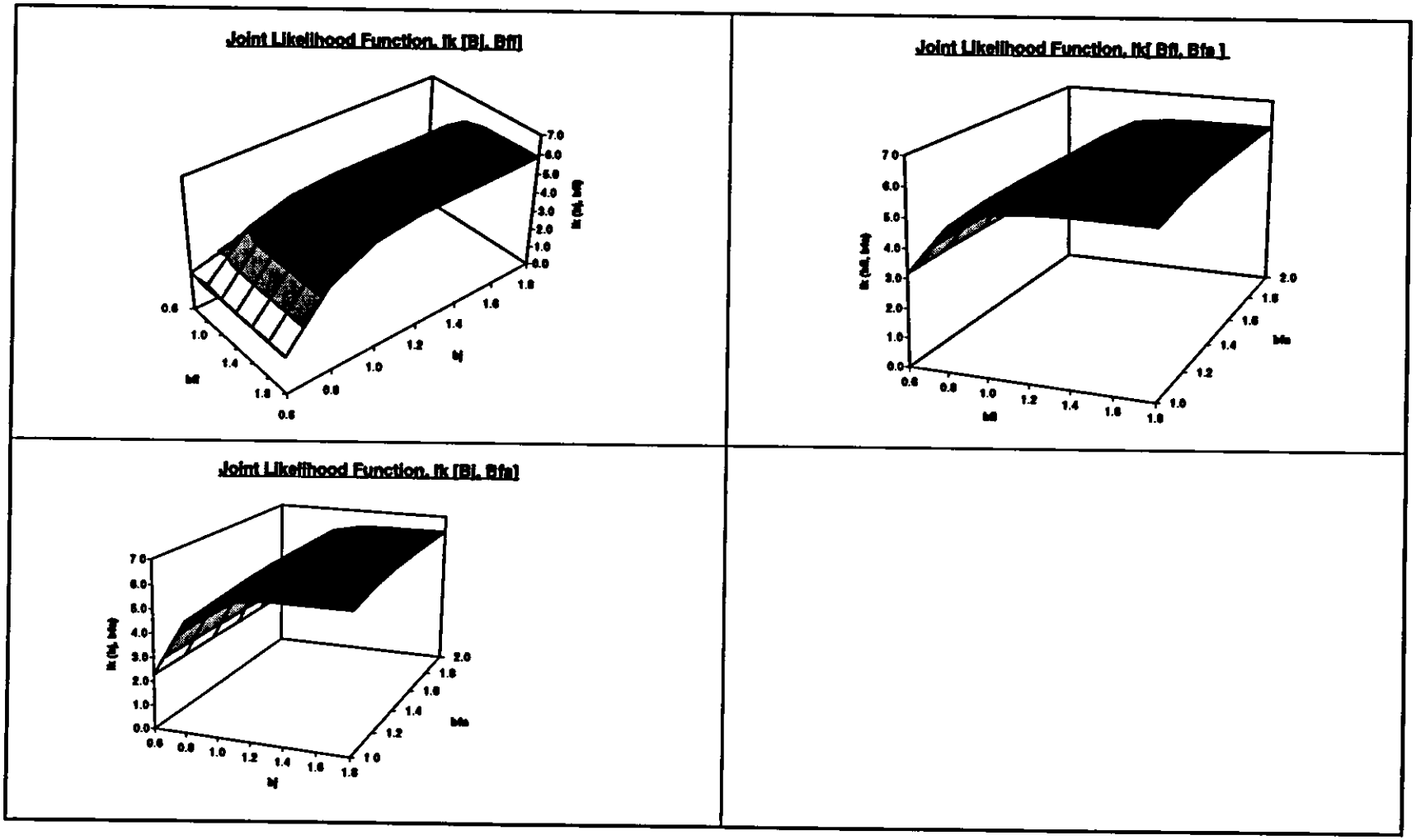

Figure E-4(a): Joint Likelihood Functions — Survival Platform WD103A

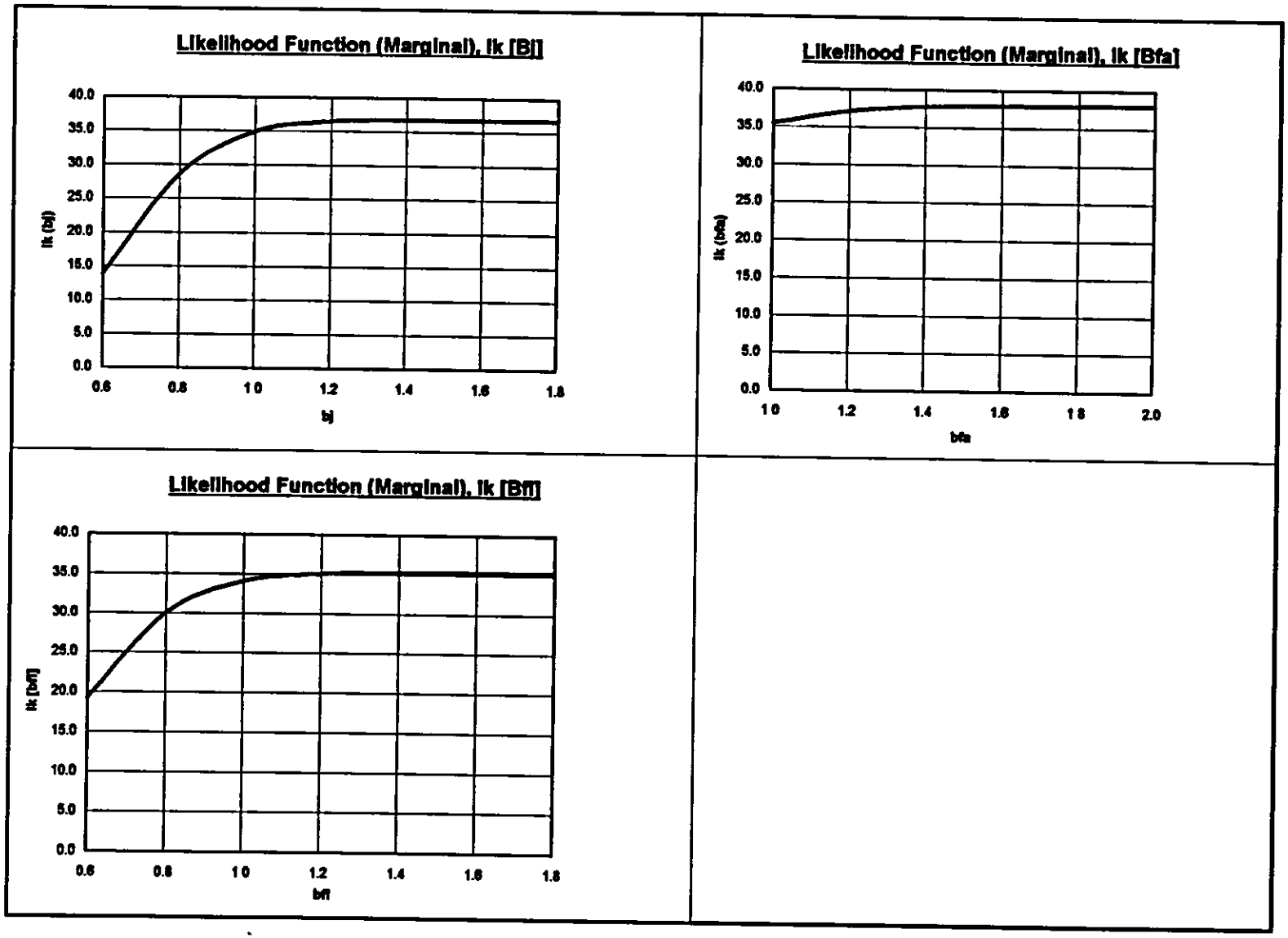

Figure E-4(b): Marginal Likelihood Functions — Survival Platform WD103A

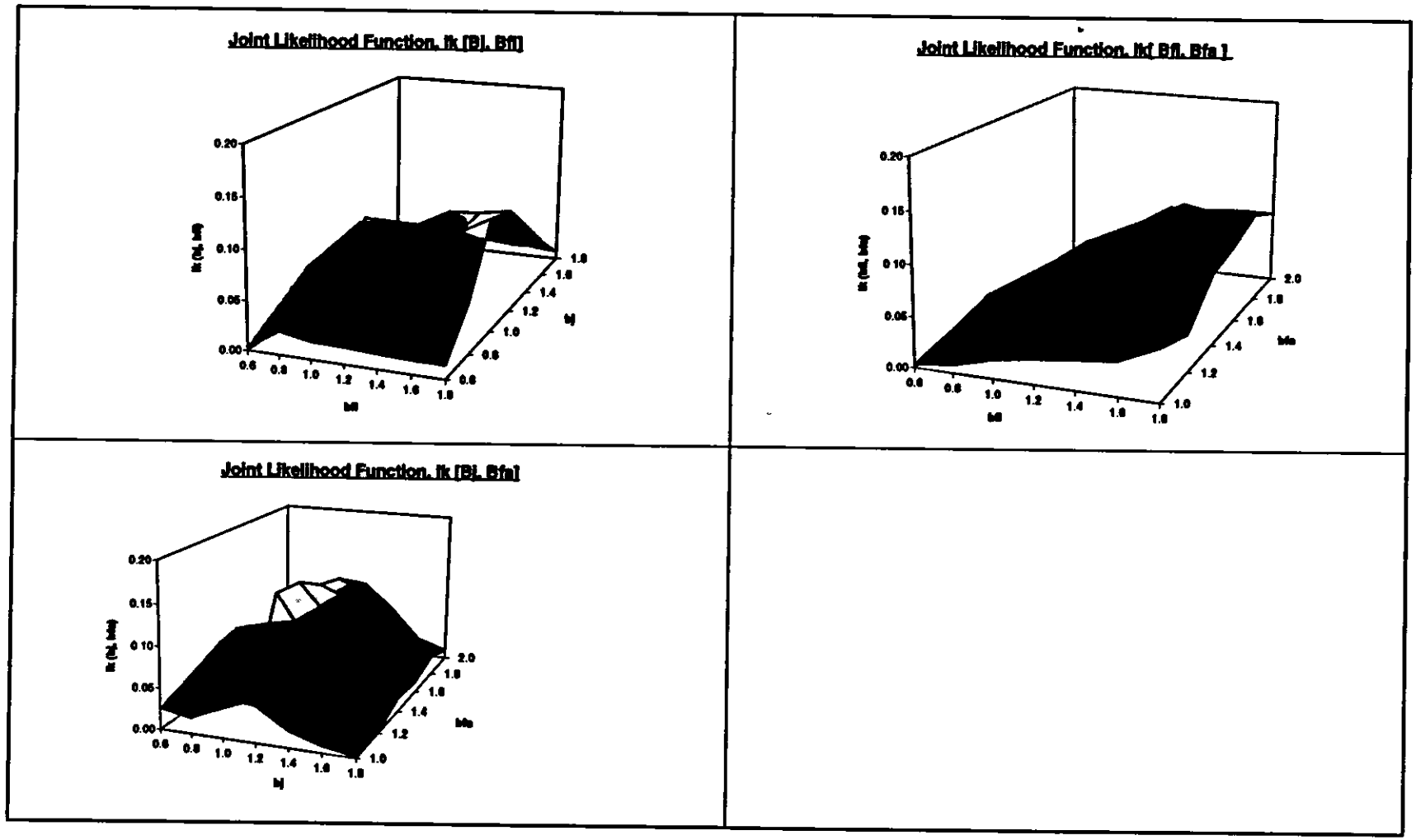

Figure E-5(a): Joint Likelihood Functions — Damage Platform ST151J

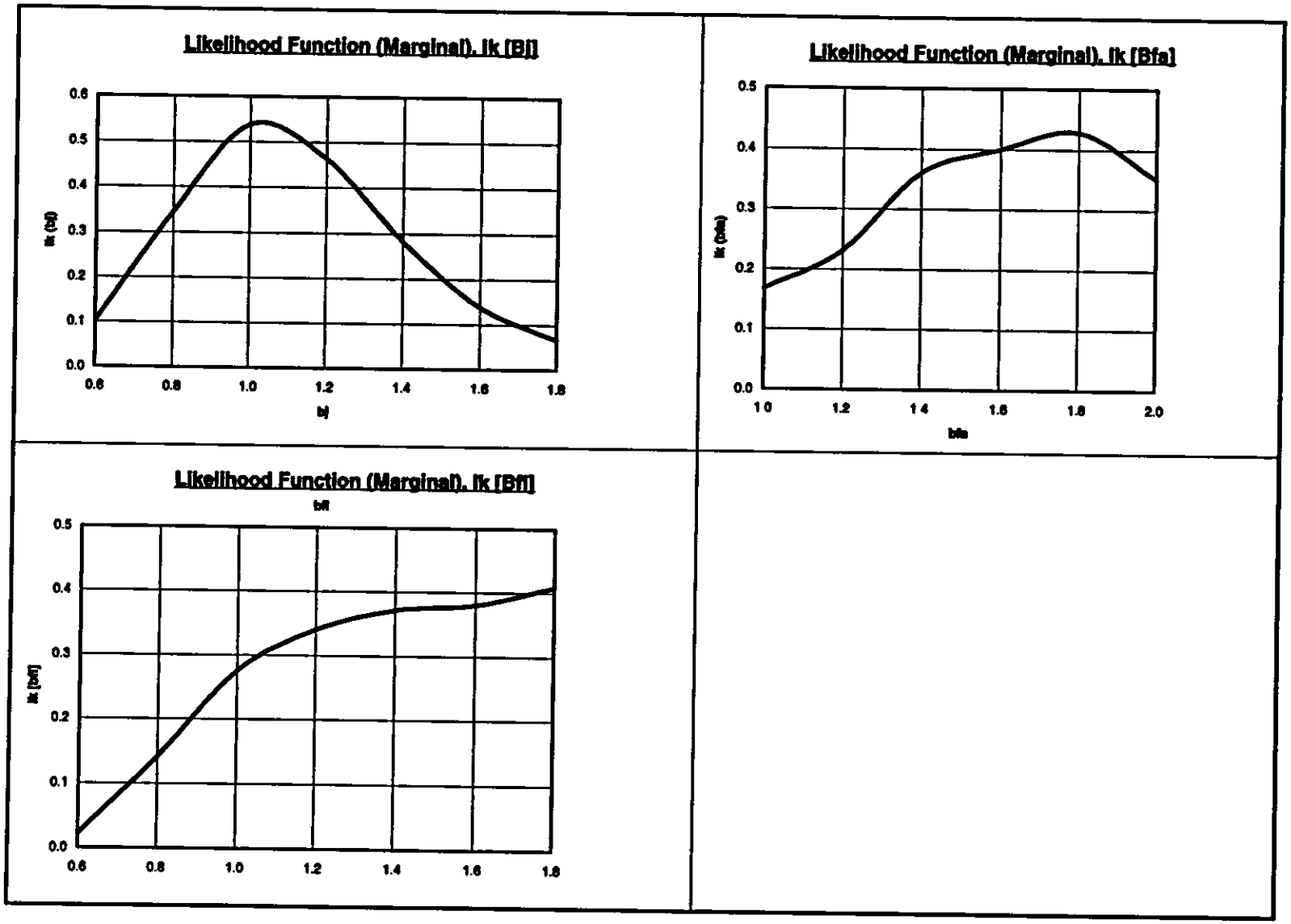

Figure E-5(b): Marginal Likelihood Functions — Damage Platform ST151J

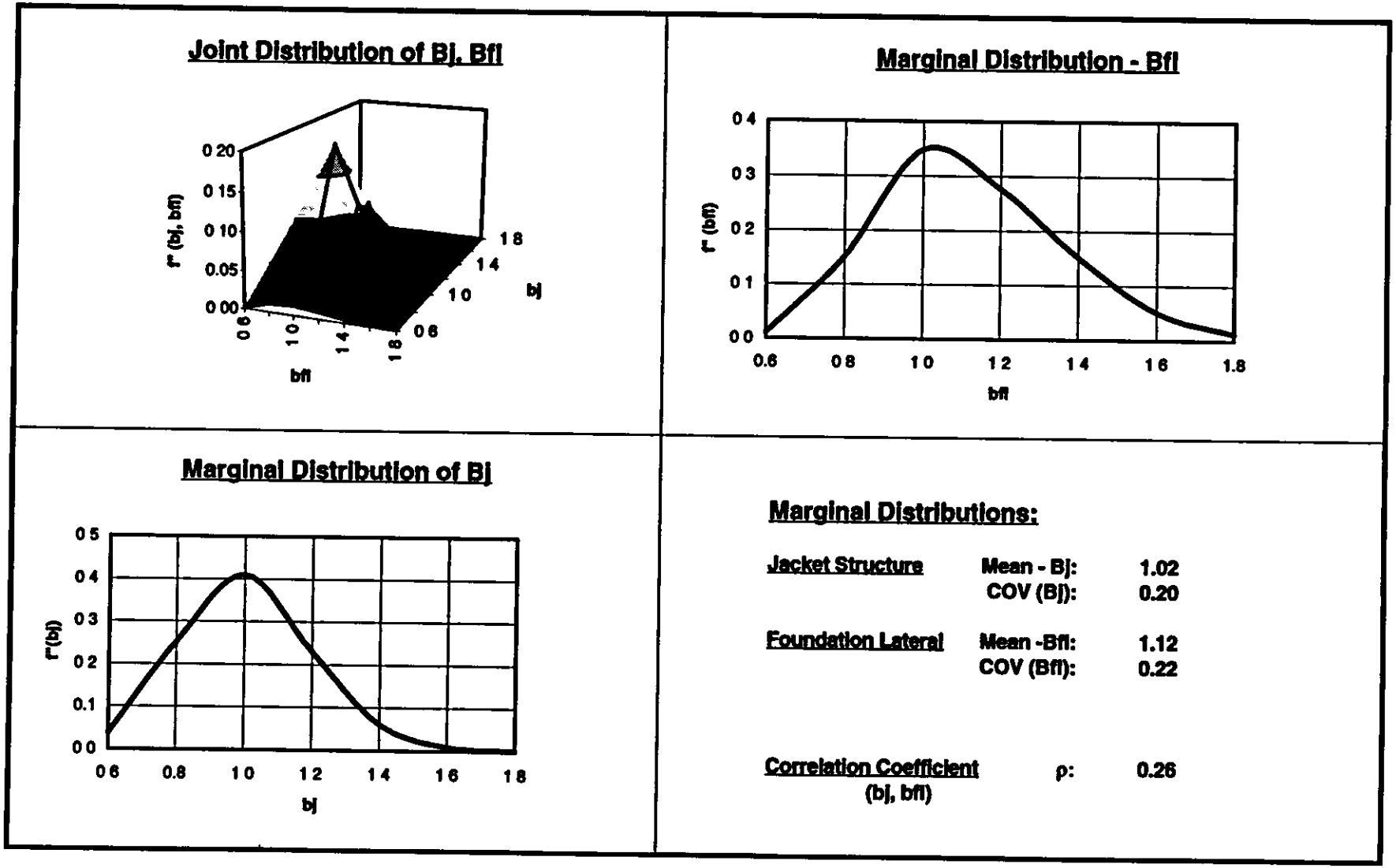

Figure E-6(a): Posterior Distributions of Bias Factors (B_j, B_{fl}) — Damage Platform ST151J

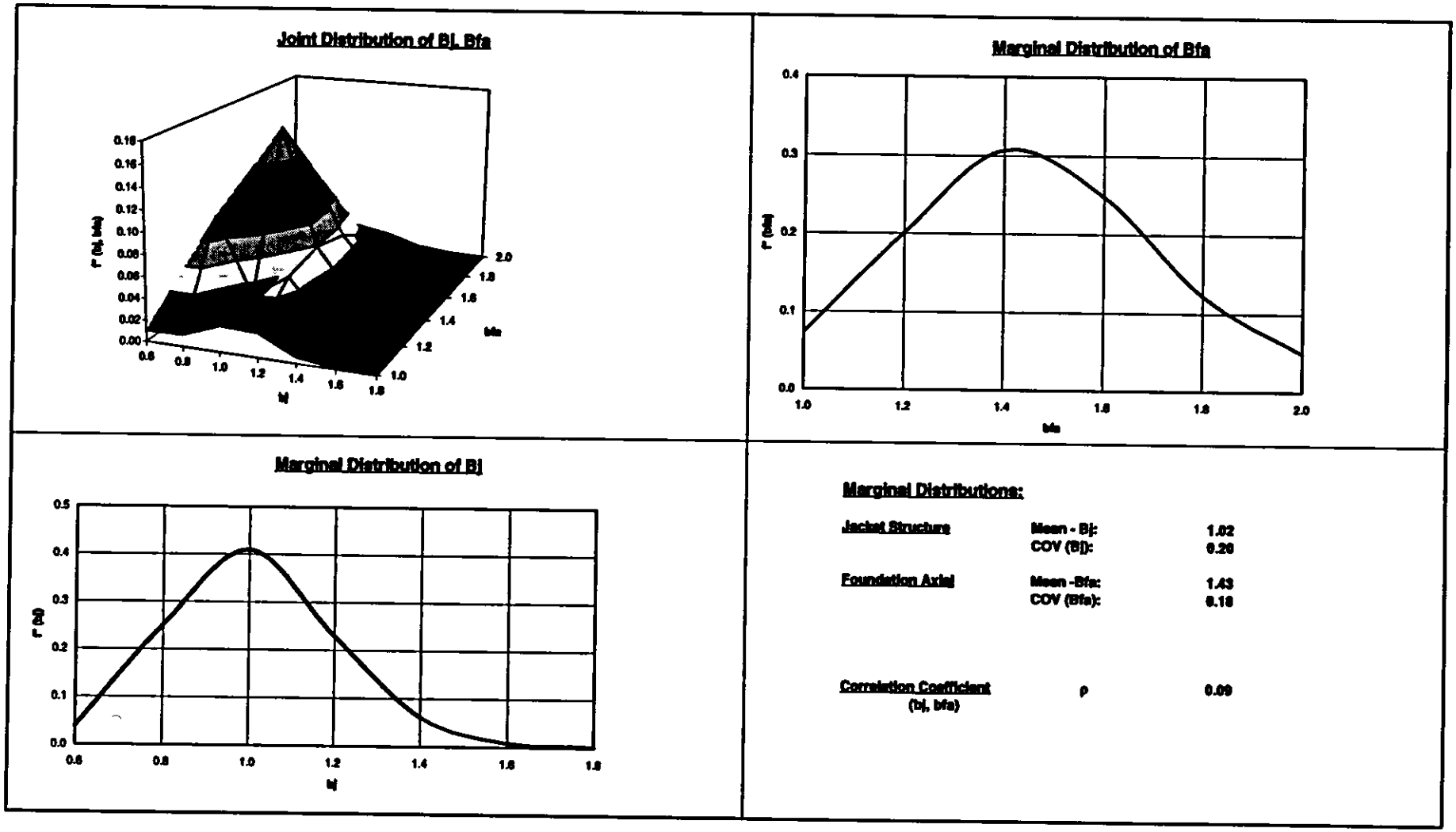

Figure E-6(b): Posterior Distributions of Bias Factors (B_j, B_{fa}) — Damage Platform ST151J

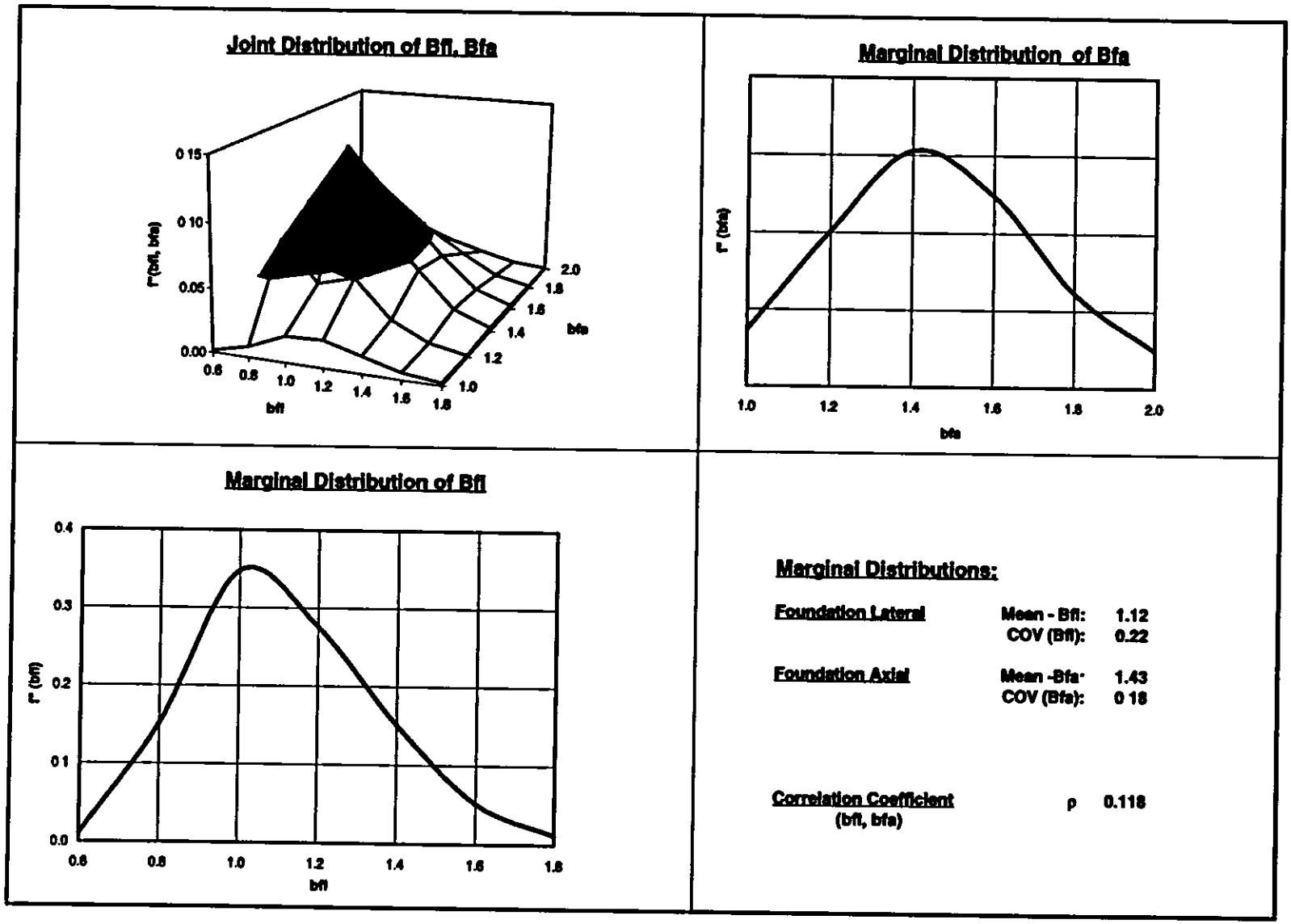

Figure E-6(c): Posterior Distributions of Bias Factors (B_{fl}, B_{fa}) — Damage Platform ST151J

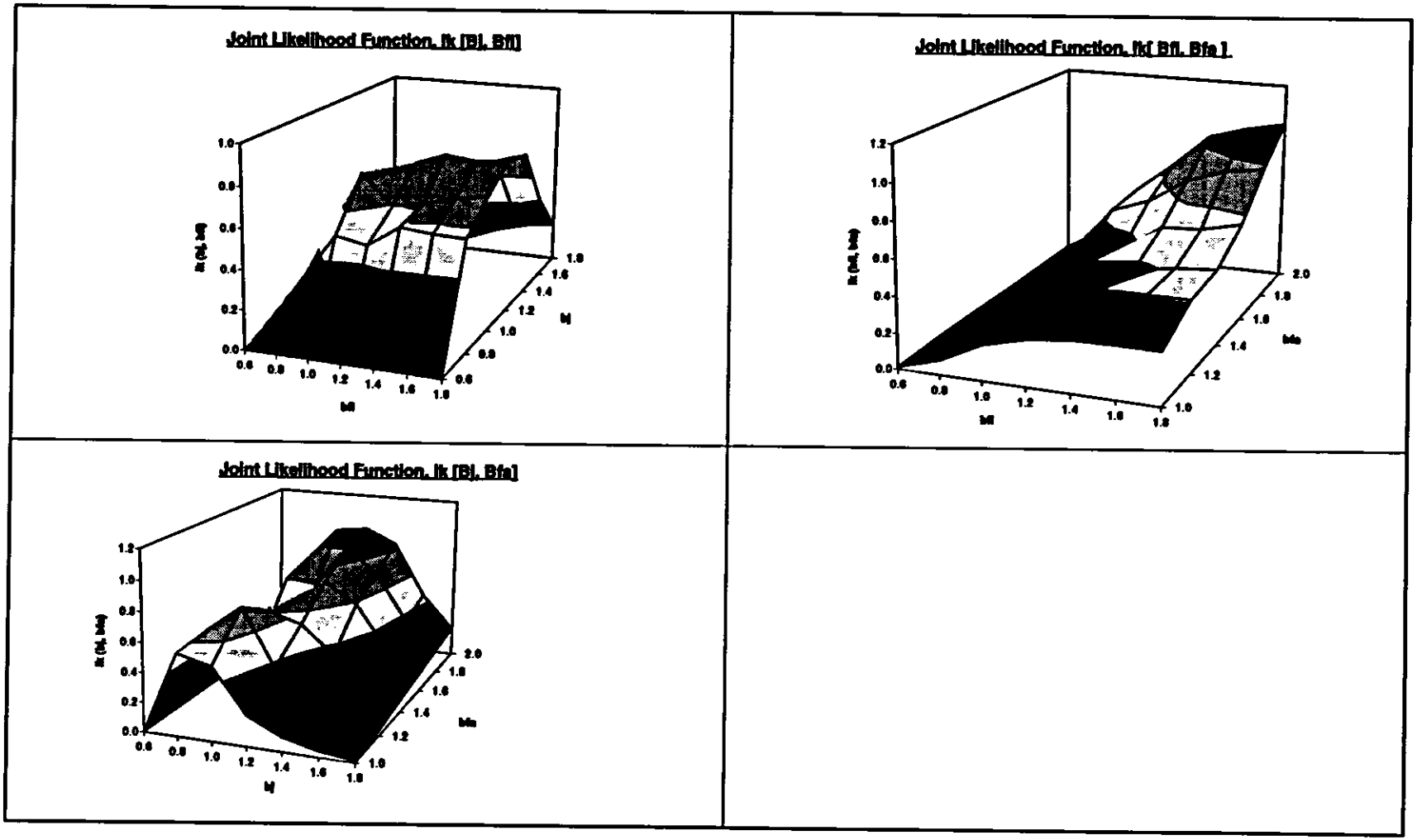

Figure E-7(a): Joint Likelihood Functions — Damage Platform ST177B

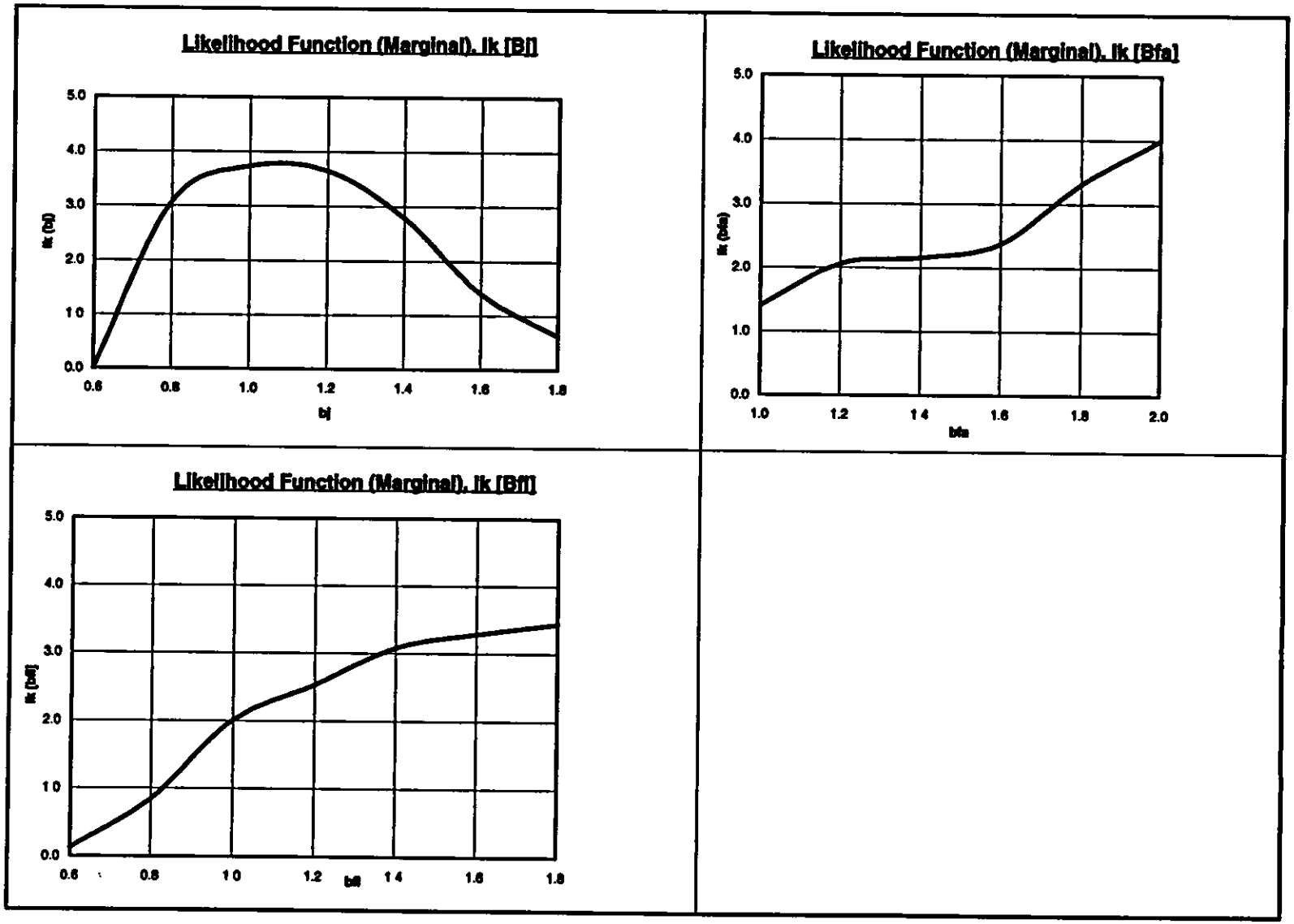

Figure E-7(b): Marginal Likelihood Functions — Damage Platform ST177B

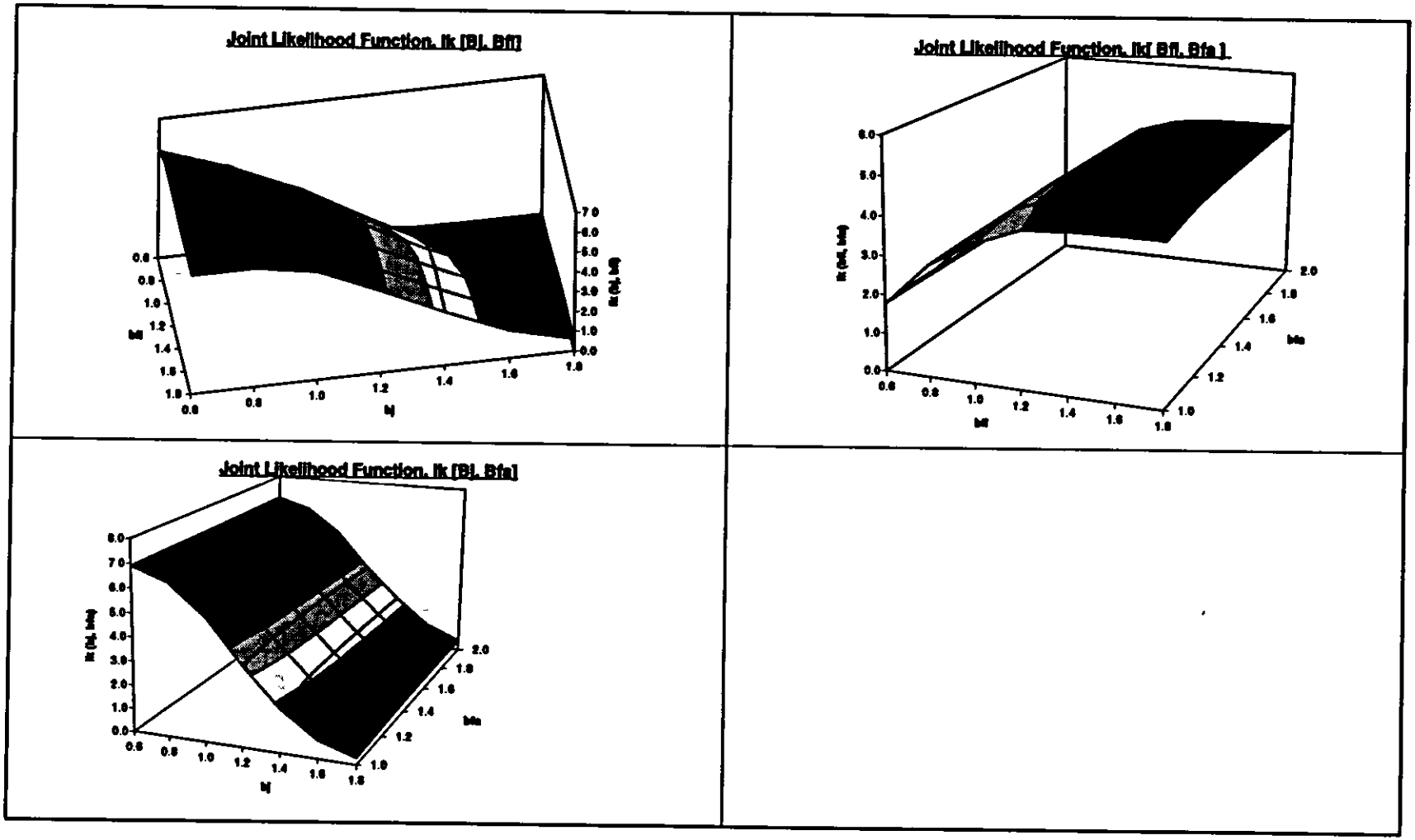

Figure E-8(a): Joint Likelihood Functions — Damage Platform SS139 (T25)

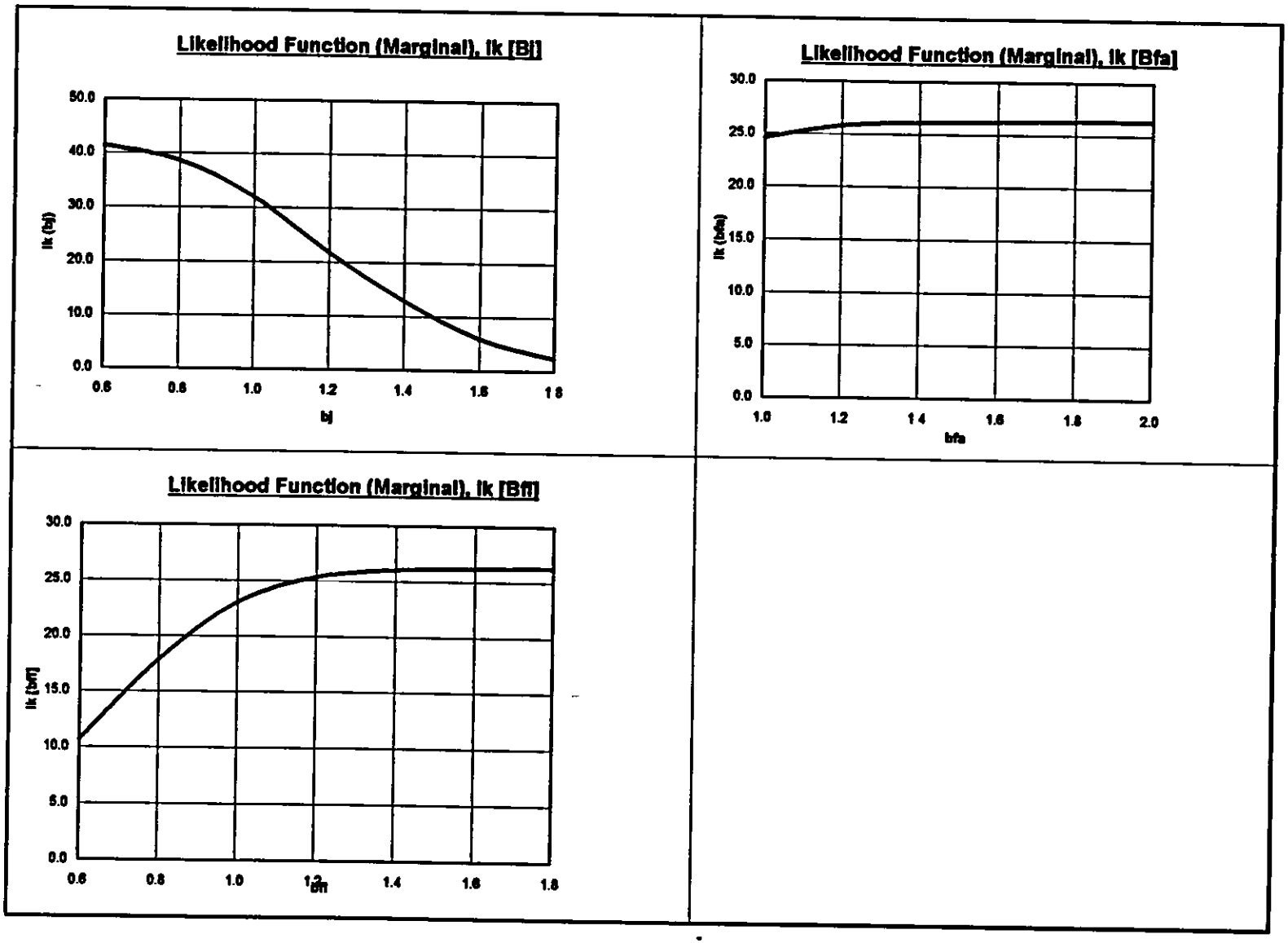

Figure E-8(b): Marginal Likelihood Functions — Damage Platform SS139 (T25)

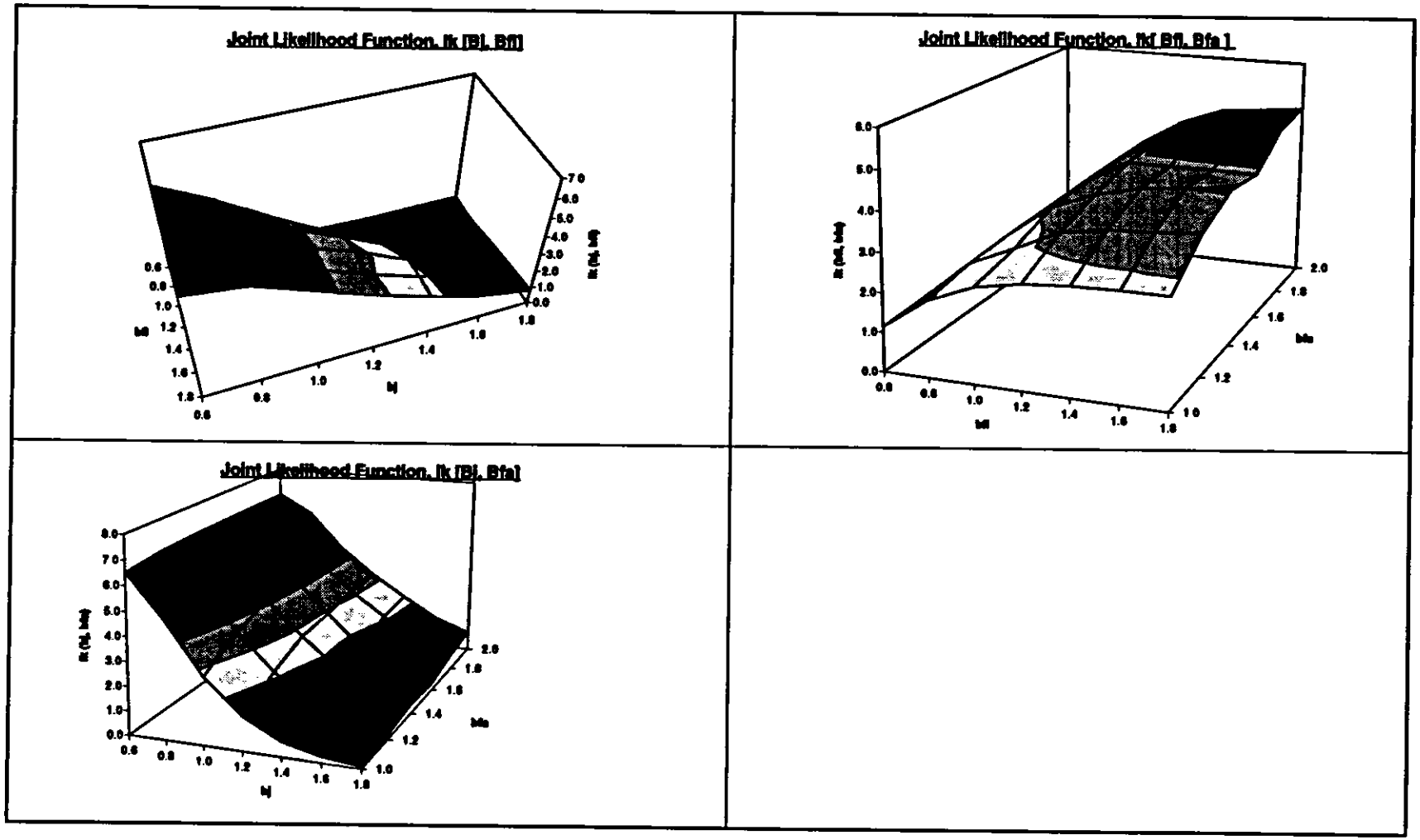

Figure E-9(a): Joint Likelihood Functions — Failure Platform ST151H

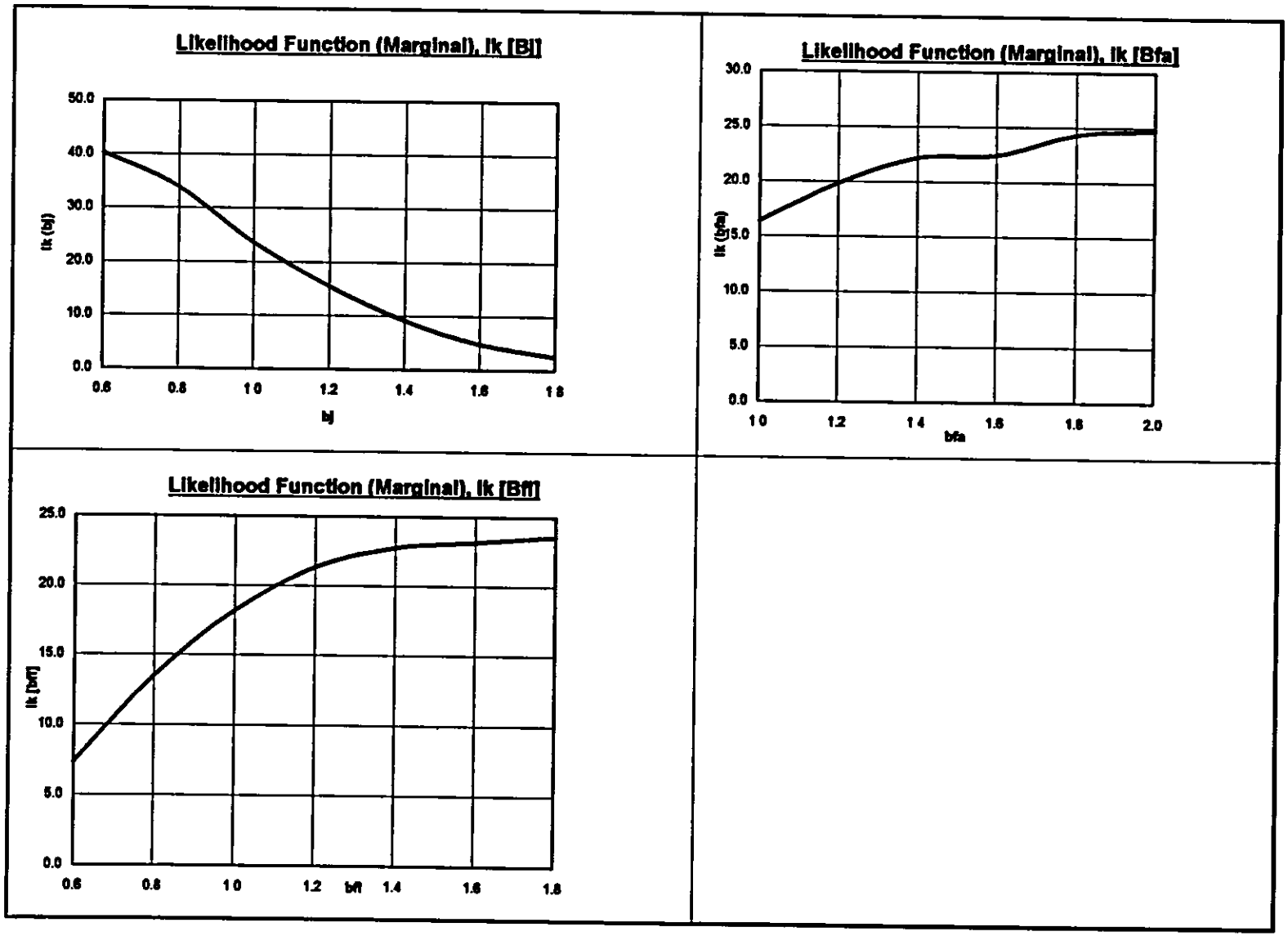

Figure E-9(b): Marginal Likelihood Functions — Failure Platform ST151H

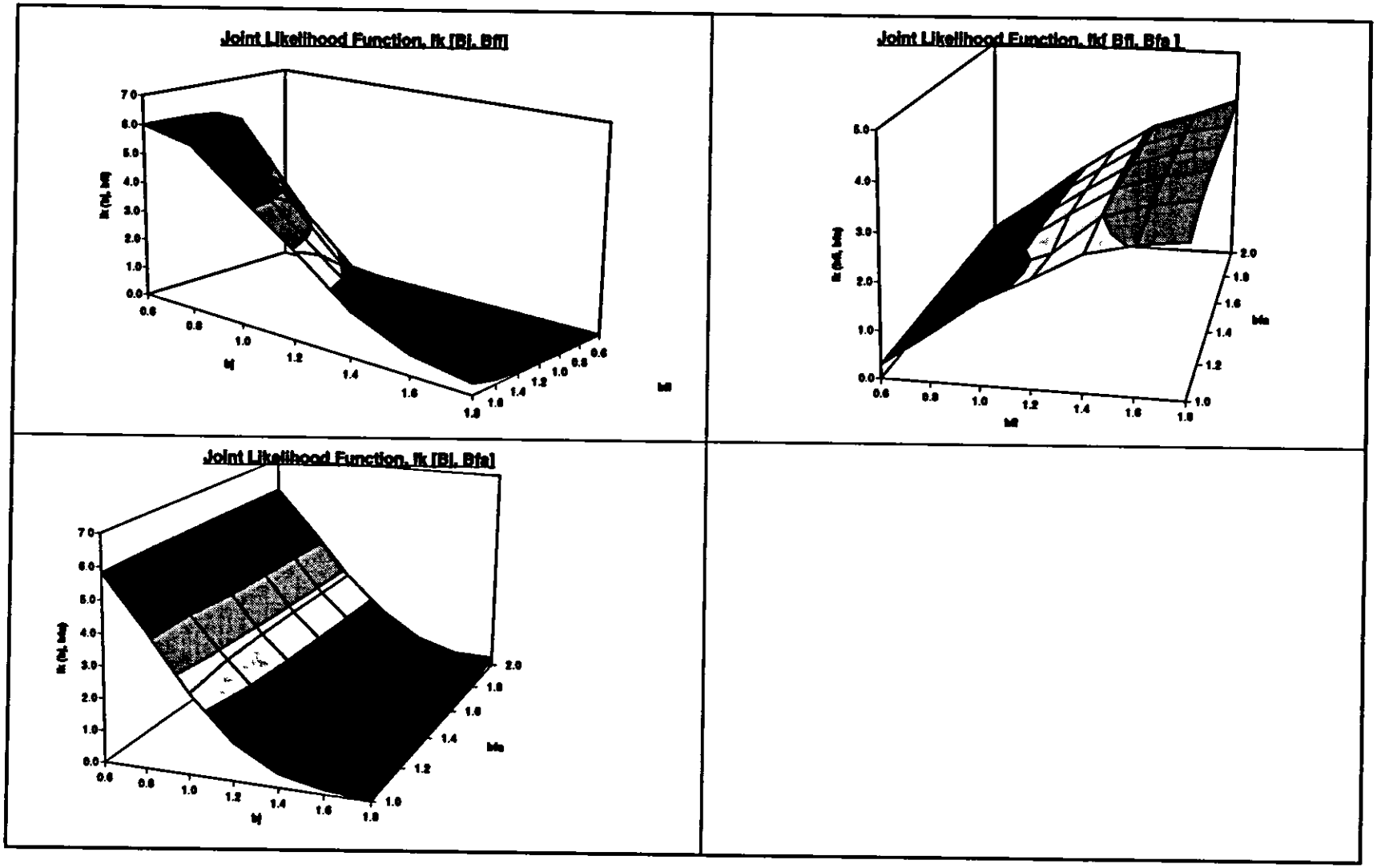

Figure E-10(a): Joint Likelihood Functions — Failure Platform ST130A

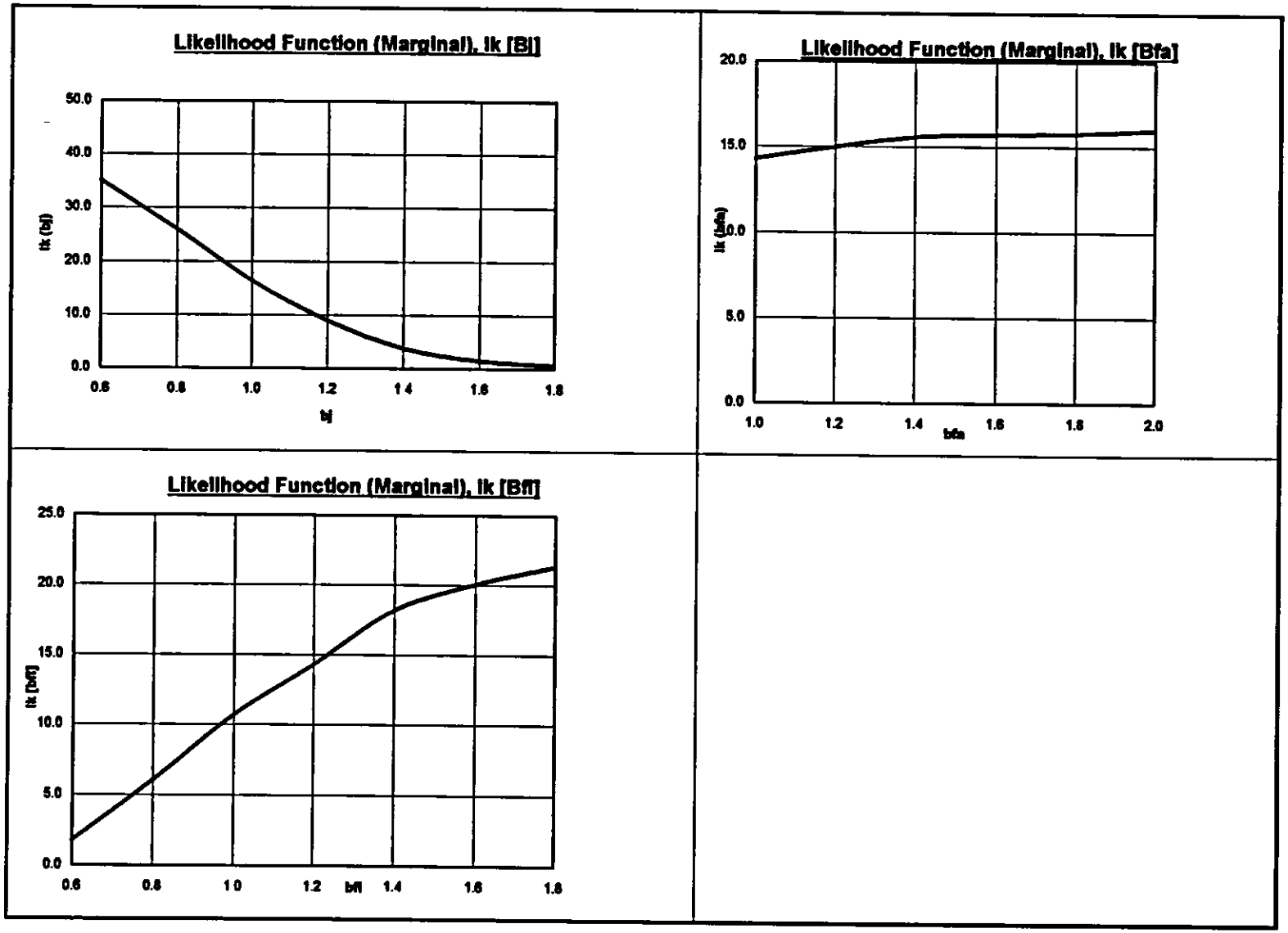

Figure E-10(b): Marginal Likelihood Functions — Failure Platform ST130A

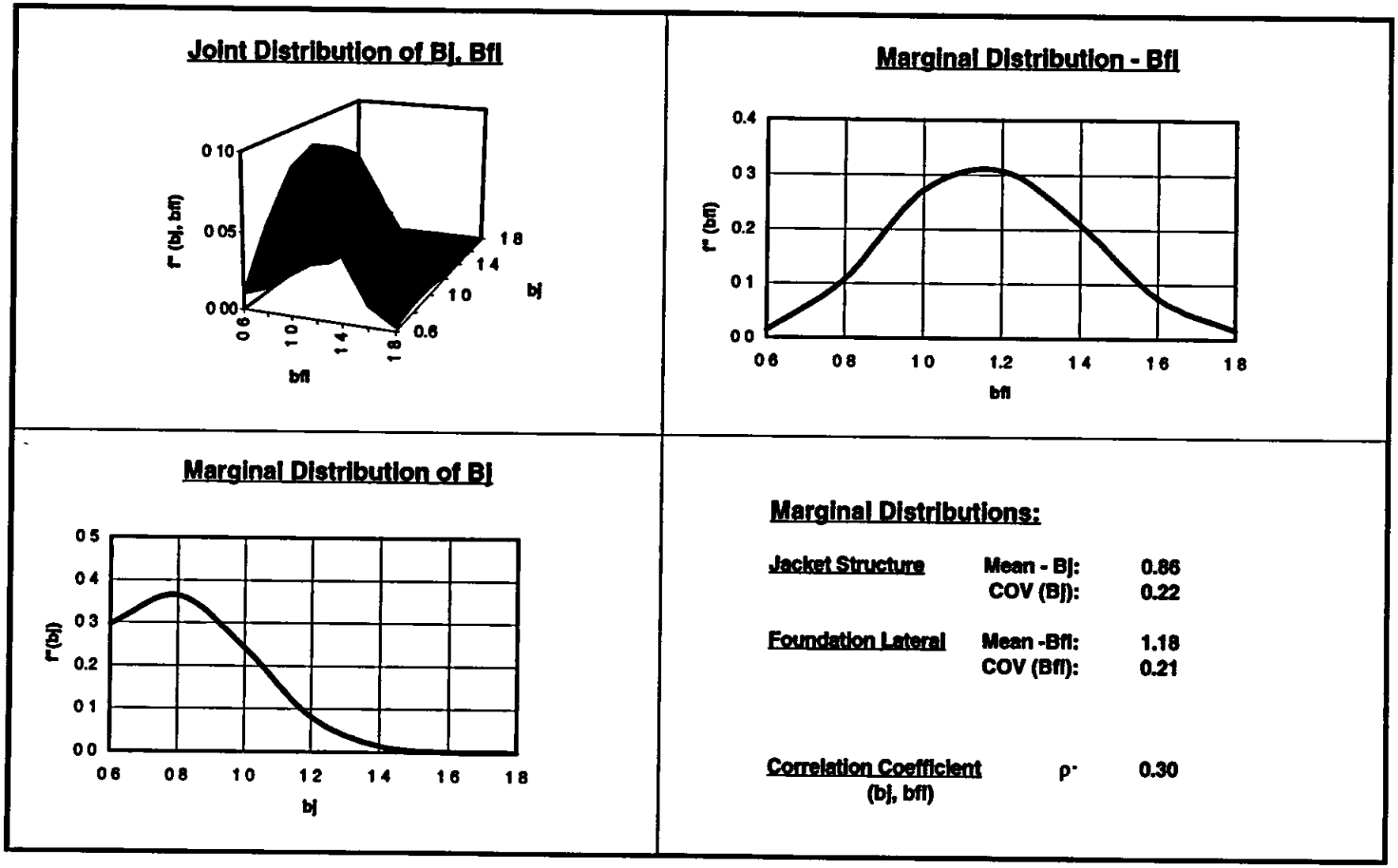

Figure E-11(a): Posterior Distributions of Bias Factors (B_j, B_{fl}) — Failure Platform ST130A

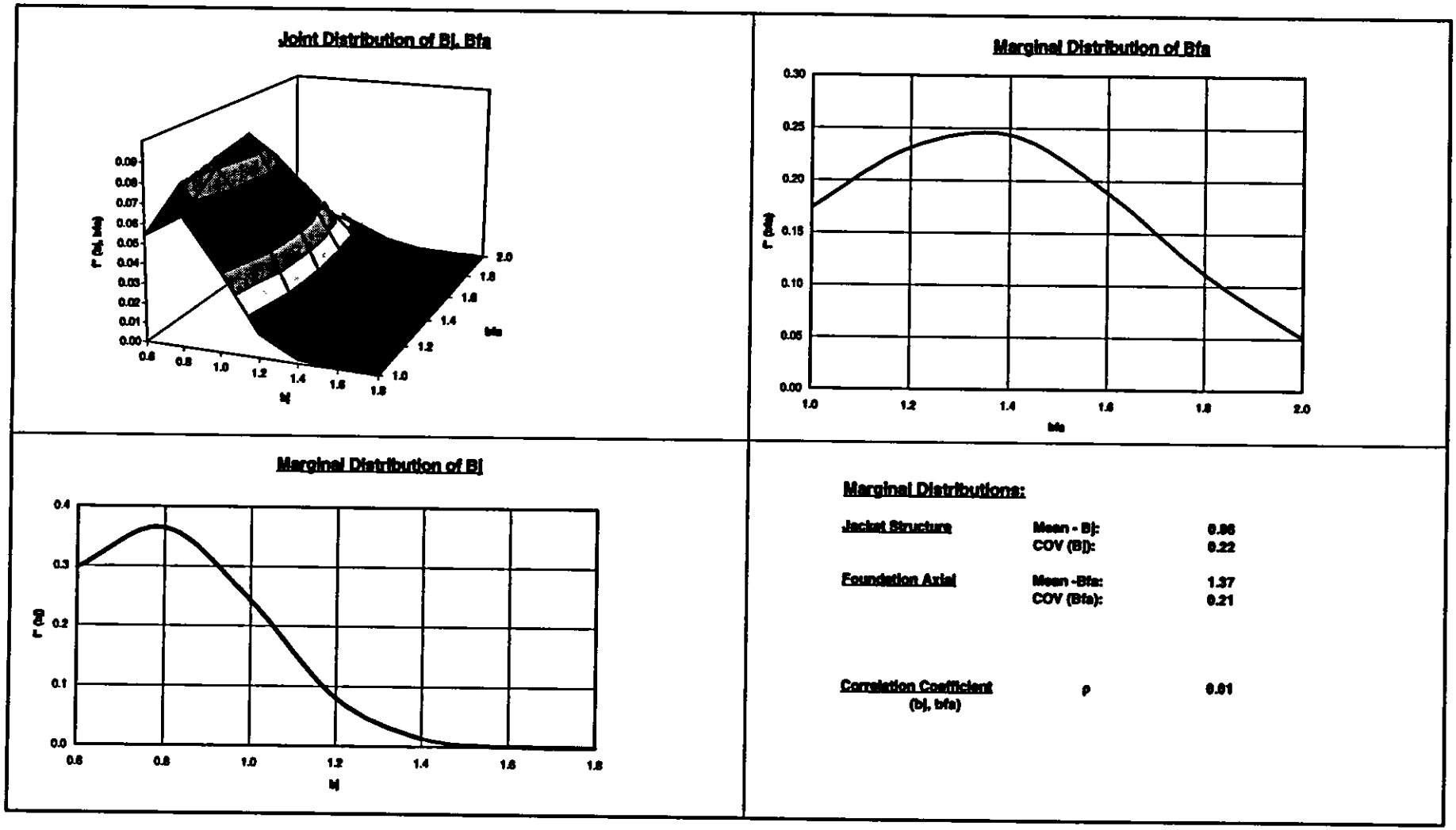

Figure E-11(b): Posterior Distributions of Bias Factors (B_j, B_{fa}) — Failure Platform ST130A

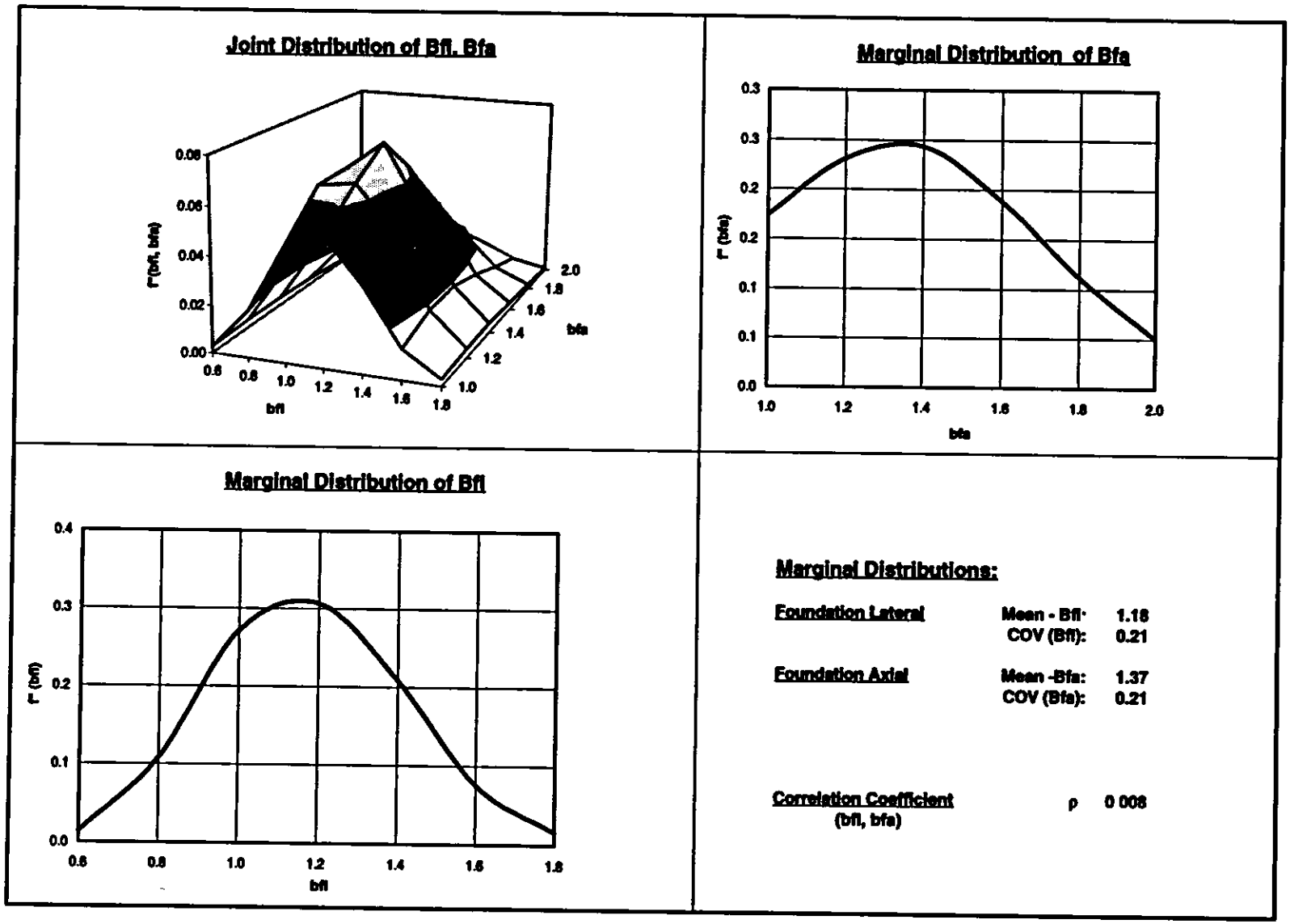

Figure E-11(c): Posterior Distributions of Bias Factors (B_{fl}, B_{fa}) — Failure Platform ST130A

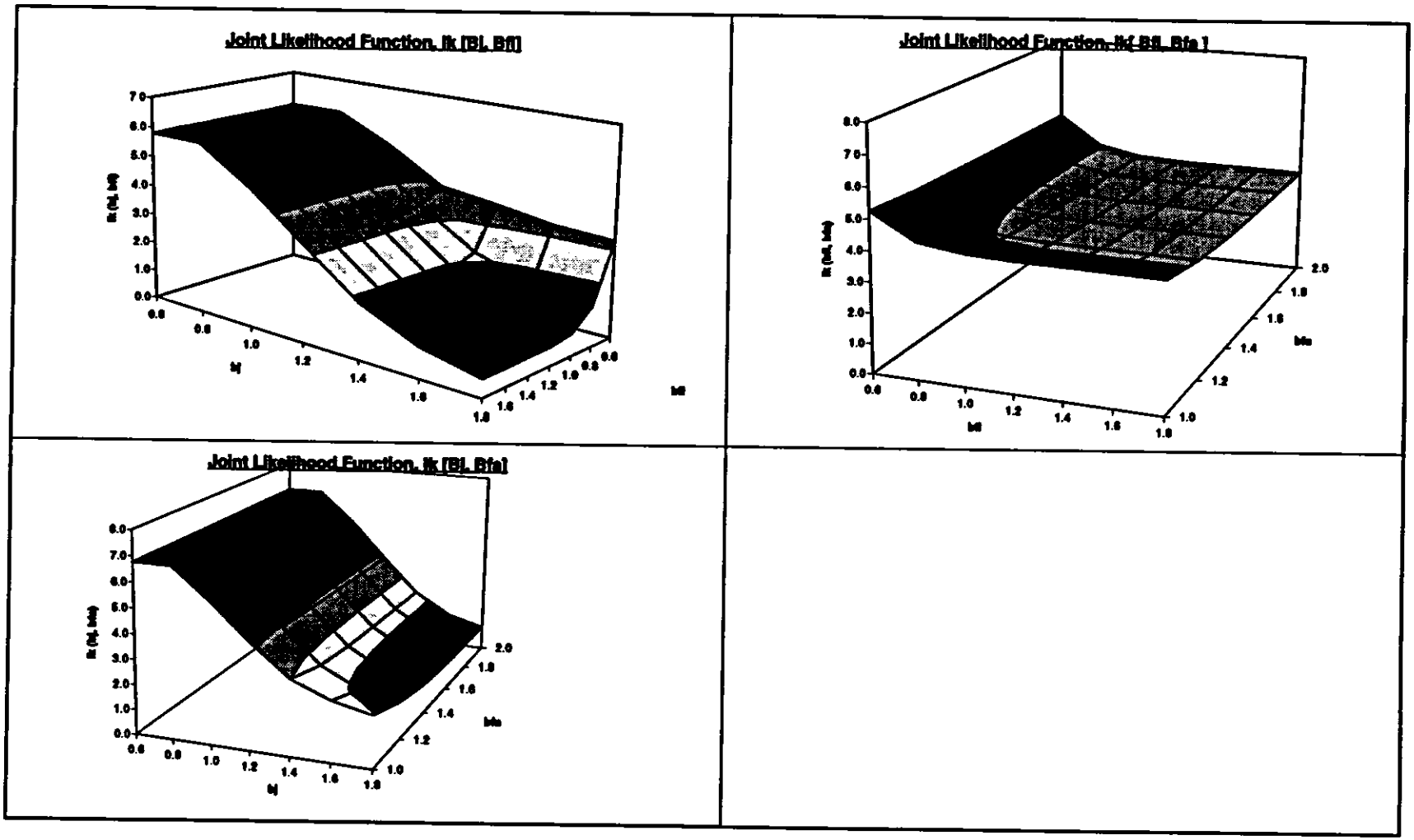

Figure E-12(a): Joint Likelihood Functions — Failure Platform ST72 (T21)

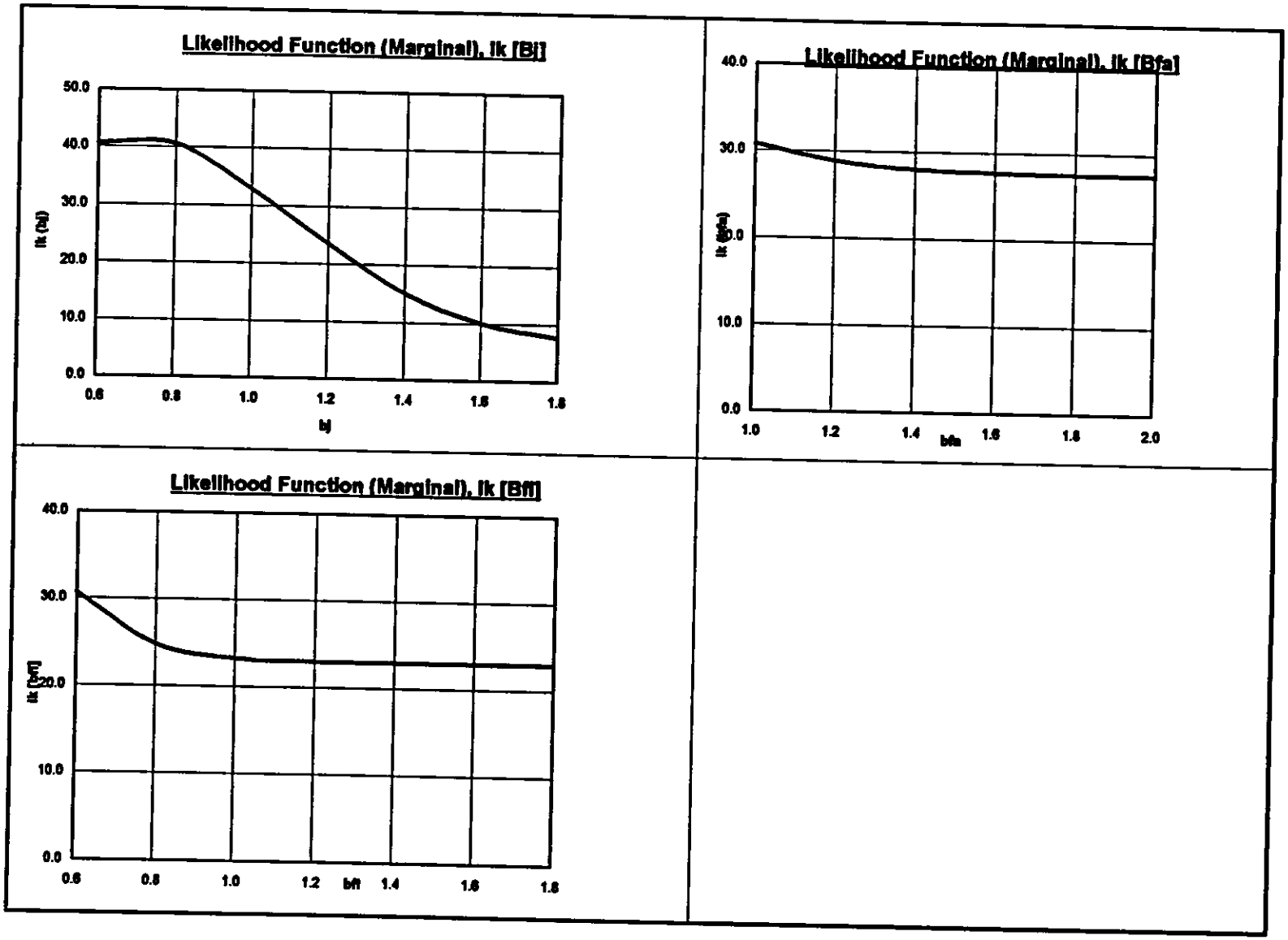

Figure E-12(b): Marginal Likelihood Functions — Failure Platform ST72 (T21)

Hurricane Andrew

In August of 1992 the Gulf States were subjected to one of the most intense hurricanes in recorded history. Hurricane Andrew exhibited peak wind speeds of over 155 miles per hour and created wave heights in excess of 70 feet. The track of Hurricane Andrew led through southern Florida, where most of its destruction occurred, progressed through the Gulf of Mexico and eventually made its final landfall near Morgan City, Louisiana. Andrew caused over 50 deaths onshore and extensive property damage. Andrew represents one of the costliest natural disasters in US history.

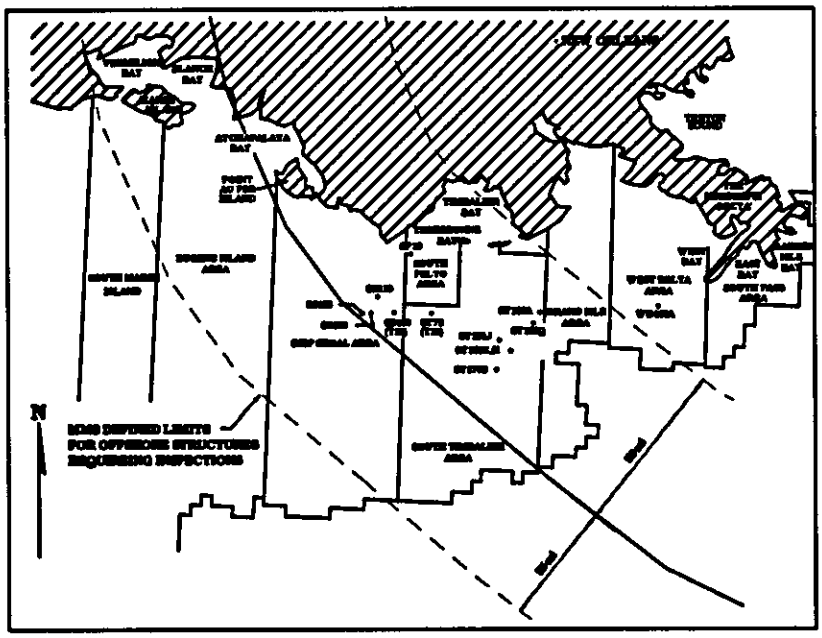

The hurricane path includes a region of the Gulf that is very densely populated with offshore platforms. As shown in the adjacent figure, the center of the hurricane traversed the Mississippi Canyon, South Timbalier, Ship Shoal and Eugene Island areas Along its path through this area, Andrew's waves typically exceeded the 100 year return period criteria used for the design of new structures. The region of platforms most significantly loaded by Andrew, as defined by the Minerals Management Service (MMS), included approximately 700 platforms located in the Eugene Island, Grand Isle, Mississippi Canyon, Ship Shoal, South Marsh, South Pelto, South Timbalier, and West Delta areas. Many of these platforms were older structures that were not designed to withstand the forces created by a hurricane of Andrew's magnitude. However, inspections following the hurricane revealed that most of the platforms affected by Andrew were not significantly damaged The vast majority of the damage reported was minor and included items such as bent handrails, damaged walkways, and damaged boatlandings. A number of structures experienced significant local structural damage both above and underwater. In many of these instances, the damage was considered to be of significant consequence possibly jeopardizing the overall structural integrity of the platform In these cases, the damage was either repaired or shown not to degrade global strength to below minimum safety limits. There were 28 jacket type platforms that suffered substantial damage resulting either in total collapse or rendering the structure unserviceable and beyond repair. In addition, 47 caissons were also significantly damaged or collapsed [1].

The number of platforms damaged by Hurricane Andrew was significant, however, the event has provided a positive demonstration of the emergency systems in place within the Gulf. This is

evidenced by the fact that, since platforms were shut-down and evacuated prior to the hurricane, no lives were lost offshore and less that 2,500 barrels (including 2000 barrels spill from a pipeline) of oil were spilled [2].

The Andrew experience has provided very valuable data that can be used to further understand the performance of offshore structures subjected to large hurricanes. The information gained through the review of platforms that survived, were damaged, or failed during the hurricane can be used to improve procedures for designing new platforms as well as procedures for assessing the integrity and safety of existing structures Andrew thus provided a unique opportunity to study offshore structures tested under "real-life", full scale, conditions.

This report documents the results of a study performed by PMB Engineering Inc. using the Andrew data to improve the procedures used for the assessment of existing platforms. This study is the second part of a two phase project that started in 1993 [1] Other related studies that have had significant input to this work are summarized below.

Overview of Previous Andrew and Other Related Studies

Over the last 3 years PMB has completed several studies that have related to Andrew and the development of current API guidelines for platform assessment [3]. This work has included a two phase study of the effects of Hurricane Andrew on offshore platforms [1, 4], a study of the effect of Hurricane Andrew on platform foundations [5], an investigation of detailed inspections of structures damaged during Andrew [6, 7], a study of caisson behavior during Andrew [8], and a study to assess the ultimate capacity analysis procedures included in the API guidelines [9, 10, 11]

Oceanweather Hindcast Study

Oceanweather, Inc. preformed hindcast studies for Hurricane Andrew [12, 13] in 1992 and again in 1994. The 1992 hindcast was used in the Phase I study of the effects of Hurricane Andrew on offshore platforms. The 1994 hindcast, which was used in this study, was developed using a finer grid and an improved surface wind model compared to that of the 1992 hindcast. In general, the 1994 study hindcast significant wave heights were lower.

Effects of Hurricane Andrew on Offshore Platforms - Phase I

In 1993, PMB began the first of a two phase study of the effects of Hurricane Andrew. This study was sponsored by the Minerals Management Service and 11 oil companies. The essential aspect of the Phase I study was the comparison of predictions of platform response against observations collected for 13 platforms. The predictions for these platforms were generated using the oceanographic data developed from a hindcast study [12] in conjunction with the state-of-the-practice structural analysis methodology. This data was used as input to a complex reliability analysis to determine bias in the analytical methods. This calibration process is illustrated in the adjacent flow chart.

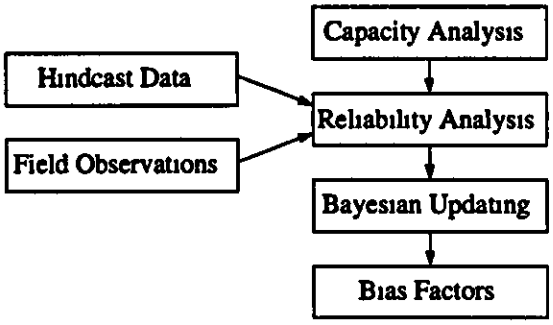

The conclusion of this initial study was that, on average, the calculation of loading and resistance led to a conservative prediction of platform behavior for the 13 platforms analyzed. The capacity to demand ratio was shown to be conservatively biased by 19%. This bias was based on a calibration described on the basis of overall response (i e., total failure, structural damage, and survival). One important conclusion from Phase I was that foundation failures were predicted for several platforms for which no foundation failures were observed Similarly, joint failures were predicted to occur in many more instances than were observed. It was therefore concluded that the level of bias that exists in formulating the strength of individual components (e g , braces, joints, piles, soils) is probably very dissimilar. This observation led to the recommendation that further comparisons be made between predictions and observations focusing on specific component behavior instead of just global response. The Phase I work also identified areas in the current platform analysis methods that could be improved. The final report of the Phase I study was issued in October 1993 [1].

Development of Bias Factors for Pile Foundation Capacity

Following the completion of the Andrew Phase I study, the MMS and API commissioned PMB to assess the bias specifically attributable to platform foundations. This study focused on structures that had either exhibited foundation failure or were predicted to have experienced foundation failure during Hurricane Andrew. The study concluded that, for the sample of structures analyzed and analysis methods used, the foundation lateral and axial strength to load ratios were conservatively biased by 30% and 70%, respectively. The results of this study were issued in May 1995 as an API PRAC report [5].

Hurricane Andrew - Detailed Platform Inspection and Analysis

Following the completion of the Phase I study, the MMS commissioned PMB to perform detailed underwater inspections and analysis of 4 structures that were subjected to extreme loading during Andrew. Of the 4 platforms, 2 survived with minimal damage, one was severely damaged and later abandoned, and one collapsed. The objective of these studies was to assess the accuracy of analytical predictions based on observed local component behavior recorded from the detailed inspections. The results of these analysis further identified specific areas within the analysis methodology needing improvement. The results of these studies were submitted to the MMS in June and August of 1994 [6,7].

API Section 17 Trials/Benchmark Study

PMB coordinated with API Task Group 92-5 to study the methodologies included in the draft recommendations of API RP2A WSD Section 17 [3] This project was sponsored by the MMS and 21 companies, each of which participated in an independent trial application of the recommended procedures. The results of these trial applications were compiled and used to develop recommendations for improvement of the draft guidelines. A second part of this study included a benchmark analyses of a single platform. Several oil companies and engineering contractors volunteered to complete an ultimate strength analysis of a common platform. The results of these analyses were compiled by PMB and used to assess the consistency and variability of analysis results. These results have also provided useful information in support of a standard recipe for ultimate strength analysis [10,11].

Effects of Hurricane Andrew on Offshore Platforms - Phase II

The primary focus of Phase II (present study) was to develop separate bias factors for the jacket structure and foundation. This study utilized a new hindcast [13] and an updated structural analysis procedure. There were four primary activities for the Phase II study:

- Development of an improved ultimate capacity analysis procedure
- Assessment of the effect of the size of the platform sample on the bias factors
- Structural capacity analysis to establish the prediction of detailed platform response to the hurricane
- Calibration to reconcile the differences between predictions and observations resulting in the definition of three bias factors

Analysis Procedure Revision

A number of specific enhancements to the analysis methodology were developed and used for the subsequent analysis These improvements included changes resulting from access to better analytical procedures (e g , joint modeling) and changes resulting from sensitivity analysis Specific improvements included:

- Use of mean joint strength formulation instead of lower bound estimates
- Detailed joint modeling where joint failure was expected
- More detailed brace modeling
- A more detailed representation of the wave load profile as wave height is increased (particularly important when deck inundation occurs)

The most significant of these changes was that of improved joint modeling which resulted in a much closer correlation of analytical results and field observations.

Sample Size (Weighting Evaluation)

The bias factor developed in Phase I was based on a total sample of 13 platforms which represents a relatively small percentage of the total population of platforms significantly loaded during the hurricane. The sample included a disproportionate number of failures and cases where damage occurred This was due mainly to the fact that these cases provided the most important input to the calibration. It was postulated from the Phase I study that a larger, more representative, sample size could improve the definition of the bias factor.

Including a large number of platforms directly in the Phase II project was not practical due to the cost and data requirements of the detailed analysis. An alternative method was developed that involved making comparisons of platforms outside of the sample to those for which detailed analyses were performed. The observations of this larger population of structures could then be used to scale the impact of, or "weight", the results of the individual calibration results from each platform.

This process was executed in a limited form to assess the sensitivity of the bias factor to sample size and stratification. An additional 156 platforms that survived were used to weight the results of the Phase I sample of 13. This extended sample provided a better representation of the actual distribution of surviving and failed platforms. These additional platforms were allocated into 3 sub-categories describing their level of expected performance. This allocation was based on platform age and estimated Andrew wave height. This analysis indicated that the bias factors that were determined based on the smaller sample are somewhat conservative

Capacity Analysis

The structural capacity analysis uses a sophisticated procedure to simulate the true response of a platform when subjected to the hurricane conditions This analysis is quite different from that used for the design of new structures. In the analysis performed for this study, all aspects of loading and response are modeled based on expected behavior (e.g., mean formulations of component strength are used instead of lower bound values typically used for design) without factors of safety. An example of this is the use of expected yield strength of steel instead of nominal yield strength (e.g., A36 material typically provides 42 ksi actual strength). Individual components are allowed to yield and fail and are monitored to assess the impact of their failure on the overall stability of the structure. An example of such an analysis is illustrated in the adjacent figure.

Such analysis requires modeling of nonlinear material and geometric behavior and provides data that is not available through conventional elastic (design) analysis. The procedures used for this analysis follow the general guidelines provided in the draft API document on assessment of existing platforms [3].

A set of 4 capacity analyses were performed for each platform to establish the capacity of the platform as controlled by each of the primary components. This was achieved by the suppression of specific failure modes (e.g., pile pullout/plunging and pile yielding were suppressed to determine the capacity of the jacket structure).

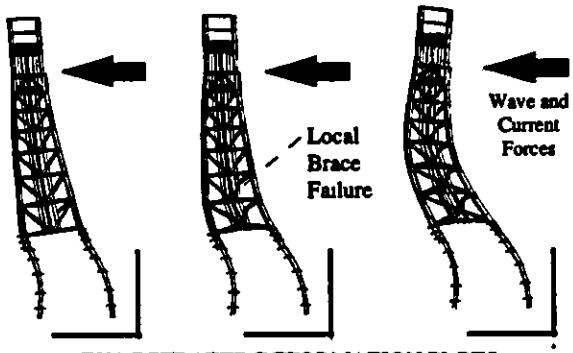

EXAGGERATED DEFORMATION PLOTS

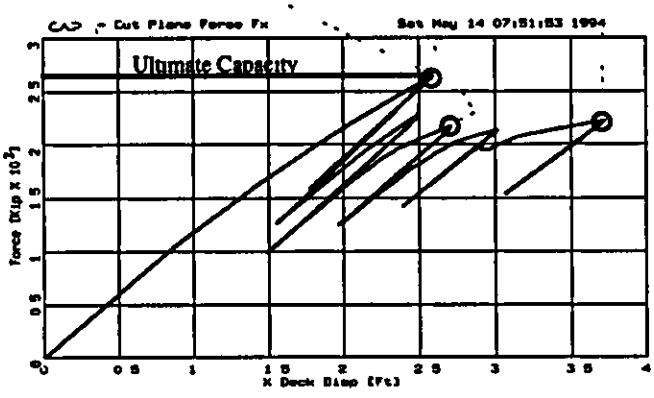

LOAD-DEFORMATION RESPONSE

Calibration

The calibration of the predictions and observations represented the majority of the work completed during the study. This task involved the following steps:

- Definition of an initial function defining the mean bias factor and its uncertainty
- A detailed reliability analysis to determine the probability of occurrence of a specific set of conditions (e.g., survival, damage and failure) for each platform
- Updating of the bias factor distribution using a Bayesian Updating procedure [33-37]

There are various ways in which the analytical predictions can be calibrated to match observed behavior more accurately. Each of the individual formulations that enters into the analysis (e.g., calculation of wave load, member strength or soil strength) could be adjusted independently to improve the overall predictions. This method would be preferable if data were available to support such adjustments. Unfortunately, while we do know, in some instances, that platforms have survived unexpectedly (i.e., predicted to fail but survived), we do not know if this is due to an overestimation of load or an underestimation of strength. The calibration procedure that was used did not attempt to adjust these individual parameters but instead assessed the bias "*B*" in the overall safety factor (resistance to load ratio). This bias factor was applied in the following form:

$$(R / S)_{true} = B(R / S)_{computed}$$

where R represents resistance or strength and S represents loading. In this form, a value of *B* greater that 1 indicates conservatism in the procedures used while values of *B* less than 1 indicate unconservative methods.

The bias factor was calculated as follows:

- The assumed, or "prior", definition of the bias factor ('*B*') was defined based on previous API PRAC studies.
- Failure probabilities were determined based on the capacity analysis results and hindcast data.

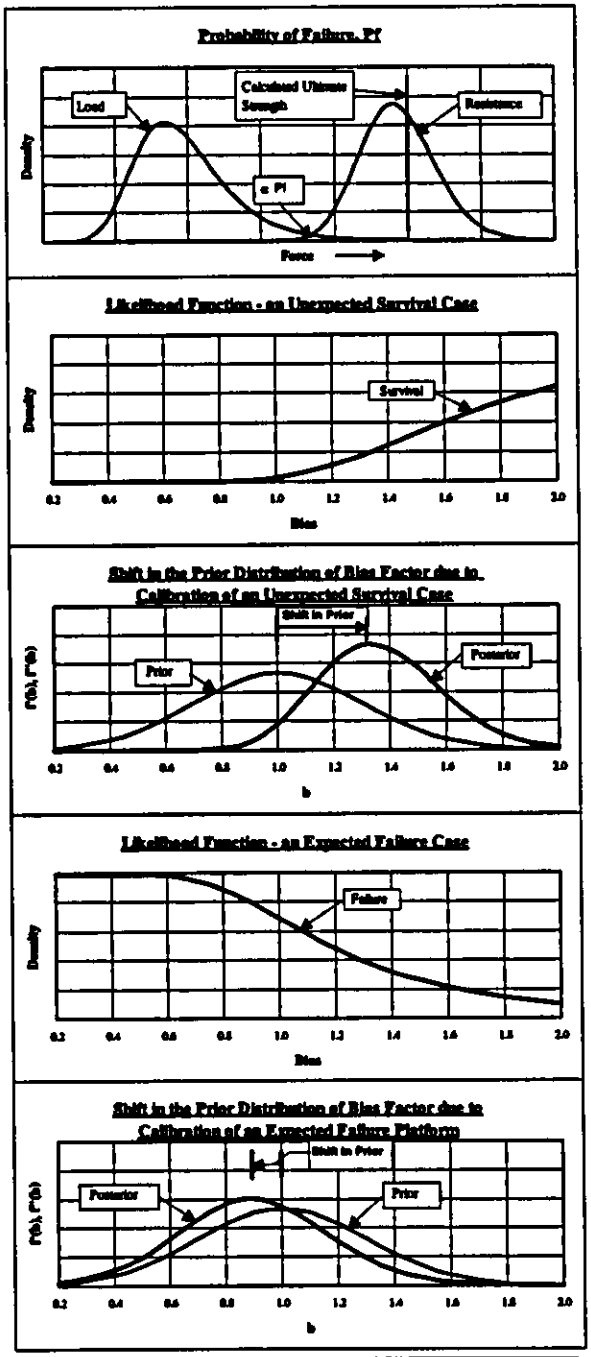

- Functions were developed for each platform to define the probability of occurrence, or likelihood, of the observed behavior.
- The updated distribution of the bias factor was calculated using the prior distribution and the likelihood function for each platform. The shift in the bias factor distribution is a function of the degree of unexpectedness of the observed results. For example, if a platform was unquestionably expected to fail during the storm, it would be assigned a relatively high failure probability. If this platform was observed to survive, the likelihood function describing the probability of survival would exhibit a significant shift to higher values of B.
- The cumulative distribution of bias factor is determined as the product of all the individual platform distributions.

Unexpected failures shift the distribution to lower values of B (to the left). Unexpected survivals shift the distribution to higher values of B. Expected failures and survivals have less effect on B. Damaged cases provide very useful information since they describe much more specific observation data than either survivals or failures. All that is known with a failure is that the load exceeded capacity. It is not known to what degree the capacity was exceeded. Similarly, survivals show that capacity exceeded load but by an unknown amount. Damaged cases describe a specific physical response to specific loading and tend to improve the definition of the bias factor by reducing the uncertainty (coefficient of variation).

This process was performed for each of the three bias factors and included the development of joint likelihood functions to include the effect of coupling between the failure modes.

Platforms Investigated

Nine jackets and 3 caissons were selected for the study. A summary of the platforms selected for the calibration is given in the adjacent table. These platforms were selected from the population of heavily loaded structures (i.e., those nearest the center path of the hurricane) on the basis of the availability of good data (e.g , drawings, pre and post-storm inspection reports, soil data) and the estimated effect on the calibration (i.e., platforms that were damaged or thought to exhibit unexpected behavior were preferred).

Case	Platform	Water Depth (ft.)	Year Installed	# of Legs
Survivals	ST130Q	170	1964	4
	ST151K	137	1963	8
	WD103A	223	1965	8
Damaged	SS139	62	1969	4
	ST151J	137	1962	8 + 2 tripods
	ST177B	142	1965	8
	SPelto 10 *	35	1984	1
	SS135*	53	1983	1
	SS136 *	50	1983	1
Failures	ST72	61	1969	4
	ST130A	180	1958	8
	ST151H	137	1964	8

* indicates caisson

There were no jacket type platforms available that were believed to have experienced a foundation failure; however, there were several caissons that experienced full or partial foundation failure. Three of the caissons that were damaged during Andrew and were included in the API/MMS Foundation study [5] were used in this Phase II study to estimate the variation in the foundation lateral capacity bias factor.

Conclusions

The primary conclusion of the Phase II study was that the definition of separate bias factors for the jacket and foundation elements was consistent with expectations in that:

- The global system bias factor was found to be very similar to that as defined during Phase I
- The foundation bias factors were significantly greater than that for the jacket, indicating significant additional conservatism in foundation design

The structural analysis procedures developed for this study showed significant improvement over that used in Phase I. The predicted behaviors matched better with the observed behaviors. This improvement was primarily due to more accurate data, refined modeling (e.g., detailed modeling of the joints) and the updated hindcast. While it is apparent that further improvement can be made in the prediction of specific component response, it is clear that an overall improvement in platform ultimate capacity analysis procedures has been gained through these new procedures

This project has demonstrated the benefit of "failure mode specific" capacity estimates which can isolate and eliminate the effect of uncertainties associated with the complementary parts of the platform (e.g., the impact of uncertainties in the definition of soil strength on jacket capacity) These analyses provide a better understanding of the platform behavior and of specific strengths and weaknesses in a platform. This helps in the development of cost effective mitigation plans that may be needed to meet API RP 2A, Section 17 guidelines. In some cases, mitigation measures based on minimal, or more simplistic, analysis could be too costly and possibly even counter productive.

A summary of the bias factors is provided in the adjacent table and includes the final values produced from this study compared against the values developed in previous work. These factors show that, on average, the jacket capacity formulation is conservatively biased to a moderate extent and that both the foundation lateral and axial strengths are biased by a much greater amount.

Study	Mode	Bias
Phase I	Global System	1.19
API/MMS Foundation	Foundation Lateral	1.26
	Foundation Axial	1.66
Phase II	Global System	1.15
	Jacket	1.10
	Foundation Lateral	1.32
	Foundation Axial	1.54

Recommendations

The results of the Phase II and related studies can assist oil companies in the assessment of their platforms A specific example was developed as part of this study to illustrate how the product of this work can be utilized.

A primary conclusion of this work is that the definition of bias factors can be further improved as additional platforms, subjected to extreme loading, are included in the calibration. This improvement can be gained through refinement of the current bias factors or by development of bias factors that can be used more directly within the analysis. This could include, for example,

bias factors specifically for joints, braces, and piles. Now that the procedure for analysis, calibration and Bayesian updating is set-up, it will be relatively easy to include additional data as they become available

Appplication of Results

The study results provide an indication of the mean bias inherent in the loading and resistance calculation procedures used. These results should be considered as evidence supporting the use of the analyses procedures developed by industry in that these procedures appear to be somewhat conservative overall. It is not recommended that the calculated bias factors be applied directly in the assessment analysis of any individual platform without a complete understanding of the capacity and reliability procedures that have been used in this study. These bias factors were derived from a specific sample of platforms that does not represent the complete range of platform configurations, site conditions and physical conditions that exist in the Gulf of Mexico or any other area. Also, the variation of bias factors amongst the platform population studied (0.86 to 1.32 for jacket structure capacity, from 1.05 to 1.18 for foundation lateral capacity, and from 1.35 to 1.44 for foundation axial capacity) indicates that use of average bias factors for individual platforms could be inappropriate.

These bias factors provide a better appreciation of the uncertainties that affect reliability analysis. The API and regulatory agencies can use the results in the development of guidelines and criteria for platform assessment for extreme storm conditions. With good engineering judgment, the results can be applied in probability based requalification of steel jacket platforms that are similar to those included in the sample investigated. These factors may be considered in determination of the average failure probability estimates and in the economic risk and cost-benefit studies for a fleet of platforms.

Section 7
References

[1] PMB Engineering, Inc., 1993. Hurricane Andrew — Effects on Offshore Platforms, Final Report to the Joint Industry Project, October 1993.

[2] Minerals Management Service, 1994. Hurricane Andrew's Impact on Natural Gas and Oil Facilities on the Outer Continental Shelf. Interim Report Prepared by G. R Daniels.

[3] American Petroleum Institute, 1995. Recommended Practice for Planning, Designing and Constructing Fixed Offshore Platforms, API RP2A, Twentieth Edition, Section 17 Draft Supplement.

[4] Puskar, F. J., Aggarwal, R. K., Cornell, C. A., Moses, F. and Petrauskas, C., 1994. A Comparison of Analytical Predicted Platform Damage to Actual Platform Damage During Hurricane Andrew, Proceedings, 26th Offshore Technology Conference, OTC No. 7473.

[5] PMB Engineering Inc., 1995. Further Evaluation of Offshore Structures Performance in Hurricane Andrew — Development of Bias Factors for Pile Foundation Capacity. Final Report to the API and Minerals Management Service (also API PRAC Report 94-81), May 1995.

[6] PMB Engineering Inc., 1994-a. Hurricane Andrew — Platform Inspection and Analysis, Final Report to the Minerals Management Service, June 1994.

[7] PMB Engineering Inc., 1994-b. Post Mortem Platform Failure Evaluation Study, Final Report to the Minerals Management Service, August 1994.

[8] PMB Engineering Inc., 1994-c. Assess the Effect of API RP 2A 20th Edition Criteria on the Design of Offshore Caisson-Type Platforms. Final Report to the Minerals Management Services, July 1994.

[9] PMB Engineering Inc., 1994-d. Trial Application of API RP2A - WSD Draft Section 17, Final Report to the Joint Industry Project, December 1994

[10] PMB Engineering Inc., 1994-e. Benchmark Analysis — Trial Application of API RP2A - WSD Draft Section 17, Final Report to the Joint Industry Project, December 1994.

[11] Digre, K.A., Puskar, F.J., Aggarwal, R.K., Irick, J., Krieger, W.F., Petrauskas, C., 1995. Modifications to and applications of the Guidelines for Assessment of Existing Platforms Contained in Section 17.0 of API RP 2A. Proceedings, 27th Offshore Technology Conference, OTC No. 7779.

[12] Oceanweather, Inc., 1992. Hindcast Study of Hurricane Andrew (1992), Offshore Gulf of Mexico, Prepared by V. J. Cardone and A. T. Cox, Oceanweather Inc., Cos Cob, CT, November 1992.

[13] Oceanweather, Inc. 1994. Hindcast Study of Wind, Wave and Current Fields in Hurricane Andrew - Gulf of Mexico, Prepared by V. J. Cardone et al, Final Report to the Minerals Management Service, November 1994.

[14] Chen, W. F., and Ross, D. A., 1977. Tests of Fabricated Tubular Columns, American Society of Civil Engineers, Journal of Structural Division, Vol. 103, No. ST3.

[15] American Petroleum Institute, 1989. Draft Recommended Practice for Planning, Designing, and Constructing Fixed Offshore Platforms — Load and Resistance Factor Design, API RP 2A LRFD, First Edition, Washington D.C.

[16] SWRI, 1977. Model Testing of Braces to Develop Earthquake Analysis Criteria for Shell Oil Co. (Confidential)

[17] Grenda, K. G., Clawson, W. C., and Shinners, C. D., 1988. Large-Scale Ultimate Strength Testing of Tubular K-braced Frames, Proceedings, 20th Offshore Technology Conference, OTC No. 5832.

[18] Earl, C. P. and Teer, M. J., 1989. A Rational and Economical Approach to the Calculation of K-factors, Proceedings, 21st Offshore Technology Conference, OTC No. 6162.

[19] Underwater Engineering Group, 1983. Design of Tubular Joints for Offshore Structures, UEG Report No. UR 21, Vol. III, London.

[20] PMB Engineering, Inc., 1987-1990. Development of Platform AIM (Assessment, Inspection, Maintenance) Program, Phase-I to Phase-IV, San Francisco

[21] Hamilton, J. M. and Murff, J D., 1995 Ultimate Lateral Capacity of Piles in Clay, Proceedings, 27th Offshore Technology Conference, OTC No. 7667.

[22] Dier, A., and Lalani, M., 1995. Strength and Stiffness of Tubular Joints for Assessment/design Purposes, Proceedings, 27th Offshore Technology Conference, OTC No 7799.

[23] PMB Engineering Inc., 1995. CAP — Capacity Analysis Computer Program, San Francisco, CA.

[24] Lloyd, J. R. and Clawson, W. C., 1983. Reserve and Residual Strength of Pile Founded Offshore Platforms, Proceedings, Symposium on the Role of Design, Inspection, and Redundancy in Marine Structural Reliability, Washington D. C., National Academic Press.

[25] Bea, R. G , Puskar, F. J., Smith, C., and Spencer, J., 1988. Development of AIM (Assessment, Inspection, Maintenance) Programs for Fixed and Mobile Platforms. Proceedings, 20th Offshore Technology Conference, OTC No. 5703.

[26] Dean, R G. and Perlin, M., 1986. Interpolation of Near-Bottom Kinematics by Several Wave Theories and Field Laboratory Data, Coastal Engineering, Elsevier Science Publishers B. V., Amsterdam, The Netherlands.

[27] Tang, W. H., 1988. Offshore Axial Pile Design Reliability, Research Report for Project PRAC 86-29B, American Petroleum Institute.

[28] Tang, W. H and Gilbert, R. B., 1990 Offshore Lateral Pile Design Reliability, Research Report for Project PRAC 87-29, American Petroleum Institute.

[29] Risk Engineering, Inc., 1995. RELACS — Reliability Analysis of Components and Systems - Version 2.0 Boulder, Colorado.

[30] Benjamin, J. R. and Cornell, C. A , 1970. Probability, Statistics, and Decision for Civil Engineers, McGraw Hill Publishing Co.

[31] Hohenbichler, M., and Rackwitz, R., 1988. Improvement of Second-Order Reliability estimates by Importance Sampling, ASCE Journal of Engineering Mechanics, 114(12):2195-2198, December 1988.

[32] Madsen, H. O., Krenk, S., and Lind, N. C., 1986. Methods for Structural Safety, Prentice-Hall Inc., Englewood Cliffs, N.J.

[33] Stahl, B. 1975. Probabilistic Methods for Offshore Structures. Presented at the 1975 Annual Meeting of Division of Production, American Petroleum Institute, Dallas, Texas, April 1975.

[34] Moses, F., 1976. Bayesian Calibration of Platform Reliability, Report prepared for Amoco Production Company, Tulsa, Oklahoma.

[35] Moses, F., 1991. Load and Resistance Factor Design — Updating and Expanded Applications, Final Report of API PRAC Project 89-22, Prepared for American Petroleum Institute.

[36] Marshall, P.W., and Bea, R.G., 1976. Failure Modes of Offshore Platforms, Proceedings, International Conference on Behavior of Offshore Structures, Vol. 2.

[37] Tang, W. H., 1981. Updating Reliability of Offshore Structures, Proceedings Symposium. on Probabilistic Methods in Structural Engineering, ASCE National Conventions, St. Louis, Mo., October, 1981, pp. 139-156.

[38] Forristall, G. Z., 1978. On the Statistical Distribution of Wave Heights in a Storm, Journal of Geophysical Research, Vol. 83, pp. 2353-2358.

[39] Wen, Y. K., and Chen, H.-C., 1987. On Fast Integration for Time Variant Structural Reliability, ASCE Journal of Structural Engineering, May 1991.

[40] Haring, R. E , Olsen, O. A., and Johansson, P. I., 1979. Total Wave Force and Moment vs. Design Practice, Proceedings, Civil Engineering in the Ocean IV, Vol. II, pp. 805-819, ASCE, September 1979.